Polyethylene blends reinforced with nanometric fillers and tire waste devulcanized by microwaves

Fabiula Danielli Bastos de Sousa

Ecole Doctorale Sciences et Ingénierie
Ressources Procédés Produits Environnement

Étude des mélanges de polyéthylène renforcé avec des nanocharges et résidus de pneus régénérés par micro-ondes

Polyethylene blends reinforced with nanometric fillers and tire waste devulcanized by microwaves

THÈSE

présentée en vue de l'obtention du

Doctorat de l'Université de Lorraine

(Spécialité: Génie des Procédés et des Produits)

Soutenance publique le 29 juillet 2016

Fabiula Danielli Bastos DE SOUSA

Composition du jury

Reviewers	Ming TIAN	Professor, College of Materials Science and Engineering, Beijing University of Chemical Technology
	Kun CAO	Professor, State Key Laboratory of Chemical Engineering, Zhejiang University
Director of thesis	Sandrine HOPPE	Researcher, Laboratoire Réactions et Génie des Procédés, Université de Lorraine
Co-Director of thesis	Guo-Hua HU	Professor, Laboratoire Réactions et Génie des Procédés, Université de Lorraine
Examiners	Alain DURAND	Professor, Laboratoire de Chimie-Physique, Université de Lorraine
	Guangxian LI	Professor, State Key Laboratory of Polymer Materials Engineering, Sichuan University

Laboratoire Réactions et Génie des Procédés
UMR 7274 Université de Lorraine - CNRS
1 rue Grandville 54000 Nancy
Tel: +33 (0)3 83 17 51 90 Fax: +33 (0)3 83 32 29 7

Dedication

This thesis is dedicated to:

My parents Domingos and Elizabete.

My sister Bruna.

My niece and goddaughter Maria Luiza.

My directors Prof. Carlos Scuracchio, PhD; Prof. Suel Vidotti, PhD;
Prof. Guo-Hua Hu, PhD and Sandrine Hoppe, PhD.

Acknowledgements

First and the foremost, I would like to thank God for my life! I am particularly grateful for this unique opportunity, for all the challenges, for all the achievements.

Some special people that have always motivated me: my parents, my sister and my niece. My parents, Elizabete and Domingos, to whom I owe you all I am! I'm very proud to have them as my parents, my examples and teachers, always! Thanks again to the good God, for giving me such a wonderful family! Finally, to my friend Babi, my gratitude for teaching me every day how to be a better person.

I would also like to thank all my directors, Carlos Scuracchio, Suel Vidotti, Guo-Hua Hu and Sandrine Hoppe. All you are examples to me and to my future as a professor. I would like to offer my special thanks to Sandrine, for all help, patience, friendship and trust she devoted to me. Sandrine, merci beaucoup pour votre aide alors que j'étais en France. Je n'ai aucun mot pour te remercier! Merci un million de fois!!!

I would like to express my gratitude to Université de Lorraine and Laboratoire de Réactions et Génie des Procédés (LRGP) by the opportunity of the doctorate in Engineering of Processes and Products.

I would like to thank all the members of the jury for accepting the invitation: Professors Ming Tian, Kun Cao, Alain Durand and Guangxian Li.

To my friend and long-time English teacher Geraldo, thanks by the availability and sincere friendship. I would like to express my sincere recognition for your remarkable help on the completion of this work. I have no words to thank you for all these years together.

A especial thank to Leandro Sumida and Professor Fabio Furlan from Universidade Federal do ABC, I would like to give you a huge thank for your efforts to help me to achieve this objective.

I wish to thank all the people who helped me to collect the stones on the road and build the podium I climb in order to make this dream comes true.

Dreams don't determine the place in which you will be,

but produce the strength needed to get you out of the place.

Augusto Cury

SOMMAIRE

Résumé étendu en français

1. Contexte de l'étude

Le traitement des déchets d'élastomères vulcanisés, notamment les pneus usagés, est aujourd'hui un vrai problème à l'échelle mondiale. En effet, de graves problèmes environnementaux et de santé publique accompagnent la fin de vie de ces matériaux puisqu'ils nécessitent de longues périodes de temps pour se dégrader naturellement en raison leur structure réticulée qui les rend infusibles et de la présence de stabilisants et de nombreux autres additifs dans leur formulation.

Une solution possible

Les mélanges de polymères constituent actuellement un point fort de l'innovation et du développement dans le domaine des matériaux plastiques et sont capables de satisfaire les exigences de performances les plus élevées.
En effet, les polymères conventionnels ne suffisent souvent pas à répondre aux exigences des utilisateurs. Pour répondre aux besoins de matériaux à propriétés multiples ou plurifonctionnels, les chercheurs ont développé toute une gamme de mélanges de polymères. L'élaboration de mélanges de polymères est une voie intéressante pour la production de nouveaux matériaux capable de satisfaire les exigences de performances élevées. Par rapport à la synthèse de nouvelles molécules de polymère cela représente également une production plus économique

Des solutions au problème de l'élimination des résidus polymères, en particulier des déchets de caoutchouc font en outre l'objet de recherches actives depuis de nombreuses années. Ainsi, l'objectif principal de ce travail s'inscrit dans le contexte de la valorisation des pneus en fin de vie, en produisant un mélange vulcanisé dynamiquement à base de polyéthylène haute densité (en anglais High Density Polyethylene ou HDPE) et de poudrettes de pneu en caoutchouc (en anglais Ground Tire Rubber ou GTR) préalablement dévulcanisées par micro-ondes.

La dévulcanisation des déchets issus du caoutchouc vise à rétablir la capacité d'écoulement du caoutchouc vulcanisé par déstructuration du réseau réticulé. Contrairement à ce que ce terme indique, le procédé de

dévulcanisation n'est pas simplement l'inversion de la vulcanisation ou la rupture des liens entre les molécules de caoutchouc, permettant ainsi à la matière d'être à nouveau mise en forme. Un certain nombre d'autres modifications peuvent se produire dans le caoutchouc au cours de la dévulcanisation, tels que la coupure des chaînes principales, des ramifications, un raidissement des molécules de polymère et une augmentation subséquente de la température de transition vitreuse, Tg.

La technique de dévulcanisation par micro-ondes est actuellement l'une des plus prometteuses, en raison des bonnes propriétés de la matière ainsi dévulcanisée et la possibilité d'une productivité élevée. Le procédé tire parti du chauffage dans tout le volume du matériau par les micro-ondes, chauffage plus uniforme que celui obtenu par les méthodes plus traditionnelles, mettant en œuvre la conduction et / ou la convection.

Cependant, la littérature ne comporte que peu d''études sur l'évolution de la morphologie au cours du traitement en extrudeuse double vis de mélanges vulcanisés dynamiquement contenant des GTR dévulcanisés par micro-ondes. De même, il existe peu de travaux de recherche sur les mélanges contenant des GTR dévulcanisés et analysant les effets de l'ajout d'argiles de différentes formes (lamellaires et tubulaires) sur leurs propriétés finales.

En résumé, ce travail vise à proposer une solution au problème de valorisation des déchets solides issu des pneus usagés en produisant un mélange vulcanisé dynamiquement à base de PEHD et de GTR dévulcanisés par micro-ondes.

L'objectif est de combler certaines lacunes observées actuellement dans la littérature par l'étude de l'évolution de la morphologie au cours de la vulcanisation dynamique de ces mélanges et de l'effet de l'addition de différentes argiles dans ces systèmes.

2. Organisation de la thèse

En raison de la complexité de ces travaux et dans le but d'en faciliter la lecture et la compréhension, les différentes parties de la thèse sont organisées de la façon suivante.

L'introduction est focalisée sur trois thèmes principaux: les nano-composites, le recyclage des matériaux élastomères et les mélanges de polymères.

Pour faciliter la compréhension de la partie expérimentale du projet, celle-ci a été divisée en trois parties, à savoir:

Partie 1: Préparation des nanocomposites, étude de l'efficacité du procédé de dévulcanisation et caractérisation des phases des mélanges;

Partie 2: Analyse des meilleures conditions de traitement des mélanges vulcanisés dynamiquement;

Partie 3: Préparation de mélanges de polymères (en utilisant les meilleures conditions de traitement obtenues dans la partie 2) et étude de l'évolution de la morphologie dans l'extrudeuse bi-vis. Caractérisation des propriétés finales des mélanges.

Par ailleurs, afin de faciliter l'analyse des résultats obtenus dans la partie 3 et, en raison de la complexité des systèmes étudiés, les résultats des différentes techniques adoptées dans ces étapes ont été présentés en fonction des différents facteurs ayant un impact sur les propriétés finales des mélanges, à savoir:

- Effet de dévulcanisation de la phase élastomère,
- Effet de la revulcanisation de la phase élastomère,
- Effet de l'addition des argiles,
- Effet de la concentration des constituants des mélanges

Le travail dans son ensemble est divisé en deux chapitres principaux, à savoir : Nanocomposites et recyclage des matériaux élastomères (chapitre 1) , et Mélanges de polymères (chapitre 2) .

Chacun d'eux se divise en :3 parties : Introduction (fondements théoriques et revue bibliographique) , Matériel et méthodes, Résultats et discussion et conclusion.

L'introduction du premier chapitre traite de deux sujets : Nanocomposites (sections 1.2 à 1.2.3) et le recyclage des matériaux élastomères (sections 1.3 - vulcanisation des élastomères , et de 1.4 à 1.4.2 - recyclage des élastomères), où la partie expérimentale du chapitre comprend la partie 1. L'introduction du deuxième chapitre traite d'un seul sujet : les mélanges de polymères (sections 5.1 à 5.3) et la partie expérimentale couvre les parties 2 et 3 .

Partie 1

Afin de rendre les poudrettes issus de résidus de pneus (GTR) plus fluides lors de la production des mélanges, avec la possibilité d'utiliser des concentrations élevées et en recherchant un bon niveau de dispersion pour la morphologie finale de mélanges, les GTR ont été préalablement vulcanisés par l'action des micro-ondes.

Les GTR ont été dévulcanisés dans un système comprenant un four micro-ondes classique et système d'agitation adapté. L'ensemble du processus de dévulcanisation est réalisé en utilisant la puissance maximale du four, qui était de 820W. La figure 1 présente l'image du système, avec le détail du système d'agitation utilisé pour homogénéiser la matière lors de la dévulcanisation du caoutchouc et éviter sa dégradation par l'action des points chauds.

Les paramètres étudiés du procédé ont été le temps d'exposition aux micro-ondes et le nombre d'interruptions. Le temps d'exposition continue varie entre 1 et 5 minutes, et le nombre d'interruptions se situait entre 1 et 2. Dans le cas d'un traitement discontinu, le matériau est refroidi à l'extérieur (micro-onde coupées lorsque la porte est ouverte), sous agitation, pendant 10 minutes dans l'intervalle de temps entre les traitements aux micro-ondes.

Figure 1 - Système de Dévulcanisation utilisé, avec le détail du système d'agitation motorisé adapté pour l'homogénéisation du caoutchouc pendant le traitement et éviter sa dégradation par la formation de points chauds (points de fortes concentrations de micro-ondes à cause des effets de résonance dans la cavité du four).

Concernant l'efficacité du processus de dévulcanisation par micro-ondes, sont présentés les résultats des mesures de la température après dévulcanisation, la teneur en gel et la densité de réticulation ainsi que les résultats des analyses ATR-FTIR et de l'analyse thermogravimétrique. Concernant la caractérisation des phases du mélange, sont présentés les résultats de la cinétique de vulcanisation des GTR dévulcanisés, de la rhéométrie capillaire et de la diffraction des rayons X du HDPE et des nanocomposites HDPE / argiles.

La figure 2 présente la fraction de gel, la densité de réticulation et la température moyenne des GRT en fonction du temps d'exposition aux micro-ondes Pour les échantillons ayant subis plusieurs étapes de traitement, la température correspond à celle mesurée immédiatement après la dernière étape de traitement.

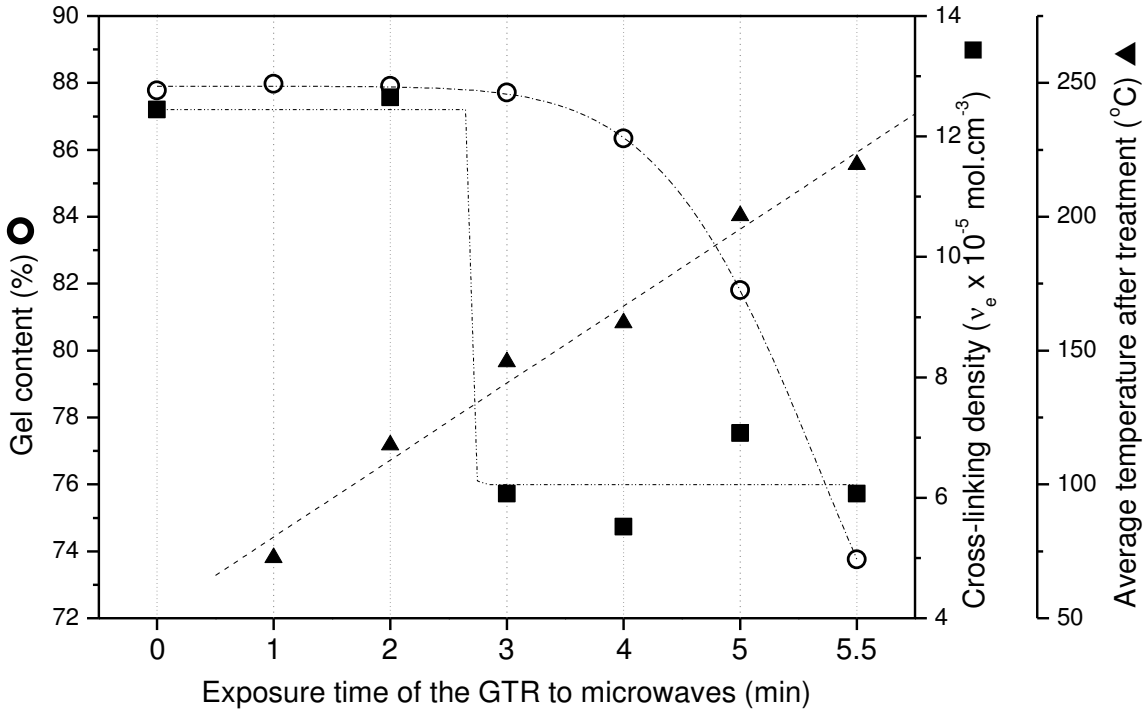

Figure 2 - Fraction de gel, densité de réticulation et température moyenne en fonction du temps après le traitement d'exposition aux micro-ondes font GTR.

En général, il a pu être observé que plus le temps d'exposition de l'échantillon aux micro-ondes est important, plus la température moyenne finale est importante et la plus la fraction de gel est faible, ce qui prouve que le processus de dévulcanisation a bien eu lieu. En d'autres termes, plus la durée du traitement par micro-ondes est longue, plus le degré de dévulcanisation est fort, en raison de la plus grande quantité d'énergie absorbée par les GTR. La température finale atteinte par l'échantillon est le principal facteur responsable du degré de dévulcanisation qui dépendait, dans ce cas, du temps d'exposition de l'échantillon aux micro-ondes.

La figure 3 montre la teneur en gel et la densité de réticulation des GTRX en fonction de sa température moyenne. Il existe une corrélation évidente entre eux, ce qui suggère que l'augmentation de température est responsable de la dévulcanisation et qu'il est probable qu'il n'y a pas d'autres mécanismes d'interaction entre les micro-ondes et les GTR.

D'après les résultats présentés dans cette section, il a été vérifié que le "meilleur" temps d'exposition examinée était celui de 5,5 minutes, en raison du plus grand degré de dévulcanisation tout en évitant une dégradation généralisée de la matière. Le résultat a également été corroboré par les résultats de rhéométrie capillaire, qui seront présentés dans la section 3.7. Ainsi, le GTR5.5 a été choisi pour être utilisé dans la production de mélanges vulcanisés dynamiquement dans l'extrudeuse bi- vis.

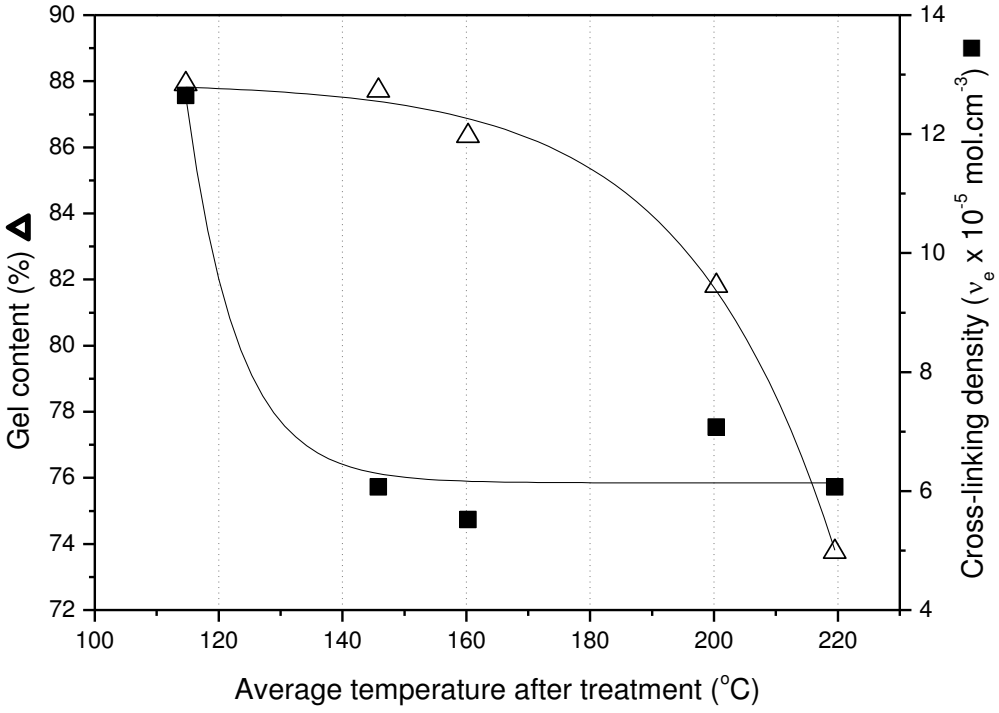

Figure 3 - Fraction de gel et densité de réticulation des GTRs vulcanisés en fonction de la température moyenne après traitement pour tous les différents temps d'exposition aux micro-ondes.

La figure 4 montre les courbes de viscosité à des taux élevés de cisaillement des phases des mélanges réalisés dans ce travail : GTR5.5 , HDPE et les nanocomposites à base d'argiles HDPE + Cloisite 20A et HDPE + halloysite .

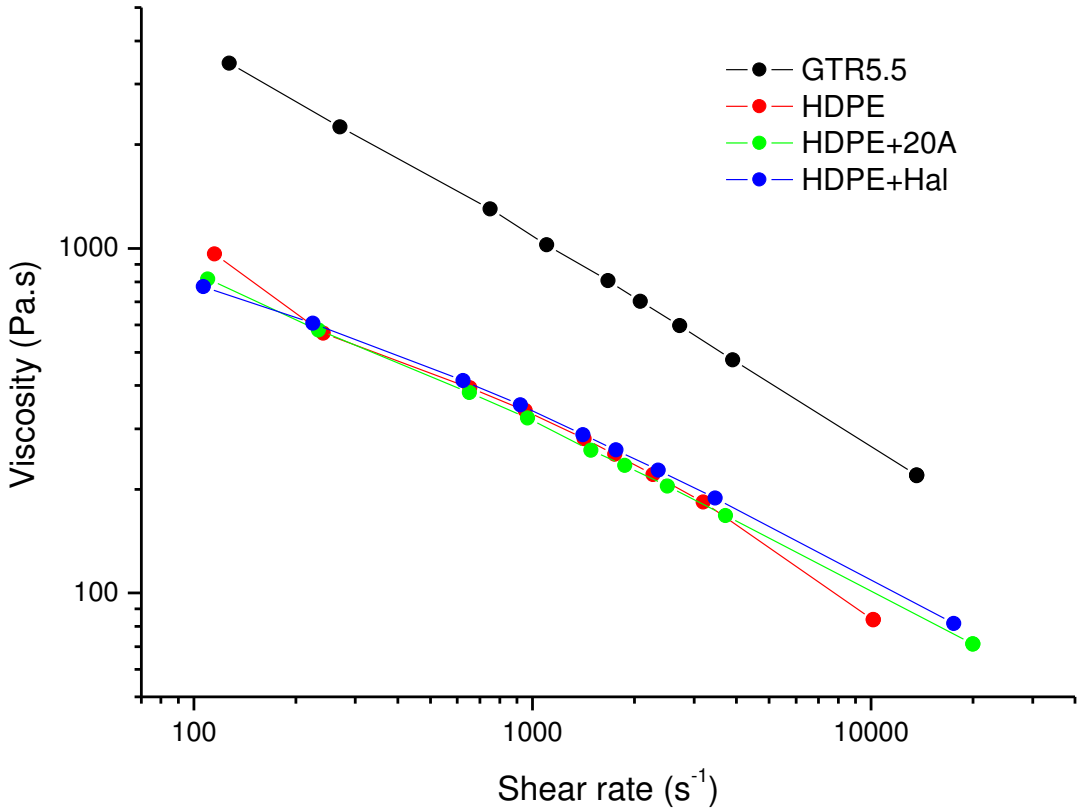

Figure 4 - Courbes de viscosité à taux de cisaillement élevés obtenus par rhéométrie capillaire à 180 ° C GTR5.5 , HDPE et de la matrice de nanocomposites HDPE utilisé dans la production de mélanges revulcanisés dynamiquement.

D'après les résultats ATR-FTIR, les atomes de soufre peuvent être brisés ou formés pendant le traitement par micro-ondes. Dans les échantillons dont l'exposition aux micro-ondes est longue, de nouvelles liaisons S-O sont formées à la suite du réarrangement des radicaux libres de soufre issus de la dévulcanisation des GTR, en présence d'oxygène.

La rupture suffisante des liaisons de soufre obtenues par dévulcanisation, permet un écoulement des GTR5 et GTR5.5 et par conséquent ces derniers peuvent être à nouveau mis en forme et revulcanisés.

La phase NR (Natural Rubber) du GTR est plus dégradée que la phase SBR (Styrene Butadiene Rubber) . Plus le niveau de dévulcanisation de l'échantillon est élevé, plus la dégradation de la phase NR (observée à partir des résultats de TGA) est importante.

La présence d'Halloysite dans le composé conduit à une dégradation des chaînes de polyéthylène haute densité par ramification et réticulation, alors

que la présence de Cloisite 20A réduit la dégradation du PEHD.

L'étude de l'efficacité du processus de dévulcanisation du GTR par micro-ondes a permis de montrer qu'il était possible de produire un caoutchouc dévulcanisé capable de s'écouler, ce qui est une exigence de base pour son utilisation dans la production de mélanges en extrudeuse. Avec l'adoption de la méthode de dévulcanisation par micro-ondes, il sera possible d'utiliser une concentration plus élevée de GTR recyclés dans des mélanges de polymères, sans grande diminution des propriétés finales et sans dommages sur la processabilité. Le procédé s'est également avéré être efficace en raison de la formation de nouveaux sites actifs pour la revulcanisation du caoutchouc.

Partie 2

Dans la deuxième étape du travail, une extrudeuse bi- vis a été utilisée pour préparer des mélanges vulcanisés dynamiquement sur la base de GTR5.5 et HDPE (contenant 40% en poids de HDPE et 60% en poids de 5,5 GTR). Deux profils de vis différents (Figure 4) et cinq vitesses de vis différentes pour chacun des profils ont été testés: 100, 150, 200, 250 ou 300 rpm. Un ou deux dispositifs d'alimentation ont été utilisés. Pour la production de mélanges réalisée en utilisant un seul dispositif d'alimentation, le PEHD et le caoutchouc dévulcanisé sont ajoutés ensemble. Pour la production de mélanges réalisée en utilisant deux dispositifs d'alimentation, on a ajouté le HDPE dans la première ligne d'alimentation et la phase GTR dans la seconde (figure 5).

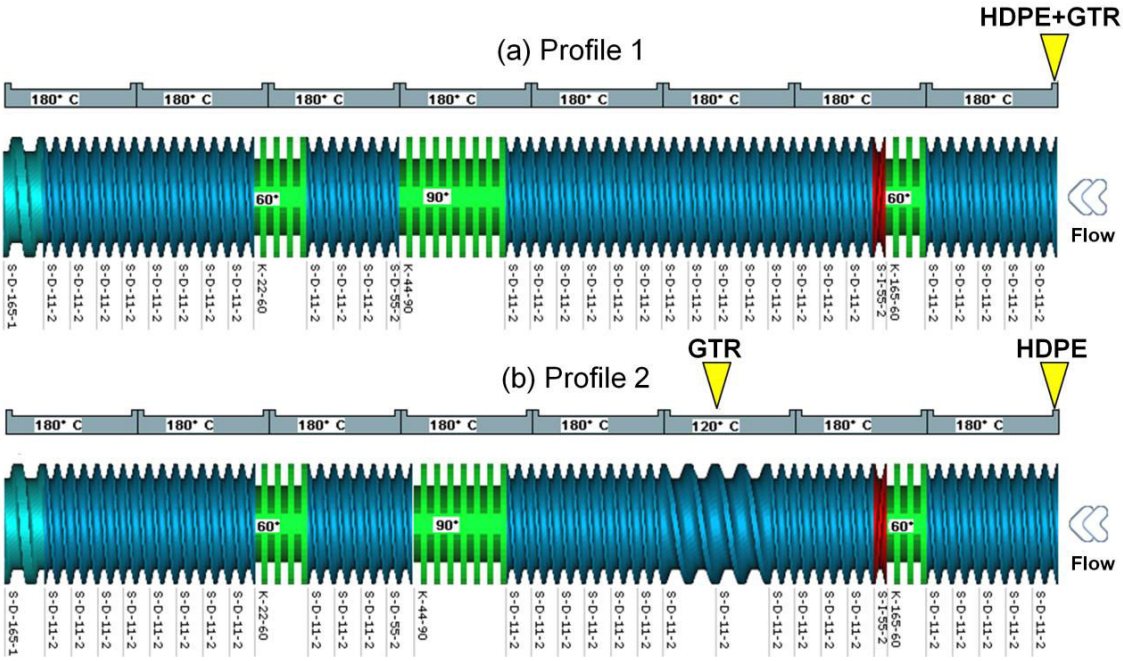

Figure 5 - Deux profils de vis différents utilisés dans la préparation des mélanges: (a) Profil 1: le PEHD et le caoutchouc dévulcanisé sont ajoutés dans le même dispositif d'alimentation, (b) Profil 2: le HDPE a été ajouté dans le premier dispositif d'alimentation et le caoutchouc dans le deuxième. Le canal de la vis à l'endroit de la deuxième ligne d'alimentation était plus profond et plus large pour faciliter l'alimentation en caoutchouc.

Dans l'ensemble, les effets de la vitesse de vis sur les propriétés mécaniques ne sont pas significatifs. En outre, les propriétés mécaniques des mélanges sont bien inférieures à ceux des TPV classiques, probablement à cause de la mauvaise compatibilité et adhérence entre GTR5.5 et HDPE.

Le tableau 1 résume les paramètres morphologiques (déterminés à partir des images MEB) du GTR5.5 / HDPE mélanges en fonction de la taille moyenne en nombre des particules (Dn), la taille moyenne en volume des particules (Dv) et de la dispersion de la taille (Dv / Dn). Il est à noter que l'impact du mode d'alimentation et de la vitesse de vis sur la taille du domaine caoutchouctique et la distribution des tailles de particules ne sont pas évidents. Néanmoins, le mélange 250-2 présente la plus petite taille, la distribution de taille de particule plus étroite et le module d'élasticité le plus élevé. Le "meilleur résultat" est une conséquence d'un compromis optimal entre la dispersion et la revulcanisation du GTR dévulcanisé dans l'extrudeuse.

Tableau 1: Paramètres morphologiques des mélanges .

Feeding mode 1				Feeding mode 2			
Sample	**D_n (µm)**	**D_v (µm)**	**D_v/D_n**	**Sample**	**D_n (µm)**	**D_v (µm)**	**D_v/D_n**
100	0.14	0.65	4.59	100-2	0.18	0.71	3.87
150	0.14	1.33	9.84	150-2	0.20	2.65	13.41
200	0.19	1.16	6.04	200-2	0.20	0.96	4.82
250	0.19	1.30	6.68	250-2	0.20	0.58	2.89
300	0.12	0.75	6.46	300-2	0.30	1.04	3.52

La figure 6 montre les paramètres de vulcanisation impliqués dans le traitement de mélanges revulcanisés dynamiquement, ainsi que le schéma d'une évolution probable de la morphologie lors du traitement. Le profil de vis est celui comportant 2 alimentations, car il permet d'obtenir une morphologie plus fine.

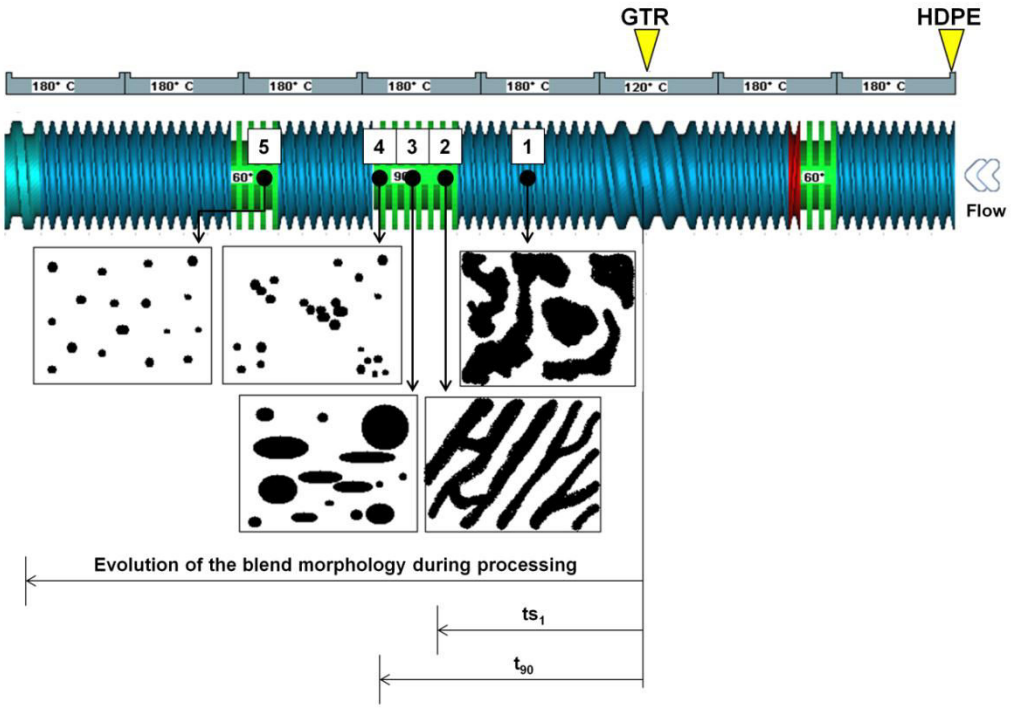

Figure 6 - Illustration de l'évolution de la morphologie et de la rhéologie de la phase élastomère impliquée au cours du traitement. Dans les images qui représentent les morphologies, la partie noire représente la phase élastomère et la partie blanche représente la phase thermoplastique.

La figure 6 montre qu'au point 1 de l'extrudeuse, il n'y a qu'un mélange physique entre les phases et il n'y a pas revulcanisation du GTR5.5 . Au début de la seconde zone de cisaillement élevé, la réaction de revulcanisation commence (le temps de séjour du caoutchouc à partir de son introduction dans l'extrudeuse à ce point est équivalent au temps ts1 de la réaction) et , autour du point 2 , le mélange présente une morphologie co-continue dans laquelle la phase élastomère est étirée dans la direction d'écoulement. A ce stade, la viscosité globale est augmentée (la phase élastomère à haute élasticité est étirée et se brise en particules plus petites en raison des taux élevés de cisaillement, (point 3), ce qui entraîne des contraintes mécaniques élevées. Au point 4, toujours sous l'effet des taux de cisaillement élevés, des particules de caoutchouc se brisent en particules plus petites, et au point 5 il y a une meilleure répartition dans la matrice thermoplastique. La fin de la seconde zone de cisaillement (point 4) correspond approximativement à un temps de durcissement optimal de la phase élastomère qui, dans le cas de GTR5.5, est de 44 s. Le temps de séjour du caoutchouc à partir de son introduction dans l'extrudeuse au point de la réaction de fin doit être équivalente à t90, et ce point devrait être dans une zone de cisaillement de l'extrudeuse pour la rupture des particules de caoutchouc de dimensions micrométriques.

Il est important de noter ici que, pour les deux profils de vis utilisés, la première zone de mélange a servi à faire fondre le HDPE, la deuxième à revulcaniser dynamiquement la phase de GTR et la dernière à améliorer la distribution spatiale des particules de caoutchouc dans le HDPE. Dans le cas des mélanges produits avec l'alimentation en mode 1 (figure 5a), le taux de cisaillement élevé dans la première zone de mélange pourrait provoquer la revulcanisation prématurée de la phase de caoutchouc, étant donné que les composants ont été ajoutés ensemble. Comme la longueur de cette zone et le temps de séjour correspondant étaient courts, le temps nécessaire pour terminer la réaction était plus long que le temps de séjour dans la zone. Ainsi, les domaines de caoutchouc ne sont pas suffisamment bien dispersés et distribués dans la matrice HDPE. Cependant, dans le cas des mélanges produits par l'alimentation en mode 2 (figure 5b), le temps de séjour de la phase de caoutchouc dans l'extrudeuse depuis son introduction jusqu'à la fin de la

seconde zone de mélange est plus proche du temps de cuisson optimal du GTR5. 5 à 180 °C (43,8 s). Par conséquent, la zone de mélange est suffisamment longue pour que la réaction de revulcanisation puisse aller à son terme et les domaines de caoutchouc dispersés puissent voir leurs tailles réduites au sein de la matrice HDPE. Le mélange 250-2 présentait une morphologie plus fine plus élevée et par conséquent de meilleures propriétés mécaniques, en dépit du fait que la compatibilité et l'adhérence entre les phases étaient médiocres. La morphologie plus fine est due à une bonne adéquation entre les conditions de traitement et les propriétés rhéologiques du GTR5.5. Les temps de séjour de GTR5.5 au sein de l'extrudeuse à partir de son introduction aux points respectifs indiqués sur la figure 6 étaient d'environ 50 et 30 s, respectivement, ce qui est très proches des valeurs de t90 et ts1 (44 et 27 s, respectivement).

Partie 3

À l'étape 3 de ce travail, les conséquences de différents facteurs (dévulcanisation et revulcanisation de la phase élastomère, l'ajout d'argile et de la concentration des phases) sur les propriétés dynamiques-mécaniques, rhéologiques et mécaniques, ainsi que sur la morphologie des mélanges ont été analysées.

D'une manière générale, l'analyse de la morphologie des mélanges a montré que la dévulcanisation du GTR est efficace pour l'augmentation de sa capacité d'écoulement en extrudeuse, étant donné que les mélanges contenant GTR0 présentaient des tailles de particules beaucoup plus grandes par rapport aux particules de GTR5.5. Le GTR5.5, plus fluide et moins visqueux, a facilité le processus de rupture des particules pendant le traitement en extrudeuse bi- vis.

En ce qui concerne la revulcanisation de la phase élastomère, on a observé que, en général, ceci a apparemment réduit le nombre de particules micrométriques de GTR. Il a été observé que les procédés de revulcanisation induisaient le durcissement par formation de microfibrilles dans les régions où les particules sous-micrométriques sont bien réparties, indiquant que la revulcanisation augmente l'adhérence entre les phases.

En ce qui concerne l'addition de l'argile, on a observé que cela a apparemment permis d'améliorer la répartition des particules de GTR dans la matrice. Toutefois, dans les mélanges non revulcanisés, la présence d'argile

Cloisite 20A semble avoir réduit l'interaction et l'adhésion entre les phases.

En ce qui concerne l'augmentation de la concentration de la phase GTR, il semble qu'elle s'accompagne d'une augmentation des particules sous-micrométriques de GTR dans la matrice. Le nombre de particules micrométriques semble également avoir été réduit avec l'augmentation de la concentration de GTR dans les mélanges.

D'après les résultats de DMA, deux transitions ont été déterminées pour les phases des mélanges: la première, autour de -40 ° C se réfère à la Tg des GTR et la seconde se réfère à la transition α du HDPE ($T\alpha$), qui se produit autour de 100 °C (les mêmes transitions ont été observées dans tous les mélanges analysés). L'existence de ces différentes transitions prouve la non miscibilité des phases des mélanges.

Même en sachant que, pour une meilleure analyse de l'évolution de la cristallinité de la phase thermoplastique, il est nécessaire d'effectuer une analyse DSC (qui n'a pas été effectué dans ce travail), certains changements dans la cristallinité de la phase de HDPE peuvent être observées sur la base de la DMA résultats.

La dévulcanisation de la phase GTR a changé la cristallinité de la phase de HDPE de certains mélanges, probablement en raison de changements dans la taille des particules de GTR5.5 et de leurs distributions dans la matrice.

D'une manière générale, dans des mélanges revulcanisés contenant GTR0, les valeurs de Tg sont plus petites par rapport aux mélanges contenant la même concentration de GTR5.5. En raison de la dévulcanisation, les chaînes polymères ont une plus grande liberté lors du traitement réactif, ce qui a probablement entraîné une augmentation du nombre de chocs efficaces et entraîné une augmentation de la densité de réticulation de la phase élastomère des mélanges contenant GTR5.5.

En ce qui concerne la revulcanisation de la phase élastomère, en général, on observe le décalage du pic de Tg des GTR à des températures plus élevées, et la réduction de la surface sous le pic de tan δ pour la Tg de la même phase, à la suite de la restriction de la mobilité des GTR par revulcanisation dynamique. De même, a également été observé le changement de la cristallinité de la phase de HDPE de certains mélanges. Comme on s'y attendait, la revulcanisation dynamique augmente la Tg de la phase

élastomère, dans la plupart des mélanges (à l'exception des mélanges contenant 20% de GTR).

Même en étant de préférence au sein de la phase PEHD, la présence d'argiles a modifié la Tg de la phase élastomère des mélanges revulcanisés. La Tg de la phase GTR des mélanges contenant de l'argile Halloysite est la plus importante de tous les mélanges analysés, en raison peut-être du plus grand nombre de chocs efficaces au cours du traitement, car la présence d'argile augmente la viscosité du PEHD par des processus de dégradation. D'autre part, la Tg de la phase GTR des mélanges contenant de l'argile Cloisite 20A est la plus faible parmi tous les autres mélanges. La présence d'argile a également modifié la cristallinité de la phase de PEHD de certains mélanges, en particulier ceux qui sont non revulcanisés.

Les résultats de rhéométrie ont montré que tous les mélanges ont présenté des réduction de la viscosité complexe avec le cisaillement, ce qui suggère un comportement pseudoplastique (fluidification par cisaillement).

A propos de la dévulcanisation de la phase GTR, en général, les mélanges contenant GTR5.5 présentent des valeurs plus faibles de la viscosité complexe par rapport aux mélanges contenant GTR0 en raison de la capacité d'écoulement plus élevée, à la suite de la rupture des réticulations du GTR pendant la dévulcanisation par micro-ondes. Les mélanges non revulcanisés contenant GTR0 ont présentés, en général, des valeurs supérieures de G ', par rapport aux mélanges contenant GTR5.5 en raison de la densité de réticulation plus élevée de la phase élastomère du mélange contenant GTR0 (non dévulcanisé). Dans le cas des mélanges revulcanisés, un comportement contraire se produit. La dévulcanisation du GTR a apparemment contribué à la formation d'un réseau percolé rhéologique.

Quant à la revulcanisation de la phase GTR, aucune tendance claire n'a été vérifiée. Les valeurs G 'ont été influencées par plusieurs facteurs: l'action de renforcement de l'argile, la dégradation de la matrice, la morphologie des mélanges et la densité de réticulation de la phase élastomère. Dans chaque mélange, en fonction de la concentration des phases et la présence ou non de l'argile, l'un des facteurs avait un impact plus important, et parfois il y avait une «concurrence» entre certains d'entre eux. Le manque d'adhérence entre les phases a également influencé les résultats obtenus.

En ce qui concerne l'addition de l'argile, en fonction de la concentration des phases et l'ajout d'un type d'argile spécifique, cela semble avoir agi comme un "renforcement" ou une "dégradation" des propriétés rhéologiques. La présence d'argile influence la formation de réseaux rhéologique percolants dans les mélanges, mais différents seuils de percolation ont été observés pour chaque argile. L'argile Cloisite 20A a réduit le seuil de percolation rhéologique (entre 40 et 60% des GTR du mélange), et pour l'autre mélange le seuil de percolation a été atteint entre 60 et 80% des GTR.

En ce qui concerne la concentration des phases, les mélanges non revulcanisés, G 'et les valeurs de n * ont augmenté en fonction de l'augmentation de la concentration de GTR présents dans le mélange. Dans le cas des mélanges revulcanisés, cette tendance n'a pas été observée. Avec l'augmentation de la concentration de GTR des mélanges, il a été observé une plus grande tendance à la formation d'un réseau rhéologique percolé, probablement en raison de la plus grande proximité entre les particules de GTR revulcanisés avec des diamètres plus petits.

Les résultats des propriétés mécaniques sont la conséquence de la morphologie des échantillons injectés qui, comme cité précédemment, a montré des particules distribuées bien dispersées ou non.

Quant à la dévulcanisation des GTR, les mélanges contenant GTR0 revulcanisés ont montré des propriétés mécaniques légèrement plus élevées par rapport aux mélanges contenant GTR5.5, probablement en raison d'une adhérence plus élevée parmi les phases (comme sur les images MEB). Comme GTR0 et les additifs et vulcanisation étaient sous forme de poudre, pour cette raison ces derniers n'étaient probablement pas bien mélangés aux GTR. On pense que, au cours du traitement, les additifs sont restés à l'interface, ce qui semble en quelque sorte d'avoir augmenté l'adhérence. Une autre possibilité pour l'augmentation des propriétés mécaniques des mélanges contenant GTR0 est la coexistence de deux réseaux de réticulation dans la phase élastomère, l'un issu de la vulcanisation et l'autre de la revulcanisation.

En ce qui concerne la revulcanisation de la phase élastomère, seuls certains mélanges ont montrés des améliorations des propriétés mécaniques. Les résultats de la microscopie électronique à balayage ont montré que la

revulcanisation dynamique augmente l'adhérence entre les phases, mais on n'a pas observé d'améliorations pertinentes dans les propriétés mécaniques des mélanges probablement en raison de la morphologie des échantillons injectés.

La présence d'argiles n'a pas modifié de façon significative la contrainte à la rupture, sauf pour quelques exceptions. L'argile Cloisite 20A a réduit l'allongement à la rupture, peut-être pour avoir réduit l'adhérence entre les phases et avoir apparemment changé la cristallinité du HDPE. L'argile Halloysite a augmenté les propriétés mécaniques pour avoir agi éventuellement à titre d'agent de compatibilisation. Le module de Young des mélanges contenant de l'Halloysite était plus faible par rapport à la valeur des autres mélanges, peut-être à cause de la dégradation du PEHD.

Quant à la concentration des phases, en général, et à quelques exceptions près, les propriétés ont diminuées avec l'augmentation de la concentration en GTR dans les mélanges, à la fois dans les mélanges revulcanisés et non revulcanisés.

Cependant, il est à noter que le mélange 60GTR5.5 / 40HDPE + 20A a présenté une haute contrainte à la rupture par rapport aux autres mélanges analysés dans le travail, ce qui était un résultat très positif, compte tenu de la forte concentration de matériau recyclé présent dans le mélange concerné.

La figure 7 présente et aide à comprendre les véritables contributions des processus de dévulcanisation et revulcanisation de la phase élastomère à la morphologie finale des mélanges.

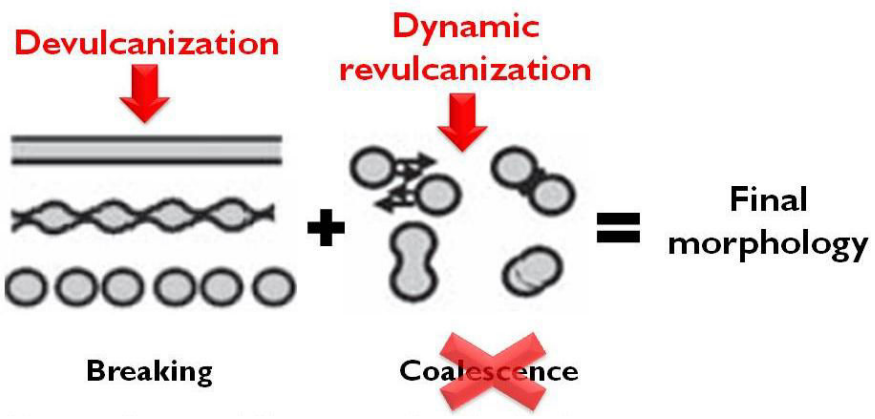

Figure 7 - Mécanismes de développement de la morphologie (rupture et coalescence des particules) des mélanges de polymères au cours du traitement .

La dévulcanisation du caoutchouc rend celui-ci plus fluide, ce qui contribue à sa rupture pendant le traitement et à la réduction de la taille des particules. Il contribue à la finesse de la morphologie, ce qui augmente par conséquent la zone de contact entre les phases et augmente la transmission de tensions. Le revulcanisation augmente l'adhérence entre les phases. La morphologie se stabilise en réduisant la fusion entre les particules de caoutchouc revulcanisées.

Conclusions

À l'étape 1, il a été analysé l'efficacité du processus de dévulcanisation du GTR par micro-ondes. Les résultats ont montré que le procédé était efficace, car la décomposition des réticulations a eu lieu et, par conséquent, la fraction de gel a été réduite, les modifications chimiques se sont produites dans la structure des GTR par dévulcanisation du caoutchouc et celui-ci est capable de s'écouler. A ce stade, ont également été analysés le meilleur moment de dévulcanisation (dans ce cas, il était de 5,5 minutes) et les propriétés des phases des mélanges qui ont été produites dans les étapes suivantes. D'après les résultats, la méthode dévulcanisation par de micro-ondes s'est avérée être une option pour le recyclage des caoutchoucs vulcanisés, en aidant à la réduction du grand problème environnemental et de santé publique qui est l'élimination des déchets solides.

À l'étape 2 ont été analysés les meilleurs paramètres intervenant dans la production de mélanges, par le traitement de mélanges 60GTR5.5 + ad / 40HDPE dans extrudeuse bi vis, en utilisant différents modes d'alimentation et vitesses d'extrusion. Les résultats soulignent l'importance dans le choix des paramètres de traitement optimaux pour chaque système particulier, étant donné que chaque système est unique, tout en respectant la cinétique de revulcanisation dela phase élastomère. Ces paramètres influent directement sur la morphologie et, par conséquent, les propriétés mécaniques des mélanges.

À l'étape 3 ont été analysées les conséquences des effets suivants: dévulcanisation et revulcanisation de la phase élastomère, addition d'argiles et concentration des phases sur les propriétés dynamiques-mécaniques, rhéologiques, mécaniques et sur la morphologie des mélanges. Sur la base des résultats présentés dans ce stade des travaux, il a été constaté que la dévulcanisation et la revulcanisation de phase élastomère a modifié les propriétés rhéologiques, dynamique-mécanique et la morphologie des mélanges. L'ajout d'argiles a également modifié les propriétés dues au changement dans le seuil de percolation rhéologique, au changement de cristallinité de la phase de HDPE de certains mélanges et à la performance possible en tant qu'agent compatibilisant entre les phases. Cependant, il n'a pas modifié de manière significative le caractère non miscible des mélanges.

Cependant, en raison du processus d'injection utilisé dans le travail pour produire des échantillons pour des essais de traction, les propriétés mécaniques ont été influencés par la morphologie des spécimens, qui ont entravé l'analyse des effets mentionnés dans ces propriétés. Bien que, même avec toute la complexité du travail en question, elle remplissait tous ses objectifs principaux. La publication des résultats permettra de combler certaines lacunes dans la littérature actuelle sur les différents aspects impliqués dans la production de mélanges revulcanisés dynamiquement contenant des résidus de pneus de camion dévulcanisé par micro-ondes. La méthode proposée pour la production des mélanges peut être une option pour le recyclage d’une partie des caoutchoucs vulcanisés, et donc être une solution à l'énorme problème mondial qui est la production de déchets solides, ce qui provoque des problèmes environnementaux et de santé publique graves.

LIST OF TABLES

LIST OF FIGURES

LIST OF SYMBOLS AND ACRONYMS

Å	Angstrom
BR	Butadiene rubber
°C	Degree Celsius
CEC	Cation exchange capacity
cm	Centimeter
cps	Count per second
D	Diameter
DCP	Dicumil peroxide
DMA	Dynamic-mechanical analysis
DRX	X-Ray Diffraction
DSC	Differential Scanning Calorimetry
E’	Storage modulus
EGMA	Copolymer ethylene-glycidyl methacrylate
EOC	Etylene octene copolymer
ENR	Epoxidized natural rubber
EPDM	Ethylene-propylene-diene rubber
EPDM-MA	Maleated EPDM
EPR	Ethylene propylene rubber
EVA	Ethylene vinyl acetate copolymer
FTIR	Fourier Transform Infrared Spectroscopy
g	Gram
G’	Storage modulus
GHz	Gigahertz
GPC	Gel Permeation Chromatography
GTR	Ground tire rubber
HDPE	High density polyethylene
HDPE-MA	Maleic anhydride grafted HDPE
Hz	Hertz
i-PP	Isotatic polypropylene
J	Joule
kg	Kilogram
kJ	Kilojoule

kV	Kilovolt
L	Length
LDPE	Low density polyethylene
m	Meter
mA	milliampere
meq	Milliequivalent
mesh	Number of meshes per linear inch
mg	Milligram
MHz	Megahertz
min	Minute
mL	Milliliter
mm	Millimeter
MMT	Montmorillonite
MPa	Megapascal
N	Newton
n°	Number
NBR	Nitrile rubber
nm	Nanometer
NMR	Nuclear Magnetic Resonance
NR	Natural rubber
OMMT	Organically modified Montmorillonite
Pa	Pascal
PA12	Polyamide 12
PA6	Polyamide 6
PB	Polybutadiene
PC	Polycarbonate
PDMS	Polydimethylsiloxane silicone rubber
PE	Polyethylene
PHBV	Poly (hydroxybutyrate-co-hydroxyvaleratelerato)
phr	Parts per hundred of rubber
PMMA	Poly (methyl methacrylate)
POE	Copolymer ethylene-octato
PP	Polypropylene

PS	Polystyrene
PVC	Polyvinyl chloride
RPA	Rubber Processing Analyzer
rpm	Revolutions per minute
s	Second
SAN	Poly (styrene-acrylonitrile)
SBR	Styrene-Butadiene Rubber
SEBS	Block copolymer of styrene-ethylene/butylene
SEM	Scanning Electron Microscopy
TEM	Transmission Electron Microscopy
T_g	Glass transition temperature
TGA	Thermogravimetric analysis
T_m	Melting temperature
TPE	Thermoplastic elastomers
TPU	Thermoplastic polyurethane
TPV	Thermoplastic vulcanizated
W	Watt
w-PE	PE residue
XLPE	Cross-linked polyethylene
µm	Micrometer
δ	Delta
Ø	Diameter
η	Viscosity

GENERAL INTRODUCTION

The search for new materials has been a constant in the human history. Likewise, solutions to the global problem of polymeric waste disposal, in particular the waste tire, which causes environmental and public health problems, have been targeted for many years by researchers.

The disposal of tires represents a serious problem to be solved, because they are items that occupy large volume and need to be stored in appropriate conditions to avoid the risk of fire and proliferation of insects and rodents [1]. Summarizing, the recycling of tires and vulcanized rubbers, in general, are far from being an easy task. The question of the disposal of scrap tires (discarded tires that are no longer useful life, or those that have irreparable damages on their structure [2]) is full of alternatives, commitments, legislation and conflicting reports about technological success [3], in addition to involve economic issues. Today, vulcanized rubber wastes are valuable materials instead of being trash, as they were in the past, but still remain a serious problem. According to Lagarinhos and Tenório [4], a major challenge for the tire recycling is, among others, the change of the concept of waste to secondary raw material.

There are currently many ways of recycling of scrap tires, which are addressed in section 1.4 of this work. On the other hand, how to convert effectively a residue in a useful material, that can be used in a wide variety of applications with security [5], still today has been the subject of much research, without reduction in the properties of the final product and high cost in the production.

An alternative that has been widely discussed in the literature is the use of recycled rubber in blends composed of one of the phases a thermoplastic polymer. Among them, blends type Thermoplastic vulcanizates (TPV) has been a good choice for improving the final properties and cost reduction in the production, since they exhibit characteristic properties of elastomers and are processed as thermoplastics.

However, in the production of this type of blend containing recycled rubber, adding a percentage of raw rubber, or the devulcanization (at least partial) of the recycled rubber, are basic prerequisites [6], since the lack of adhesion and compatibility among the phases may deteriorate its final properties.

The devulcanization by microwaves provides to recycled rubber the ability to flow and to be remolded [7] due to the break in the three-dimensional structure of cross-linked polymer chains. So, in the case of the use of a devulcanized elastomer in a polymer

blend, devulcanization acts directly on the ability of particle breakage of the dispersed phase, aiding in the refinement of the final morphology [8], in addition to the possibility that a higher concentration can be used without large depreciation on the mechanical properties of the blend.

Another possibility that has been discussed in the literature is the use of nano-sized fillers in blends containing recycled rubber. This new type of high performance material combines the advantages of polymeric blends and nanocomposites, by using small concentrations of nanofillers. In many cases, the nanofillers act as a compatibilizing agent among the phases, decreasing the interfacial tension and promoting a greater particle breakage during processing, decreasing the coalescence of the particles and increasing also the refinement of morphology [9].

OBJECTIVES

The main purpose of this work was the production of a dynamically revulcanized blend composed of matrix HDPE and dispersed phase GTR devulcanized by microwaves. However, it is known that when high concentrations of a recycled material are used as phase of a polymer blend, its final properties tend to degrade due to lack of compatibility and adhesion among phases and due to the final morphology. In order to reduce these problems, the work has suggested to devulcanize the recycled phase GTR by microwaves and carefully study the devulcanization process, to find the better exposure time of the material to microwaves that could trasform it into a fluid material without widespread degradation, which would result in the final morphologies of the blends more refined.

Another very important aspect in the production of this type of blend that changes directly its morphology is the processing. For this reason, a detailed study was proposed for verification of the most suitable parameters of twin screw extruder processing and that would result in blends with refined morphology which, consequently, would improve their mechanical properties. This stage was recommended given the lack of available works in the literature of at least similar systems to the one analyzed in this work.

About the lack of compatibility and adhesion among phases, the work proposed to analyze the effect of the introduction of nano-clays of different shapes (lamellar and tubular) in the properties of the blends, with the main purpose to increase the adhesion level and refinement of morphology.

The work has also examined the influence of different effects on the final properties of the blends: effect of devulcanization and revulcanization of the elastomeric phase, the addition of clays and the variation in the concentration of the phases.

As a result, the present work aspires to fill in some gaps found in the current literature on the various aspects involved in the production of dynamically revulcanized blends containing residues of truck tires devulcanized by microwaves, aiming to increase the added value of the final material and allowing it to be used on noble properties materials, as well as being a possible solution to the disposal of solid material of tough natural degradation such as tires, which cause several environmental and public health problems.

ORGANIZATION OF WORK

Due to the complexity of this work and with the purpose of facilitating its reading and comprehension, the constituent parts were arranged in distinct ways.

To facilitate the understanding of the experimental part of the project, the Methods were divided into stages, namely:

Stage 1: Preparation of the nanocomposites; devulcanization of GTR by microwaves and study on the efficiency of this process; and characterization of the phases of the blends;

Stage 2: Analysis of the best processing conditions of dynamically revulcanized blends;

Stage 3: Preparation of the blends (by using the best processing conditions obtained in Stage 2) and characterization of the final properties.

Likewise, in order to facilitate the analysis of the obtained results in Stage 3, due to the complexity of the systems studied, the results of the different analytical techniques adopted in this stage were divided according to the different factors that have influenced the final properties of the blends, namely:

- Effect of devulcanization of elastomeric phase;
- Effect of revulcanization of elastomeric phase;
- Effect of addition of clays; and
- Effect of concentration of phases.

The work as a whole is divided into two main chapters, namely: Nanocomposites and recycling of elastomeric materials (Chapter 1), and Polymer blends (Chapter 2). Each of them is divided into Introduction (theoretical foundations and bibliographic review), Materials and methods, Results and discussion and Conclusion.

The Introduction of the first chapter addresses two topics: Nanocomposites (sections 1.2 to 1.2.3) and recycling of elastomeric materials (sections 1.3 - vulcanization of elastomers, and 1.4 to 1.4.2 - recycling of elastomers), where the experimental part of the chapter includes the Stage 1. The Introduction of the second chapter addresses a single topic: polymer blends (sections 5.1 to 5.3), and the experimental part covers the Stages 2 and 3.

Even with the purpose to avoid difficulties throughout the text (duplicity), the sections were listed following, independent of the chapter to which they belonged.

CHAPTER 1: Nanocomposites and recycling of elastomeric materials

1 - INTRODUCTION

Topic 1: Nanocomposites

1.2 - Nanocomposites - general concepts

Nanocomposite is the result of the union of two or more types of materials with different properties, and the dispersed phase presents at least one of its dimensions in nanometer scale [10]. It is formed by continuous phase or matrix, dispersed phase or reinforcement and interfacial region [11].

Nanoscale materials are those whose dimensions range from approximately 1 to 100 nanometers, and a nanometer (nm) is one billionth of a meter (10^{-9} m) [12]. Nano-scale structures, such as nanoparticles and nanolayers, have high levels of specific surface (surface area of a given portion of material, being given in m^2/g) and lenght to diameter ratio (L/D, i.e., the largest measure of nanofiller divided by minor), making them ideal for use in polymeric materials [10].

Nanocomposites typically contain from 2 to 10% by weight of nanofiller [13, 14], with improved properties equal to or greater than the effect observed in traditional composites containing from 20 to 35% load. Due to its high lenght to diameter ratio and low density, nanofillers can be used as replacements to traditional fillers in polymeric composites, and among the most common there are the mineral clays [15].

1.2.1 - Clays

In general, macroscopic reinforcing elements contain imperfections. In this way, greater structural perfection is reached if the reinforcement elements become smaller and smaller. The final properties of a compound containing elements of reinforcement can be expected if the dimensions atomic or molecular levels are reached [16].

The reinforcements in nanoscale more common are the clays, consisting of layered silicates [15]. Among them, one of the most used for production of polymer matrices nanocomposites is Montmorillonite clay (MMT), a group of silicate smectits belonging to subclass of phyllosilicates 2:1 [17], which have a crystalline structure in the form of

layers, intrinsically anisotropic characteristics and ability to swell in water [18]. Each layer consists of two types of sheets together in sandwich form, which is called a lamella [19, 20]. One is called the tetrahedral sheet is composed of silicon dioxide, while the other is called the octahedral sheet, a polyhedron with eight triangular equilateral faces, composed of aluminum hydroxide or magnesium [20]. The thickness of a lamella is approximately 1 nm, and its lateral dimensions can vary from 30 nm to a few micrometers, depending on the particular lamellar silicate [15, 21-23]. The layers (or lamellae) are maintained by dipole forces stacked or van der Waals interactions, and have a uniform spacing among the layers, called basal spacing, interlayer or gallery [21]. Isomorphic replacements within the layers (for example, Al^{+3} by Mg^{+2} or Fe^{+2}) generate negative filler, which is balanced by cations among the galleries [17, 24]. This type of lamellar silicate is characterized by moderate surface filler, known as cation exchange capacity (CEC) and is usually expressed as meq/100 g [18, 25]. This surface filler is not locally constant, and may vary between one and another layer and should be considered as an average value of crystalline structure [15, 17]. A diagram representing the structure of a lamellar silicate is shown in Figure 1.

Another type of clay also widely used, the nanotube Halloysite (referred to in this work only as Halloysite or Hal), has molecular formula $Al_2Si_2O_5(OH)_4.nH_2O$ [26-28]. The length of nanotubes varies from 1-15 µm, the inner diameter of 10-30 nm and the external of 50-70 nm [26, 29]. Figure 2 shows the crystalline structure of Halloysite.

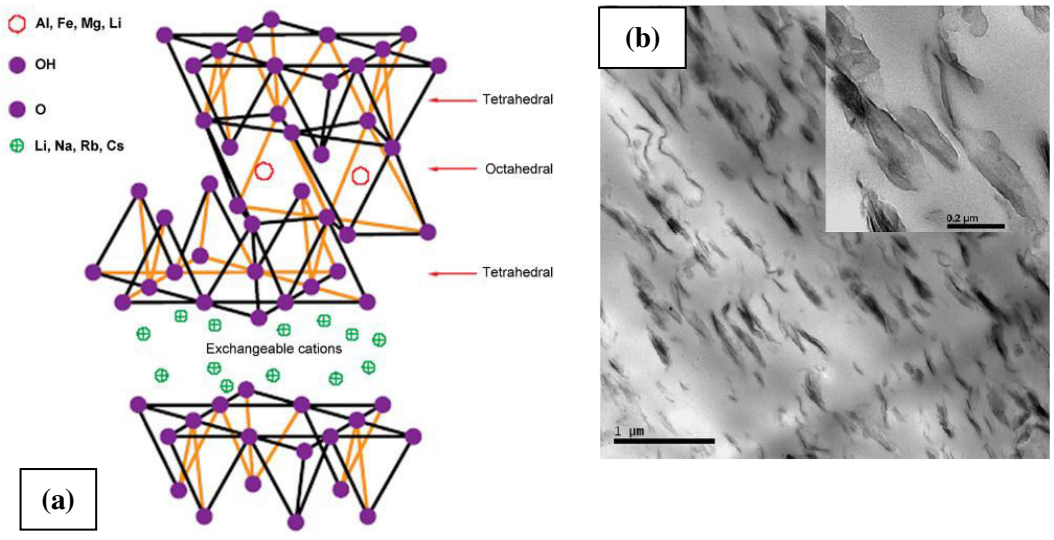

Figure 1: (a) A lamellar silicate structure [25] and (b) TEM micrograph of the compound poly (hydroxybutyrate-co-hydroxyvaleratelerato) (PHBV)/Cloisite 30B (5 wt%) [28], and clay is a type of lamellar silicate.

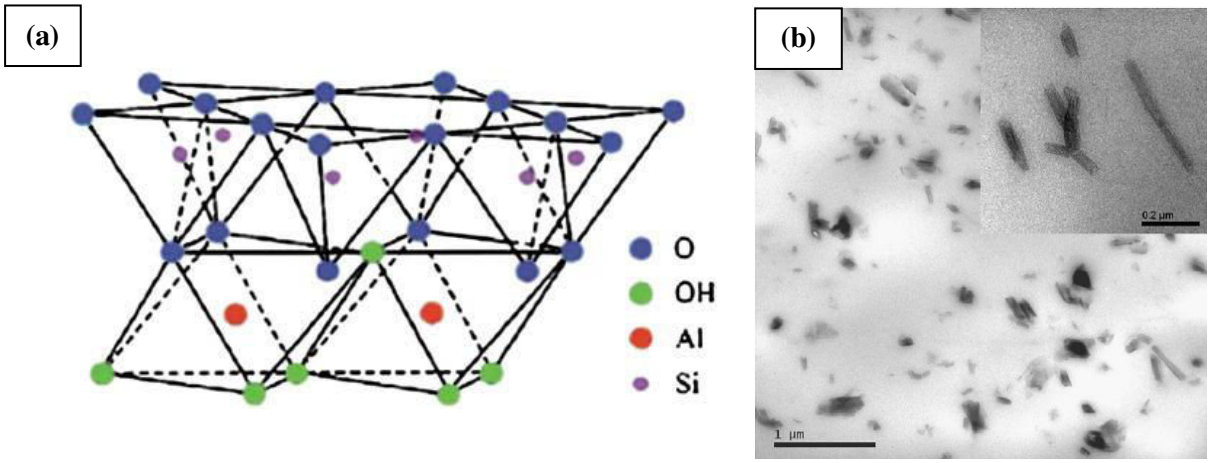

Figure 2: (a) Crystal structure of Halloysite [30] and (b) TEM micrograph of the compound PHBV/Halloysite (5 wt%) [28].

The nanofiller is considered ideal for the production of polymeric composites due to the following factors: (a) it is a rigid material and with high lenght to diameter ratio; (b) compared with other nanofillers such as silica, Montmorillonite, and nanotubes can be more easily dispersed in polymeric matrices due to geometric and chemical factors. Geometrically, for its stick format, it is easily dispersed due to limited intertubular contact area [27]. Chemically, they are tubular structures at the nanoscale with a surface composed of siloxane and a few hydroxyl groups, possessing potential ability in the formation of hydrogen bonds [30].

A method for producing nanocomposites widely used, especially in the case of thermoplastic matrices, is the method for molten state, which will be approached with greater details in the next section.

1.2.2 - Production method of nanocomposites in the molten state

The preparation of nanocomposites can be reached by different ways, including in situ polymerization, solution and molten state [31]. Among them, the method of production of nanocomposites in the molten state is the most attractive due to its advantages such as low cost, high productivity, no need for the use of chemical solvents and compatibility with the techniques commonly employed in the processing of polymers. The production of nanocomposites from this method is made, usually, in a twin screw type extruder.

The dispersion and distribution of nanofillers in the matrix happen thanks to shear forces during processing and compatibility among the phases. The agglomerate of nanofillers is broken due to the action of shear and extensional forces, while the compatibility among the phases ensures the dispersion of nanofillers in the polymer

matrices. When the clay and the polymer do not have a good compatibility, optimization of process conditions will determine the final morphology of the nanocomposite [32], and the dispersion of nanofillers can also be achieved through the use of a compatibilizing agent [33]. Therefore, the choice of the parameters used during processing may be responsible for the final properties of a nanocomposite polymer matrix. The typical states of clay dispersion in polymeric matrices and some typical properties of nanocomposites will be addressed in section 1.2.3.

1.2.3 - Dispersion states of clays in polymeric matrices and properties of nanocomposites

Depending on the nature of the components used (clay, organic cation and polymer matrix) and the method of preparation, three main types of composites can be obtained when clay layers are associated to a polymer (Figure 3).

When the polymer is unable to penetrate among the lamellae of silicate, a separate phase compound (Figure 3a) is obtained, whose properties remain in the group of traditional microcomposites. In addition to this classic family of composites, two types of nanocomposites can be obtained: intercalated structure (Figure 3b), in which polymer chains are located among the lamellae of the clay, but these don't lose their spatial ordering, only increasing its basal spacing, built with alternating polymer and inorganic layers. When the silicate layers are completely and evenly dispersed in polymer matrices, exfoliated or delaminated structure is obtained (Figure 3c) [34, 35].

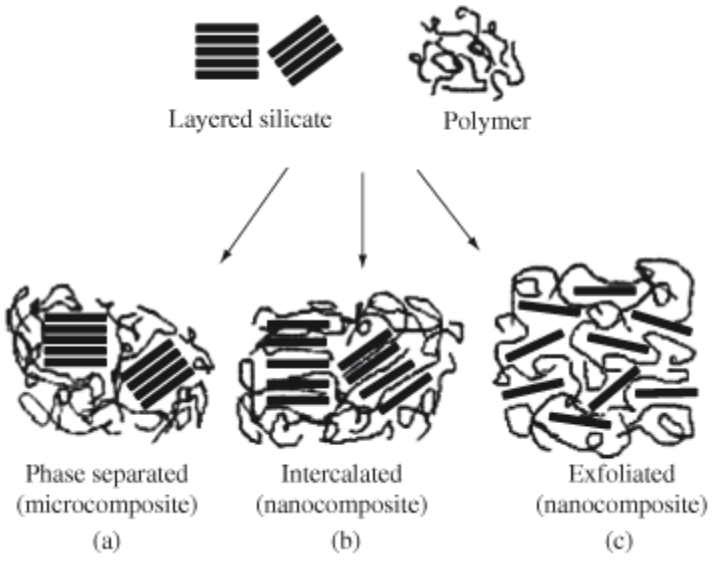

Figure 3: Typical states of dispersion found in lamellar silicate nanocomposites: (a) microcomposite, (b) intercalated nanocomposite and (c) exfoliated nanocomposite [34].

Some examples of improvements on the properties of polymers by adding nanofillers are improvement in thermal stability, mechanical properties, flame resistance and barrier to gases [36]. However, these improvements are linked to the state of dispersion of clays in the matrices, the concentration of the dispersed phase and compatibility among the phases.

With the purpose of studying the state of dispersion of clays in the matrices, a technique widely used is the X-Ray Diffraction (DRX), being that it is generally supported by Transmission Electron Microscopy (TEM). According to Goettler et al. [37], the interlayer spacing serves as a measurement of the degree of intercalation of clay, which can be measured by DRX, although the final verification of morphology should be made by TEM. The literature presents several works using the DRX [28, 31, 38-40] and TEM [27, 28, 31, 40-44], and the technique of DRX was also adopted in the work in question in the study of dispersion of high density polyethylene (HDPE) matrix clays and the results will be presented on the Results and Discussions from Stage 1.

From this point, some examples taken from the literature showing the importance of the addition of clays in polymeric matrices forming nanocomposites produced in the molten state are here briefly described and discussed.

According to Goettler et al. [37], with the increase in concentration of clay in addition to a concentration limit (varying according to the analyzed system and representing the percolation threshold), often result in reduction in mechanical properties, and low concentrations of fillers are preferred and should be able to provide significant reinforcement when properly structured and linked to the polymer matrices.

Carli et al. [28] have achieved improvements in mechanical properties of PHBV with the addition of 5 wt% of Cloisite 30B and Halloysite clays. The Young's modulus increased in 103 and 63% to nanocomposites containing Cloisite 30B and Halloysite, respectively. According to the authors, the increase in stiffness is due to good dispersion of the clays in the matrices and the strong interaction between the polar PHBV and nanofillers. Other authors also obtained similar results in their works [38, 45].

Du et al. [44] produced nanocomposites with matrix HDPE, polypropylene (PP) and polyamide 6 (PA6) and Halloysite clay. According to the authors, the formation of hydrogen bonds between the clay and the matrices occurred, increasing the bending properties of the compounds. Similarly, Lee and Han [40] observed the formation of hydrogen bonds between the hydroxyl groups present at the end of chain of surfactant present in the Cloisite 30B clay and the carbonyl groups present in matrix polycarbonate (PC), which formed a sort of interphase and increased compatibility between the PC

matrix and the clay.

Minkova et al. [39] analyzed the properties of nanocomposites matrices HDPE and low density polyethylene (LDPE), and Cloisite 20A and 30B clays containing compatibilizing copolymer ethylene-glycidyl methacrylate (EGMA). The use of the copolymer as compatibilizing facilitated the intercalation of the lamellaes of Cloisite 20A clay, and exfoliation and partial degradation of the organic surfactant of the lamellae of Cloisite 30B clays. The thermal properties and microhardness of nanocomposites depend on the concentration of clay, and the microhardness of the ternary nanocomposites was increased significantly due to the action of the copolymer. The nanocomposites also presented good flame retardance properties. The literature presents other works with similar results [31, 46].

Another function of the clays is to act as nucleating agent in semi crystalline matrices. Liu et al. [27] produced nanocomposites isotatic polypropylene (i-PP) and Halloysite in different concentrations and observed that the presence of clay altered the process of crystallization of the thermoplastic, having acted as an interlayer agent. Depending on the concentration of clay and kind of crystallization, the degree of crystallinity was changed of α or β. In the work of De Oliveira et al. [47], the addition of clay did not alter significantly the crystallinity degree of the matrices, but favored the formation of γ crystals.

Sadeghipour et al. [43] produced nanocomposites HDPE matrix, and Cloisite Na^+ and 20A clays in different concentrations. Organically modified clay has greater potential to merge the matrix due to greater interaction among the phases. The modulus of the nanocomposites increased with the increase in the clay concentration, but the increase was greater in the low-frequency region, because the interaction matrix/filler decreased with increasing frequency.

As described in the section on Organization of work, the introductory part of the first chapter was divided into two main topics, the first of which is nanocomposites and the second, elastomeric materials recycling. From this point, the approach of the second major topic will be made, starting with the definition of the concept of vulcanization of elastomers.

Topic 2: Recycling of elastomeric materials

1.3 - Vulcanization of elastomers

Elastomers consist in a class of materials widely used today in many fields of application. Their typical properties as high levels of elasticity and damping are what make this class so important. For this, the elastomers must, before, to go through a complex process known as vulcanization [48]. Vulcanization (or cure), word derived from Roman mythology (Vulcan, God of fire and of working with metals) [49] is the process of treating elastomers with chemicals to reduce their plasticity, stickiness, sensitivity to heat and cold, and to add useful properties like elasticity and resistance [48].

Chemically, the vulcanization of rubber conversion is through a process of formation of cross-linkings, i.e., a process in which the molecular chains, independents, are joined by chemical bonds forming primary cross-linkings, which lead to the formation of a three-dimensional network in the material. This structural organization allows to maintain or increase the elastic properties and to reduce the plastic behavior of the material. The elastomer becomes insoluble and with greater mechanical resistance in temperatures greater than that of non vulcanized rubber [50]. The formation of a network of cross-linkings can be obtained by using sulphur or other chemical compounds as cross-linking agents [51].

The vulcanization can lead to different kinds of cross-linkings, namely: polysulphidic (Figure 4a), disulphidic (Figure 4b), monosulphidic (Figure 4c) and cyclic bonds (Figure 4d).

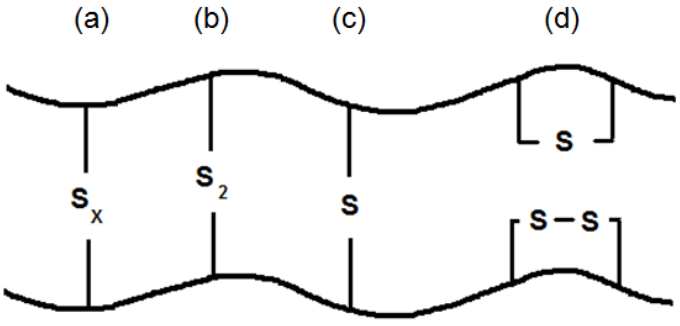

Figure 4: Types of cross-linkings resulting from the attack of the sulphur to the elastomeric chains: (a) polysulphidic, (b) disulphidic, (c) monosulphidic, and (d) cyclic bonds, based on [52].

However, while the vulcanization provides improvements in the properties of the elastomers and with it the possibility of a wide use as consumer goods, it brings

difficulties for recycling after use, once the vulcanized polymer becomes a thermosetting plastic, making it impossible for subsequent molding into another product. The general concepts on elastomeric materials recycling will be covered in the next section.

1.4 - Recycling of elastomers - general concepts

Tire rubber residues do not decompose easily due to its cross-linked structure (they are not biodegradable), presence of stabilizers and other additives [53, 54], and being that the time necessary for them to degrade naturally is undefined [2]. They cannot be reprocessed as thermoplastic materials [3] for being not fusible and insoluble in organic solvents due to the presence of three dimensional chemistry networks [55]. Currently, the tire recycling is even harder due to the addition of new components in the mixture and additives in order to increase their performance and service life, safety, noise reduction, comfort and well-being of passengers. Moreover, their current composition is unknown because it is a confidential information.

The interest in new applications for scrap tires has become a new challenge for researchers. The recycling of waste tires in general has important implications such as environmental protection, energy conservation, use as industrial raw material, reduction in costs and improving the processing behavior of rubber compounds [56]. According to Hassan et al. [57], GRT recycling not only helps to solve the problem of the disposal of solid waste and maintain environmental quality, but also helps to save the valuable and limited resource of fossil raw materials. According to Vergnaud and Rosca [3], an "ideal solution" should be based on the following factors:

"i. Waste disposal processes of rubber should not present any adverse effect to our environment.

ii. Preferably, the processes should conserve our natural resources through the recovery and recycling of raw materials.

iii. Proceedings should have a minimal adverse impact on established industries, consistent with the goals of conservation and recycling.

iv. The processes should be adapted for widespread use, and the products should have commercial value.

v. Minimum cost would be necessary in order to be truly competitive in our economic system."

Almost all molding and vulcanization processes generate waste. The disposal of this waste is one of the largest costs of rubber industry, because the material used has high

added value, and therefore its removal is considered a waste. The ideal solution to this problem, therefore, is that the material is added back into the process within the industry itself, which is not so simple in the case of rubbers [58].

There are basically four different levels of recycling: recycling of materials, recycling of monomers, energy recycling and recycling as fuel [59]. One of the alternatives of energy recycling, for example, is the burning of tire for using of its energy value. 128 J of energy is consumed to produce a kilo of tire rubber. However, the calorific value retrieved by its burns is 27-33 J/kg, not much bigger than the burning of a low-cost coal, i.e., valuable rubber material is lost. Moreover, the burning of tires for energy production generates air pollution [60]. Some toxic gases such as SO_2, H_2S, HCl, HCN, and others are produced, requiring additional systems to proper treatment and, consequently, more investments will be needed in the project of incinerators using suitable materials [61]. A form of recycling as fuel is the co-processing of GTR with coal as a way to produce liquid fuels transport [62-67]. The present work is focused only on one of the levels of recycling: recycling of materials, in which case it is the recycling of rubber used in tread of truck tires.

Some industries grind the vulcanized rubber and reintroduce it on the production line as filler on raw rubber, as a way of recycling and reduction of cost [68]. However, this process tends to degrade the mechanical properties and the performance of the final product [68] and the amount of rubber to be reincorporated, without affecting these properties, is much shorter than the ideal [58], due to the cross-linked structure of ground rubber that restricts the movement of its chains and reduces its processability [69]. A recycling method able to minimize the problem is the devulcanization, which is defined and covered with more detail in the next section.

1.4.1 - Devulcanization

Devulcanization of elastomers is defined as the process of total or partial cleavage of the polysulphidic, disulphidic and monosulphidic cross-linkings formed during the initial vulcanization [70-73] (scheme shown in Figure 5). This rubber is known as regenerated or reclaimed rubber [70], namely, devulcanized rubber which recovered its viscous properties (or regained its mobility [69]), as well as some features of the original compound [74].

The known methods for production of regenerated rubber include thermo-mechanical, thermo-chemical, physical (methods of microwaves and ultrasound) and biological processes that involve complex transformations that lead to depolymerization,

oxidation, and in many cases the degradation of polymeric chains of rubber, which reduces its viscosity [70]. In general, all of these methods are ways to provide energy to destroy, in whole or in part, the three-dimensional network of vulcanized rubber [75].

Figure 5: Schematic of devulcanization, where the red blocks represent the breaking of the cross-linkings of the elastomer due to process of devulcanization.

When the goal is to reintroduce the recycled material in the process, the role of devulcanization of rubber is, exactly, to increase the interaction between the raw and recycled material, reducing the degradation of the properties of the finished product, and making it possible to increase the amount of recycled rubber in the compound raw phase/recycled phase [52].

Despite the devulcanization process increase the molding material capacity, the higher the degree of devulcanization, the greater the amount of breakage of the main polymer chain links. The effect of this degradation in polymer is the significant reduction of stiffness and other mechanical properties when the material is revulcanized. Therefore, the choice of the parameters of the devulcanization process must take into account the balance between the processability and mechanical properties of the final material [7].

The literature presents several works that discuss the different methods used to devulcanize rubbers, as mechanical process and chemical mechanical [6, 57, 76-100], microwaves method [7, 58, 72, 101-110], ultrasound method [52, 71, 75, 111-146], chemical method [55, 80, 147-158], microbial method [69, 159-168], and there are still other methods as bioreactor and spraying for solid-state shear [169-173]. Some authors demonstrate the importance and the value of scrap tires through its transformation into a large number of raw materials that can be used in the rubber industry, residential and commercial buildings, construction of roads, sea walls, artificial habitats for coral reefs in shallow seas, steel production and sports facilities [174]. However, some authors [175] claim that the surface of decks and playgrounds, where the vulcanized rubbers are

widely used, contains hazardous organic chemicals that can cause serious health problems. In addition, in general, work on the recycling of rubber through the addition of vulcanizates in concrete work normally only on workability of mixture, i.e., the ability of the concrete to be easily placed and evenly compressed in a given location. Depending on the properties and size of rubber particles added to concrete, this capacity can be improved or not. The use of ground rubber on the asphalt has great importance according to Myhre et al. [68]: "this application simply did not develop without environmental concerns, but also from a need to improve the performance and service life of the asphalt pavement". A great advantage is that the GTR can be used in a variety of industrial applications due to its thermal and chemical stability, in addition to the low cost [176].

Warner [73] presented a series of chemical compounds also used on devulcanization of rubber like sodium di-n-butyl phosphate, thiol-amina, di-tiotreitol, lithium aluminium hydride, phenyllithium, methyl iodide. The vast majority of them is able to break poly and disulphide-connections and, according to the author, the latter compound is able to break the monosulphidic links. This method is not widely used today due to lack of efficiency, since it results only in rubber partially devulcanized and uses hazardous chemicals to human health and to the environment, many of which are carcinogenic. Another chemical method currently not widely used is the catalysis [73]. According to Isayev et al. [136], in chemical recycling methods, the process of devulcanization is usually very slow. In addition, "it creates a problem by removing the solvent and additional waste that are generated in the form of mud" and, with that, the total cost may be increased.

In the following section, the method of devulcanization by microwaves, which was used in this work, will be addressed with more details.

1.4.2 - Devulcanization by microwaves

The technique of devulcanization by microwaves is very promising, both by good devulcanized material properties, and the possibility of high productivity. The process uses the volumetric heating of the material by microwaves, promoting a more uniform heating than that achieved by more traditional methods of heating conduction or convection-based. As the interaction between the material and the microwave depends on the dielectric characteristics of the material, in mixtures with different types of materials is possible the selectivity of heating of certain regions, property that has been

explored in thermoset processing with mineral fillers [7, 177].

The processing of materials by microwaves is a relatively new technology, which has created alternatives to the improvement of some properties, including the recyclability with economic advantages over other types of processes, such as lower power consumption and reduced processing time. This method is very useful because it provides an economic and environmentally friendly form of reuse of waste rubber, making it possible, in some cases, its return to the same process and originally produced products, thus creating a similar product with equivalent physical properties [178]. The process has physical nature, that is, does not involve chemicals during the process (it's a type of thermal or controlled degradation [68]), allowing the implementation of high amount of energy to the material in a short time, resulting in high productivity [7].

The microwaves are electromagnetic oscillatory fields with frequencies in the range of 300 MHz to 300 GHz, corresponding to the wavelength λ between 10 cm and 1 mm [179]. As the microwaves are also used in telecommunications, two specific frequencies are reserved for heating: 0.915 and 2.45 GHz. Most of the interactions between the microwaves and the material that are of chemical relevance are due to induced electric field and polarization phenomena of reorientation [180] or, in other words, the interaction between the microwave and the material depends on this to have polar characteristic.

The polarity of the material can be an intrinsic feature or be induced by the presence of a second component, or filler, of conductive nature. Carbon black, which is a common filler widely used in rubber, presents sufficient electrical conductivity to promote this interaction between the wave and the material [181]. This filler is widely used in rubber tires in general due to improvements in tensile strength, modulus of elasticity, hardness, resistance to tear, abrasion, resistance to fatigue and break [145]. The susceptibility of the material when heated to high-frequency electromagnetic waves is due to ion polarization or interface, i.e., accumulation of free electrons in interface of different stages with different dielectric constants and conductivities [182].

It is possible to quantify the dielectric properties of a material and, consequently, its ability to interact with the microwaves through the dielectric constant (ε') and the dielectric loss factor (ε") which refer, respectively, to capacitive and conductive components of the material and are usually written in terms of complex dielectric constant (Equations 1 and 2) [183].

$$\varepsilon * = \varepsilon' - i\varepsilon" \qquad \text{Equation 1}$$

Another common term used to express the answer is the tangent of dielectric loss:

$$\tan \delta = \frac{\varepsilon'}{\varepsilon''} \qquad \text{Equation 2}$$

ε' represents the ability of a material to be polarized by an external electric field, and therefore is a relative measure of energy density of microwave, while ε" the efficiency with which the electromagnetic energy is converted into heat [184]. The value of tan δ is related to the ability of the material to be heated, so the higher the value of tan δ, the greater the heat generation [180].

Due to the restriction of internal rotation of the dipoles, there will be a delay between the applied electric field and polarization of molecules of the material. This delay, known as the relaxation time, is due to the dissipation of energy as heat in the material. Microwave heating is the result of this dielectric relaxation. The phenomenon is similar to that found on the rheology of viscoelastic materials subjected to mechanical stress.

According to Scuracchio et al. [7], the technique of microwave devulcanization is able to generate a material with properties quite different from the original vulcanized rubber. One of the properties, perhaps the most prominent, with regard to the possibility of the material to be recycled, is the ability to flow and to be remolded. This feature, along with the ability to revulcanization, points out to the wide applicability of microwave devulcanization. Once the heating of the material has been achieved, it is necessary that the amount of energy absorbed by the rubber is enough to break the cross-linkings formed by C-S and S-S, but not enough for the main chain degradation of rubber, formed by C-C and C=C, being that the energy required to break bonds C-S, S-S e S_X is, respectively, 285, 268 and 251 kJ/mol, while the C-C bond is 346 kJ/mol [72, 89, 185]. One of the ways to improve the selectivity of the breaking of chemical bonds in the vulcanized tridimensional network is by the control of process parameters. Consequently, it is important to have knowledge about the influence of the conditions of application of microwaves in devulcanized rubber properties.

Bani et al. [101] report that the use of microwaves has shown to be a quick method and a simple technique with many advantages, among them the high heating rate, that allows the reduction of the total time without any need of additional mechanical or chemical treatments. To Hirayama and Saron [105], microwave treatment causes breakages mainly in polysulphidic links, as well as the decomposition of sulphur-containing chemical groups attached to the chemical structure of Styrene-Butadiene Rubber (SBR), while the chemical bonds of higher energies, such as the

monosulphidics, remain preserved.

For checking the occurrence of devulcanization in elastomers, it is very common among the authors the use of the techniques of extraction and solvent swelling [69, 71, 77, 83, 88, 89, 91, 105, 108, 109, 115, 119, 121, 126-131, 149, 160, 186]. The devulcanization changes the density of cross-linkings, which consequently alters the fraction of sol-gel of the sample. The relative amount of gel (insoluble material) and the sol (soluble material) is a direct measure of the level of devulcanization and/or aging. Greater the amount of sol and lower the amount of gel in the recycled rubber means that there was breaking of three-dimensional network formed by cross-linkings [141], i.e., the higher the sol fraction, the more efficient was the devulcanization process [94]. The swelling index is one of the indicators of the devulcanization degree [96, 187, 188]. Generally, the cross-linking density is determined by the swelling and use of the Flory-Rehner equation [189]. Tukachinsky et al. [146] presented an equation (Equation 3) to measure the devulcanization degree:

$$\zeta = 1 - {}^{\upsilon}/_{\upsilon_o} \qquad \text{Equation 3}$$

where υ is the cross-linking density of elastomer, and υ_o is its density of initial cross-linkings.

The study of sol fraction can also be very helpful in verification of degradation during the process, which can also be verified through the use of other techniques, such as Gel Permeation Chromatography (GPC) [71, 84, 98, 127, 128, 130, 136, 142, 144, 145], by Fourier Transform Infrared Spectroscopy (FTIR) [55, 77, 84, 88, 89, 99, 105, 108, 109, 160, 190], Nuclear Magnetic Resonance (NMR) [52, 55, 98, 99, 126, 128, 131, 142-145, 166, 190-192], Spectra Photoelectron excited by X-Rays [94], or even for the determination of free sulphur content [89].

Many authors have analyzed the kinetics of revulcanization of blends containing devulcanized elastomers through rheology studies [71, 75, 96, 108, 116, 125, 127, 136, 138, 146, 193, 194]. Rubber Processing Analyzer (RPA) is a rheometer whose results are based on the principle that the cross-linking density is proportional to the viscosity of rubber [195, 196]. Rubber, after the process of devulcanization, has lower viscosity relative to its initial viscosity and thus flows more easily. The higher fluidity of the rubber facilitates the processing, facilitates its dispersion into other polymers to form a polymer blend, as well as assists its reaction to revulcanization. The study of the rheological properties of a rubber has paramount importance and also helps in verifying

the efficiency of the process of devulcanization adopted. At this point, it is necessary the presentation of important aspects involved in this analysis, which will be addressed not only in this section, but along great part of this work.

The kinetics of vulcanization is studied by using curometers or rheometers measuring the torque development as a reaction to the imposed elongation to rubber as a function of time at a given temperature. Figure 6 shows a typical curve of vulcanization of elastomers. It is divided into 3 regions: induction or reaction delay period (the period prior to the beginning of the reaction itself); cure or vulcanization; and overcure (it is the period after the end of the reaction, and can present 3 distinct behaviors: increase, equilibrium or reversion).

Several important values are derived from the characterization of the rate and the extension of vulcanization of a compound:

- ML or R_{min}: minimum torque at the rheometer. This parameter is usually connected with the Mooney viscosity of the compound;
- MH or R_{max}: the maximum torque reached at rheometer. It represents the final stage of vulcanization and is proportional to the cross-linking density [197];
- ts_1: time for the onset of vulcanization (scorch time);
- t_{90}: time required to achieve 90% of total cure (MH-ML), known as optimum cure time [198-200]. It is the state of cure in which the physical properties have optimal results [201].

In general, in the works involving that technique, the ts_1 and t_{90} values relating to the revulcanization reaction of devulcanized rubbers are smaller in relation to the same values concerning vulcanization reaction of raw rubber, namely, the revulcanization reaction occurs more rapidly; according to Oh and Isayev [71], it is a feature of recovered rubber. This fact is due to the degradation [71, 116, 125, 127, 136], the presence of carbon black on the recycled rubber [75], or even for the existence of accelerators of the vulcanization reaction remnants of the first reaction.

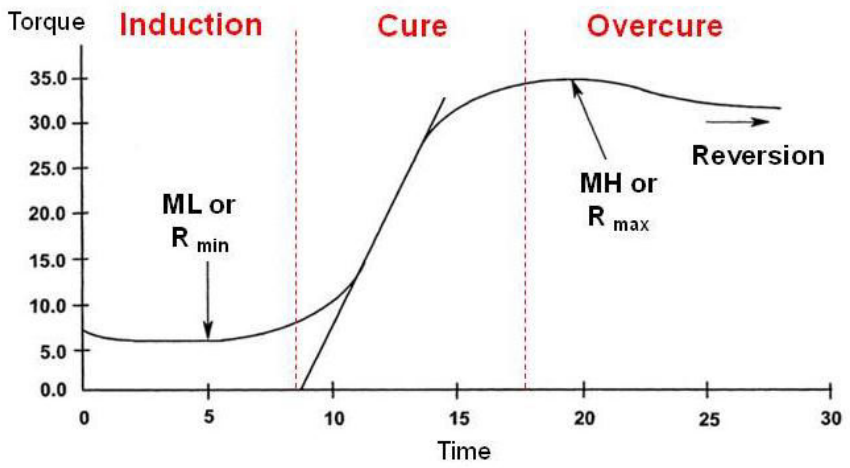

Figure 6: Typical vulcanization or cure curve of elastomers based on [202].

The following sections will address the experimental part related to the Stage 1 of the project.

STAGE 1: Preparation of nanocomposites, devulcanization of GTR by microwaves and study of process efficiency, and characterization of the phases of the blend

2 - MATERIALS AND METHODS

2.1 - Materials

2.1.1 - HDPE

The HDPE used was a commercial product of Braskem with the trade name IA-59, used for injection moulding applications. According to its data sheet [203], the profile of temperature is from 160 to 230°C, and other properties are shown in the Table 1. HDPE offers high stiffness and impact strength, low cost, high chemical resistance, good processability. It is a material largelly used in TPV blends.

Table 1: HDPE type IA-59 description used in the project [203].

Properties	Nominal value	Unit	ASTM method
Physical			
Melt Mass-Flow Rate (MFR) (190°C/2.16 kg)	7.3	g/10 min	D 1238
Specific gravity	0.96	g/cm^3	D 792
Mechanical			
Yield tensile strength	28	MPa	D 638
Tensile strength at break	25	MPa	D 638
Elongation at break	1700	%	D 638
Notched Izod impact	73	J/m	D 256
Thermal			
Vicat softening temperature	129	°C	D 1525
Brittleness temperature	-70	°C	D 746

2.1.2 - GTR

Ground waste truck tire (GTR) separated from non-elastomeric components, was kindly donated by Pirelli Pneus Ltda.

2.1.3 - Montmorillonite

Organically modified Montmorillonite Cloisite 20A® (named in this work just as Cloisite 20A or 20A), kindly donated by Bentonit União Nordeste. This is a modified sodium clay with a quaternary ammonium salt, formed by 2 methyl groups and 2 carbon chains di-hydrogenated (Figure 7). The argilomineral presents CEC of 95 meq/100g, moisture content below 2.0%, loss on ignition of 38%, X-ray diffraction d-Spacing (001) of 31,5 Å.

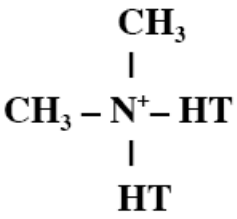

Figure 7: Structure of organic modifier of OMMT Cloisite 20A, where HT represents the carbonic chain (~65% $C_{18}H_{37}$; ~30% $C_{16}H_{33}$; ~5% $C_{14}H_{29}$). The anion used is chlorine.

2.1.4 - Halloysite

Halloysite nanotubes of specification #685445 produced by Sigma-Aldrich (kindly donated by the research group of Prof. Rosario Bretas from Universidade Federal de São Carlos - UFSCar, Brazil). This material presents a cylindrical shape, surface area of 64.6 m^2/g, internal diameter of 15 nm and external between 30-70 nm, length between 1-3 μm, CEC of 800 meq/100g, linear formula $Al_2Si_2O_5(OH)_4 \cdot 2H_2O$, molar mass 294.19 g/mol and pH between 6.5-6.9.

2.1.5 - Compatibilizing agent

It was used maleic anhydride grafted HDPE (HDPE-MA) Polybond® 3029 (kindly donated by Chemtura) to increase compatibility between Halloysite clay and HDPE. The specification of compatibilizing agent is shown in the Table 2.

2.1.6 - Vulcanization additives

It were used rubber accelerator TBBS (N-tert-Butyl-2-benzothiazole sulfenamide) and sulphur, both kindly donated by Pirelli Pneus Ltda. The TBBS is accelerant agent and sulphur the vulcanization agent.

Table 2: Specification of the compatibilizing agent Polybond® 3029 used in the project [204].

Properties	Nominal value	Unit	ASTM method
Maleic anhydride conten	1.5-1.7	%	D 6047
Physical			
Melt flow rate (190°C/2.16 kg)	4	g/10 min	D 1238
Density (23°C)	0.95	g/cm^3	D 792
Thermal			
Melting point	130	°C	

2.2 - Methods

The analyses carried out during Stage 1 of the project followed the flowchart shown in Figure 8.

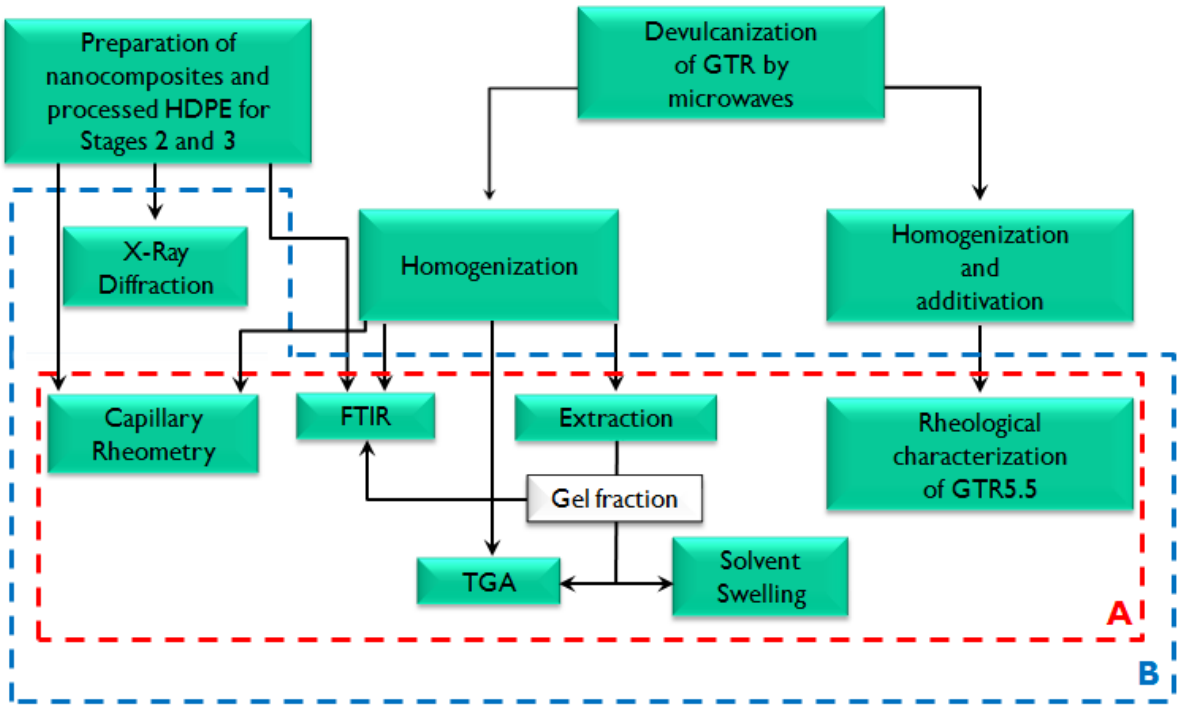

Figure 8: Flowchart of activities performed during Stage 1. A: Study of efficiency of devulcanization process by microwaves; B: Characterization of the phases of the blends.

2.2.1 - Granulometric analysis

Granulometric analysis of the GTR0 was performed according to ASTM D5644-01, by using an electromagnetic sieve shaker Contenco. It was used 100 g of rubber, 19.8 g of talcum powder, sieves of 50, 60, 70, 80, 100 and 400 Mesh, and two rubber balls for each sieve.

2.2.2 - Devulcanization the GTR by microwaves

Purposing the increase of the GTR fluidity, in order to achieve a good level of refinement of the final morphology of blends to be produced in the following stages, GTR was previously devulcanized by the action of the microwaves.

GTR was devulcanized in a system comprised of a conventional microwave oven (Brastemp, model BMS35BBHNA) adapted with a motorized stirring system (IKA, model RW 20) with a speed control, as shown in Figure 9.

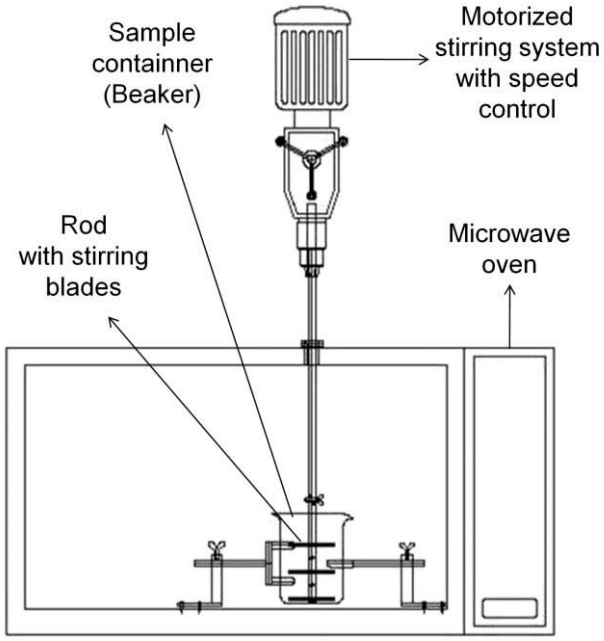

Figure 9: Scheme of the devulcanization system used in this work.

Figure 10 presents the photo of the devulcanization system, with the detail of the stirring rod used to homogenize the material during devulcanization of rubber and avoid degradation by hot spots (points of concentration of energy caused by resonance phenomena inside the cavity). The stirring system consists of a main stem with 13 mm of diameter, 217 mm length (the upper wall of the interior of the oven until the end of the rod that is in contact with the sample) and 5 paddles with length of 50 mm and 3 mm of diameter, perpendicular to the main stem. The paddles are adjustable in direction of the diameter of the agitator, which provides set capable of sweeping all over the wall of the container (beaker) used for placing the sample, thus preventing its overheating, which can cause degradation of the material and bring the risk of fire.

The whole devulcanization process was done by using the maximum power of the oven, i.e., 820W. About 65 g of the GTR sample was put into a 250 mL glass beaker with a stirring speed of 100 rpm. To avoid possible unwanted movement of the beaker along

with movement of the stem, it was designed a system of clutches, which is also adjustable and able to promote good attachment to the beaker during the process, even at high temperatures. All parts of the system contained within the oven were made of stainless steel.

Figure 10: Devulcanization system used, with detail of the stirring rod responsible for rubber mixing during treatment, which prevents its degradation by the action of hot spots (points of high concentration of microwaves due to resonance effects in the cavity of the oven). It can be also observed the clutches system designed to promote good attachment to the container during the process.

The time at which the material was exposed to microwaves ranged from 1 to 5, and 5.5 minutes (GTRX, where X is the exposure time of GTR to microwaves). The temperature after devulcanization was measured by using a rod thermometer.

During devulcanization of GTR5.5 (5.5 minutes of exposure to microwaves), it has been found in some samples the presence of clusters of coal, as a result of thermal degradation of the material. Or even, when the sample was taken out of the oven and held in the beaker, part of the material also degraded due to high temperatures of the material inside. So, in order to prevent the degradation of samples, they were kept under mechanical agitation for about one minute after the end of treatment, and then were scattered in a metallic form, as shown in Figure 11.

Figure 11: Photo of the GTR5.5 spread in a metallic form to avoid thermal degradation.

2.2.3 - Homogenization of devulcanized GTRs and mixing with additives

After the devulcanization process, all the samples were homogenized and mixed with additives in a laboratory two roll mill (Prenmar). The samples to be later used in the analysis of extraction, thermogravimetric analysis (TGA), FTIR and capillary rheometry were just homogenized, while those to be used in the characterization of revulcanization were homogenized and mixed with vulcanization additives.

The additivated samples, shortly after their homogenization, were added 1 phr of TBBS and 1 phr of sulphur, respectively. The total time of homogenization and mixing with additives was about 6 minutes [120].

2.2.4 - Study of revulcanization behavior of GTR5.5

Rheological measurement was performed in the GTR5.5 in order to study its revulcanization characteristics, by using a RPA Tech Pro, model Rheo Tech MDPT, according to ASTM D 1646-07. The curve of torque *versus* time was obtained at 180°C (1° and frequency of 1 Hz), and approximately 5 g of material was required for the test. The nomenclature adopted is type GTR5.5+ad, where '+ad' represents the presence of vulcanization additives in the sample.

2.2.5 - Extraction

The soluble (sol) and insoluble (gel) fractions of each GTRX sample, after the devulcanization process, were determined by extraction, according to ASTM 2765-11, by using toluene as a solvent. About 1 g of GTRX was placed in a cage (pouch) made of

stainless steel blanket (Figure 12a). They were completely immersed in boiling toluene for 24 h (Figure 12b), and about 1 g of Irganox 1010 of Dow Corning was added in to avoid degradation. After the extraction, the gel fraction (GTRXg) sample was dried for 24 h at 40°C to remove the solvent and its mass was measured. The percentages of the sol and gel fractions were calculated according to equations 4 and 5, respectively:

$$Extract\ (\%) = \frac{(Weight\ lost\ during\ extraction)}{(Weight\ of\ original\ specimen)} = \frac{(W_3 - W_4)}{(W_2 - W_1)} \qquad \text{Equation 4}$$

where:

W_1 = weight of the pouch (sealed on three sides, one side open),

W_2 = weight of the specimen and the pouch (sealed on three sides, one side open),

W_3 = weight of the specimen and the cage, after being stapled shut,

W_4 = weight of the specimen and the cage after extraction and drying.

$$Gel\ content = 100 - Percent\ extract \qquad \text{Equation 5}$$

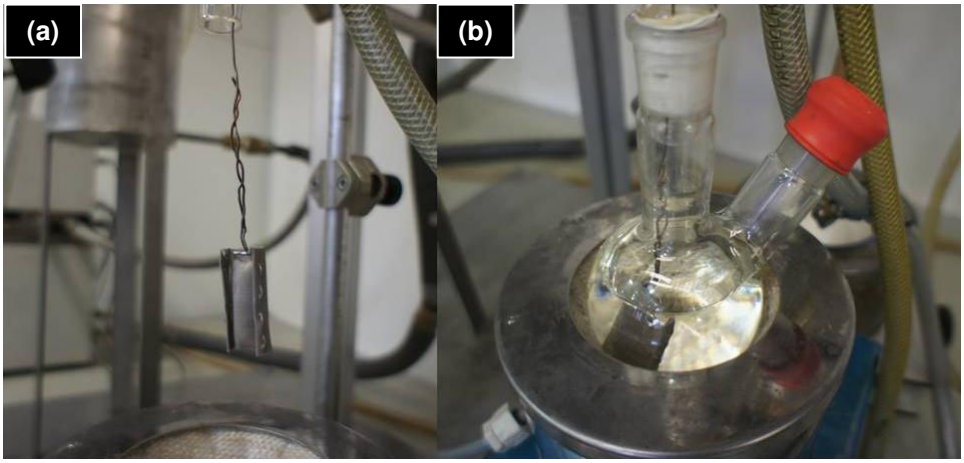

Figure 12: (a) Photo of the cage made of stainless steel containing GTR and (b) photo of the cage completely immersed in boiling toluene.

2.2.6- Swelling by solvent

After the extraction, the gel fractions (GTRXg samples) were pressed in a hydraulic press at 170°C using a circular mold (Ø25x1 mm) for 5 min. The pressed samples were immersed into 100 mL of toluene at controlled temperature (25°C) for 72 h, according to ASTM D6814-2. The excess of solvent on the surface of the samples was removed by using an absorbent paper. The mass of the swollen sample was measured, and the cross-linking density was calculated by using the Flory-Rehner equation [189]

(Equation 6):

$$\nu_e = \frac{-[\ln(1-V_r)+V_r+\chi_1 V_r^2]}{[V_1\left(V_r^{1/3}-V_r\right)/2]} \qquad \text{Equation 6}$$

where: υ_e is the cross-linking density (mol/cm^3), V_r is the volume fraction of rubber in the swollen sample, V_1 is the solvent molar volume (106.2 cm^3/mol [205]), and χ is the polymer-solvent interaction parameter (0.391 [206]).

2.2.7 - TGA

A thermogravimetric analyzer STA 449 F3 Jupiter device was used to carry out TGA. It was conducted to provide information about the thermo-oxidative degradation of the samples after the devulcanization. The analysis was performed on the extracted samples (GTRXg) and samples before the extraction (GTRX). About 10 mg of each sample was heated from room temperature (25°C) to 550°C under nitrogen atmosphere to monitor the weight loss of oil and elastomers. At 550°C, the gas flow was changed by oxygen atmosphere and the samples were heated to 800°C in order to observe the carbon black degradation. Both ramps were heated at a rate of 10°C/min.

2.2.8 - Production of nanocomposites HDPE/clay by extrusion

About 6 kg of HDPE, initially in the form of granules, were pulverized in a cryogenic mill Micron Powder Systems, model Mikro-Bantam. After the HDPE have been dried in an oven at 60°C for 24 hours, it was mixed with Cloisite 20A clay (production of nanocomposite HDPE/Cloisite 20A), and Halloysite clay and compatibilizing agent (production of nanocomposite HDPE/Halloysite) in an extruder to form masterbatches, being dried in a vacuum oven at 60°C for 8 hours to ensure the elimination of moisture.
The nanocomposites were prepared in a co-rotating twin screw extruder Werner & Pfleider, model ZSK 30. The screw profile used in the process is showed in Figure 13. The screw profile was used in research conducted by the group of Prof. Rosario Bretas (UFSCar, Brazil), being that the resulting nanocomposites by using such processing parameters obtained satisfactory results. The heating system of the equipment is divided into six zones, and during processing were used the following temperatures: zone 1: 160°C, zone 2: 170°C, zone 3: 180°C, zone 4: 190°C, zone 5: 200°C, and zone 6: 210°C.

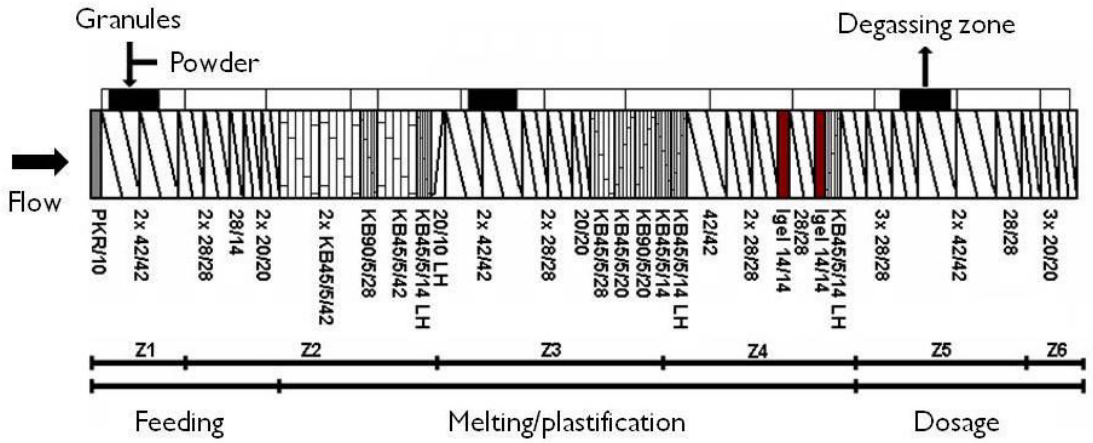

Figure 13: Screw profile used, where: 42/42, 28/28, 20/20 are right-handed screw elements; 20/10 LH is a left-handed screw element; KB 45/5/14, KB 45/5/28, KB 45/5/42, KB 90/5/20, KB 90/5/28 are right-handed kneading disc blocks; KB 45/5/14 LH is a left-handed kneading disc block; Igel 14/14 is a mixing element type "turbine“.

The nanocomposites were prepared by direct method, in which all components are fed at the same time in the feeder (masterbatch and neat HDPE). The final concentrations of clay and compatibilizing agent (when used Halloysite clay) in the matriz were 5 wt%. The flow rate used was 3 kg/h; were produced 15 kg of HDPE/Cloisite 20A and HDPE/Halloysite nanocomposites, and were also processed 15 kg of neat HDPE (processed HDPE). Nanocomposites and processed HDPE were used in stages 2 and 3 of the project.

2.2.9 - FTIR

ATR-FTIR analysis was performed on gel fraction samples (GTRXg), as well as on the samples before extraction (GTRX), in order to obtain information about chemical modifications of the GTR as a result of the devulcanization process. The spectra were recorded on a Thermo Nicolet Avatar 370 FT-IR with ATR accessory, from 4000 to 500 cm^{-1} at a resolution of 4 cm^{-1} over 20 scans at room temperature.

2.2.10 - Capillary rheometry

The melt-viscosity of the devulcanized materials, as well as the phases of blends to be produced in the next stages of the project, was measured by using a high pressure capillary rheometer Ceast SR20 (Instron) with a capillary die of 1 mm and a L/D ratio of 20. Measurements were performed at 180°C over a shear rate range between 100 and 5000 s^{-1}. The data were corrected according to Rabinowitsch corrections for non-

Newtonian behavior. However, the Bagley correction was neglected due to the high L/D ratio.

2.2.11 - X-ray diffraction of HDPE/clay nanocomposites

The study of the clays dispersion on HDPE matrix was performed by analysis of X-ray scattering in a Rigaku diffractometer Mini Flex II operated at 30 kV and 15 mA at a scan rate of 1°/min, in an interval of 2θ from 2 to 10°. Cloisite 20A and Halloysite clays were analyzed, as well as the processed HDPE and nanocomposites prepared in the section 2.2.8.

All the samples were first immersed in liquid nitrogen and ground in a mill Ika A11 Basic. The samples were dried in a vacuum oven at 100°C for 1 hour.

In the next section, the results of the analyses performed during Stage 1 of the project will be presented and discussed.

3 - RESULTS AND DISCUSSION

3.1 - Granulometric analysis

Figure 14 shows the results of granulometric analysis of GTR used in the project (GTR0 as received).

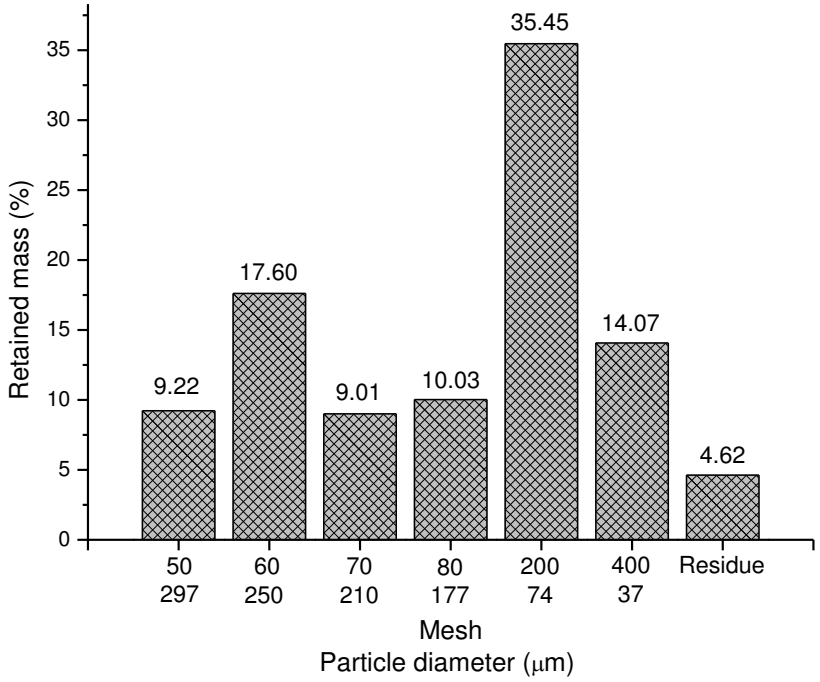

Figure 14: Granulometric analysis of GTR0, with mesh distribution and the diameter of the retained particles.

The result shows that, approximately, 35% of the GTR0 was retained on 200 mesh sieve, which demonstrates that the GTR used consists mostly of 74 μm sized particles. However, the particle size distribution ranged between 297 and 37 μm.

3.2 - Temperature measurements after devulcanization by microwaves

Table 3 shows the temperatures of the GTR samples just after their exposure to the microwaves. The temperature measurements were done immediately after the end of the treatment, by using a rod thermometer. The average temperature was calculated from the temperatures of 20 samples exposed to the same conditions of treatment.

The results show that the temperature increases with increasing the exposure time of the sample to microwaves, as also observed by other authors [7, 58, 105, 107-109]. GTR is mainly composed of NR and SBR, which are known as low microwaves absorbers. On the other hand, GTR contains high concentration of carbon black, a typical conductive

filler [145, 181], which induces a phenomenon known as Maxwell-Wagner polarization [104, 207, 208].

Table 3: Temperatures of the GTR samples immediately after their exposure to microwaves.

Sample	Temperature (°C)
GTR1	72.6 (± 2.4)
GTR2	114.7 (± 5.7)
GTR3	145.8 (± 10.2)
GTR4	160.3 (± 9.9)
GTR5	200.4 (± 32.2)
GTR5.5	219.5 (± 26.8)

De Sousa and Scuracchio [208] studied the influence of the carbon black concentration on the NR devulcanization by microwaves. It was concluded that the factor that dictated the degree of devulcanization was the final temperature reached by the sample, which was dependent on the exposure time of the sample to microwaves and the amount of carbon black it contained. Another important observation was that the carbon black content allowed the improvement of the devulcanization process by microwaves, which was as high as 45 phr. Hirayama and Saron [105] conducted a similar study by using SBR. They also observed that the heating of the material during the exposure to microwaves was caused by the presence of carbon black, and that the final temperature achieved by the sample was influenced by the carbon black present on it. Garcia et al. [209] studied the change in morphology of GTR as a result of devulcanization by microwaves. They observed that the amount of carbon black in each of the phases of the material, i.e., NR and SBR, changed with the exposure time to microwaves. In samples exposed for 5 minutes, the carbon black was preferably located in the NR phase, while for a longer exposure time, it was preferably located in the SBR one.

According to Dubkov et al. [210], around 30% of a tire is composed of carbon black, which corresponds to around 40 phr of carbon black in the tire. Since carbon black is preferably in the NR phase, its content would be enough to devulcanize the sample, considering the fact that the minimum carbon black for improving the devulcanization process is 45 phr, as mentioned above. Another important observation is that if carbon black is preferably located in the NR phase, the probability for this phase to be overheated would be high. This observation is validated by TGA results, which will be presented later.

In summary, no matter if one phase in the material is preferably devulcanized, the

longer the time of treatment, the greater the amount of energy absorbed by the elastomer due to carbon black. Since the microwave devulcanization takes advantage of the volumetric heating [177], the higher the amount of energy absorbed along the treatment due to the presence of carbon black, the higher the transformation of this energy into heat, and the higher also the degree of devulcanization (to be seen ahead), since the determining factor for the degree of devulcanization is the final temperature reached by the sample [208].

3.3 - Gel content and cross-linking density

Table 4 shows the results of the gel content and cross-linking density of microwave treated GTR.

The higher is the sol fraction, the more efficient is the devulcanization process [58, 211]. According to Table 4, the values of the gel fraction and cross-linking density of the samples decrease as the exposure time of the GTR to microwaves increases, confirming that the GTR was devulcanized by the action of microwaves [208]. The value of the gel fraction of GTR1 was slightly larger than that of GTR0, due to experimental errors or possibly as a real increase in the degree of vulcanization, as also observed by Hirayama and Saron [105].

Table 4: Gel contents and cross-linking densities of the GTR samples devulcanized by microwaves.

Sample	Gel content (%)	Cross-linking density (υ_e x 10^{-5} mol.cm^{-3})
GTR0	87.8	12.44
GTR1	88.0	NA
GTR2	87.9	12.65
GTR3	87.7	6.07
GTR4	86.3	5.52
GTR5	81.8	7.07
GTR5.5	73.8	6.07

NA: The cross-linking density of GRT1 was unavailable because it broke during the swelling in toluene.

According to some authors [105, 109], the degree of devulcanization (Equation 7) can be calculated by the difference in gel content between the devulcanized rubber (DR) and the vulcanized one (VR).

$$Degree\ of\ devulcanization = -(DR - VR) \qquad \text{Equation 7}$$

Figure 15 shows the degree of devulcanization of the GTR as a function of the exposure time of the sample to the microwaves. The overall trend is that the degree of devulcanization became significant only when the time of exposure to the microwaves exceeded 3 min. It became significantly more important as the time of exposure to the microwaves further increased. GTR1 and GTR2 showed negative values for the degree of devulcanization, namely, the degree of formation of new bonds seems to be higher than the degree of breaking of cross-linkings during the time of exposure to microwaves. However, as discussed earlier, those values could also be within experimental errors.

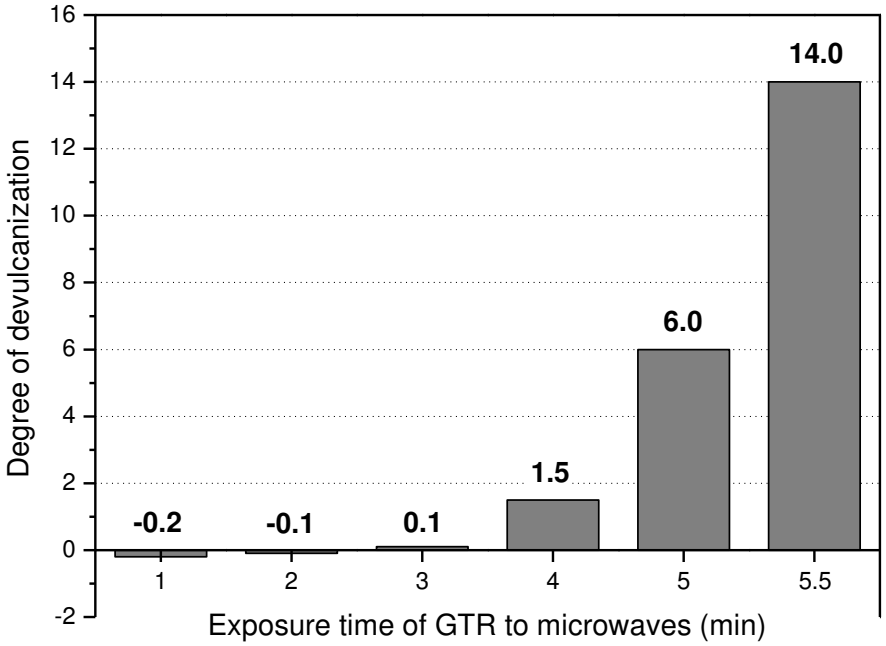

Figure 15: Degree of devulcanization of the GTR as a function of its time of exposure to the microwaves.

Figure 16 shows the gel content, cross-linking density and average temperature of the GTR as function of the time of exposure to microwaves. The overall trend is that the longer the exposure time of the sample to the microwaves, the higher is the final average temperature and the lower is the gel fraction, confirming the occurrence of devulcanization. In other words, the longer the time of the microwave treatment, the higher the degree of devulcanization (as observed from Figure 15), due to the greater amount of energy absorbed by the GTR. As mentioned above, the final temperature reached by the sample is the primary factor responsible for the degree of devulcanization which depended, in this case, on the time of exposure of the sample to microwaves [208].

On the other hand, the cross-linking density reached a plateau after 3 minutes of microwaves treatment. As observed in Figure 15, in the samples which were exposed to the microwaves for a short time, the values of the degree of devulcanization were negative, showing that the number of new bonds formed likely exceeded that of bonds which were broken. Also the FTIR spectra (to be shown later) indicate that the exposure of GTR to microwaves changed its chemical structure. Some cross-linkings were broken down and new ones were formed at the same time.

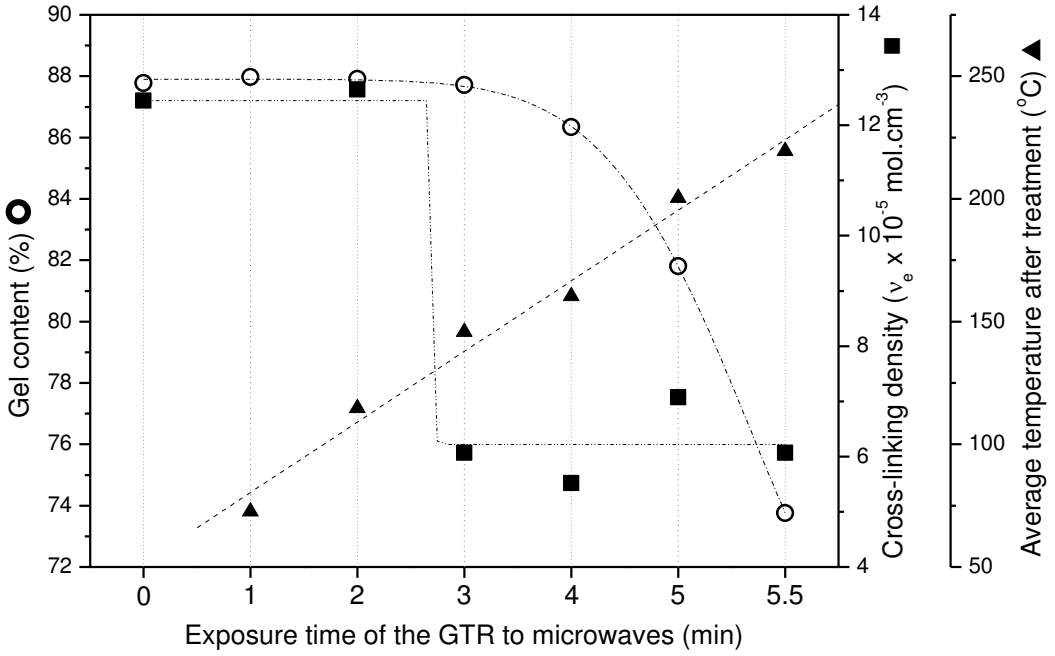

Figure 16: Gel content, cross-linking density and average temperature after microwave treatment *versus* exposure time of the GTR to microwaves.

Figure 17 shows the gel content and cross-linking density of the GTRX as a function of its average temperature. There is an obvious correlation between them, suggesting that the temperature rise is responsible for the devulcanization [208], and that it is likely that there is no additional mechanisms of interaction between the microwaves and the GTR.

From the results presented in this section, it was verified that the "best" exposure time examined was the one of 5.5 minutes, due to the greater degree of devulcanization without encountering widespread degradation of the material. The result was also corroborated by the results of capillary rheometry, to be presented in section 3.7. So, the GTR5.5 was chosen to be used in the production of dynamically revulcanized blends in twin screw extruder. The results of the analysed blends containing GTR5.5 will be presented in the Stages 2 and 3 of this work.

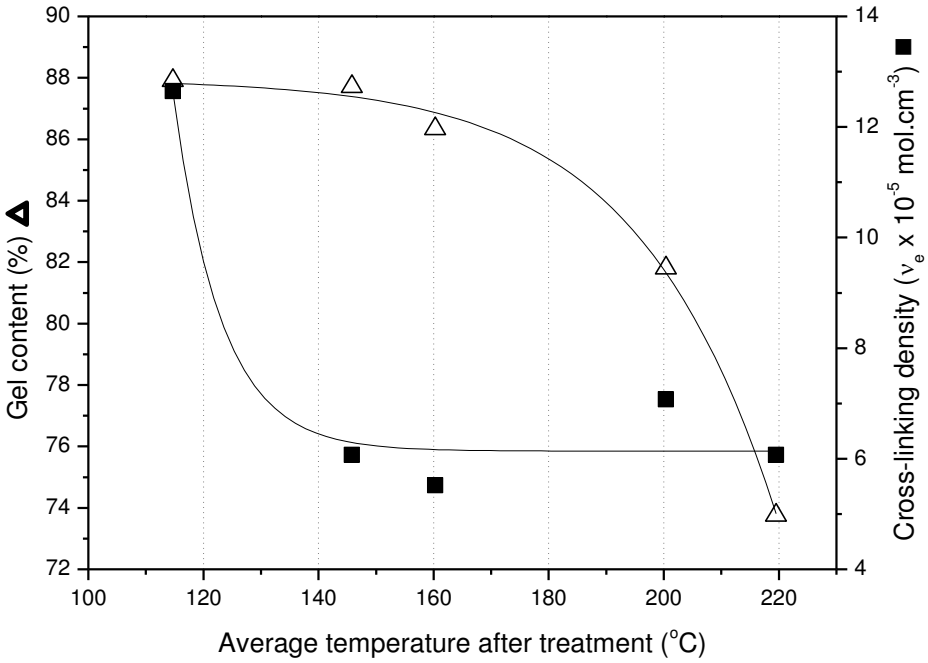

Figure 17: Gel content and cross-linking density of the GTRX as a function of its average temperature.

3.4 - ATR-FTIR

3.4.1 - ATR-FTIR of the devulcanized GTR

Figure 18 shows the FTIR spectra of the devulcanized samples before solvent extraction (GTRX) and of their gel fractions (GTRXg) obtained under different times of exposure to microwaves.

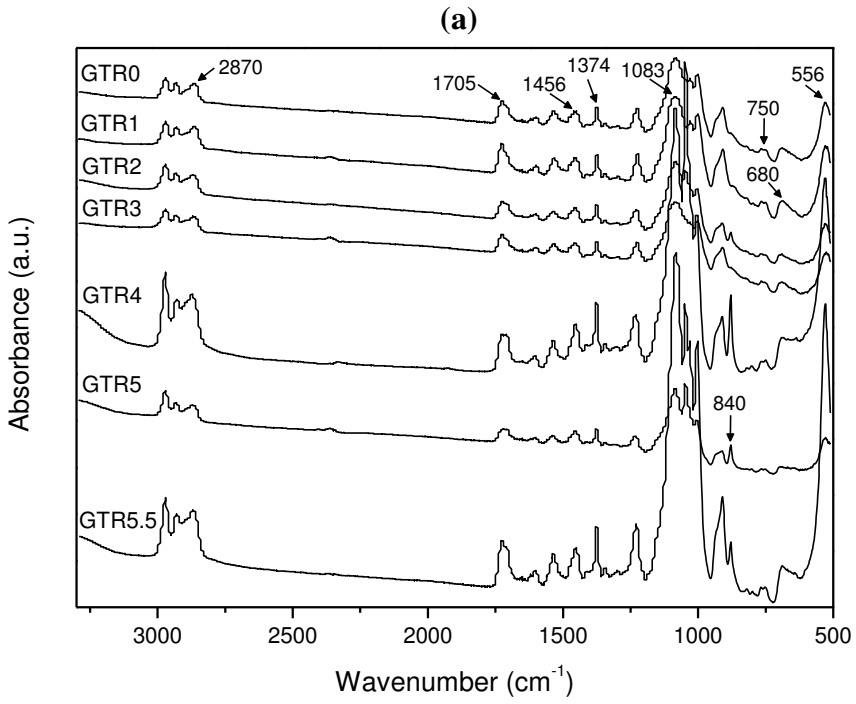

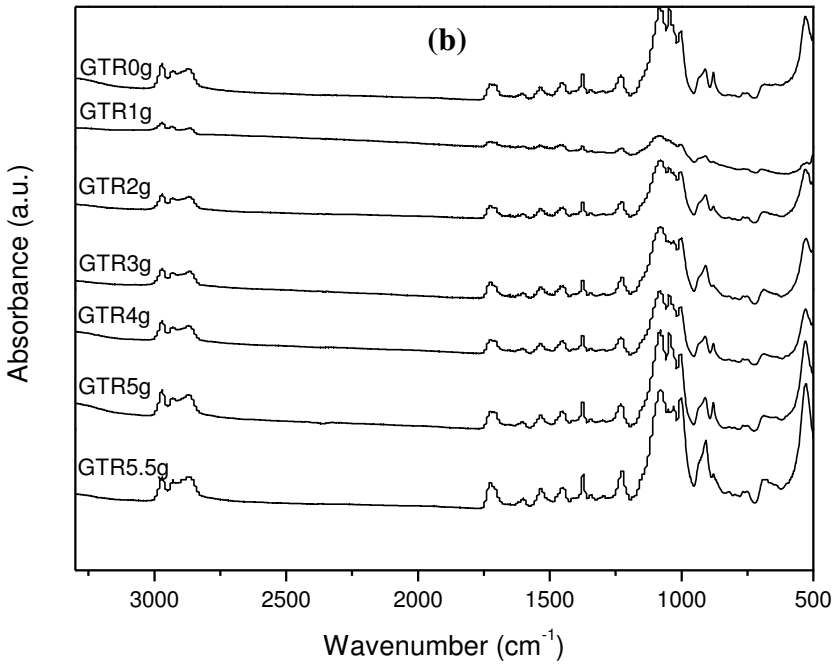

Figure 18: FTIR spectra of (a) the devulcanized samples before solvent extraction (GTRX) and (b) their gel fractions (GTRXg).

The CH_2 bands (1475-1450 cm^{-1}) [80, 108, 160, 211, 212] refer to the vibrations of stretching and aromatic bending of the SBR, and the CH_3 bands (1390-1372 cm^{-1}) [89, 108, 211] are groups of the NR [213]. Those bands were observed in all the FTIR spectra, indicating that the GTR did not undergo significant degradation when exposed to the microwaves [108]. In other words, whatever the time of exposure of the GTR to microwaves, it did not degrade completely by the action of the microwaves.

A peak around 680 cm^{-1} refers to the presence of C-CH_3 group, which is characteristic of the elongational vibration of the styrene ring [211], which also confirms the presence of SBR in the composition of the GTR. A peak around 1705 cm^{-1} is related to the lactone ring (C=O), confirming the presence of carbon black in the GTR [214]. It is important to mention that this peak is present in all samples, both in the devulcanized GTR and their gel fractions. This means that the carbon black present in the samples remains in the gel fractions after the extraction of the sol fraction by toluene. This result is in agreement with that of Dubkov et al. [210], who analyzed the sol and gel fractions of the GTR after devulcanization by nitrous oxide. According to them, the gel fraction contained that carbon black which was present in the initial GTR.

In GTR2, GTR5 and GTR5.5, there was a new peak around 840 cm^{-1} which, according to Rooj et al. [89], refers to C=C links of the NR of the GTR. The formation of this new peak would have a positive effect, since they are active sites for the revulcanization of the devulcanized GTR during subsequent processing [105]. However, this peak cannot

be clearly observed in the gel fractions of the devulcanized samples (Figure 18b), indicating degradation of the main chains of the NR of the GTR. According to Dubkov et al. [210], who performed Nuclear Magnetic Resonance (NMR) analysis on the sol fraction of the GTR, the signal of the internal twin bonds (>C=CH–) in 1,4-units of polyisoprene indicates that the sol fraction contained isoprene oligomers.

In order to perform a quantitative analysis on the sulphur links, the peaks related to S-S, C-S and S-O bonds (556, 750 and 1083 cm^{-1} respectively) were normalized by dividing their heights by that of the absorbance peak at 2870 cm^{-1}, which corresponds to the C-H bonds of the main chains of the NR of the GTR (Figure 19). From Figure 19, as the time of exposure to microwaves increased, the intensity ratio of the S-S (556 cm^{-1}) [89, 215] bond (especially for gel fraction samples) and that of the S-O (1083 cm^{-1}) bond [105] (especially for GTR5.5) slight increased, and that of the C-S bond (750 cm^{-1}) [105, 215] slightly decreased.

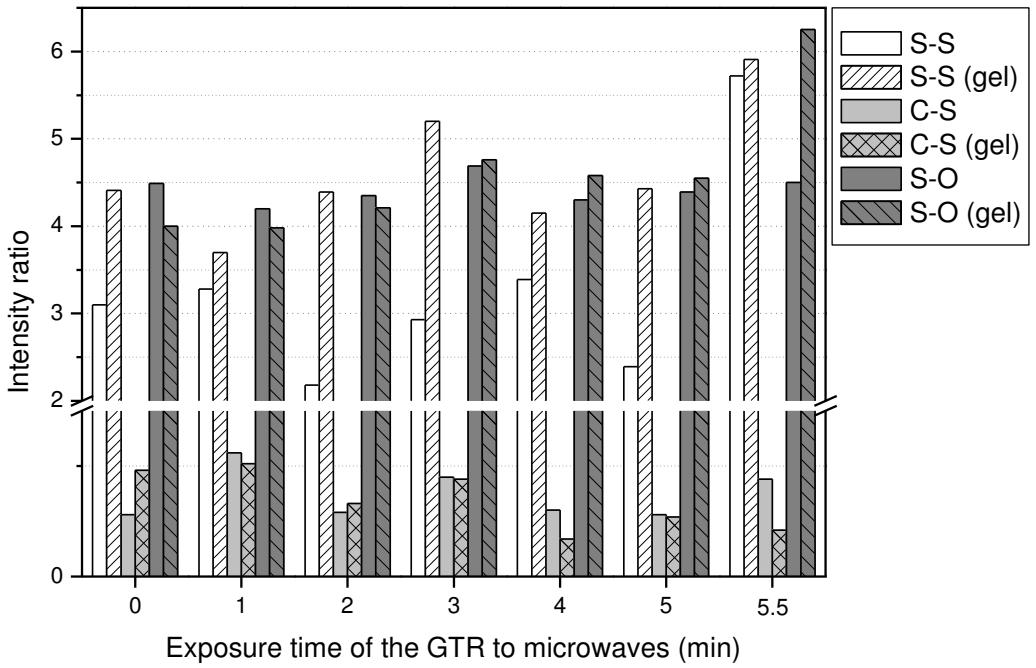

Figure 19: Intensity ratio of chemical bonds as a function of exposure time of the GTR to microwaves.

Similar to the degree of devulcanization (Equation 7), the degree of bonding, which is the difference in the intensity ratio of a bond between a devulcanized GTR and the initial one (Equation 8), can be used to quantify the degree of chemical modifications of the GTR after the exposure to the microwaves.

$$Degree\ of\ bonding = IR_{Sample} - IR_{GTR0} \qquad \text{Equation 8}$$

where IR_{Sample} and IR_{GTR0} are the intensity ratios of a devulcanized GTR (GTRX) and GTR0, respectively. In the case of the gel fractions (GTRXg), IR_{GTR0g} was used instead of IR_{GTR0}.

As some authors concluded [105, 216], heating as a result of the exposure to the microwaves may induce the breaking of sulphur bonds and the formation of new ones. The resulting degree of devulcanization is related to the balance between them. The swelling results showed that, the longer the exposure time of the GTR to the microwaves, the less its cross-linking density. However, this is an overall result and does not imply that all different kinds of cross-linkings in the GTR were broken. This is clearly shown in Figure 20. The degree of bonding depends on the exposure time of the sample to the microwaves and the energy necessary to break each kind of sulphur bond.

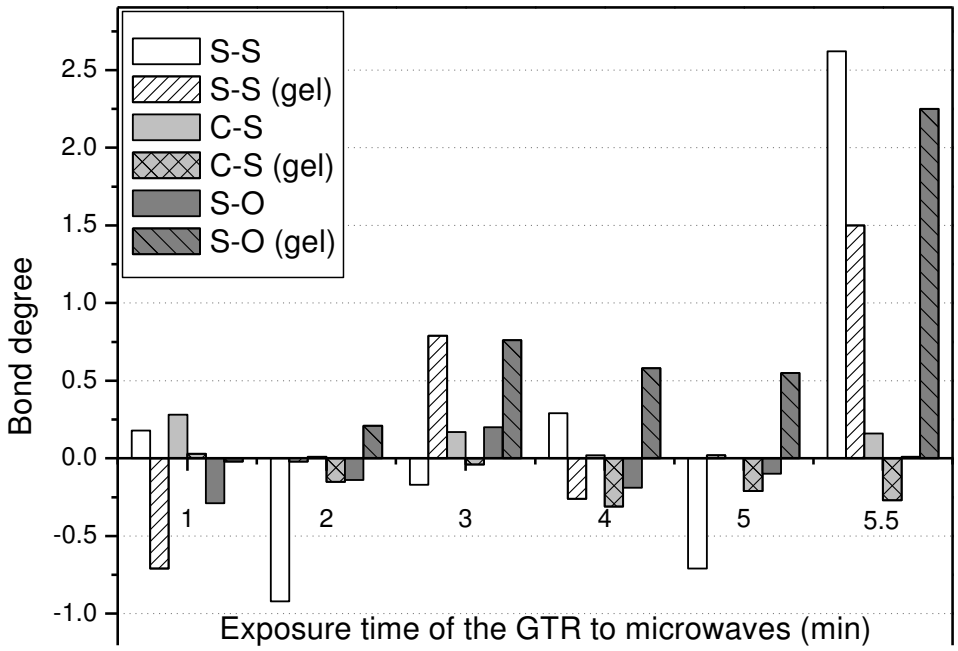

Figure 20: Degree of bonding from intensity ratio values of the devulcanized samples.

The analysis of the gel fraction allows better understanding of chemical modifications of the GTR as a result of the exposure to the microwaves. In general, the formation of S-S bonds outperformed their breaking in samples which were less exposed to microwaves, whereas the breaking of C-S bonds outperformed their formation in those which were exposed to microwaves for longer times. In the latter cases, S-S and S-O bonds were formed. The formation of the new S-S bonds in the samples with longer exposure times to microwaves would likely result from the breaking of the C-S bonds. Another possibility would be the reaction of an excess of unconsumed sulphur in the first vulcanization process (free sulphur), which would tend to form polysulphidic links.

On the other hand, the formation of the S-O new bonds would result from rearrangement of the sulphur free radicals from the devulcanization of the GTR in the presence of oxygen. Those results confirm that the GTR was indeed subjected to devulcanization upon exposure to microwaves, and that, different types of sulphur bonds could be broken and formed as a result of the microwave radiation, depending on the exposure time and consequently the final temperature of the sample. In the case of the IIR devulcanization by microwaves, disulphidic bonds were broken, releasing sulphurs which were transformed into new mono and polysulphidic bonds [216].

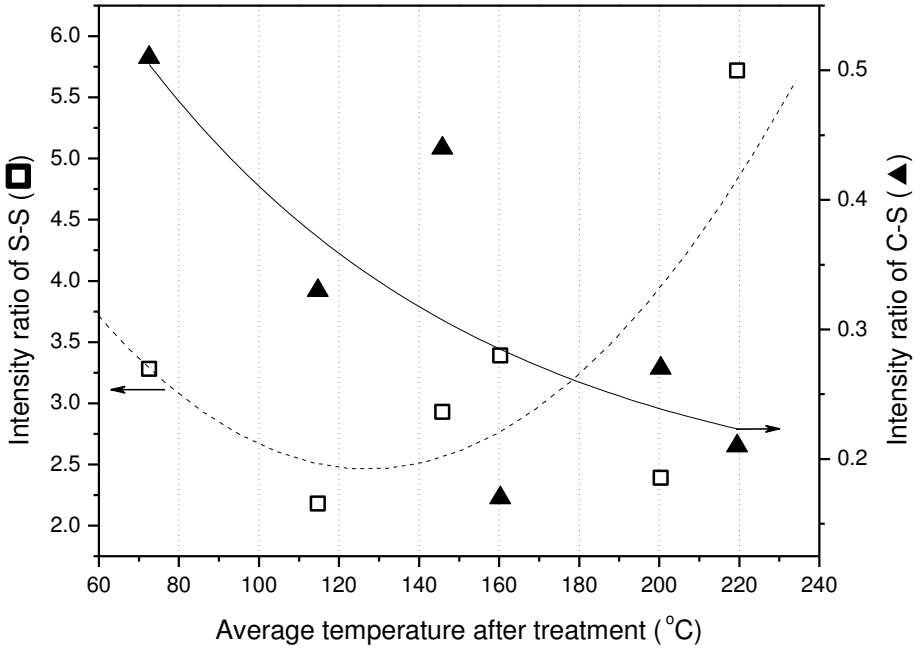

Figure 21: Intensity ratios of the S-S and C-S bonds as a function of the average temperature after the microwave treatment for all devulcanized samples.

As discussed above, the degree of bonding depends on the temperature of the sample after the microwave treatment. Figure 21 shows the intensity ratios of S-S and C-S bonds as a function of the average temperature of the sample after the microwave treatment. Despite the scattering of the data, there seems to be an overall trend that the intensity ratio of the S-S bonds increases (from approximately 120ºC) with increasing average temperature, while that of the C-S bonds decreases. This seems to show that as the average temperature increased, more C-S bonds broke while new S-S bonds were formed. Also, regarding the S-S bonds, the smallest value of intensity ratio is observed at temperatures around 120-140°C, i.e., it seems to be the smallest number of links, showing that their breakdown is effective when the sample reaches such a temperature. According to the literature [72, 89, 185], the energy necessary for breaking C-S, S-S

and S_X bonds is 285, 268 and 251 kJ/mol, respectively, while it is 346 kJ/mol for C-C bonds. Therefore, the breaking of the C-S bonds is more sensitive to temperature than that of the S-S bonds.

3.4.2 - ATR-FTIR of HDPE and nanocomposites HDPE/clays

The ATR-FTIR spectra of processed HDPE and nanocomposites (HDPE+20A and HDPE+Hal) are presented in Figure 22.

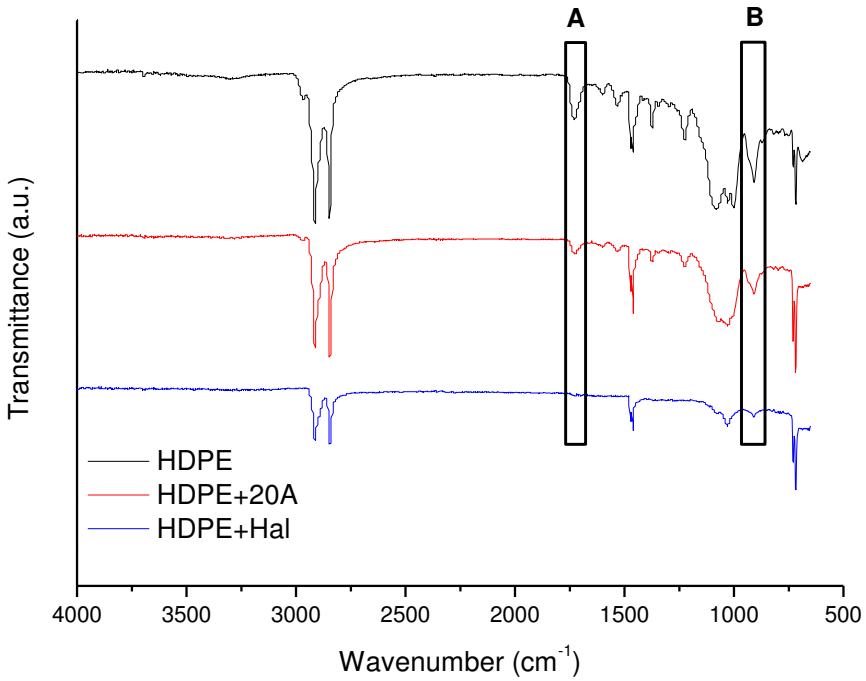

Figure 22: ATR-FTIR spectra of HDPE, HDPE+20A and HDPE+Hal.

The spectra exhibit two characteristics bands of HDPE, between 2950-2600 cm^{-1} representing the $-CH_2$ group, where its bending vibration exists within the range 1450-1380 cm^{-1} [211].

With the formation of HDPE/clay nanocomposites, it is clearly the disappearance or reduction in the intensity of some bands. However, in order to study the degradation of HDPE, just the characteristic bands will be reviewed. According to Hinsken et al. [217], the main HDPE degradation mechanisms are the chain cision, and chain branching followed by cross-linking. The regions A and B in the spectra (Figure 22) represent the characteristic bands of carbonyl groups (1720 cm^{-1}) [218] and vinyl groups (990 and 910 cm^{-1}) [217, 218], respectively. The peaks of these regions were normalized (to eliminate the thickness effect of the films) by dividing their respective heights by 2910 cm^{-1}, which corresponds to the height of the transmittance peak of $-CH_2$ groups (Figure

23). From carbonyl index of HDPE+Hal is already discounted the amount of the same group from maleic anhydride compatibilizing agent in the compound.

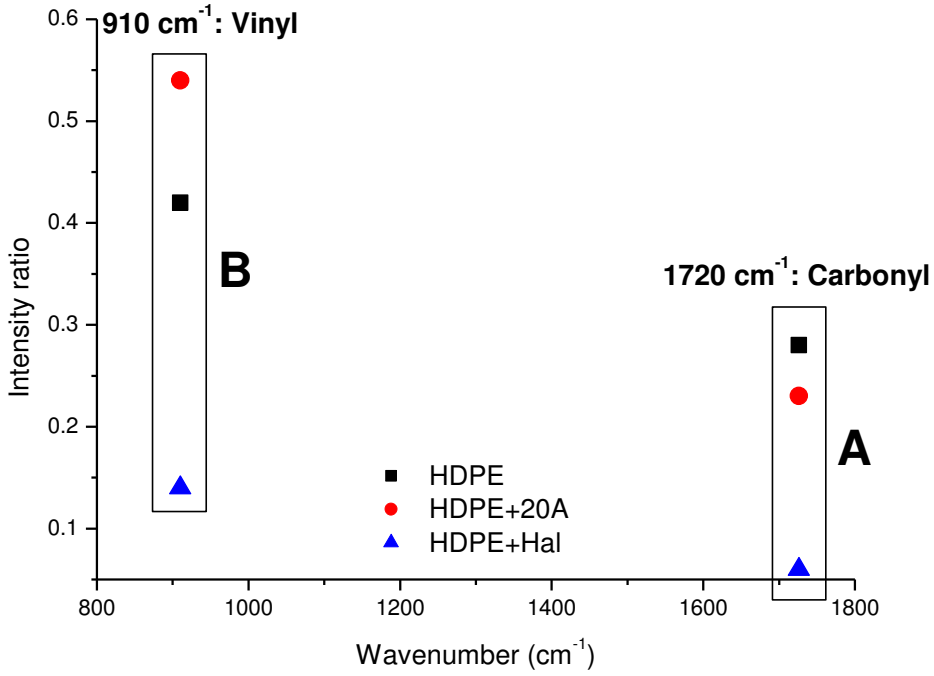

Figure 23: Intensity ratios of the groups carbonyl and vinyl of HDPE, HDPE+20A and HDPE+Hal referring to bands A and B shown in Figure 22.

According to Hinsken et al. [217], alkyl radicals may react with vinyl groups (Figure 24), and this will result in the addition reaction and subsequent cross-linking of macromolecules.

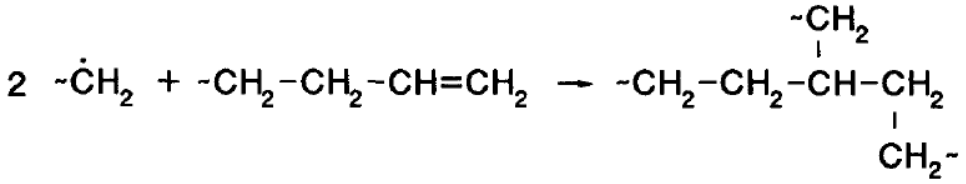

Figure 24: Degradation reaction of HDPE chains, resulting in branching and subsequent cross-linking [217].

According to Figure 23, the addition of Halloysite clay reduced the vinyl intensity ratio, which is due to the degradation of HDPE chains by the addition of this clay. This type of degradation increases the molar mass of the HDPE, as verified by Hinsken et al. and Pinheiro et al. [217, 218].

The region A in spectra refers to the carbonyl groups (1720 cm^{-1}) [218]. Silvano et al. [219] depicted that the increase in the intensity of this peak represents the degradation of the polymer chains due to oxidation. In that work, the presence of MMT clay reduced

the degradation of PP polymeric chains due to the blocking action of clay lamellae, which reduced the oxygen diffusivity in molten polymer, reducing the formation of carbonyl groups.

In Figure 23, the carbonyl intensity ratios of compounds were smaller in relation to the HDPE, especially in HDPE+Hal compound indicating that, as well as in the work of Silvano et al. [219], the presence of clays reduced the oxidative degradation index of polymeric chains, reducing the oxygen diffusivity in molten HDPE and reducing the formation of carbonyl groups, especially the Halloysite clay.

According to Pinheiro et al. [218], the mechanism of thermo-mechanical degradation begins with the cision of longer chains, due to their higher probability of entanglement. On the other hand, the smaller chains, for presenting a greater mobility, suffers less cision, but have the tendency of branches formation, which may have occurred in this work.

Based on the results, it can be concluded that the clays acted in different ways in the compounds. In the one containing Halloysite clay, there was an increase in the degradation by branching and subsequent cross-linking of the macromolecules, while cision chain degradation was reduced. In the compound containing Cloisite 20A clay, the two different degradation ways were reduced, i.e., Cloisite 20A helped in reducing both the degradation by cision, and by branching and subsequent cross-linking. However, Halloysite clay was more efficient in reducing degradation by cision of chain when compared to Cloisite 20A clay.

It is known that the compound HDPE+Hal also contains maleic anhydride as compatibilizing agent, which contains peroxide and may have influenced the largest level of degradation by branching and cross-linking of HDPE. One possible corroboration of these results is the capillary rheometry results (section 3.7). It was verified that the viscosity of HDPE+Hal presented slightly superior to the viscosity of neat HDPE, which is possibly due to the occurrence of cross-linkings and consequent increase in the molar mass of the HDPE, in addition to the polymer interaction.

3.5 - TGA

According to Cui et al. [220], when using TGA, a problem associated with the identification of mixtures of rubbers is encountered. Fernández-Berridi et al. [221] reported that the first mass reduction of GTR under N_2 atmosphere between 200 and 300°C (about 9% of the total mass) corresponded to the volatilization of the processing oil and/or other components of low boiling points. The next mass reduction, still under

N_2 atmosphere (about 37% of the total mass), corresponded to the NR, and the subsequent mass reduction corresponded to the SBR. Hassan et al. [211] also reported two mass reduction stages that occurred between 300 and 500°C, and corresponded to the decomposition of elastomeric components of the GTR.

Figure 25 shows the TGA and Figure 26 the DTG curves of the devulcanized GTR after different times of exposure to microwaves before (GTRX samples) and after Soxhlet extraction (GTRXg samples). According to Figure 25, the first mass loss (from room temperature to approximately 300°C) refers to the decomposition of processing oil and other organic polymeric additives [58], the second mass loss corresponds to the decomposition of NR (from approximately 300 to 400°C), the third one corresponds to the decomposition of the synthetic rubber (from 400 to 550°C) and the last one (from 550 to 800°C) refers to the decomposition of the carbon black, which occurs under oxidizing atmosphere.

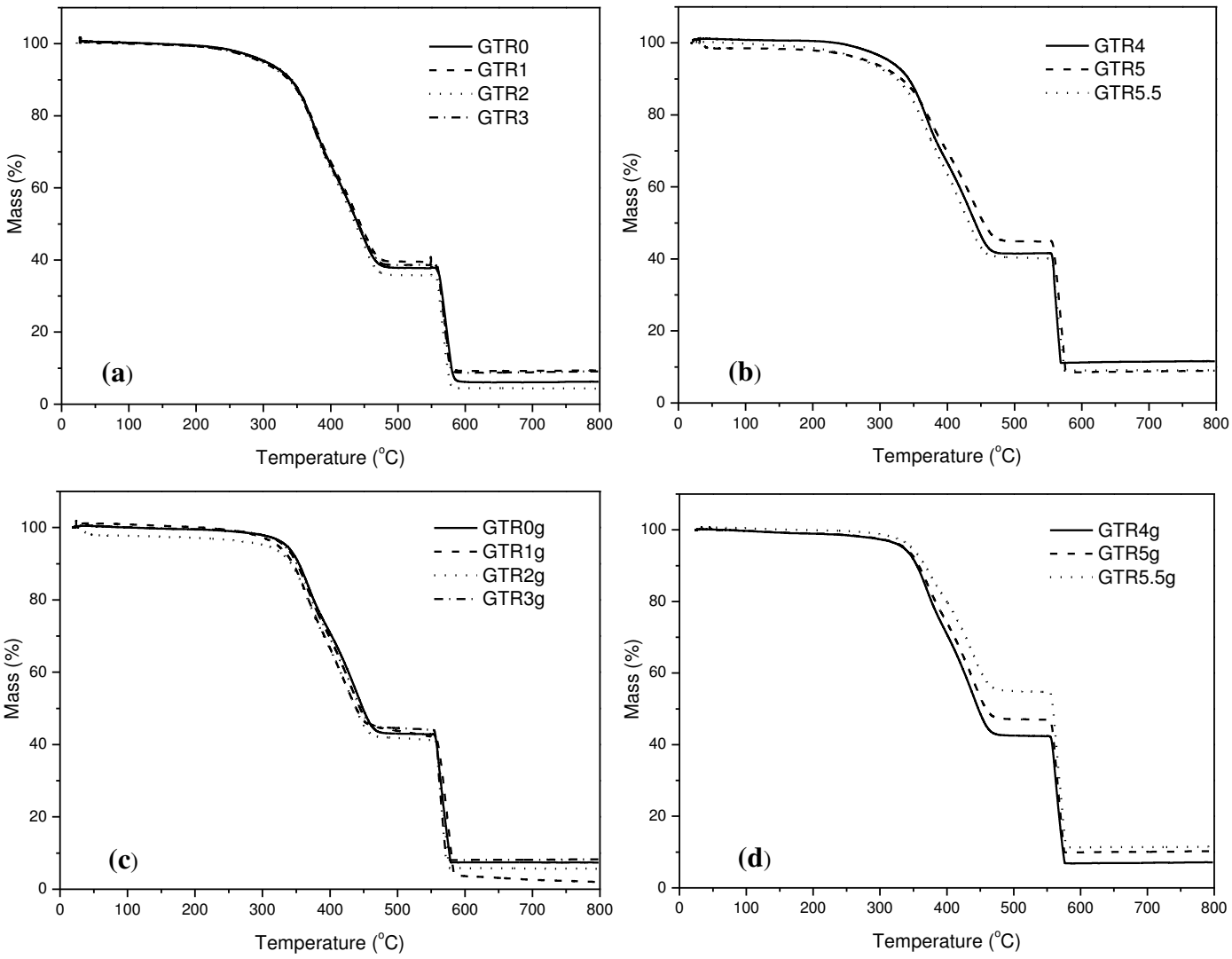

Figure 25: TGA curves of the devulcanized GTR (a) and (b), and their gel fractions (c) and (d). The curves are separated for the sake of clarity.

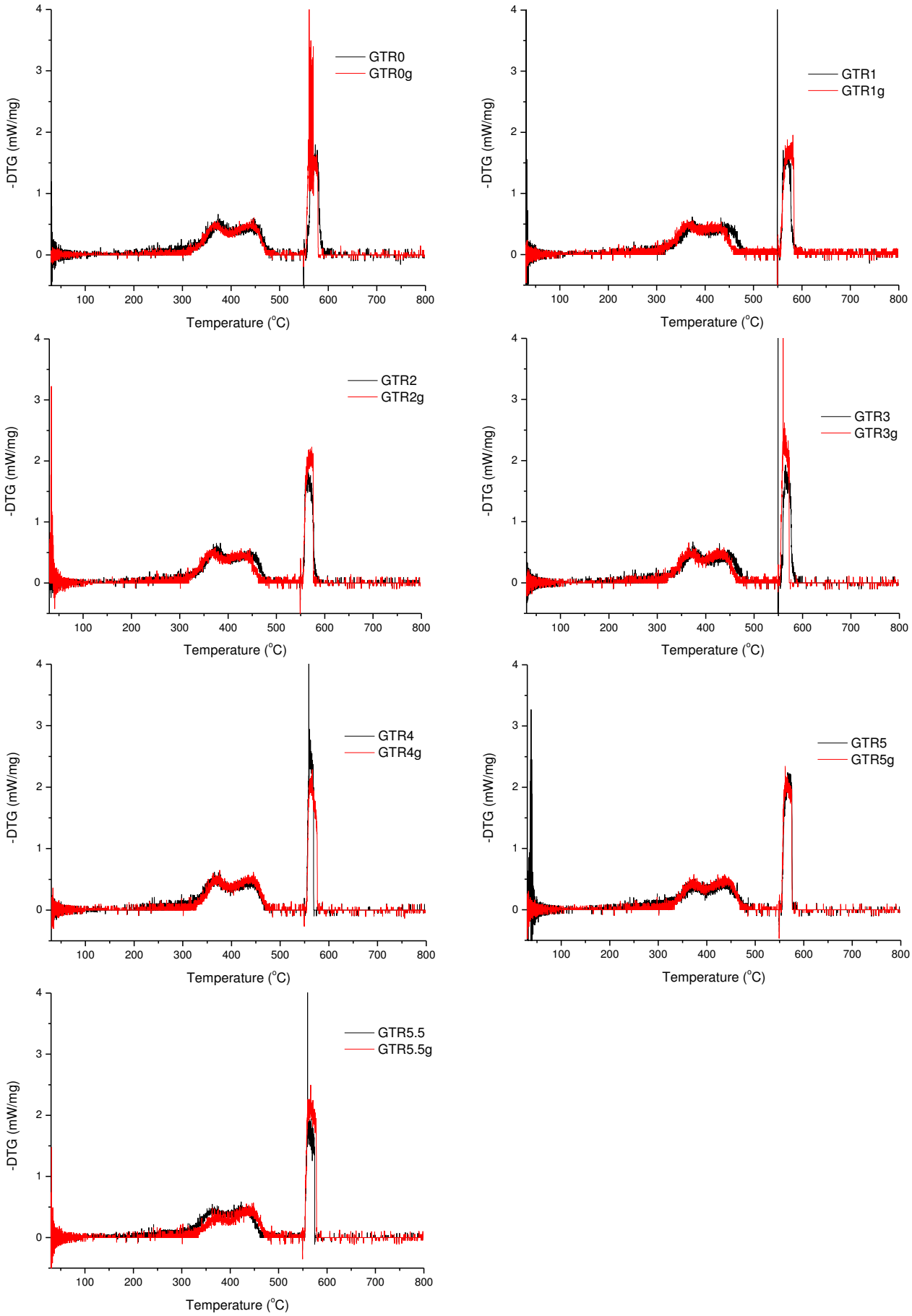

Figure 26: DTG curves of the devulcanized GTRs and their gel fractions.

Table 5 shows the mass loss values and the temperature ranges from TGA curves of the devulcanized samples (left column) and the gel fractions after Soxhlet extraction (right column). The mass loss in percentage of each organic component of the GTR (processing oils and rubbers) tends to decrease as the exposure time of the GTR to microwaves increases, while the opposite trend is observed for the percentage of the carbon black.

In the case of the gel fractions, the same trends were observed. It turns out that the devulcanization process adopted acted more strongly in the breaking of the NR cross-linkings (mass loss from about 300 to 400°C). As found by Garcia et al. [209], carbon black is preferably located in the NR phase of the GTR. Recently, Hong et al. [222] analyzed the devulcanization of EPDM by microwaves and found that the devulcanization effect was limited to the surroundings of polar fillers due to the ion polarization effect. In this work, the NR phase was shown to be the most degraded, since there was no significant variation in the synthetic rubber content in the GTR before and after the extraction (gel fraction).

Table 5: Mass loss values (△m) and the temperature ranges (ΔT) from TGA curves of the devulcanized samples (left column) and the gel fractions after Soxhlet extraction (right column).

Sample	Δm (%)	ΔT (°C)	Sample	Δm (%)	ΔT (°C)
GTR0	3.4	25-280	GTR0g	2.9	25-315
	30.8	280-400		25.4	315-400
	27.8	400-550		28.9	400-550
	31.9	550-800		35.4	550-800
	Residue: 6.1			Residue: 7.4	
GTR1	4.8	25-300	GTR1g	3.4	25-300
	28.5	300-400		25.8	300-390
	27.5	400-550		28.7	390-550
	30	550-800		38.2	550-800
	Residue: 9.2			Residue: 3.9	
GTR2	5	25-300	GTR2g	5	25-300
	30.3	300-400		24.4	300-400
	28.9	400-550		28.9	400-550
	31.5	550-800		35.8	550-800
	Residue: 4.3			Residue: 5.9	
GTR3	6.4	25-300	GTR3g	3	25-320
	29.3	300-400		22.5	320-390
	25.7	400-550		30.3	390-550
	30	550-800		36	550-800
	Residue: 8.6			Residue: 8.2	
GTR4	4.3	25-300	GTR4g	4.5	25-320
	27.8	300-400		23	320-400
	26.3	400-550		30.1	400-550
	30.4	550-800		35.4	550-800
	Residue: 11.2			Residue: 7	
GTR5	6.6	25-300	GTR5g	4.4	25-330
	22.9	300-400		19.6	330-400
	25.5	400-550		29.2	400-550
	36.4	550-800		36.8	550-800
	Residue: 8.6			Residue: 10	
GTR5.5	5.6	25-290	GTR5.5g	3.2	25-330
	26.7	290-390		16.2	330-400
	27.4	390-550		25.7	400-550
	31.3	550-800		43.6	550-800
	Residue: 9			Residue: 11.3	

3.6 - Revulcanization behavior of GTR5.5

As previously mentioned, from the results of the study of the efficiency of devulcanization by microwaves, the GTR5.5 sample was chosen to be used in the production of dynamically revulcanized blends in the next stages of the project. For this reason, only the revulcanization behavior of GTR5.5 was analyzed.

The torque *versus* time curve of GTR5.5+ad is shown in Figure 27.

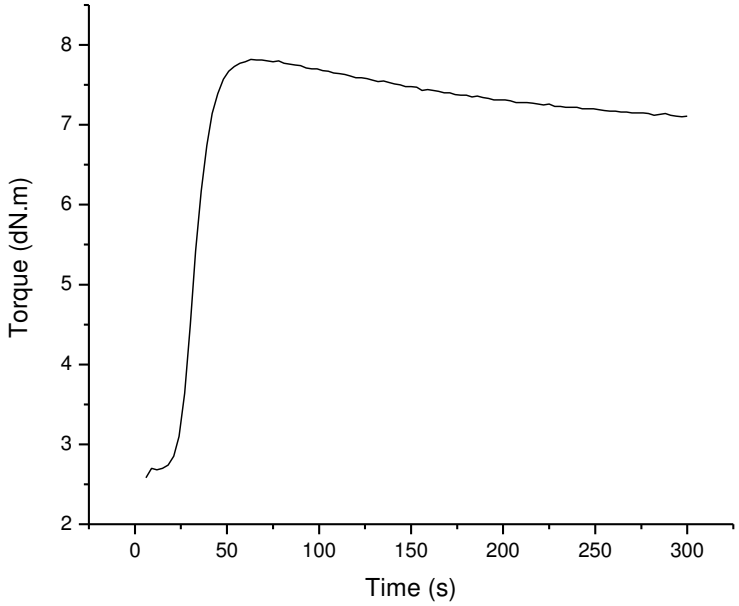

Figure 27: Torque *versus* time curve of GTR5.5+ad.

In the Figure 27, it can be observed a sort of "shoulder" in low times (up to 25), which refers to the compression of the material, and then an increase of the torque due to revulcanization reaction. During the reaction, cross-linkings formed among the rubber chains became the material more rigid, causing an increase in the torque measured by the equipment during the analysis.

According to the rheological measurements of the GTR5.5 with the vulcanizing agents, the values of ts_1 and t_{90} were 27.0 and 43.8 s, respectively. These values are very useful for the production of blends containing GTR5.5+ad in extruder. More details will be given ahead.

3.7 - Capillary rheometry

Figure 28 shows the viscosity of GTR5 and GTR5.5 as a function of shear rate at 180°C. Both samples were able to flow as a result of the devulcanization by microwaves. They showed a shear-thinning behavior [209]. The viscosities of both samples were very close. GTR4 was unable to flow, therefore GTR with an exposure

time to the microwaves less than 4 minutes were not analyzed.

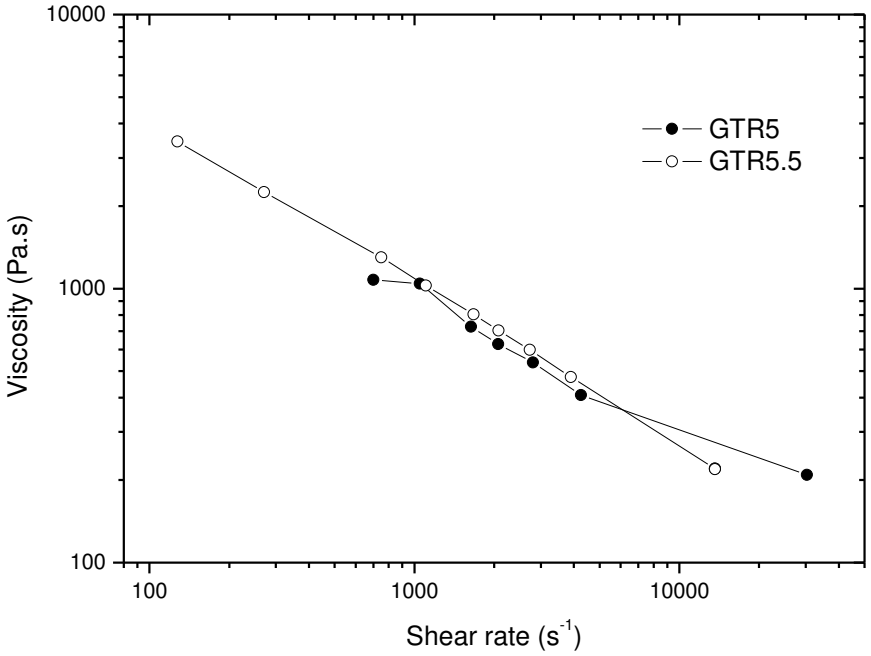

Figure 28: Viscosity *versus* shear rate for GTR5 and GTR5.5 samples.

As a conclusion, the devulcanization by microwaves returned the flow capacity of the GTR, which may be subsequently revulcanized and remolded. This conclusion was validated by some previous works [8, 223, 224], in which blends composed by HDPE and GTR devulcanized by microwaves were produced, both by internal mixer and extruder. In the two ways, the rubber was able to flow during processing, resulting a blend with a finely dispersed GTR phase in the HDPE matrix.

It is worth to point out the texture of the devulcanized samples after remixing them in the two roll mill. Figure 29 shows the appearance (photos) of GTR0, GTR5 and GTR5.5. The difference between GTR5 and GTR5.5 is likely due to a higher relative amount of carbon black and the smaller amount of processing oil in GTR5.5, as shown in the TGA results (Table 5).

As shown in the other results, even being very close the viscosities of both samples analyzed, GTR5.5 was chosen to be used in the production of dynamically revulcanized blends due to its superior results presented in relation to the efficiency of the devulcanization process.

Figure 29: Photos of GTR0, GTR5 and GTR5.5 after remixing in a two roll mill.

Figure 30 shows the curves of viscosity at high shear rates of the phases of the blends produced in this work: GTR5.5, HDPE, and the nanocomposites HDPE+Cloisite 20A and HDPE+Halloysite.

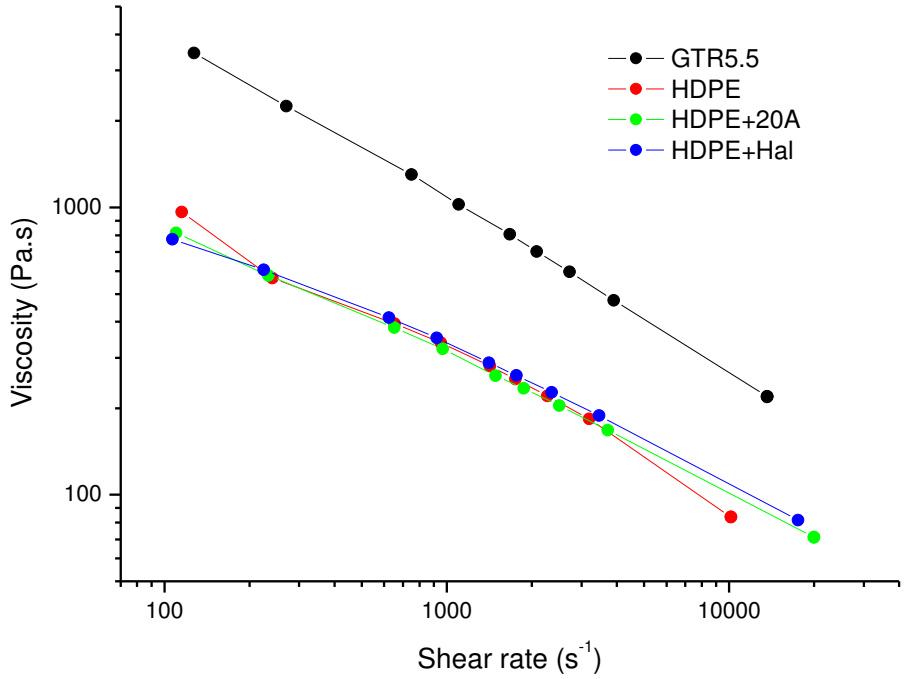

Figure 30: Viscosity curves at high shear rates obtained by the capillary rheometry at 180°C of GTR5.5, HDPE and nanocomposites matrix HDPE used in the production of dynamically revulcanized blends.

Figure 30 shows that all the samples presented reduction of the viscosity with increasing the shear rate, which shows the pseudoplastic behavior of them.

From the same results it was possible to calculate the consistency (m) and the power law index (n), according to the Power Law equation (Equation 9)

$$\eta = m\dot{\gamma}^{n-1}$$ Equation 9

where η is the apparent viscosity and $\dot{\gamma}$ is the shear rate.

The n value presents important information about the behavior of the material under shear flow. It indicates whether the molten polymer presents Newtonian character, dilatant or pseudoplastic, being that the material will be dilatant if the n value is greater than 1 and pseudoplastic if the n value is less than 1 [225].

Table 6 presents the 'm' and 'n' values calculated from Figure 30.

Table 6: Consistency and power law index values obtained from Figure 30.

Sample	Consistency m (Pa.s^n)	Power law index n	Shear rate range (s^{-1})
GTR5.5	64081	0.41	127.47 - 13653.57
HDPE	11835	0.47	115.10 - 10167.18
HDPE+20A	7877	0.53	110.14 - 20000.91
HDPE+Hal	6695	0.56	106.68 - 17556.17

It is observed that the GTR5.5 presents viscosity far superior than other materials. All of them present high shear thinning, between 0.41 and 0.56.

From the results of viscosity at high shear rates obtained at 180°C from capillary rheometry, it was calculated the viscosities ratio among the phases of the blends (Figure 31).

There are some equations used to describe the effect of viscosity of the phases in the breaking process of the particles of the dispersed phase. Wu [226] developed the Equation 10 from the blend nylon/rubber

$$\frac{\gamma \eta_m D}{\sigma} = 4\left(\frac{\eta_d}{\eta_m}\right)^t$$ Equation 10

where γ, D, η_m, η_d and σ are shear rate, diameter of the particles of the dispersed phase, viscosities of the matrix and the dispersed phase, and interfacial tension, respectively.

The equation indicates that smaller particles of the dispersed phase are obtained when the viscosity of the two phases have close values, and that the elongation of the particles is increased by high shear rates, high viscosity of the matrix and low interfacial tension

[227].

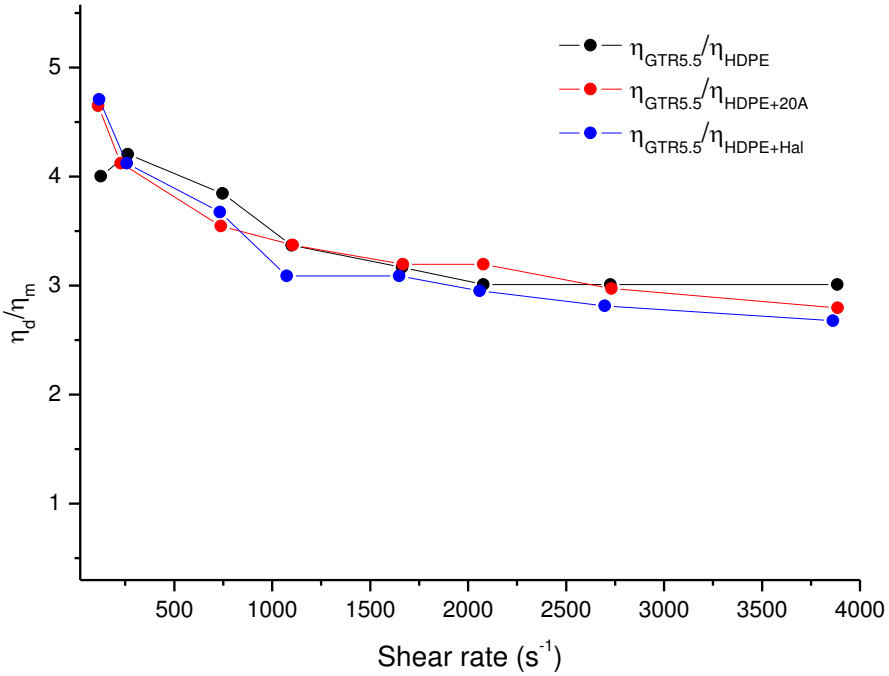

Figure 31: Viscosities ratio between the phases of the blends.

There is also the viscosities ratio equation among the phases of the blend (Equation 11)

$$p = \frac{\eta_d}{\eta_m} \qquad \text{Equation 11}$$

where η_d and η_m are the viscosities of the dispersed phase and matrix phase, respectively.

When the viscosity ratio approaches to the unit, the dispersed phase is capable of elongating in long filaments and breaks into micro spheres due to surface tension.

Some authors report that it is not possible the break of the dispersed phase into small particles when p>4 in shear flow [228] due to elastic effects, presence of the elongational field, and the complex profile viscosity-temperature along the extruder barrel [226]. However, Oderkerk and Groeninckx [229] obtained ethylene-propylene-diene rubber (EPDM)/Nylon blends with rubber particles finely dispersed in the matrix with p≥8 due to reduction in the interfacial tension and coalescence suppression by reactive compatibilization and dynamic vulcanization.

In the case of the results obtained, as the viscosity of the GTR is far superior to HDPE and nanocomposites used in the production of the blends, the viscosity ratio between them was higher than a unit. However, as the nanocomposite HDPE+Hal presents

slightly higher viscosity compared to neat HDPE, it turns out that the viscosities ratio of GTR5.5/HDPE+Hal showed slightly lower compared to the others, which may have facilitated the break of the GTR phase into small particles, to be checked on the results of Stage 3 of this work.

3.8 - X-ray diffraction of nanocomposites HDPE/clays

The X-ray patterns of neat Cloisite 20A and Halloysite clays, processed HDPE and nanocomposites HDPE/clays (5 wt%) are shown in Figure 32.

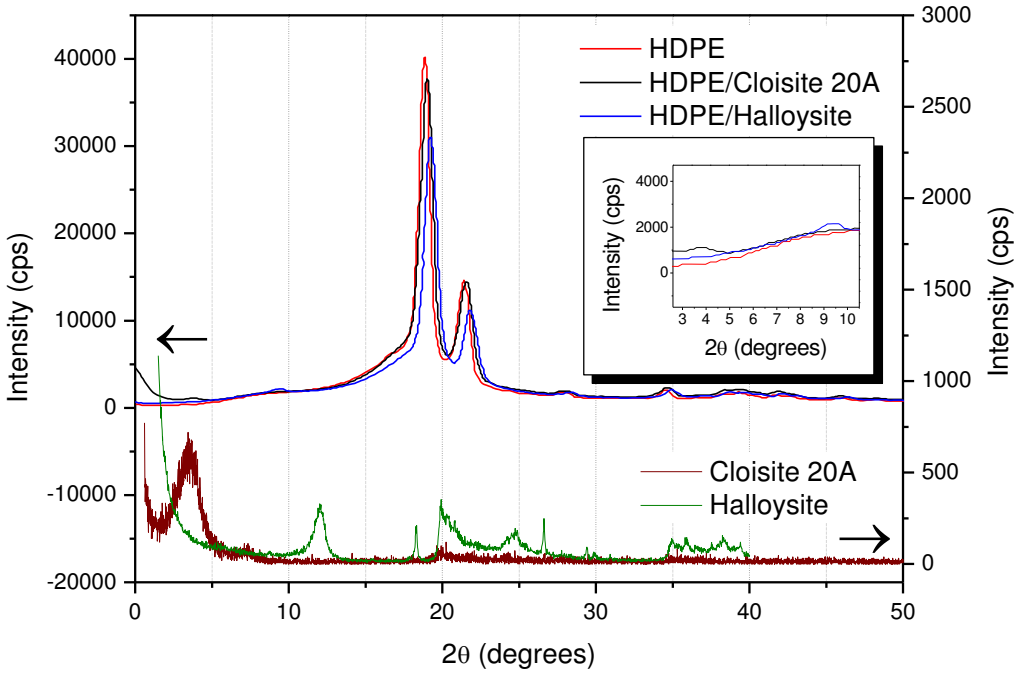

Figure 32: X-ray patterns of clays, HDPE and nanocomposites.

No significant differences were found between the results of neat HDPE and nanocomposites.

The X-ray pattern of the HDPE/Cloisite 20A presented the characteristic peak of clay with far less intensity, possibly due to the smaller amount of clay present in the compound [230]. According to Ray et al. [231], the reduction in peak intensity of the compound compared to the neat clay demonstrates good interaction among the phases. Such behavior can also demonstrate some degree of disorder of the lamellaes: they can be partially exfoliated [232] or intercalated [233], that is, it is the sign of a disordered structure.

4 - PARTIAL CONCLUSION

In the first stage of the work, the GTR was devulcanized by microwaves and the process efficiency was evaluated based on the results of extraction, solvent swelling, TGA, FTIR, capillary rheometry and revulcanization behavior.

According to the results of solvent extraction and swelling, the longer the exposure time of GTR to microwaves, the higher the degree of devulcanization due to the decrease of cross-linkings. In other words, the higher the amount of energy absorbed during the microwave treatment due to the presence of carbon black, the higher the temperature of the GTR, and the higher the degree of devulcanization. The temperature of the GTR is the primary factor responsible for the devulcanization.

Sulphur bonds can be broken or formed during the microwave treatment. In the samples whose exposure to microwaves is long, S-O new bonds are formed as a result of the rearrangement of the sulphur free radicals from the devulcanization of the GTR in the presence of oxygen.

Sufficient break of the sulphur bonds by devulcanization, GTR5 and GTR5.5 can flow and consequently can be remolded and revulcanized.

The NR phase of the GTR is more degraded than the SBR phase. The higher the devulcanization level of the sample, the higher the degradation of the NR phase observed from TGA results.

The presence of Halloysite in the compound resulted in degradation of the HDPE chains by branching and cross-linking, whereas the presence of Cloisite 20A reduced the degradation of HDPE.

The study of efficiency of devulcanization process of GTR by microwaves proved to be efficient and capable of producing a devulcanized rubber able to flow, which is a basic requirement for its use in the production of blends in extruder. With the adoption of the method of devulcanization by microwaves, will be possible to use a higher concentration of recycled GTR in polymer blends, without large depreciation of the final properties and with small damage on processability. The process also proved to be effective due to the formation of new active sites for the revulcanization of rubber.

5 - INTRODUCTION

Topic 3: Polymer blends

5.1 - Polymer blends - general concepts

Before addressing the theme itself, it is necessary the definition of some terms that will be widely covered in all the work.

Polymer blends are physical mixes of two or more polymers that can be miscible or immiscible. In general, they can present two distinct morphologies: morphology of dispersed phase (Figure 33a and 33c) and morphology of co-continuous phases (Figure 33b). In the first case, one of the phases is continuous forming the matrix, while the other is dispersed, forming the dispersed phase itself. In the second case, the two phases coexist continuously, and are interconnected throughout the blend [234] or, in other words, it is a completely continuous structure formed by the polymers that make up the blend [235].

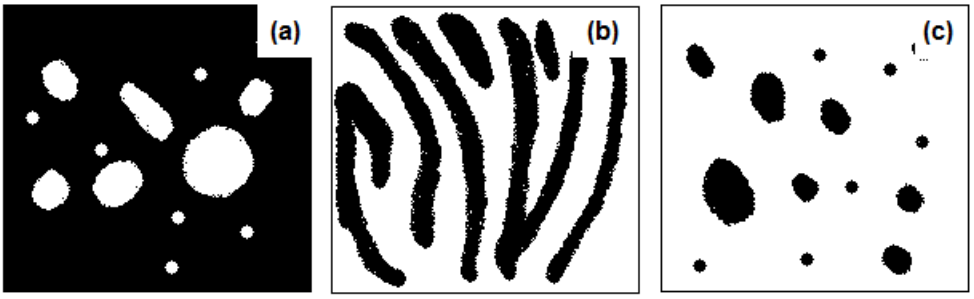

Figure 33: Schema showing morphologies of blends: (a) and (c) morphologies of dispersed phase and (b) morphology of co-continuous phases. The dark part represents polymer 1, while the clear part represents the polymer 2.

Some blends pass, during processing, by a process known as phase inversion. According to Antunes et al. [235], inversion phase is defined as the point at which the blend components change their discontinuities, i.e., the matrix phase becomes the dispersed phase, while the dispersed phase becomes the matrix phase. However, for that

to happen, the blend acquires an intermediate morphology which is the morphology of co-continuous phases. Figure 33 shows in a very simplified way the process of phase inversion, being that in Figure 33a the polymer 1 forms a matrix phase and the polymer 2, the dispersed phase; in Figure 33b both are continuous phases (co-continuos); and in Figure 33c polymer 1 forms the dispersed phase and the polymer 2 forms the matrix.

Immiscible blends are those that do not form continuous homogeneous solutions. The vast majority of blends is immiscible. However, these can be modified through the use of additives to form systems with useful properties, creating compatible blends [236].

Another very important aspect involving blends with the morphology of dispersed phase are the levels of dispersion and distribution of elastomeric particles in the thermoplastic matrix. There are four different possibilities, namely: badly dispersed particles and badly distributed ones (Figure 34a); badly dispersed particles and well distributed particles (Figure 34b); well dispersed particles and badly distributed (Figure 34c); and well dispersed and well distributed particles (Figure 34d).

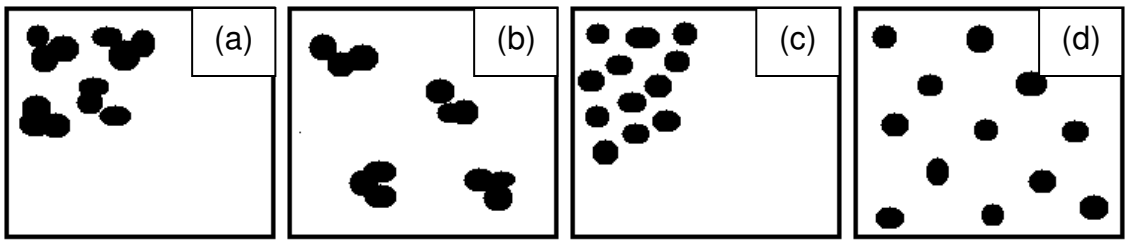

Figure 34: Levels of dispersion and distribution of elastomeric phase particles in thermoplastic matrix: badly dispersed and badly distributed (a); badly dispersed and well distributed particles (b); well dispersed and badly distributed particles (c); and well dispersed and well distributed particles (d).

The ideal to achieve good properties in blends, especially the mechanic ones, is that particles are well distributed and well dispersed in the matrix to prevent the concentration of stresses, which doesn't always happen.

Due to the fact that two or more properties of the polymers can be combined, the blends and polymer alloys have been studied extensively with the aim of improving the physical properties compared to neat polymers, i.e., obtain materials with additional properties, and minimal loss of original properties [237], as well as being more economically viable to unite two existing polymers to synthesize another nonexistent [238], for the creation of a new molecule. Some benefits of the blends may be cited: (i) supply of materials with a set of properties that you want at a lower price; (ii) increase in the performance of engineering resins; (iii) improvement of specific properties; (iv) provision of means for recycling industrial plastic waste and/or municipal. The blends

also benefit manufacturers by providing: (i) improvement in processing power, product uniformity and scrap reduction; (ii) rapid formulation changes; (iii) flexibility in the plant and high productivity; (iv) reduction in the number of bars that need to be manufactured and stored; (v) inherent recycling [237, 239].

A plethora of polymeric blends can be obtained, including polymer blends composed of elastomers. There are basically two types of polymeric blends composed of at least one of the elastomeric phases: the blends composed of two or more types of elastomers (elastomeric blends) and blends composed of a thermoplastic phase and the other elastomeric. These can be of two types: when there is a high concentration of elastomer (thermoplastic elastomers - TPEs) and when there is low concentration of elastomer (toughened plastic). In all cases, the goal of the mix is the obtaining of materials with desired properties, additional to the properties of the neat materials. The class of TPEs will be addressed in more details in the following section.

5.1.1 - Thermoplastic elastomers

Thermoplastic elastomers contain high concentrations of elastomeric phase (usually above 50%), combining the processability of thermoplastics and the functional performance of vulcanized rubbers at room temperature [240-244]. There are three distinct classes of thermoplastic elastomers, namely: block copolymer, thermoplastic/dynamically vulcanized elastomer blends and ionic thermoplastic.

The unique combination of properties allows the processing of TPEs in conventional equipment used for processing of thermoplastics in processes such as injection molding, blow molding, film production and extruded profiles, keeping the elastomeric properties without becoming thermosetting. Such behavior is attributed to their structures that contain both flexible and elastic fields of high extensibility with low T_g, and rigid low extensibility areas with a T_g and/or crystalline melting temperature (T_m) high [60].

Thermoplastic elastomers have advantages and limitations on conventional rubbers. The key advantages of TPEs include [60]:

- The ability of TPEs to become fluid with heat and then hardening with cooling gives manufacturers the possibility to produce articles with rubber behavior using equipment commonly used in the processing of plastics. In some TPEs, a reversible transition similar to the transition from solid to fluid can be used in the addition of solvent. On the other hand, vulcanization of rubbers is a thermosetting process, which is slow, irreversible and that occurs through heating.
- There is little or no mixing of additives necessary for the production of TPEs. The

majority is ready for manufacturing. Rubbers, however, require the mixture of vulcanizing agents, stabilizers, fillers, auxiliary processing, among other additives.

- TPEs, once prepared, do not need more the step of vulcanization. As shown in Figure 35, the processing consists of fewer stages in the processing of vulcanized rubber.
- The scrap produced in the production process of the TPE can be reprocessed (Figure 35). Scrap generated in processing vulcanized rubbers, however, have their potential reuse limited and the cost of its production is greater, due to the loss of material and cost of disposal of scraps.
- Thermoplastic processing consumes less total energy by having a more efficient processing and with smaller time cycles.

Some limitations [60]:

- TPEs are relatively new materials intended to replace some rubbers. However, the behavior during the processing of these materials even today is not fully known.
- They have a permanent elongation greater than the elongation present in elastomers.
- Many of them require a step of drying before processing of the final products.

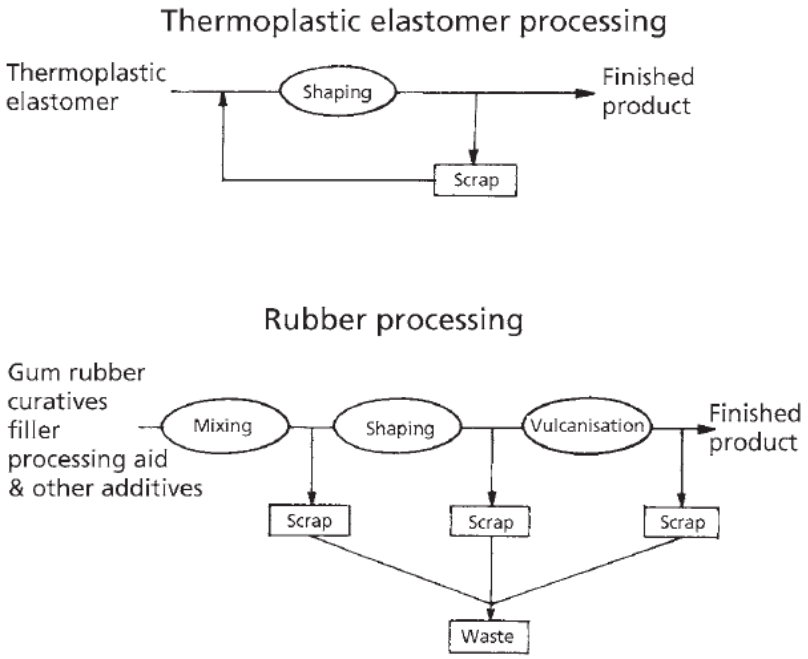

Figure 35: Processing of TPEs *versus* rubber processing [60].

In addition, so that there are no problems in the use of such material, it needs to be used within a specific temperature range for each type of TPE, and which depends on the transition temperatures of each of the constituent phases, known as service temperature (Figure 36). At very low temperatures, below the T_g of the elastomeric phase, the

material is rigid and brittle. Above the T_g, the elastomeric phase softens and the material is elastic, similar to a conventional vulcanized rubber. Around that point to the T_g or T_m of rigid phase it is found the service temperature range, in which the material can be safely used. However, at the temperature of T_g or T_m of rigid phase, the material becomes a viscous fluid [245].

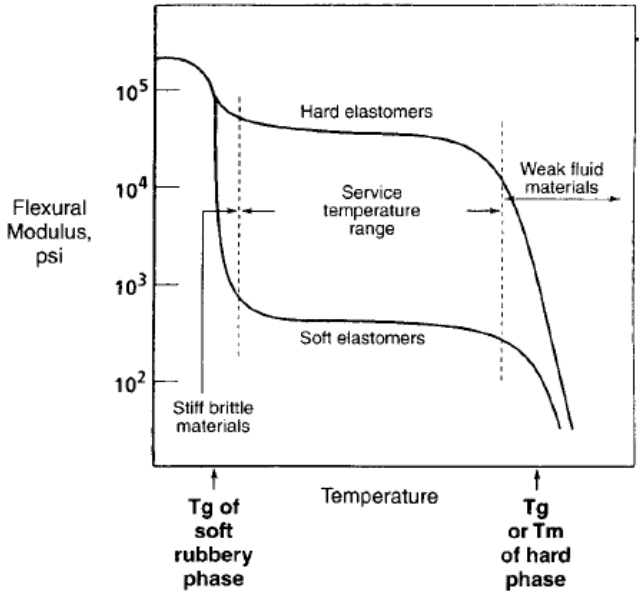

Figure 36: Hardness of TPEs and their dependence with temperature [245].

The thermoplastic/dynamically vulcanized elastomer blends, main objective of study of this work, will be described in more details in the following sections.

5.1.2 - Thermoplastic/dynamically vulcanized elastomer blends

This type of blend, known as TPV, is a type of TPE produced via dynamic vulcanization of the elastomeric phase of an immiscible blend of thermoplastic in molten state and rubber under high shear rates [50, 235, 246-248]. TPVs are materials widely used in the automotive industry (for example, bumpers, fuel tank covers, gaskets, interior components [57, 249]), the electronics industry, civil construction, wiring and cables, biomedical products, among others [57, 250-252].

Dynamic vulcanization is the vulcanization of an elastomeric reticulation for the molten mixture with other polymer(s) [253]. The process produces a cross-linked polymer dispersion in a continuous polymer matrix phase not cross-linked [50, 60, 188, 254-256]. The continuity of the thermoplastic phase provides the thermo-plasticity and mechanical resistance necessary to blends [257], while the dynamically vulcanized

rubber particles give elasticity, flexibility and stability [243, 251, 258].

The dynamic vulcanization process for thermoplastic elastomers can be described as follows: after enough fusion-blend of thermoplastic and rubber, vulcanization agents are added. The vulcanization of rubber phase occurs with a continuation of the mixture. After the output of the mixer, the cold blend can be chopped, extruded, injected, molded, pelletized, etc [188, 248]. They are prepared commercially by a continuous process by using twin screw extruders [254]. Figure 37 presents an outline of the morphology of EPDM/PP blend by dynamic vulcanization, in which vulcanized EPDM elastomeric particles are dispersed in thermoplastic PP matrix [259].

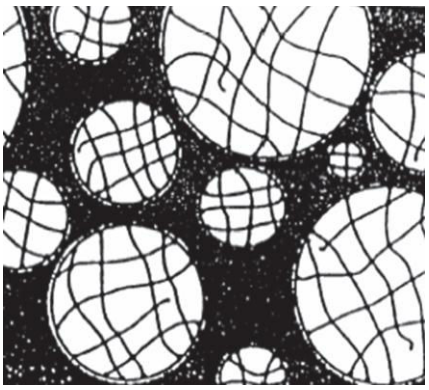

Figure 37: Scheme of the morphology of formation of cross-linkings on EPDM/PP blend by dynamic vulcanization, where the dark part represents the matrix phase and the light parts represent the dynamically vulcanized elastomeric particles [259].

According to Anandhan and Bhowmick [260], the dynamic vulcanization increases the elasticity and stabilizes the morphology of TPVs. The literature presents a vast number of works showing the differences in the properties of polymer blends resulting from dynamic vulcanization, among them: improvement in mechanical properties [134, 260-266], greater thermal stability [262, 264, 267], minor swelling of the extruded [248, 258, 263, 264], better reprocessability [84, 251, 257], increase in the service temperature [248, 254, 263], greater weather resistance [57] among others, depending on the system analyzed. Several papers also feature improvements in mechanical properties as a result of the dynamic vulcanization, but through the use of compatibilizing agents [243, 253, 268-272] and, in general, the improvement in mechanical properties of the blends came about as a result of greater refinement of morphology [240, 273]. Among the improvements, it is found also reduced permanent elongation, increased fatigue resistance, greater stability of morphology and better chemical resistance.

Among other factors, the decrease in the size of the particles of the elastomeric blends

type TPV is an important factor in the improvement of their stress-strain properties (Figure 38).

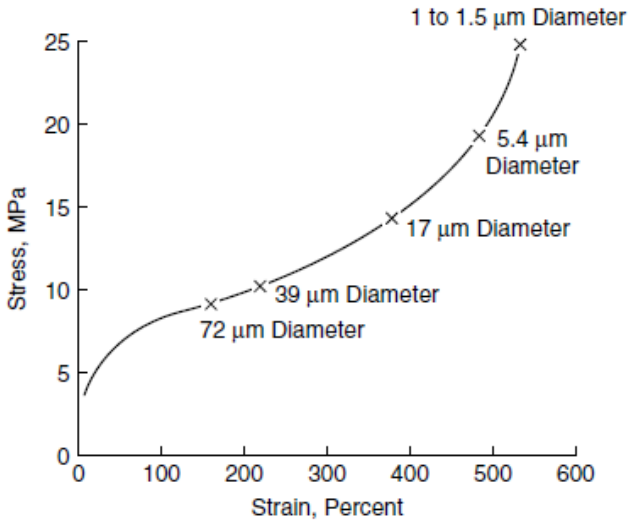

Figure 38: Effect of rubber particle size on stress-strain properties of TPVs [5, 228, 245, 248].

According to van Duin [274], elasticity of TPVs is still a mystery, since the matrix consists of a thermoplastic polymer and the vulcanized elastomer is the dispersed phase. However, Huy et al. [275] managed to describe it: as soon as a stress is applied to the material, the orientation of all components starts in the direction of the applied stress, and the orientation of the elastomeric particles is greater. Plastic elongation begins as soon as reached the yield stress. The concentration of stresses on thermoplastic (more specifically, in the interfacial region) reaches the maximum in equatorial areas of the particles, so in those regions the plastic elongation begins first. With the increase of elongation, the plastic elongation zone spreads from the equatorial zone to the polar regions and the orientation of the thermoplastic phase increases even more. When the applied force is removed, the elastic rubber particles forces stretched pull highly deformed plastically interfacial region [276], resulting in an intermediary permanent elongation between the permanent elongation of the components that form the blend. Figure 39 shows a scheme of the model of elasticity of TPVs and its permanent elongation after the relaxation of tension applied [274]. However, the schema is only valid for blends with good adhesion among phases, because otherwise occurs the detachment of vulcanized elastomeric particles of the matrix with the application of stress.

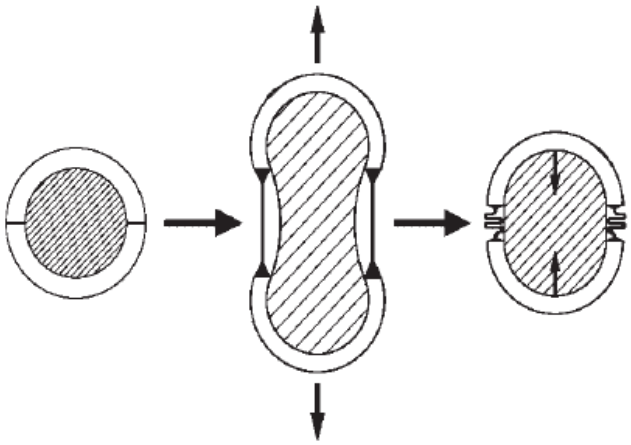

Figure 39: Schema of elasticity model of TPVs. After the relaxation of the applied stress, the polymer chains of the interfacial region deformed plastically are pulled by the elastomer, then occurs the formation of a sort of "spring" with these chains in the equatorial regions of the particle, known as permanent elongation [274].

In the next section, the introduction of nanofillers in dynamically vulcanized blends and its consequences in the final properties will be addressed.

5.1.3 - Dynamically vulcanized blends containing nanofillers

Polymeric reinforced blends are widely produced to increase the stiffness, or even improve existing blends properties for a given specific function of the final product. However, conventional fillers like talc, mica and calcium carbonate not only increase the stiffness, but also the density and molten viscosity, besides reducing the toughness. Others like fiberglass increase the difficulty of manufacturing, beyond all of them are used at high concentrations [277].

In recent years, a new type of polymer material has emerged: reinforced polymer blends with fillers in the nanoscale, such as organically modified clays and carbon nanotubes. This new type of high performance material combines the advantages of polymeric blends of nanocomposites, and use small concentrations (usually from 2 to 5 wt%). In many cases, these fillers act as compatibilizing agents among the phases, decreasing the interfacial tension, promoting greater particle breakage during processing and decreasing the coalescence of the particles, assisting in stabilizing their morphology [9]. The synergistic improvement in properties such as stiffness, barrier to gases and flammability of the hybrid polymer/clay blend results from good dispersion of clay lamellaes on polymer matrix. The good dispersion depends on the interfacial energy of the system, that tries to achieve the minimum interfacial energy state.

According to Taguet et al. [9], one of the important conditions for which fillers may be efficient as compatibilizing agents is their size: the radius of the particle must be of the same order of magnitude of the gyration radius of the polymer. With that, the stabilization energy is particularly effective when the inorganic filler has great surface area per unit weight, as in the case of the nano-sized fillers. If the rays are similar, the filler starts to influence the configuration entropy.

Fang et al. [278] presented a schema by comparing the mechanisms for making a diblock copolymer and clay lamella (Figure 40). According to them, to the diblock copolymer, blocks A and B are compatible with the phases A and B respectively, and the covalent bond occurs at the interface of two phases by creating the connection among them. In the case of clay, both polymers A and B have a strong interaction with the lamella exfoliated clay, which is located in the interface. The lamella acts as a sort of compatibilizing agent among polymers.

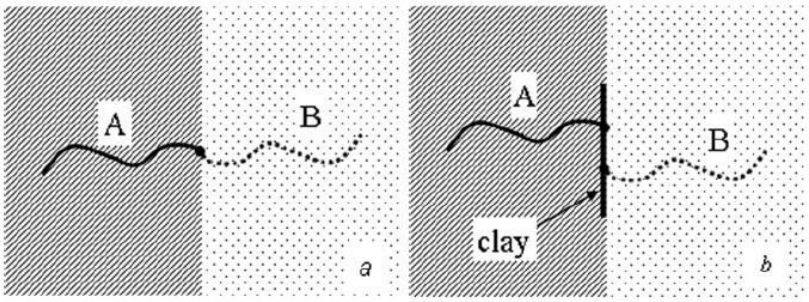

Figure 40: Comparative schema among compatibilization mechanisms: (a) copolymer diblock and (b) lamella of clay [278].

It is known that, in order for the compatibilizing effect be effective, the lamellae of the clays need to be well dispersed in at least one of the phases of the blend, and the crucial factor in the control of dispersion (and, therefore, morphology) is the degree of interaction among the modified lamellae and the polymer matrix. Fang et al. [279], in another later work, complemented the results showing a new schema comparison, demonstrating that the interface among two polymers can be stabilized by lamellae depending on the strength of interaction among them and the polymers (Figure 41). When the two polymers have a strong interaction with the clay, the lamellae can exfoliate, and the lamella acts as compatibilizing agent among the phases (Figure 41a). When they have no interaction with the clay, the lamellae agglomerate or just are intercalated, not acting as a compatibilizing agent (Figure 41b). In the case of only one of the polymers have interaction with the clay, the lamellae become partially exfoliated,

being that the lamella acts as compatibilizing agent only with the polymer which has strong interaction (Figure 41c).

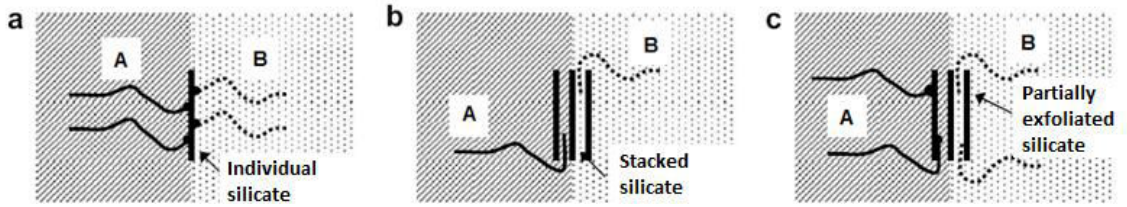

Figure 41: Schemes of compatibilization mechanisms among lamellae of clays and polymers: (a) both polymers A and B have a strong interaction with the lamellae; (b) both polymers A and B do not have interaction with the lamellae; and (c) the polymer A has strong interaction with the lamellae, while B does not have [279].

The presence of nanofillers in polymer blends can change substantially their morphology, and the factors that result in this change were listed by Fenouillot et al. [280], namely: (a) reduction in interfacial energy; (b) inhibition of coalescence by the presence of a solid barrier around the dispersed phase; (c) change in the viscosity ratio due to the presence of the filler at least in one of the phases [281]; (d) creation of a physics network of particle (when the percolation threshold is reached) that inhibits the movement of the matrix or particles; and (e) the interaction of macromolecules adsorption on the surface of solid particles.

Still, according to the same authors [280], the stabilization mechanism of morphology of polymer blends by nanoparticles happens due to the mechanical barrier effect generated by their presence on the surface of the particles of the dispersed phase (Figure 42), called by drops in the scheme shown in Figure 42. The nanofillers hamper the mobility of interface during drainage process, and in the case of contact among the drops, they are able to move to prevent the coalescence.

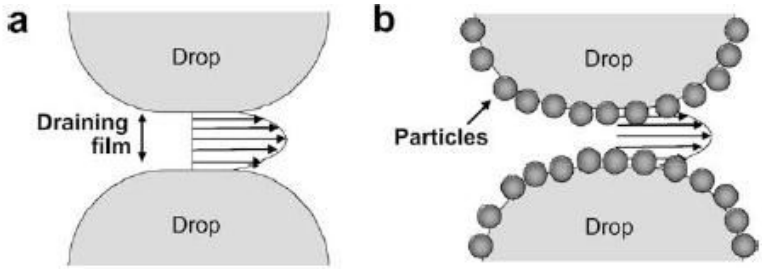

Figure 42: Schema showing the stabilization of drops by the presence of nanoparticles: (a) free drops and (b) drops covered by a layer of particles [280].

An interesting work that exemplifies the change in morphology of polymer blends by addition of nanofillers is that of Zhang et al. [282], in which the authors produced PP/polystyrene (PS) 70/30 blends in extruder with or without silica. In blends containing silica was observed a drastic reduction in the size of the dispersed phase due to the reduction in interfacial tension and coalescence of the particles by the presence of nanofillers on the interface. In another work with the same blend and filler, the authors [283] observed similar behavior (Figure 43). The same behavior also could be verified in other works of literature [233, 278, 279, 281, 283-285].

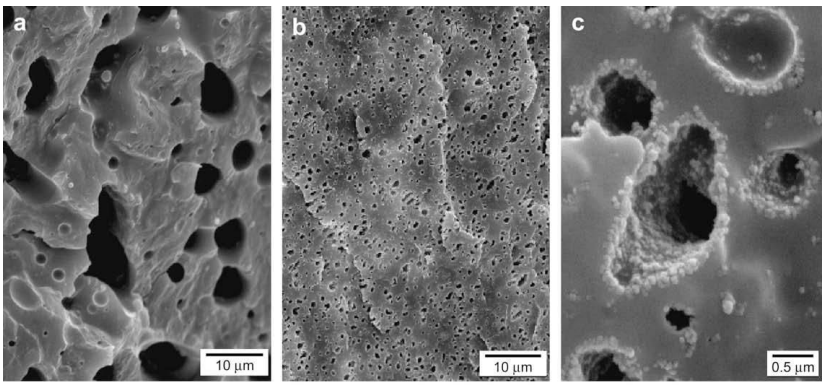

Figure 43: Morphology of the PP/PS blends, being that the PS phase was selectively extracted by solvent. (a) PP/PS blend without silica; (b) blend containing 3 wt% of silica; and (c) amplification of image b showing the silica particles concentrated in the interface [283].

Mani et al. [285] produced TPVs polyamide 12 (PA12)/Polydimethylsiloxane silicone rubber (PDMS) 80/20 in an internal mixer. In order to study the variation in morphology of the TPV, Lotader 3410 compatibilizing agent was used (3 wt%) and nanosilica (6%). Figure 44 presents the SEM images of the analyzed blends.

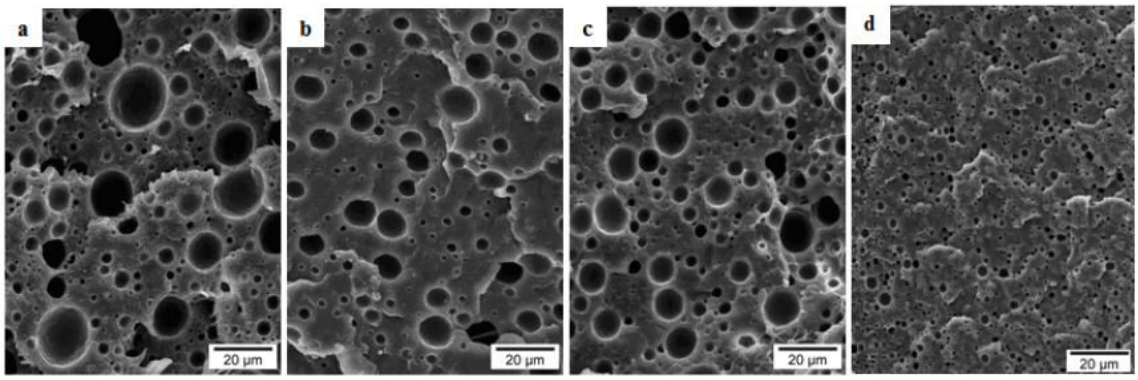

Figure 44: SEM images of cryogenically fractured surfaces of blends: (a) no compatibilizing agent and no filler, (b) containing only filler, (c) containing only compatibilizing agent and (d) containing compatibilizing agent and filler [285].

According to Figure 44, it was found that the PDMS phase was dispersed roughly on PA12 matrix, and the average radius of the particles was 16.5 µm (Figure 44a). The addition of nanosilica or Lotader separately did not affect the morphology of the blend, with average radius of particles of the dispersed phase between 15-16 µm (Figures 44b and c). However, when silica and Lotader were added together, the coalescence of the particles of the dispersed phase was inhibited and the average radius of the particles was divided by a factor of 3, going from 15-16 µm in the addition of silica and Lotader separately to 5.5 µm when added together to the blend (Figure 44d) [285].

However, so that the nanofilllers can stabilize the blends, you must use the nanofiller with lenght to diameter ratio such that do not slow down its transference speed for the interface during processing in the molten state [9].

Göldel et al. [286-288] revealed in their works that the lenght to diameter ratio of solid fillers have an important role in the dynamic transference and stability in interface in mixtures in the molten state of multiphase blends. They proved that fillers with higher lenght to diameter ratio were transferred more quickly compared to the fillers with lowest lenght to diameter ratios due to changes in the curvature of the interface during the transfer process. Fillers with low lenght to diameter ratio such as silica and carbon black tend to be located in the interface of non-reactive immiscible blends (Figure 45b). The same authors [286] showed that in poly (styrene-acrylonitrile) (SAN)/PC blends, carbon nanotubes multi layers moved from the lower viscosity phase to the larger viscosity one during processing (Figure 45a). Changes in curvature of the interface during the process of transferring explain the rapid and complete transference of the nanotubes of the less favorable wettability phase to the most favorable wettability phase of the blend.

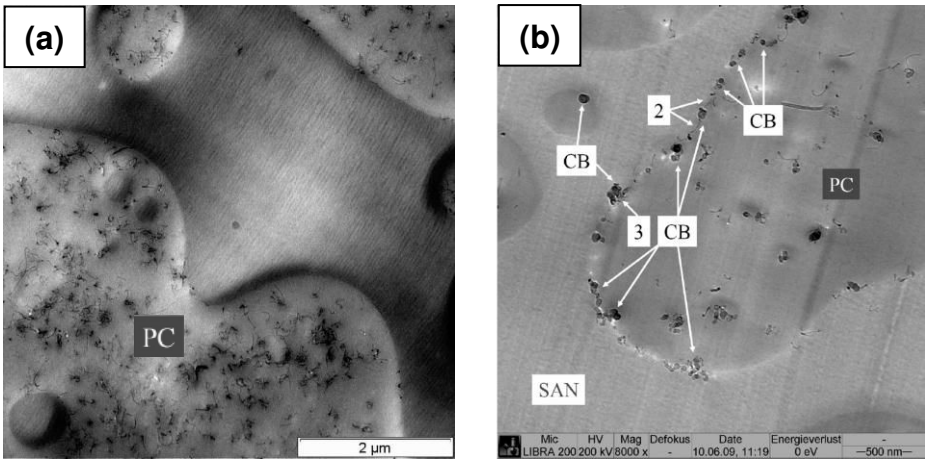

Figure 45: TEM images of the SAN/PC blend showing nanotubes located on PC phase (a); and the same blend showing the carbon black (CB) located on the interface (b) [287].

In the same manner as in the production of nanocomposite containing lamellar clays, its compatibility with the polymers of the blends strongly affects its dispersion. In general, the higher the affinity, the greater the dispersion of lamellae and, the better the strengthening effect. It is possible to control the dispersion of clays in polymeric blends through different addition sequences during processing, which can change the morphology and, consequently, change its final properties [289, 290]. According to Fenouillot et al. [280], the order of addition of components is important and strongly affects the kinetics and mixing intensity, since the filler influences directly the phase in which it is in contact during its incorporation.

A good example of work that shows the variations in morphology caused by different sequences of addition of the components of blends is the one by Zhang et al. [290]. PA6/EPDM modified with maleic anhydride (EPDM-MA)/organically modified Montmorillonite (OMMT) blends were produced in twin screw extruder with different sequences of addition of the components: N1 (all components were added together); N2 (first added PA6 and OMMT, and after the EPDM-MA); N3 (first added PA6 and EPDM-MA, and after the OMMT); N4 (first added PA6 and EPDM-MA, or PA6 and OMMT, and then PA6 and OMMT, or PA6 and EPDM-MA). Figure 46 shows the TEM and SEM images showing the location of clay lamellae and morphology of blends, respectively. In the images, the black lines are the lamellae of clays, the white parts are the particles of EPDM-MA and grey part PA6. On N1 and N3, part of the clay lamellae penetrated in the EPDM-MA particles, while on N2 and N4 few lamellae were able to penetrate. The different sequences of addition also changed the morphology of blends. For the performance of the micrographs, EPDM-MA particles were selectively extracted.

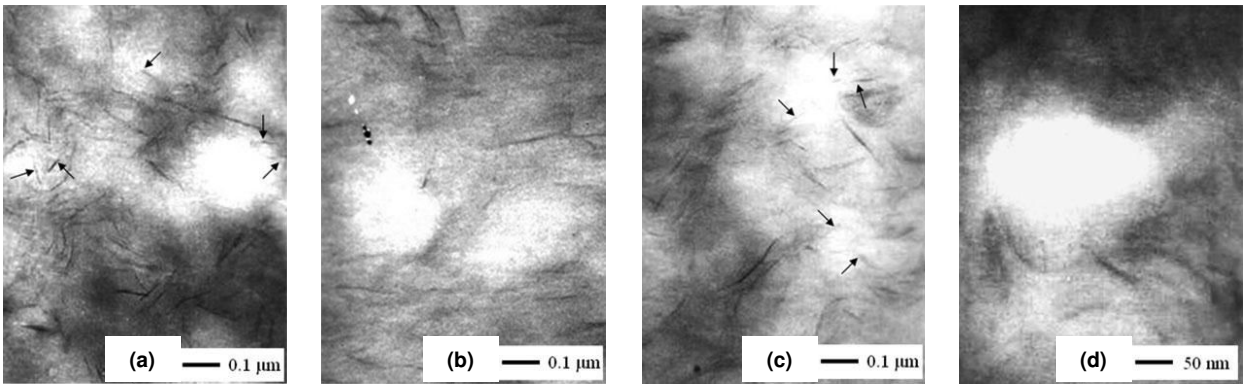

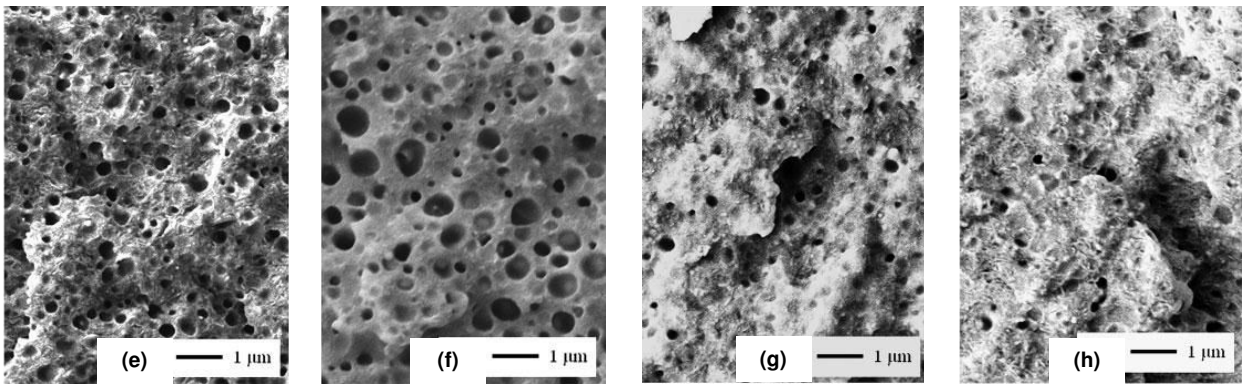

Figure 46: TEM and SEM images of blends, respectively: (a) and (e) N1; (b) and (f) N2; (c) and (g) N3; and (d) and (h) N4 [290].

For immiscible polymer blends with high interfacial energies, the lamellae of clay with polar nature usually tend to be located in the high polarity component. If the component of greatest polarity makes the most concentrated phase; the clay lamellae may be well dispersed in the matrix. But when this component is the one with the lowest concentration, the lamellae of the clay tend to form isolated structures intercalated/exfoliated at the least concentrated phase. However, in the case of blends of partial miscibility with polar component, in which the components have similar molecular structures, the interfacial energy continues to be low enough to accommodate the lamellae of clay in both phases. But for partially miscible blends with non-polar components, despite having low interfacial energy, the lamellae of clay may not have a good dispersion and mainly remain in their original not intercalated states. For this type of blend it is necessary to modify the interface with the use of a compatibilizing agent. Grafted maleic anhydride is widely used as a compatibilizing agent for PP and PE-matrix nanocomposites. It is believed that the polar characteristic of anhydride causes affinity for clay materials such that the polyolefin with maleic anhydride can serve as a compatibilizing agent among the matrix and the filler [284].

A major factor and that will also influence the location of nanofiller in the blend is the parameter of wettability of polymer particles, i.e., the filler ability to get wet by the polymer, which depends mainly on the chemical interaction between filler-polymer [280].

An interesting work to illustrate the effect of the wettability was directed by Feng et al. [291]. PP/poly (methyl methacrylate) (PMMA)/carbon black blends were produced by using three different types of different PMMA molar masses and a single type of PP, and the effect of the viscosities ratio was investigated. All components were added at the same time in an internal mixer and PMMA was the least concentrated phase. The

calculation of the wettability parameter predicted that the particles would be dispersed in PMMA phase. However, the TEM images showed that the carbon black was located on PMMA phase only in the blend with viscosities ratio close to 1. With the increased viscosity of PMMA, the filler tended to be located on the interface.

In short, it appears that the presence of the nanofillers can change, in general, the final properties of the blends. The improvement in properties of blends containing nanofillers takes place thanks to the interaction between its large surface areas and the polymer chains [277]. However, great attention should be given as regards the interaction among the fillers/phases of blend and parameters involved in the processing (to be discussed in the following sections), since these can change the location of the fillers in the blend and its state of dispersion (as shown in section 1.2.3 of this work), and in this way change any desired specific property of the blend or of one specific phase.

The production of blends containing recycled materials, a very important subject today, will be discussed in the next section.

5.1.4 - Dynamically vulcanized blends containing recycled materials

The reuse, recycling and recovery of waste of cross-linked rubber are of great scientific and technological interest. As discussed in section 1.4 of this work, there is great difficulty in recycling, as they are infusible and insoluble materials; which have difficult processing [84] due to their structure of cross-linkings. Due to the large public and environmental health problem caused by the disposal of tires, on 26 August 1999 the CONAMA (National Environmental Council) resolution n° 258/99 was approved in Brazil [292], which establishes the responsibility of the producer and importer for the total cycle of tires, i.e., the collection, transportation and disposal. Since 2002, manufacturers, importers, distributors, resellers, reformers and consumers of tires are co-responsible and contributors for its collection. From 2005, for every four produced or imported tires (new or reformed), the manufacturers and the importers must give final destination to five scrap tires [292]. In this context, many efforts have been made regarding the preparation and characterization of polymer blends containing GTR and various thermoplastics, as an alternative to recycling [293, 294].

The properties of these materials depend on the concentration of the recycled material, as well as the adhesion among phases [260, 295]. According to some authors [100], the adhesion between the GTR and the polymer matrix is usually very weak due to the three-dimensional structure of the cross-linkings, in the case of blends, in which the

GTR is just ground. Cañavate et al. [294] report that the lack of adhesion among phases is due to the large particles of GTR, their superficial characteristics and structure of cross-linkings, hindering its adsorption by molecules of the thermoplastic matrix, being that the use of only ground GTR into blends makes the processability a difficult step [296]. For Kumar et al. [6], for the production of TPVs containing recycled rubber, the addition of a raw rubber or the devulcanization (at least partial) of recycled material are prerequisites.

In order to improve adhesion and interaction among phases, many authors have used compatibilization techniques [100, 187, 244, 253, 281, 297-303], devulcanization of elastomeric phase [57, 84, 100, 117, 120, 134, 304], addition of a third elastomeric phase or replacing part of recycled rubber for a raw one [6, 187, 257, 294, 295, 305-315], superficial treatment of the rubber [178, 316], functionalization [78, 303, 305, 316, 317], filler addition [233, 252, 277-279, 281-291, 302, 313, 318, 319], beyond the dynamic vulcanization, which notoriously increases the adhesion and interaction among phases of the blends [6, 84, 120, 187, 240, 258, 263, 273, 297, 300, 320]. Additionally, the dynamic vulcanization in blends containing recycled material gives them greater added value [244].

Some works taken from the literature containing recycled materials will be presented and briefly discussed.

Cañavate et al. [294] prepared TPVs HDPE/EPDM/GTR. Figure 47a shows the composite without EPDM and peroxides, only HDPE and GTR. These two materials are incompatible due to different chemical compositions, which can be seen in Figure 47a, in which the particles of GTR appear almost isolated, without being wetted by the HDPE matrix. The addition of an elastomeric component that contains a high amount of PE improved the compatibility between HDPE and GTR, since the particles are not so isolated as they are in EPDM compound (Figure 47b). However, it can be observed that the EPDM was unable to encapsulate all the particles of GTR. The effect of encapsulation can be seen in figures 47c and 47d with the addition of the peroxides. In Figure 47d, corresponding to the composition with 0.5% Trigonox + 0.1% dicumil peroxide (DCP), the encapsulation is more visible. The fact of the GTR particles are completely encapsulated means that the EPDM formed a three-dimensional network with it, and at the same time the EPDM created a co-continuous phase with the HDPE. This effect leads to a better adhesion, and better mechanical properties [33].

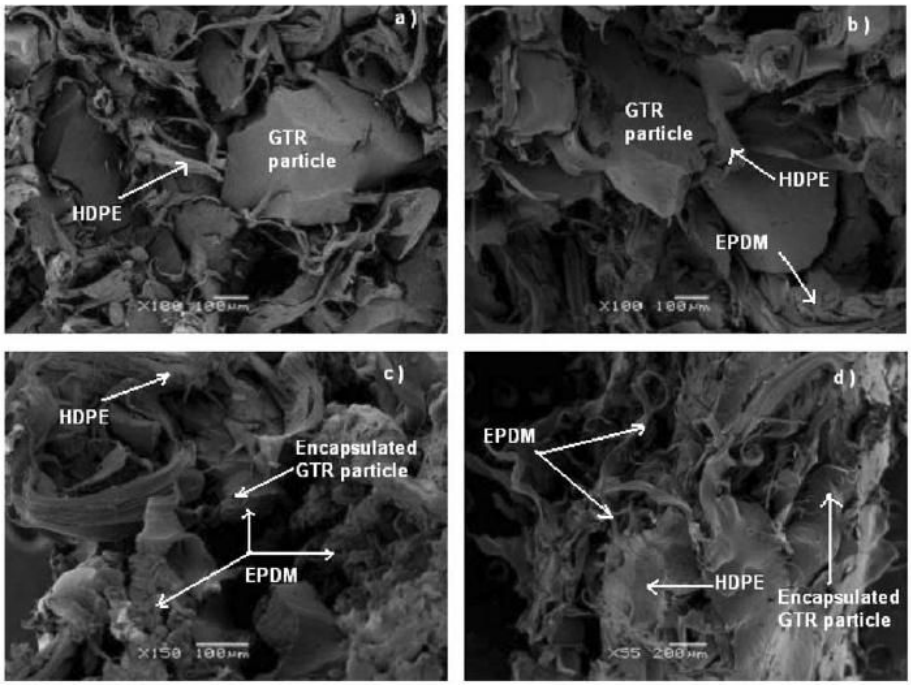

Figure 47: SEM images: (a) 40/60 HDPE/GTR, 40/30/30 HDPE/EPDM/GTR, (c) 40/30/30 HDPE/EPDM/GTR + 3% Trigonox, (d) 40/30/30 HDPE/EPDM/GTR + 5% Trigonox and 0.1% DCP [294].

Babu et al. [255] produced TPVs based on PP, etylene octene copolymer (EOC), EPDM, GTR, and dicumil peroxide cross-linking system on an internal mixer, with varied concentrations of phases. The morphologies and, consequently, the properties of the blends were changed completely with the variation in the concentration of the phases. In short, according to the authors, the state and the mode of the dispersed phase were determined primarily by the ratio of viscosities and elasticities of the components of the blend.

Grigoryeva et al. [321] produced TPEs of matrix phase recycled and raw LDPE, and dispersed phase raw BR, and analyzed the properties of both, concluding that the blends containing recycled material can be used in compositions of TPEs with useful properties. The authors produced also the same blends containing compatibilizing agents, and it was verified that the amorphous phase of the recycled LDPE was dissolved on rubber phase and a co-continuous morphology has been verified, ensuring improvement in the mechanical properties of TPEs.

Magioli et al. [296] produced blends type TPV GTR/SBR/PP and GTR/PP. According to the authors, all blends presented an excellent combination of tensile strength and stress at break, and possibility of reprocessing without depreciation of properties, which are features of TPV type blends.

Kumar et al. [6] produced blends containing GTR, LDPE and other rubbers (EPDM,

NR and SBR). Some blends have been the GTR phase mechanically devulcanized without oil (GTR^M) and with oil (GTR^{RM}). The authors observed that the non vulcanized blends containing GTR^M presented better mechanical properties due to the increased possibility of entanglement of the devulcanized GTR chains with the other phases, while the blends containing GTR^M and EPDM showed higher values of elongation at break due to greater compatibility among the phases. The dynamic vulcanization proved to be effective in improving the mechanical properties of the blends.

Hong and Isayev [120] produced blends GTR/HDPE in different concentrations in internal mixer and extruder, by using GTR, GTR devulcanized by ultrasound (DGTR) and revulcanized DGTR (RGTR). In general, the revulcanized blends and the ones produced on extruder presented better mechanical properties due to their morphologies. Figure 48 shows the SEM images of 80/20 blend produced on extruder containing GTR, DGTR and RGTR.

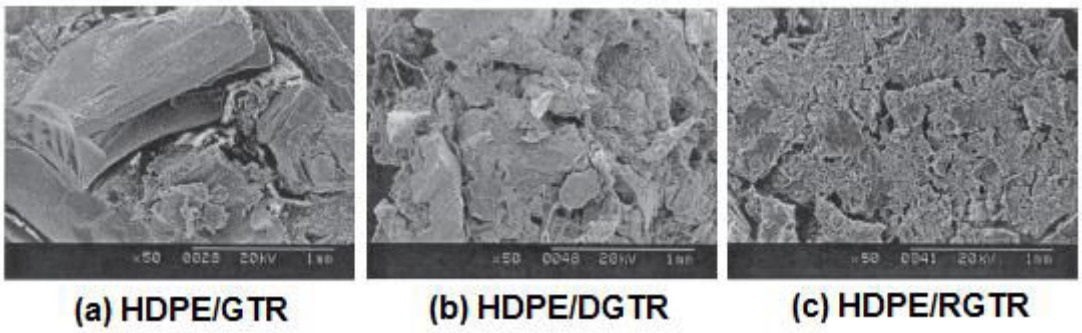

Figure 48: SEM images of blends GTR/HDPE 80/20 produced on extruder [120].

According to Figure 48, HDPE/GTR blend offers smooth surfaces, which shows lower resistance to fracture. On the other hand, the HDPE/RGTR blend presents greater roughness and porosity, and the diameter of the rubber particles are smaller. The dynamic vulcanization increased the wettability and interfacial adhesion among phases.

Similar to the previous work,, Zhang et al. [84] produced GTR mechanically devulcanized/cross-linked polyethylene (XLPE) 50/50 blends in internal mixer. The mechanical properties of revulcanized blends were higher than those of non revulcanized blends and, in general, they have increased with the increase in the number of cycles of grinding of the GTR (Figure 49). According to the authors, the increase in the number of cycles increased the breaking of cross-linkings, which increased the fluidity of the GTR and facilitated the breaks into small particles and dispersion during the production of the blends, which resulted in the increase of mechanical properties.

Ismail and Suryadiansyah [241, 242] produced RR/PP and NR/PP blends in different concentrations, being that RR is recycled NR, composed of residual dust from sanding of rubber balls and artificial eggs. The blends containing RR showed higher values of stress at break, Young's modulus, lower values of elongation at break and greater thermal stability than the blends containing NR due to cross-linkings presence in RR. According to the authors, the difference in the mechanical properties of blends containing RR is because they need more energy to the occurrence of catastrophic failure.

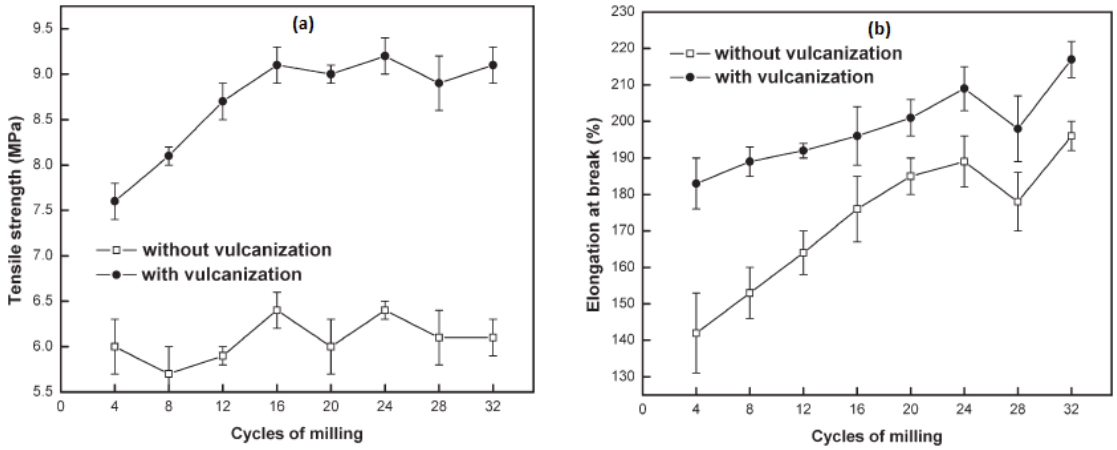

Figure 49: Tensile strength (a) and elongation at break (b) in relation to the number of cycles of the GTR of GTR/XLPE blends [84].

In the next section will be reviewed some important factors capable of influencing or even change the morphology of dynamically vulcanized blends.

5.2 - Microrheology and morphology of polymer blends

Polymer blends can have two distinct morphologies: morphology of dispersed phase and co-continuous phases, which were defined at the beginning of section 5.1. The final morphology of a blend occurs during its processing, so it is a crucial stage in getting the final desired properties.

Many factors can change the morphology of polymer blends during processing such as temperature, residence time (processing on extruders), intensity of the mixture (speed of the extruder and setting of the screw), composition of the blend, viscosities ratio, elasticities ratio and interfacial tension among the phases [322]. In this way, the final morphology of immiscible polymer blends depends on the properties of the individual components, as well as processing conditions [323, 324] (Figure 50).

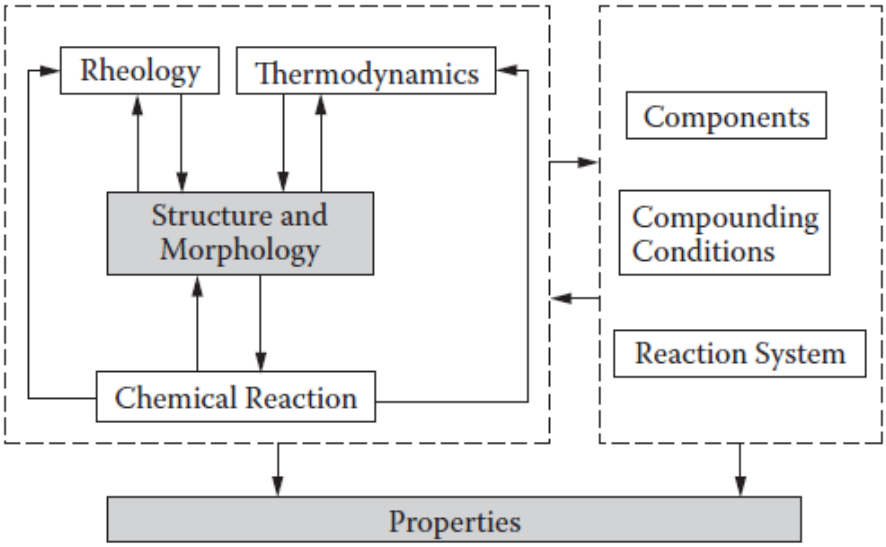

Figure 50: Complex relationship between processing, morphology and properties during the processing of reactive polymer blends [228].

An example of change in properties with the variation in the concentration of one of the phases of blend was presented on the work of Khonakdar et al. [326], who analyzed the dynamic-mechanical properties of HDPE and LDPE/ethylene vinyl acetate copolymer (EVA) blends. With the increase in the EVA content, there was a decrease in all the transition temperatures of the blend. This was attributed to the decrease of the crystallinity of the system, which increased molecular movements of the amorphous phase.

A work that exemplifies the importance of reactional system and components factors is the one of Naskar and Noordermeer [327], in which they produced EPDM/PP blends type TPV in different concentrations and with different chemical natures of various peroxides. The various peroxides used changed the cross-linking density of elastomeric phase and degrees of degradation of PP phase, which consequently have altered the physical properties of the blends. Likewise, Punnarak et al. [300] produced GTR/HDPE blends in different concentrations and different cross-linkings systems (sulphur, peroxide or mixture of the ones used before). The authors reported that the best method was by sulphur, because these blends presented greater values of resistance to impact and tensile strength, while peroxide was the worst of them. This is due to the higher cross-linking density, greater contact among the phases of blends and differences in the linkings, since sulphur produces predominantly polysulphidic links, while the peroxide C-C bonds type. He et al. [328] analyzed the properties of the same blend containing DCP and DCP+phenolic resin, and the compound containing 0.3 phr of DCP and 4 phr of phenolic resin presented the best mechanical properties due to the synergistic effect

among them. Good levels of particle dispersion of GTR and adhesion among phases were observed in the SEM images. Other works also show differences caused on the properties of TPV type blends due to the use of different concentrations of DCP [57, 310].

Processing can also alter the particle size distribution of rubber, in the case of morphology of dispersed phase. Studies show that blends produced on extruder tend to have smaller particle sizes compared to blends produced in internal mixer [120, 134, 329-331] due to the higher rate of shear during processing in extruders and intensive flow field [330]. The elastomeric phase of the blends produced on extruder can also present greater cross-linking density, as verified on the work of Sengupta and Noodermeer [329]. However, the distribution of sizes of particles is more uniform in the blends produced in internal mixer due to longer residence time and greater total shear stress, promoting the breakdown of particles [329]. According to Shahbikian et al. [330], that produced EPDM/PP blends in internal mixer and extruder, even with the shortest residence time for processing in extruders, the cure reaction occurred quickly, resulting in EPDM particles of sizes more heterogeneous and with greater cross-linking density.

The authors [329] proposed a schematic representation of the development process of morphology in twin screw extruder and in internal mixer (Figure 51), which is in accordance with the results obtained by Shahbikian et al. [330]. According to them, the development of morphology is governed by the dispersion of highly viscous rubber in molten thermoplastic matrix less viscous (in the case of work, block copolymer of styrene-ethylene/butylene (SEBS) and PP, respectively). By combining the effects of time, temperature and shearing, the matrix phase acquires elasticity and it is extruded into sheets. At the same time, there is a break of these sheets due to elongational and shear forces generated in the mixing equipment. So, there is a dynamic balance between the process of breakdown of phases and coalescence. The process also depends on composition, and will be more easily checked in blends with lower concentration of rubber due to the lower probability of coalescence.

Among other factors mentioned, the final morphology is the result of processes of coalescence and breakage of the elastomeric phase particles (in the case of blends with the morphology of dispersed phases) during processing, per schematic shown in Figure 51. In the case of dynamically vulcanized blends containing devulcanized rubber, the

devulcanization acts on the process of breaks, while the dynamic revulcanization acts on reduction of the coalescence process of particles (Figure 52) [223].

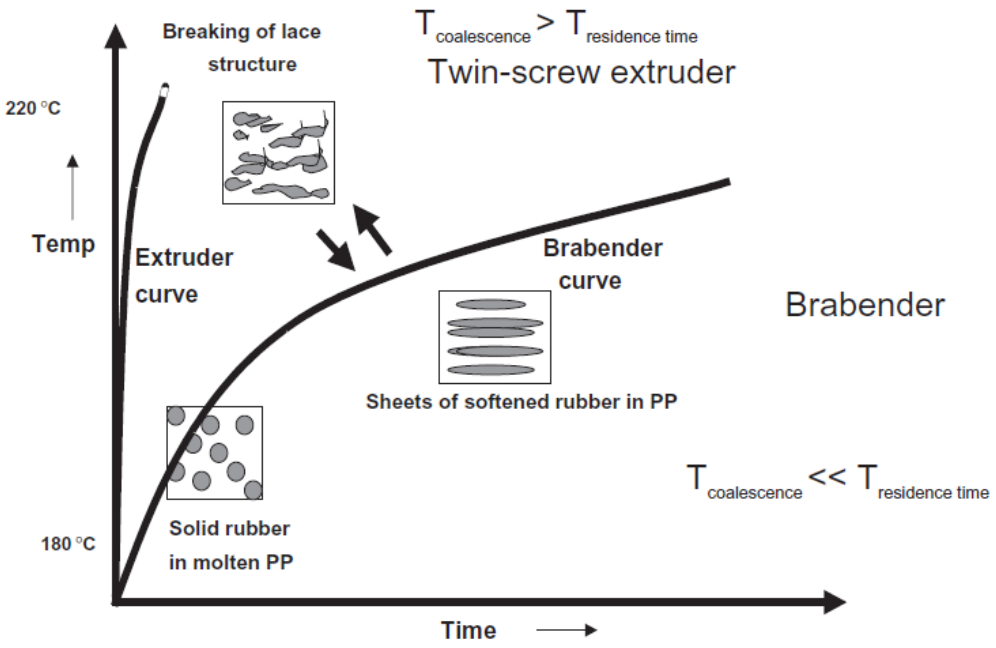

Figure 51: Schematic representation of the development of morphology of rubber/thermoplastic blends, showing the dynamic equilibrium between coalescence and breakage of rubber particles in thermoplastic matrix [329].

In short, the process of devulcanization makes fluid rubber, aiding in the process of breaking what, consequently, helps in reducing the size of the particles, increases the contact area among the phases and increases the transmission of tensions. While the dynamic revulcanization helps in stabilizing the morphology by inhibition of coalescence process among the particles of the dispersed phase [11, 223, 332].

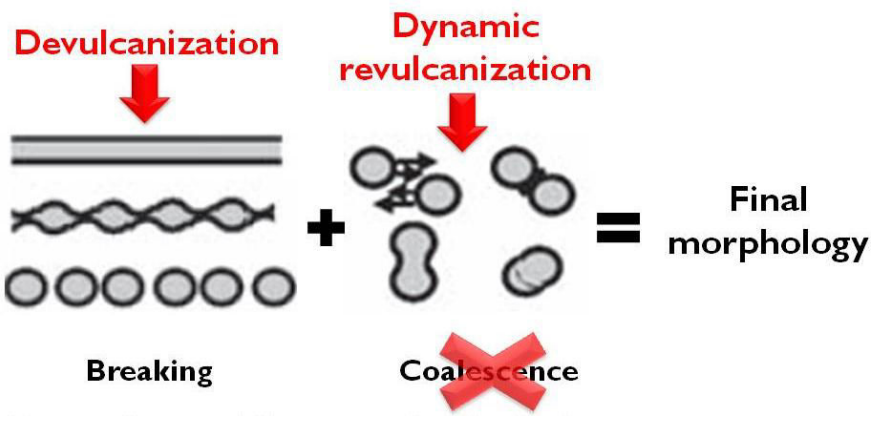

Figure 52: Morphological development mechanisms (breaking and coalescence of particles) of polymer blends during processing.

The elongation and breakage of polymeric particles suspended in another polymer under shearing flow was first studied by Taylor [333]. According to him, two dimensionless parameters that enable the prediction of morphology in the molten state are the number of Capillarity (Equation 12) and the viscosities ratio (Equation 13):

$$C_a = \frac{\sigma R}{\alpha} \qquad \text{Equation 12}$$

where σ represents the shear stress, R the radius of the particle or drop, and α the interfacial tension between the phases of the blend.

$$p = \frac{\eta_d}{\eta_m} \qquad \text{Equation 13}$$

where η_d and η_m are the viscosities of the dispersed phase and the matrix phase , respectively, as described earlier in section 3.7.

If the value of C_a is small, interfacial forces dominate and the particles acquire the shape of ellipsoids. Above a critical value $C_{a\ crit}$, the particles become unstable and break down [234].

When two immiscible polymers are mixed to form a blend, in accordance with the principle of minimum dissipation of energy, it is expected that the most viscous polymer forms the dispersed phase and the less viscous forms the matrix phase. When this principle is satisfied, means that the viscosities ratio (Equation 13) was the predominant factor in determining the state of dispersion of the blend [334].

Grace [335] built a chart from the number of critical capillarity depending on the viscosities ratio under two flow types: simple shear flow and hyperbolic flow (elongational) (Figure 53). According to the author, the drops are stable when the C_a value is less than the critical value; the elongation and breakages occur more easily when the viscosity ratio is between 0.25 and 1 for shear flow, while the elongational flow is more effective for breakage and dispersion. For viscosities ratios between 4 and 5, it is not possible to break particles in simple shear flow.

However, as previously mentioned, Oderkerk and Groeninckx [229] obtained EPDM/Nylon blends with rubber particles finely dispersed in a matrix with $p \geq 8$ due to reduction in interfacial tension and coalescence suppression by reactive compatibilization and dynamic vulcanization.

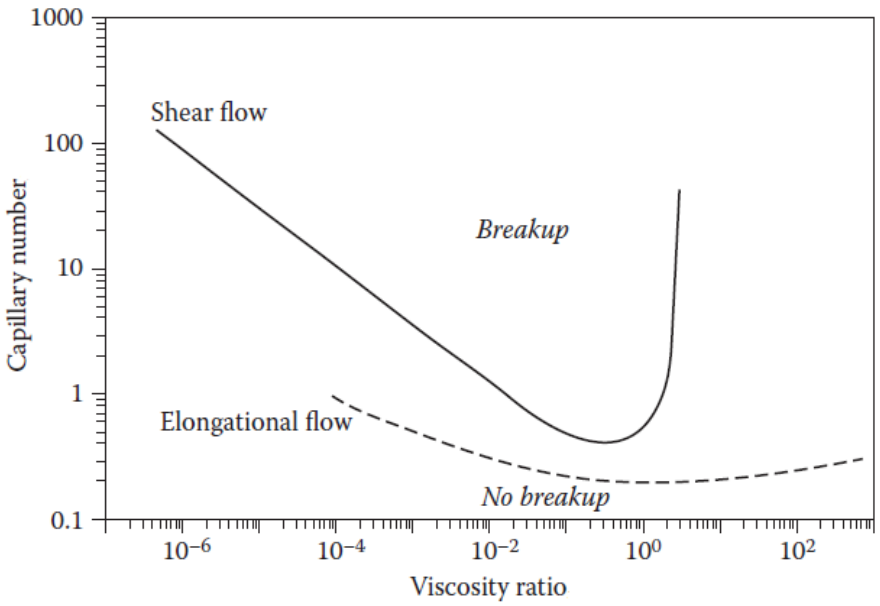

Figure 53: Number of critical capillarity *versus* viscosities ratio in shearing and elongational flow [335].

Immiscible polymer blends, especially the dynamically vulcanized ones, usually undergo a process of inversion of the phases during its processing. To study the development of the phase morphology and predict the inversion phase region in immiscible polymer blends, Avgeropoulus et al. [336] developed an empirical model based on torque ratio in internal mixer and volumetric fraction of each phase (Equation 14). Jordhamo et al. [337] proposed a similar equation (Equation 15), based on the viscosities ratio:

$$\frac{\emptyset_1}{\emptyset_2}.\frac{T_2}{T_1} = X \qquad \text{Equation 14}$$

$$\frac{\emptyset_1}{\emptyset_2}.\frac{\eta_2}{\eta_1} = Y \qquad \text{Equation 15}$$

which results in the following variants morphologies:

X, Y > 1 - Phase 1 is continuous or matrix and phase 2 is dispersed.

X, Y < 1 - Phase 2 is continuous or matrix and phase 1 is dispersed.

X, Y = 1 - Two phases are continuous or region of inversion phase.

Where Φ_1, Φ_2 are volumetric fractions, T_1, T_2 are measures of torques at a same temperature and η_1, η_2 are viscosity values for phases 1 and 2, respectively [255].

In addition, for dynamically vulcanized blends, a factor of utmost importance is the characterization of their vulcanization kinetics (according to section 1.4.2 of this work),

and the adequacy of the system while processing so that these characteristics are respected. The evolution of morphology of these blends according to rheological characteristics of rubber phase of blend will be examined in the following sections.

As mentioned, the stage of dynamically vulcanize processing is of extreme importance and all aspects involved should be carefully analyzed and optimized, as they may change the final morphology of blends and, with it, completely alter their final properties [338]. An essential factor is, first, the choice of the appropriate screw profile, in case of blends produced on extruder. This factor will be analyzed with greater detail in the next section.

Another very important factor is the choice of the temperature (or temperatures of each zone in the case of extruder) during processing, which should be close to the melting temperature of the thermoplastic phase (or greater) [249], and be able to activate the vulcanization reaction of the elastomeric phase [251]. It is known that the behavior of vulcanization of the elastomeric phase varies according to the adopted temperature, besides that it should not be high enough for that, combined with the high shear rates involved in the process (especially in twin screw extruders), high level of degradation occurs in both phases of the blend.

For the case of blends in which all phases are added together in the extruder in one feeder, studies show that as soon as the complete melting of the thermoplastic phase is reached, the blend reaches quickly its final morphology [246, 339] due to generated interfaces among phases. According to Covas et al. [340], increasing in the interfacial area raised soon after the melting of the thermoplastic induces chemical conversion and the evolution of morphology. Therefore, the choice of the parameters of the processing, the number of feeders to be used depending on the screw profile adopted is a factor of great importance.

Another very important factor during processing is the degree of filling of the channels within the extruder due to the amount of shear transference to the molten. Generally, with the reduction of the degree of filling, the effective average depth of the channel to be taken into consideration becomes smaller and thus results in higher rates of local apparent shear [330].

The literature presents some works in which the processing variables are changed and analyzed [84, 117, 249, 263, 304, 339, 341-348], and some of them are presented below.

In a study done by John et al. [342], the rheological behavior of EVA/HDPE polymer blends was checked in relation to variations in the ratio of the components, shear rate,

temperature, presence of compatibilizing agents and the occurrence or not of dynamic vulcanization, as well as the variation of the concentration of additives. In short, it was verified that all the studied variables altered the viscosity of blends and, with it, have changed their final morphology.

In the same way as for nanocomposites there is an optimum concentration of nanofillers, Joseph and Thomas [345] showed in their work that there is an optimum condition for processing of TPEs. They analyzed different parameters of processes involved in the production of polybutadiene (PB)/PS blends in different concentrations and observed that, for each system, there is an optimum condition, and that it does not mean to be the limit. For example, they produced blends in different concentrations in internal mixer and varied the speed (20, 40 and 60 rpm), the mixing time (30 s, 1, 2, 4, 8, 15 and 25 min) and temperature (140, 180 and 200°C). For the 80/20 blend, optimal processing conditions were 60 rpm, 180°C and 8 minutes.

Zhang et al. [84] produced blends type TPV GTR/residue of XLPE 50/50 (with GTR mechanically devulcanized) in internal mixer at various temperatures. As well as in the work of Joseph and Thomas cited previously, there seems to be an optimum processing temperature, according to the mechanical properties of the blends produced at different temperatures (Figure 54). According to the authors, at low temperatures the vulcanization was not achieved, resulting in low values of mechanical properties.

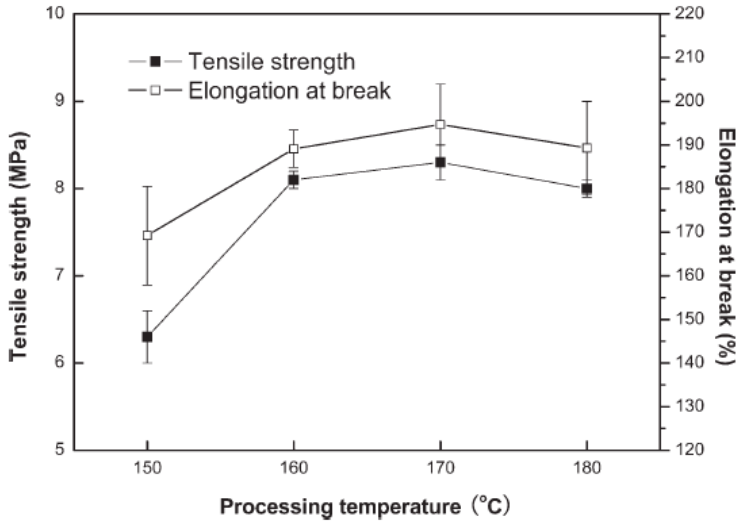

Figure 54: Effect of processing temperature on the mechanical properties of the blends GTR/XLPE [84].

Kalkornsurapranee et al. [346] analyzed, among others, the influence of mixing parameters (in internal mixer) in the production of TPVs NR/thermoplastic polyurethane (TPU) on their mechanical properties. It was verified that the tensile

strength decreased with the increase in temperature and mixing time due to degradation of polymeric chains of NR. Another important result was that the speed of the rotors influenced directly the final morphology of blends. Initially, the tensile strength increased with the increase in the speed of the rotors to 100 rpm, by decreasing then with higher speeds, corroborating with the work of Joseph and Thomas [345]. High shear rates during processing lead to mechanical degradation of NR due to high shear rates between the chains. On the other hand, low shear rates produce blends with poor mechanical properties due to insufficient reduction of particle size and its distribution on TPU matrix.

Yquel et al. [339] analyzed the effects of processing conditions on chemical conversion and evolution of morphology of PA6/PE blend along the twin screw extruder. According to them, by increasing the speed of the screw or by using more high-shear elements, the melting was accelerated, promoting greater speed of compatibilizing reactions; both have strong effect on the distributive and dispersive mixing rates and intensity. The melting of the thermoplastic is a very important stage, because only after its complete melting the vulcanization reaction is initiated, thanks to the increase of the interfacial area among the phases. The results were corroborated by other studies available in the literature [117, 340].

Scaffaro et al. [304] produced blends GTR/PE residue (w-PE - composed of HDPE and LDPE) in different concentrations in extruder, ranging some process parameters such as temperature, residence time and method for producing specimens for tensile test. The authors found that the temperature was the most important parameter, since high temperatures can increase the degree of devulcanization of GTR and reduce the incompatibility among the phases, but can also cause carbonization of this phase and increase the filler-filler effect, which can increase the viscosity, the modulus, stress at break and decrease the elongation at break. However, the variation in residence time did not cause major changes in the final properties of the blends. The production of specimens by injection resulted in blends with better mechanical properties than by compression method, due to greater mixing of the phases during the injection process and back pressure have improved the quality of the samples.

Section 5.3 will present the stages involved during the evolution of morphology of dynamically vulcanized blends and the influence of processing parameters on the development of the final morphology of these blends.

5.3 - Evolution of morphology of dynamically vulcanized blends during processing

Figure 55 shows in a schematic way the transformation the morphology of dynamically vulcanized blends during processing.

Very simplified, in general the blend completely changes its morphology, from co-continuous to dispersed phase. However, so the blend presents typical final properties for noble uses, the stage of processing must be carefully analyzed and optimized. In the case of using an extruder, the analysis becomes more complex because of the large number of variables involved, but at the same time it becomes a big advantage in the improving of the technique.

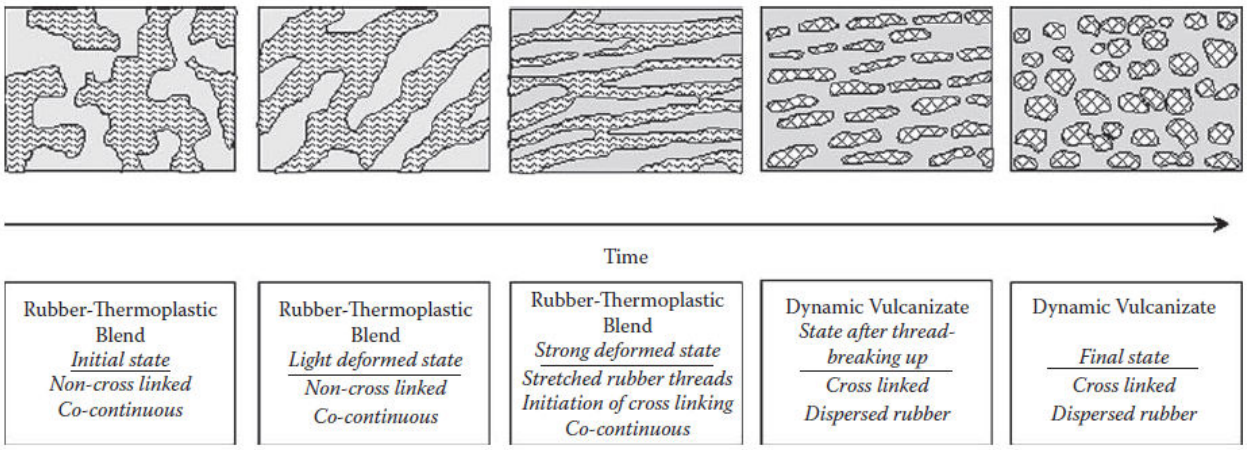

Figure 55: Schematic morphology transformation during the dynamic vulcanization of polymeric blends [228].

Figure 56 shows the stages involved during production of a dynamically vulcanized blend in extruder containing two feeders, in which the phases of the blend are added separately in each of them.

The profile presented has two feeders. In the case of blends in which the elastomeric phase was previously mixed to vulcanization additives, this will be added in the second feeder, as occurred in this work. In the case of elastomeric phase not be previously mixed to additives, the two phases of the blend can be added together in the same feeder (feeder 1), while the additives are added in the second feeder (feeder 2). The detailed explanation of the stages involved in the production of dynamically vulcanized blends in relation to the extruder zones that will be made below refer to the first case.

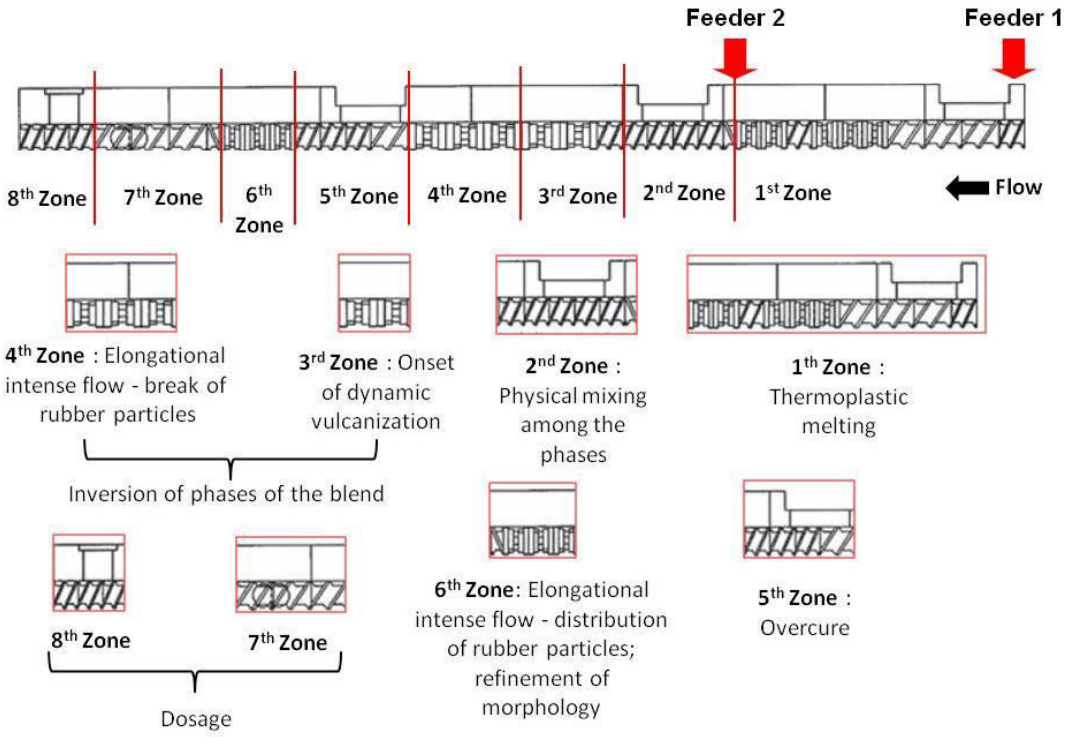

Figure 56: Extruder zones according to the stages involved in the production of a TPV, modified from [228].

In the feed zone of the extruder is added only the thermoplastic. In this zone are used screw elements of big pitch, a quantity of elements capable of providing a sufficient residence time for the complete melting of the material. Shortly thereafter, mixing blocks are used for homogenization of the melting. Then, at the beginning of the zone 2 in Figure 56, the elastomer (previously mixed to cross-linking system) is added. So, in the zone 3 occurs the beginning of vulcanization reaction (long enough to reach the value of ts_1 of vulcanization reaction of elastomer since its introduction in the zone 2 up to zone 3 of extruder), and are therefore required the use of blocks to the mixture. Due to the high elongational flow in this zone (use of mixing or kneading blocks), the rubber along vulcanization process can deform (due precisely to the three-dimensional structure formation of cross-linkings and consequent increase in viscosity of the blend [273]) enough for break of their particles in other smaller than the ones before [270] and phase inversion occurs. According to Harrats et al. [228], the elastomeric phase deforms until it reaches a critical tension, when it breaks up into small particles. As the values of ts_1 obtained from rheological analysis of rubbers are usually very small, it can be less than the residence time required for the melting and homogenization of thermoplastic, so for this reason rubber is added to the process separately, in a second feeder. The residence time of the elastomer since its introduction in the extruder until the end of the

zone 4 is proportional to the t_{90} value of vulcanization reaction, while the residence time of the blend between zones 3, 4 and 5 is related to overcure (Figure 57). The biggest changes of morphology occur in the first high-shear region, in which both phases are together [246, 349-351]; in the case of work in question, this area refers to the zone 3.

In zone 6, cross-linked rubber particles now have a very high viscosity and elasticity, and it occurs only the distribution of the particles in the matrix, improving macroscopic homogeneity, so it is necessary the use of mixing elements. It must be pointed out that the dispersion process occurs instantly with the vulcanization reaction and both processes are influencing each other. The rapid increase in the cross-linkings of rubber also leads to an increase in the surface tension of the elastomeric phase. Cross-linkings and superficial tension increased will reduce the driving force for the coalescence and therefore the characteristic of the particles of vulcanized rubber phase will be preserved, even in a new mixture after the completion of the cross-linking process [228].

The increase in interfacial tensions as a result of cross-linkings and the high elasticity of the particles produces the relaxation of the deformed structures; in an ideal case, spherical particles are formed. Due to the high viscosities ratio, elastomeric cross-linked particles can only be distributed, and no longer dispersed on a new mixing cycle [228].

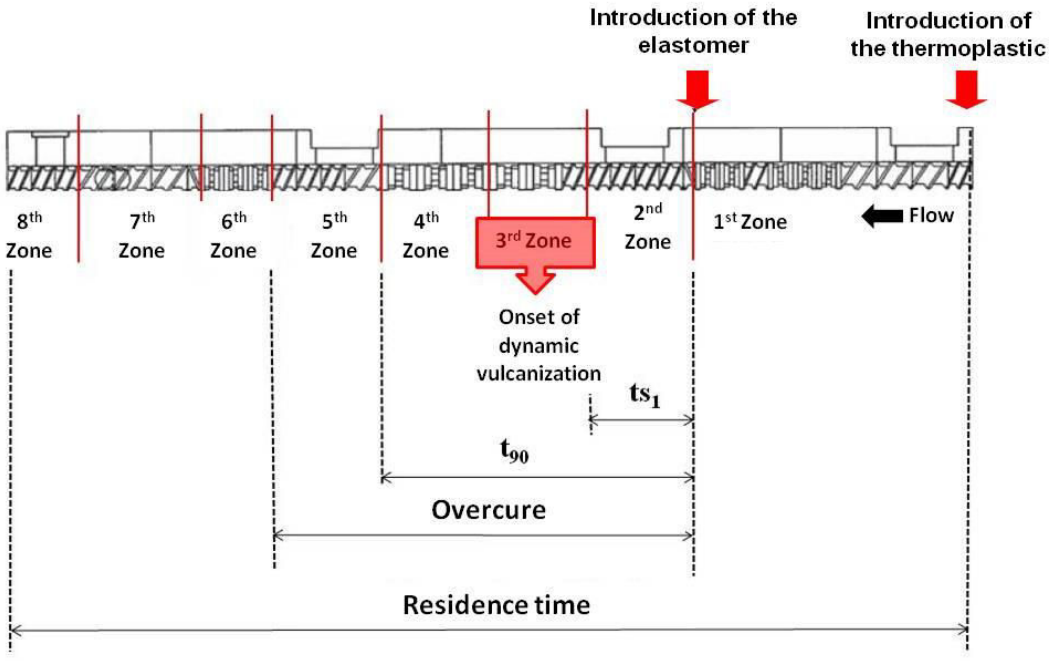

Figure 57: Kinetics of vulcanization on elastomeric phase during the processing of TPV type blends in extruder, modified from [228].

Zhang et al. [84] presented in their work a diagram showing the dynamic vulcanization process (Figure 58). Soon after the end of the dynamic vulcanization, vulcanized rubber

particles present a high surface tension, which carries on agglomerate. Therefore, for them to be undone, it is necessary the application of high shear rates, which are generated due to the presence of mixing blocks in processing performed in extruder, as zone 6 in Figure 56.

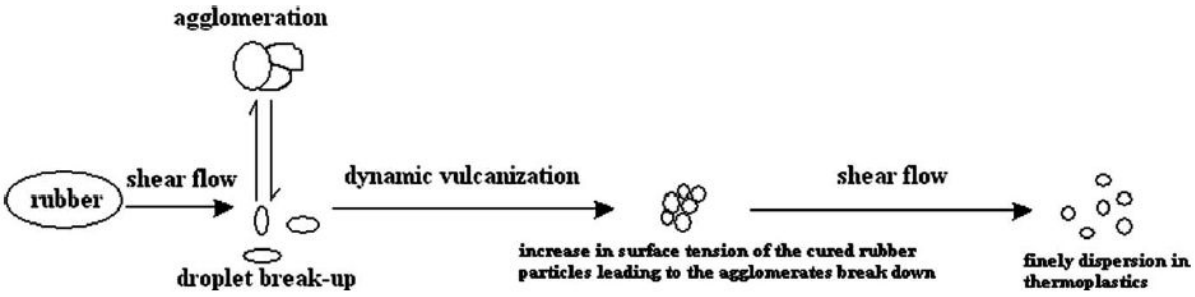

Figure 58: Schematic diagram describing the dynamic vulcanization mechanism [84].

A work that demonstrates the importance of observation and adequacy of vulcanizing kinetics of the elastomeric phase to the characteristics involved in the processing of dynamically vulcanized blends is of Kalkornsurapranee et al. [346]. According to the authors, when the value of ts_1 of the elastomeric phase is too small, the kinetics of vulcanization is beyond the time necessary for the dispersion of particles, leading to an increase in the size of the particles and changing the final morphology of blends (blend studied by the authors was the NR/TPU in different concentrations). The model proposed by the authors is present in Figure 59.

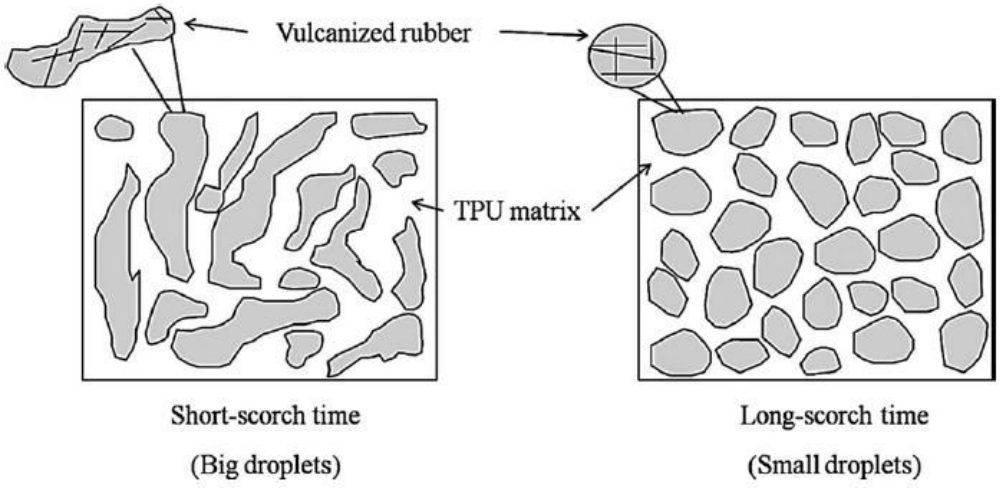

Figure 59: Proposed model for the morphology of dynamically vulcanized blends with different values of scorch time [346].

The authors [228] produced TPVs ethylene propylene rubber (EPR)/PP 60/40 using

peroxide as a cross-linking system on twin screw extruder with L/D ratio of 30. The viscosities ratio was approximately 1.5.

Figure 60 shows the differences in morphology between the non vulcanized blend (left column) and dynamically vulcanized blend (right column), revealing the changes during the course of the process. It is interesting to note that the general character of the phase morphology of non vulcanized blend does not vary. After passing through zones of high intensity mixing screw, there was no variation in the co-continuous morphology. Due to viscosities ratio and the composition, the co-continuous morphology is a dominant feature. Elastomeric not cross-linked phase might be more deformed by the application of shear stresses, but co-continuous morphology persisted [228].

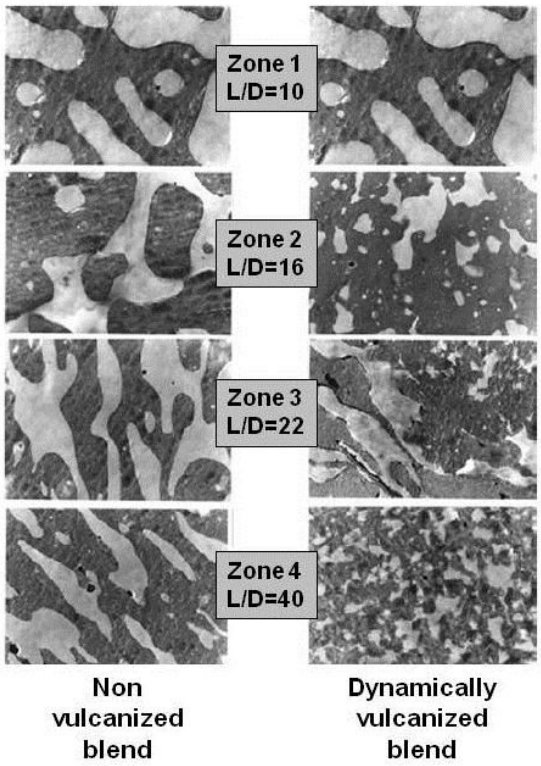

Figure 60: TEM images of non vulcanized blend (left) and dynamically vulcanized blend (right) monitored along the extruder screw [228].

The cross-linking reaction was initiated on zone 3, associated with the transformation of phase morphology. The initial morphology of co-continuous phase with large areas of PP and EPR was changed to particle-matrix morphology (dispersed phase). Due to cross-linking reaction, the elastomeric phase and system viscosities increased, which is a precondition for occurrence of the specific breakage mechanism [228].

The average particle size of EPR of 1 µm could be achieved under appropriate

conditions of processing. The residence time measured for the continuous dynamic vulcanization process was approximately 30 seconds, which was long enough for the cross-linking process and the transformation of the blend morphology.

Due to differences in morphology, the blends also showed significant differences in their mechanical properties. As can be seen from the behavior of a stress-strain curve (Figure 61), there was an increase both in stress and elongation at break for vulcanized blends. While the elongation at break increased from 350% to around 600%, the stress at break of vulcanized blend has reached the value of 24 MPa, six times greater than the value of the non vulcanized blend. In addition, EPR/PP vulcanized blends are highly transparent and have excellent processability, features which are desirable in the production of films or thin-walled products [228]. These results were supported by the work of Covas et al. [340].

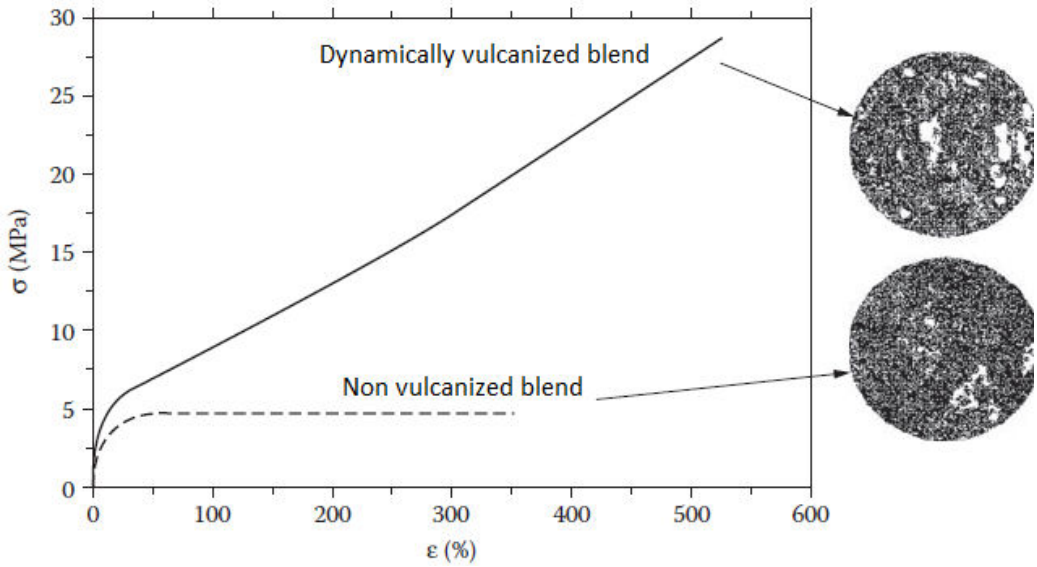

Figure 61: Stress-strain behavior of non vulcanized and dynamically vulcanized blends EPR/PP 60/40 [228].

Antunes et al. [188] investigated the development of morphology and phases inversion during the processing of vulcanized blends EPDM/PP. The evolution of one of the blends produced is in Figure 62, and phase inversion can be clearly observed. It was started shortly after the addition of the reticulation system (45 s) with the formation of a co-continuous phase, and the EPDM phase, which initially was the matrix phase, became then the dispersed one. Using a low EPDM molar mass and increasing the viscosity of the PP, the authors found that there has been acceleration in the development of morphology, and that the phase inversion occurred in smaller times, showing that the viscosities ratio affects the development of morphology during the

reaction. However, when the authors varied the average molar mass of EPDM, it was verified that the cross-linking density increased with increasing the molar mass. The composition of the blend influenced the final morphology, but caused minor effect on morphological development mechanism.

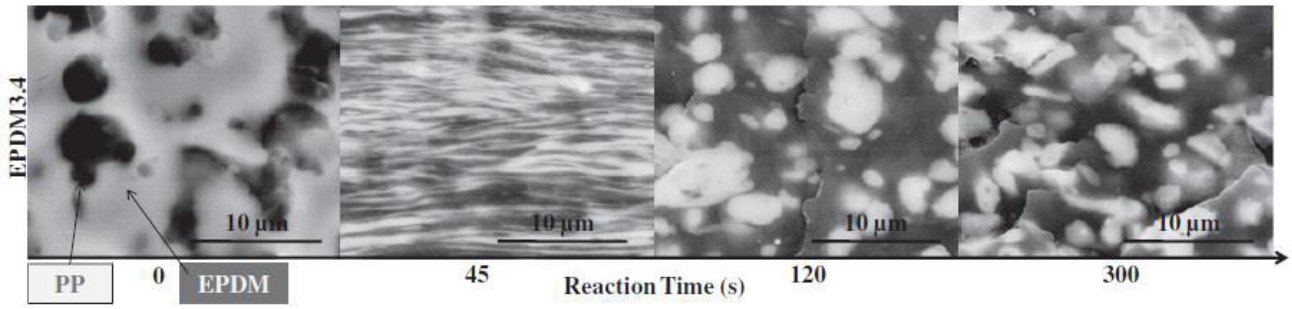

Figure 62: SEM images of vulcanized blend EPDM/PP 50/50 collected to 0, 45, 120 and 300 s mixture in internal mixer. Modified from [188].

Based on the findings, the same authors [188] proposed a mechanism of phase inversion driven by formation of cross-linkings (Figure 63).

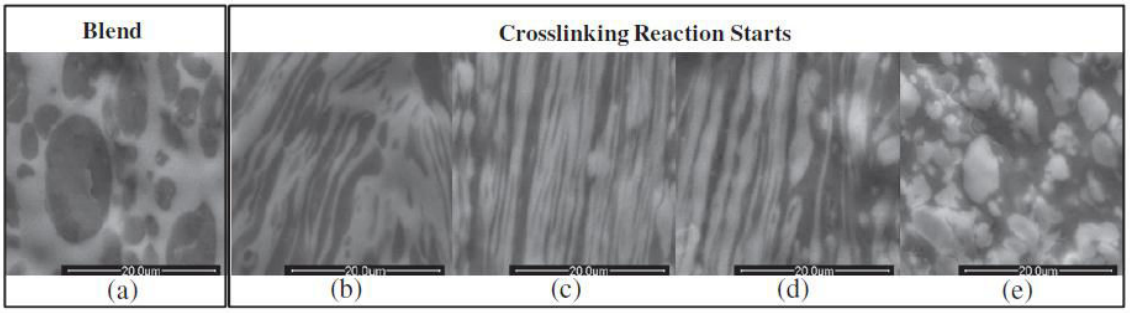

Figure 63: Morphological development mechanism proposed for the phase inversion led by formation of cross-linkings [188].

The mechanism can be described by the following stages [188]:

- before the addition of the reticulation system (Figure 63a);
- after adding the system, so that the cross-linking system comes into contact with the EPDM and the reaction starts immediately. EPDM particles begin to deform, while the PP begins to coalesce and becomes the continuous phase (Figure 63b);
- PP becomes continuous phase with the advancement of reaction; shear and elongation stresses increase, resulting in greater elongations of both phases and in the formation of lamellar structure (Figure 63c);
- EPDM is increasingly deformed and begins to break up due to capillary instabilities

(Figure 63d);

- finally, PP becomes the matrix phase and EPDM the dispersed phase (Figure 63e).

Machado and van Duin [352] analyzed the properties of EPDM/HDPE TPV type blends and found that, the higher the content of EPDM, the greater the viscous dissipation, the higher the melting and, consequently, the greater the rate of cross-linking.

Van Duin and Machado [246] studied the dynamic vulcanization reaction of EPDM/HDPE 50/50 blend through the withdrawal of peer-to-peer samples on twin screw extruder during processing. According to the authors, the cross-linking of EPDM phase began when the HDPE still was not fully melted, and the final morphology of blends was reached very quickly. The phase inversion occurred due to formation of cross-linkings.

To sum up this section of the work, it was possible to observe the importance of choice of processing parameters of TPV type blends, as well as the prior knowledge of the kinetics of vulcanization of the elastomeric phase and the union of these during processing, to obtain blends with refined phase morphology, good dispersion and particle distribution of vulcanized elastomer in the thermoplastic matrix.

From this point on, will be discussed the experimental aspects related to Stages 2 and 3 of the project.

STAGE 2: Analysis of the best processing conditions of dynamically revulcanized blends

6 - MATERIALS AND METHODS

6.1 - Materials

6.1.1 - Phases of the blends

For the production of dynamically revulcanized blends, it was used as the thermoplastic phase the processed HDPE (as previously described in section 2.2.8) and GTR5.5+ad. The GTR was devulcanized by 5.5 min as described in section 2.2.2. The homogenization and additivation of the elastomeric phase will be described in the section 6.2.1.

6.2 - Methods

The analyses performed during the Stage 2 of the project followed the flowchart shown in Figure 64.

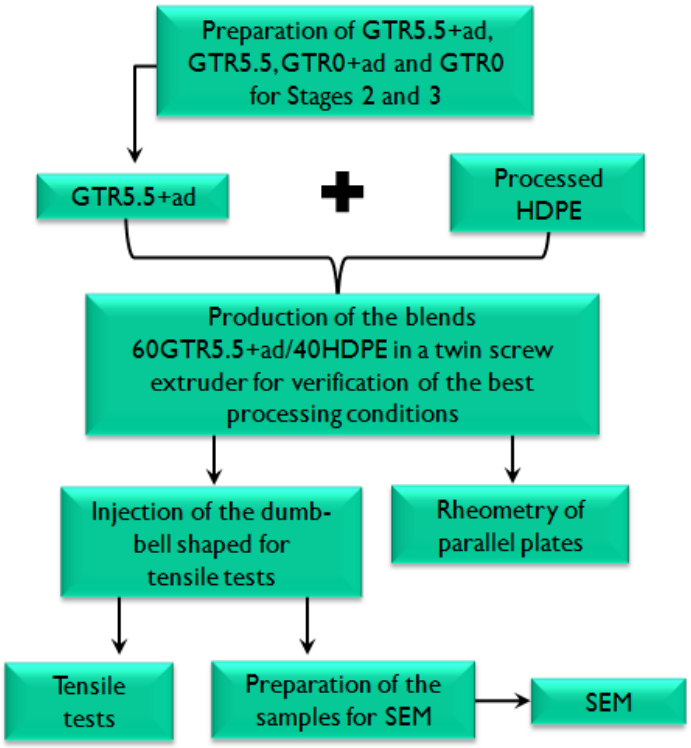

Figure 64: Flowchart of activities performed during Stage 2.

6.2.1 - Homogenization and additivation of GTR

About 5 kg of GTR5.5 were homogenized and mixed with vulcanization additives as described in section 2.2.3 for using in the production of dynamically revulcanized blends. Other 5 kg GTR5.5 have just been homogenized as the same procedure for using in the production of non revulcanized blends, with the purpose of analyzing the effect of dynamic revulcanization on the properties of the blends.

Shortly after the process, the resulting tacky rubber sheets were cut manually (dimensions of approximately 3 mm x 3 mm) for using in the production of blends in twin screw extruder.

In order to analyze the influence of devulcanization of elastomeric phase on final properties of blends, it was also produced blends containing non devulcanized GTR (GTR0). Even though the GTR0 is a powder, same procedures were adopted, including mixing with vulcanization additives (procedure described in section 2.2.3).

GTR5.5+ad was used in Stages 2 and 3; GTR5.5 was used in Stage 3; GTR0 and the GTR0+ad were used in Stage 3. In the flowchart of activities performed during Stage 2 shown in Figure 64, this was termed as "Preparation of GTR5.5+ad, GTR5.5, GTR0+ad and GTR0 for Stages 2 and 3".

6.2.2 - Production of the blends in twin screw extruder

Blends were prepared in a twin-screw extruder of type Process 11 Thermo Scientific with 2 different feeding modes (Figure 65).

The temperatures of the barrel zones were fixed at 180°C, except the third zone for the second feeding mode (Figure 65b) whose temperature was fixed at 120°C to facilitate the introduction of the rubber phase. The effects of screw speed and feeding mode were studied with blends composed of 40 wt% of HDPE and 60 wt% of GTR5.5+ad. The screw speed was 100, 150, 200, 250 and 300 rpm, respectively. The blends produced in the extruder through feeding mode 1 were denoted by the corresponding screw speed in rpm, and those produced through feeding mode 2 were designated as the corresponding screw speed in rpm followed by 2.

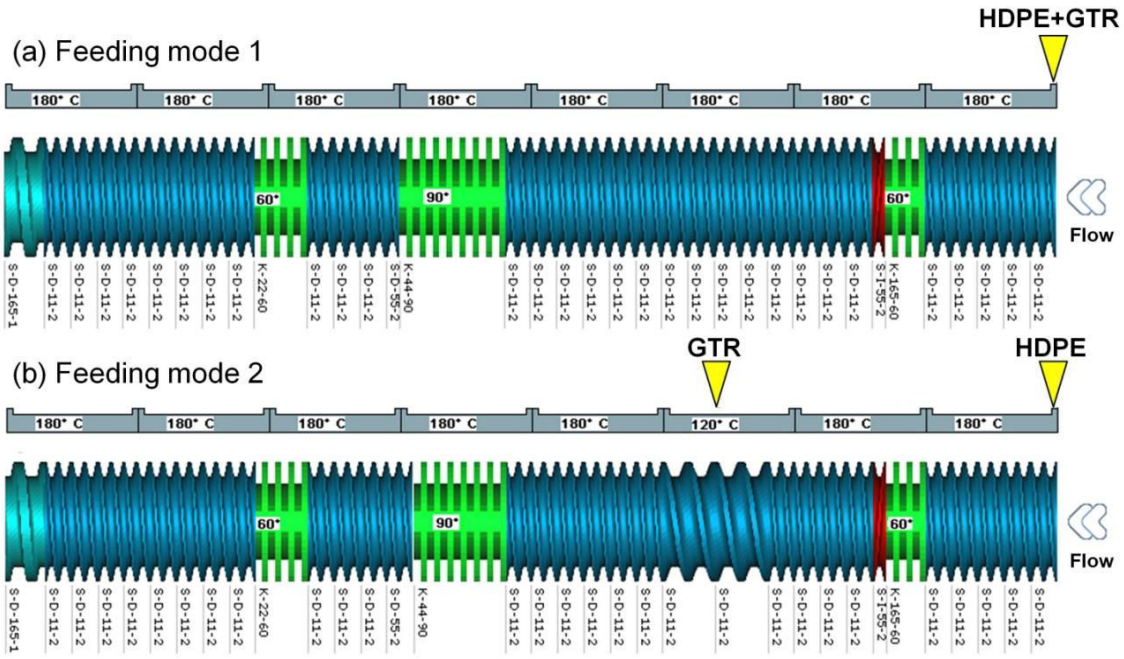

Figure 65: Two different feeding modes used for the preparation of the blends: (a) Feeding mode 1: both HDPE and GTR5.5 were added in the same feeder; (b) feeding mode 2: the HDPE was added in the first feeder and the GTR5.5 in the second one. The screw channel in the region of the second feeder was deeper and wider to facilitate the GTR5.5 feeding.

6.2.3 - Injection of specimens for tensile tests

The materials were taken directly from the extruder die and were injected using a micro injection molding machine 12cc Explore. The temperature of the injection unit was 180°C and that of the mold was 45°C. The material inside the mold was maintained at 15 bars for 10 s. The mold dimensions were based on ASTM D 412 type A.

6.2.4 - Tensile tests

The tensile properties of the blends were evaluated by using a dynamometer MTS Systems Qtest 150 Elite. The rate of grip separation was 50 mm/min.

6.2.5 - SEM

A Jeol JSM-6490LJ Scanning Electron Microscope (SEM) was used to characterize the morphology of the blends. The injected molded samples for the tensile tests were fractured in liquid nitrogen and the GTR phase was selectively extracted by cyclohexane at 70°C for 12 min. The samples were dried in a vacuum oven at 100°C for 30 min and then coated with a mixture of gold and palladium (80 and 20%,

respectively) by using a sputter coater Fine Coat Ion Sputter JFC-1100.

Different micrographs were taken for each blend and were analyzed by the image analyzer software ImageJ to determine the diameter of each particle. At least 100 particles of each blend were analyzed. The number average diameter (D_n) and the volume average diameter (D_v) were calculated according to Chen et al. [353]. More information about the mentioned method can be found in the work of Mani et al [285].

6.2.6 - Rheometry of parallel plates

Rheological properties of the blends were analyzed by oscillatory rheometry in a parallel plate rheometer Anton Paar CTD450 (diameter 25 mm, gap 1.3 mm, 1 % of strain at 180°C). Frequency sweep experiments were carried out in the linear viscoelastic range to characterize the viscoelastic properties of the blends. The frequency ranged from 0.1 to 100 rad/s and pre-strain sweep tests were performed to determine the linear viscoelastic range of the blends.

7 - RESULTS AND DISCUSSION

This stage of work was carried out in order to verify what the best conditions for processing the analyzed system are. The literature presents several works on dynamically vulcanized blends processed on extruders, with a wide range of extrusion speeds used during processing, as shown in Table 7, in addition to being different systems from the one studied in this work. Then, as each system is unique, it was decided to check what the best conditions for the system in question are.

Table 7: Extrusion speeds used in the processing of some dynamically vulcanized blends found in the literature.

Polymer blend	Extrusion speed (rpm)	Reference
Epoxidized natural rubber (ENR)/polyvinyl chloride (PVC)	10	[341]
Nitrile rubber (NBR)/PP	60	[354]
EPDM/Nylon 6	80	[229]
EPDM/Nylon 6	80	[355]
GTR/PP	100	[297]
EPDM/PP	100	[330]
GTR/HDPE	100	[120]
EPDM/PP	80-125	[249]
EMA/PP	150	[347]
GTR/PP	150	[134]
EPDM/iPP	150	[356]
EVA/PP	160	[348]
EPDM/HDPE	200	[246]
EPDM/HDPE	290	[352]
EPDM/PP/óleo	350	[329]
EPDM/PP	600	[252]
EPDM/PP/OMMT	800	[319]

The choice of temperatures used in each zone of the extruder was resulting also from literature. One of the conditions of dynamically vulcanized blends processing is to be processed at temperatures above the thermoplastic phase melting. The recommended temperature profile, according to the technical data sheet of HDPE used [203], is from 160 to 230°C. According to the TGA results of GTR5.5 (section 3.5), it was found that the thermal degradation temperature of the NR present in the GTR is 290°C.

Also according to Kalkornsurapranee et al. [346], the ts_1 value of elastomeric phase of TPV type blends is one of the most important factors that affect the final properties of this blend. The results obtained in their work show that, when the ts_1 value is small, the kinetics of vulcanization is beyond the time necessary for the dispersion of particles, which results in large particle sizes and poor dispersion. It is known that the ts_1

value of GTR tends to decrease with increasing the adopted temperature during vulcanization [223]. So, based on all these aspects, was adopted the processing temperature of 180°C in all zones of the extruder during processing.

7.1 - Tensile properties

Figure 66 compares the tensile properties of the blends between feeding modes 1 and 2. Overall, the effects of screw speed on the mechanical properties are not significant. Moreover, the mechanical properties of the blends are far below those of classical TPVs, probably because of the poor compatibility and adhesion between GTR5.5 and HDPE.

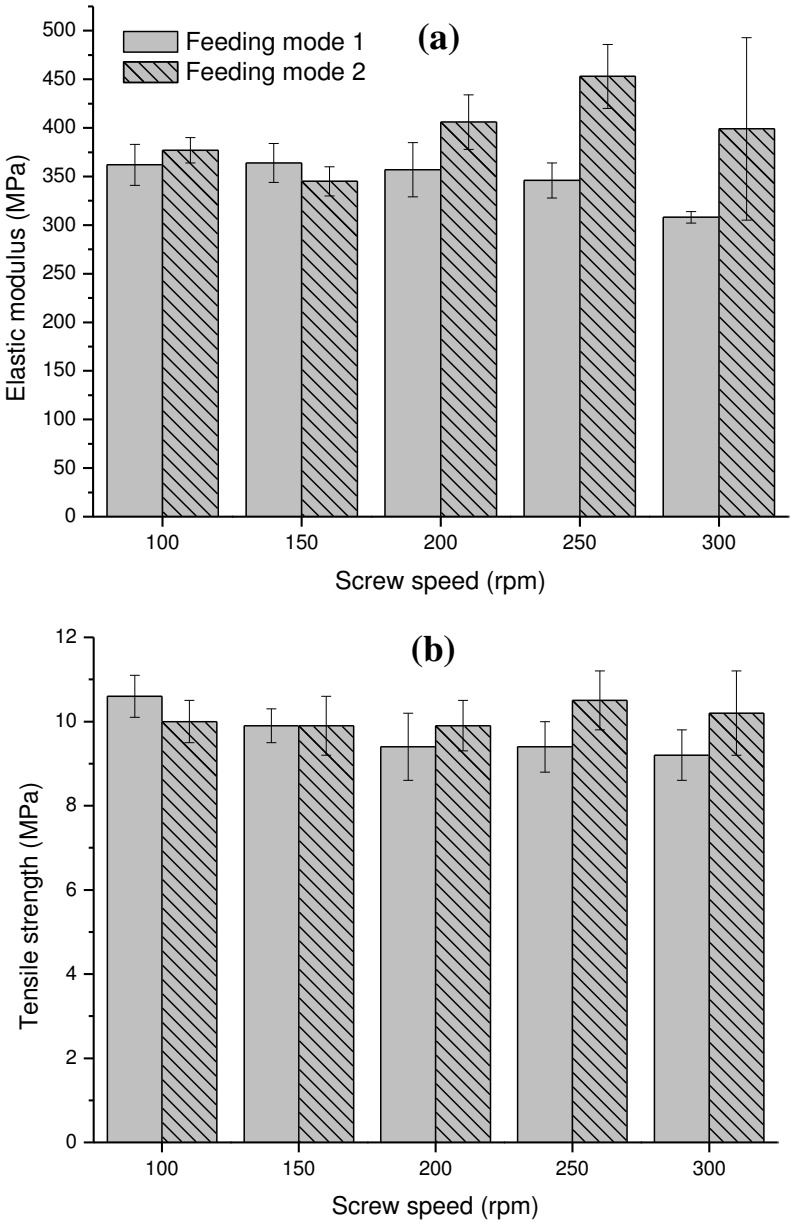

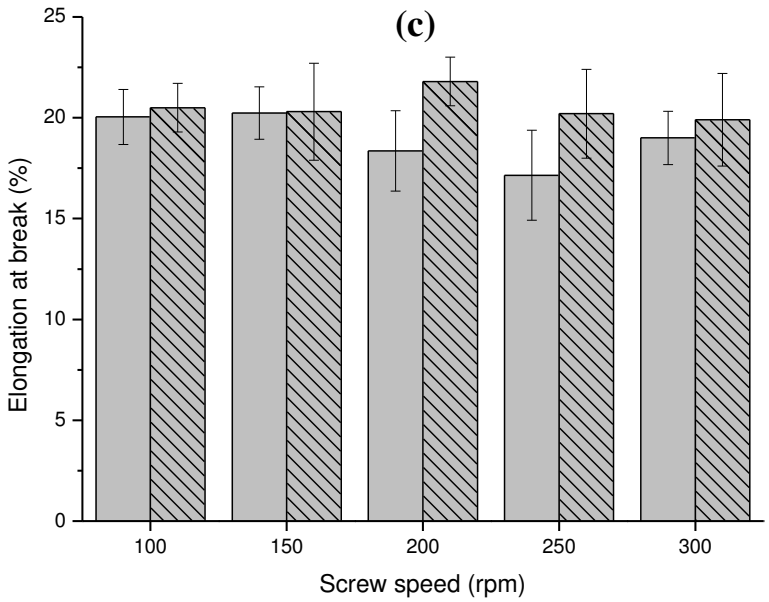

Figure 66: Tensile properties of the blends produced through feeding modes 1 and 2: (a) elastic modulus, (b) tensile strength and (c) elongation at break.

Mahallati and Rodrigue [357] observed the influence of feeding strategy on the mechanical properties of blends of PP/recycled ethylene-propylene-diene monomer (r-EPDM). According to them, the location of the second feeder needed to be optimized to reach a good balance between dispersion and rubber particle treatment. They found better mechanical properties when the r-EPDM was separately introduced in the first feeder due to better interaction between the phases. As a conclusion, feeding sequence had a strong influence on the properties of the blends due to the dependence of the properties on the mixing quality during processing.

On the other hand, properties of a TPV composed of a recycled material depend on the concentration of the regrind, as well as on the adhesion between the polymer phases [260]. When the compatibility or adhesion between the phases is poor, whatever the processing parameters, their influences on the mechanical properties of the blends may not be large. However, in this work the tensile properties of the blends produced through feeding mode 2 slightly outperform those through feeding mode 1, especially elastic modulus. This is probably due to differences in morphologies, as will be shown later.

In an earlier study [223], revulcanized blends composed of devulcanized GTR/HDPE were produced in an internal mixer, and the exposure time of the GTR was varied. As observed in the present work, the mechanical properties were far from typical TPV due to the lack of adhesion between the phases. Adding a nanometer scale filler to the system [8] did not make much difference. However, the properties of the blends

produced in the extruder in this work are much better than those produced in the internal mixer, due to better dispersion of the GTR in the matrix.

According to Lee et al. [297], it is not easy to produce polymer blends composed of a thermoplastic and GTR due to the lack of thermodynamic compatibility between them. The latter can be improved through surface treatment of the rubber and dynamic vulcanization of the elastomer phase. The devulcanization of the elastomer phase by microwaves improves the compatibility between the phases of the blend. However, according to Kumar et al. [6], the prerequisites of manufacturing blends containing GTR are: use of an additional (fresh) elastomer and/or devulcanization of the GTR at least partially, what is performed on the present work in order to increase the compatibility between the phases. Even performing devulcanization of the GTR phase, both the lack of compatibility and adhesion between the phases contributed to the deterioration of the mechanical properties of the blends, no matter the processing parameters adopted.

7.2 - SEM

Figures 67 and 68 show the SEM images of all the blends produced through the two different feeding modes and their particle size distributions. The black areas correspond to GTR5.5 particles selectively extracted by cyclohexane.

First of all, it is seen that devulcanized GTR particles are all finely dispersed in the HDPE after the extrusion stage in the twin screw extruder. Moreover, the higher the screw speed, the finer the rubber particles, and the narrower the particle size distribution. The rubber particles are smaller in size for the blends obtained by feeding mode 2 (Figure 68). This is probably due to a higher shear stress/rate imposed to the rubber particles, or due to the absence of premature revulcanization of the rubber phase. This tendency was also observed by Yquel et al. [339] and George et al. [263]. The latter prepared nitrile rubber (NBR)/HDPE TPVs under different processing conditions in terms of barrel temperature, screw speed, among other factors. They found that the size of the rubber particles decreased with increasing the screw speed.

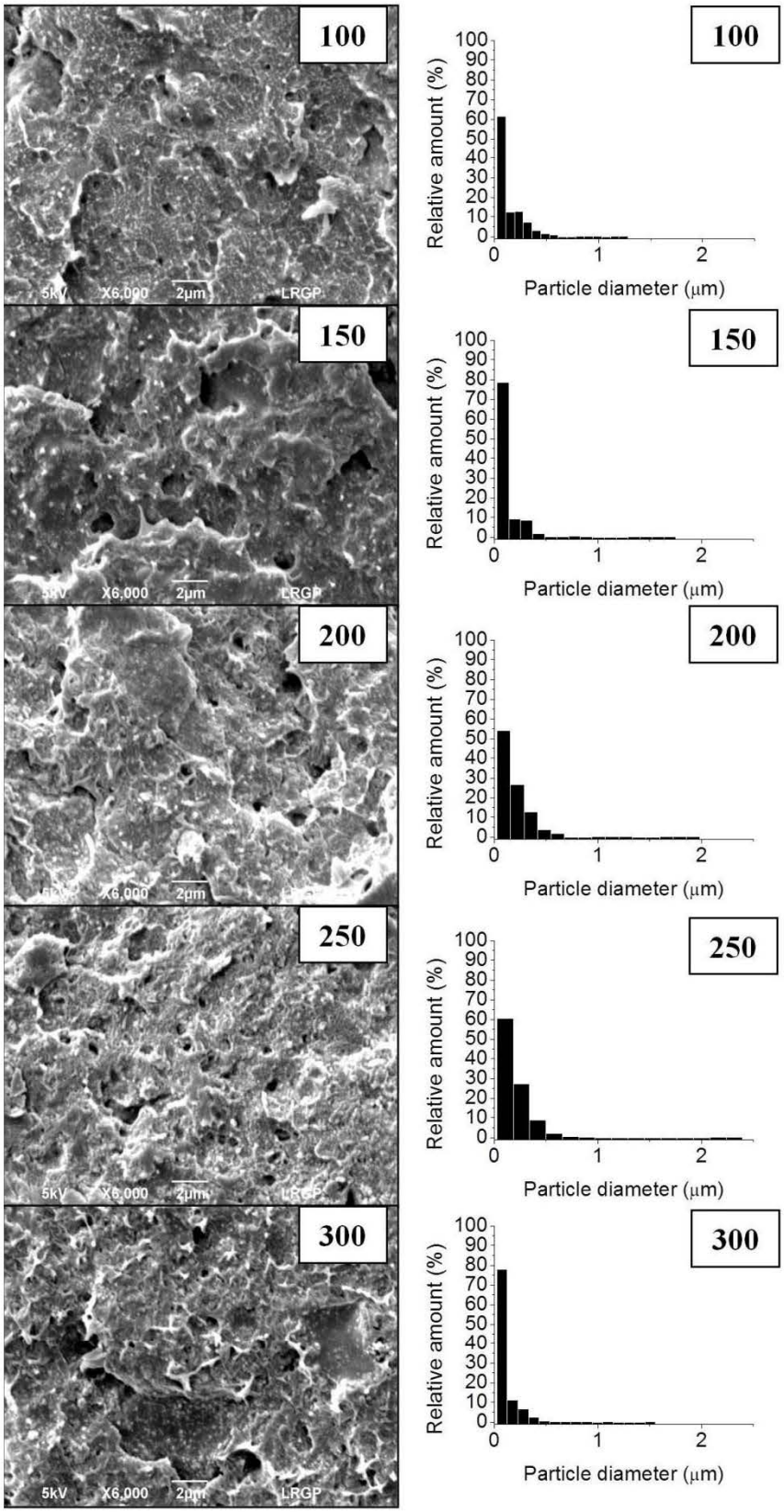

Figure 67: SEM images of the blends produced through feeding mode 1 for 5 different screw speeds and their particle size distributions.

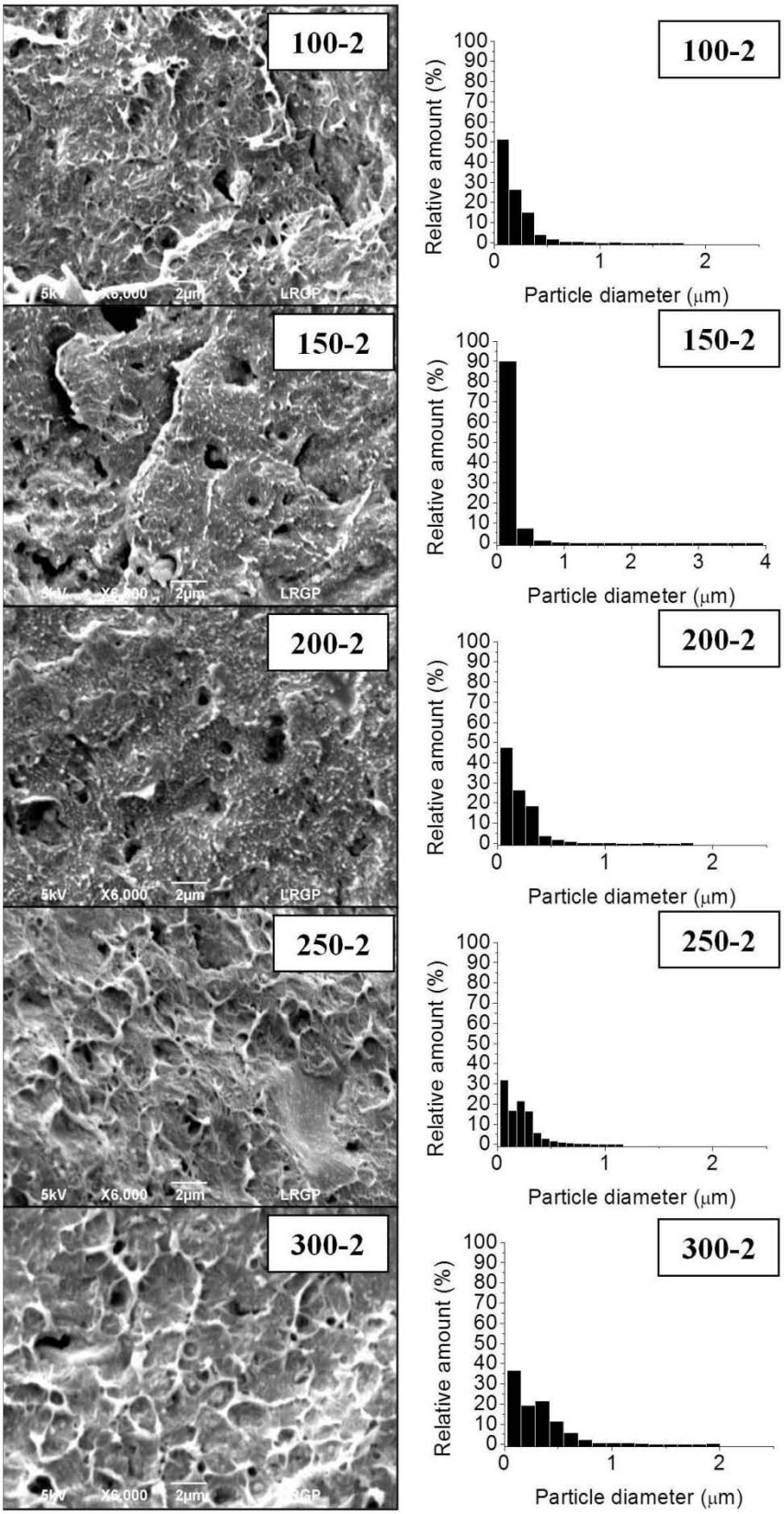

Figure 68: SEM images of the blends produced through feeding mode 2 for 5 different screw speeds and their particle size distributions.

Table 8 summarizes the morphological parameters from the SEM images of the GTR5.5/HDPE blends in terms of the number average particle size (*Dn*), volume average particle size (*Dv*) and size dispersion (*Dv/Dn*). It is noted that the effects of the feeding mode and screw speed on the rubber domain size and the particle size distribution are not obvious. Nevertheless, the blend 250-2 presents the smallest size, the narrowest particle size distribution and the highest elastic modulus. The "best result" is a consequence of an optimum trade-off between the dispersion and revulcanization of the devulcanized GTR in the extruder.

Table 8: Morphological parameters of the blends.

Feeding mode 1				**Feeding mode 2**			
Sample	**D_n (µm)**	**D_v (µm)**	**D_v/D_n**	**Sample**	**D_n (µm)**	**D_v (µm)**	**D_v/D_n**
100	0.14	0.65	4.59	100-2	0.18	0.71	3.87
150	0.14	1.33	9.84	150-2	0.20	2.65	13.41
200	0.19	1.16	6.04	200-2	0.20	0.96	4.82
250	0.19	1.30	6.68	250-2	0.20	0.58	2.89
300	0.12	0.75	6.46	300-2	0.30	1.04	3.52

7.3 - Oscillatory rheological properties

Figure 69 shows the storage modulus (G') and complex viscosity (η*) as a function of the frequency of the blends produced through feeding modes 1 and 2.

It is seen that the complex viscosity of the blends decreased with increasing frequency. This is a typical shear thinning behavior, according to the Cox-Merz rule [251, 255, 358-360]. Moreover, the values of G' and η* of the blends produced through feeding mode 1 were higher than those of the blends produced through feeding mode 2 because the elastomeric phase of the former to be more highly cross-linked.

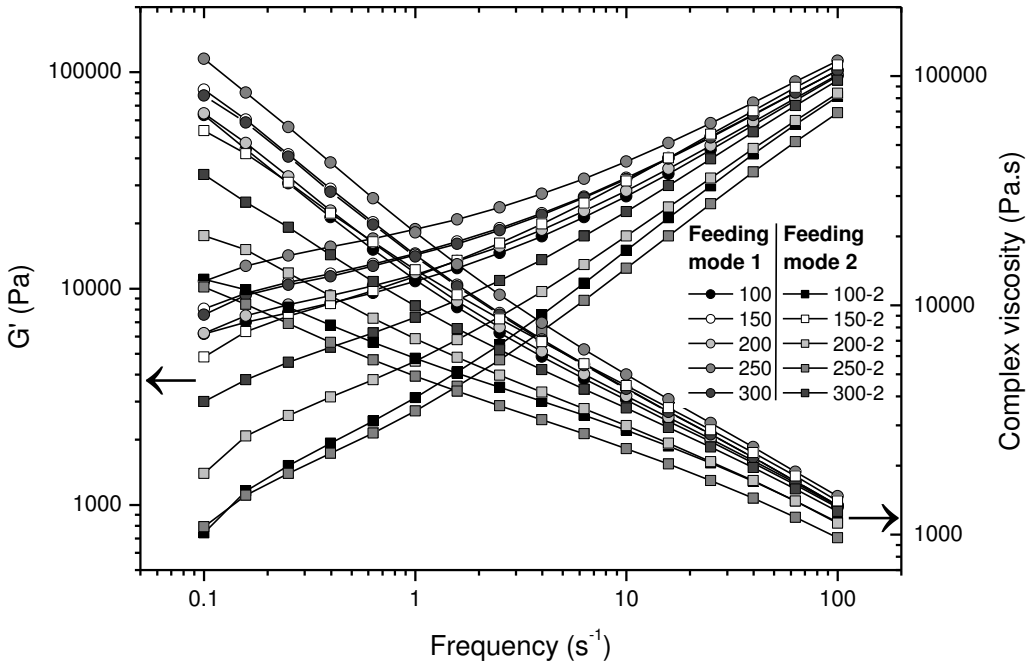

Figure 69: Evolution of G' and η* of the blends produced through feeding modes 1 and 2.

The storage modulus decreased as the size of rubber particles reduced, as confirmed by the SEM images. Since the morphology achieved through feeding mode 2 was finer, G' was expected to increase due to more efficient stress transfer among the phases. However, the results of elongation at break showed poorer adhesion between the phases of the blends, which probably caused a decrease in G'. The same behavior was previously observed [8, 223], and the authors correlated the decrease in G' with the deterioration of the mechanical properties of the blends of GTR devulcanized by microwaves and HDPE, due to particle detachment from the matrix when an external stress was applied.

7.4 - Final provisions of Stage 2

Figure 70 shows some vulcanization parameters involved in the processing of dynamically revulcanized blends, as well as the scheme of a probable evolution of morphology during processing. The screw profile is for feeding mode 2, since it produced finer morphology.

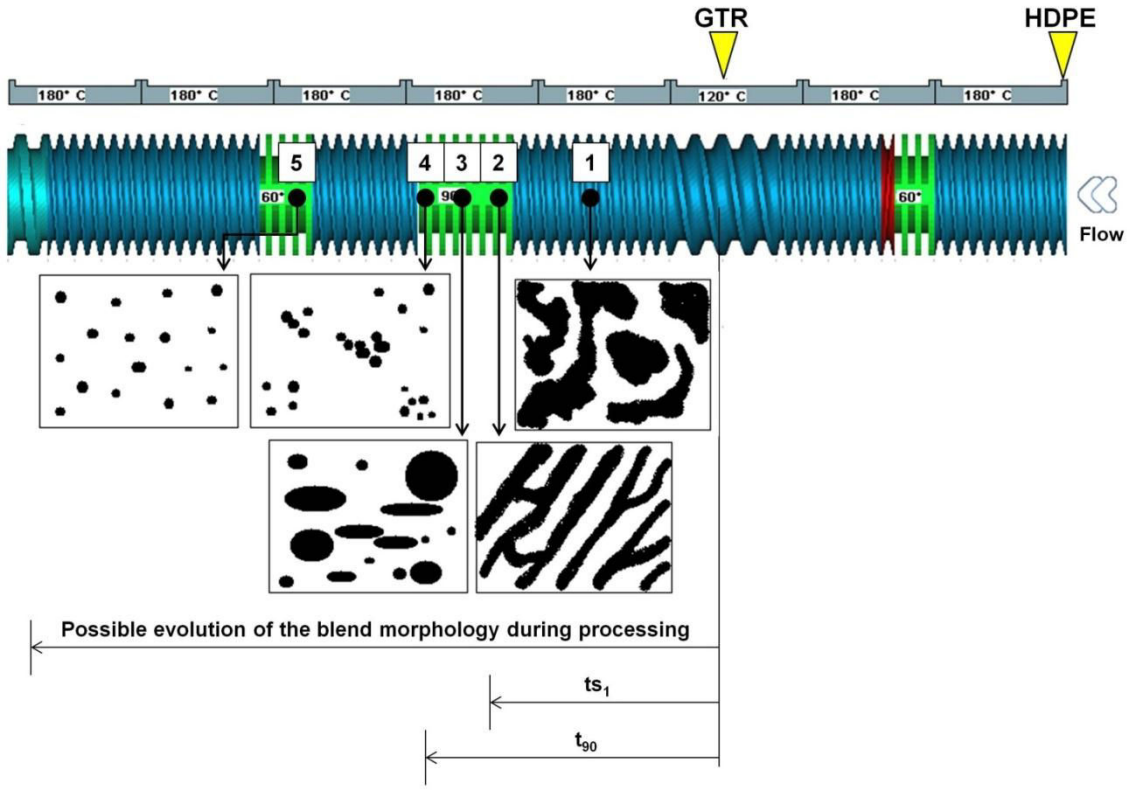

Figure 70: Screw profile relative to Figure 65b (feeding mode 2) used in the preparation of the blends, showing the schema of the possible evolution of the morphology and rheology of the elastomeric phase involved during processing. In the images that represent the morphologies, the black part represents the elastomeric phase and the white represents the thermoplastic phase.

Figure 70 shows that at point 1 of the extruder, there is only physical mixing among the phases and there is no revulcanization of the GTR5.5. At the beginning of the second high shear zone, the revulcanization reaction starts (the residence time of the rubber from its introduction in the extruder to this point is about the same of ts_1 of the reaction) and, around point 2, the blend presents a co-continuous morphology in which the elastomeric phase is stretched in the flow direction.

At this stage, the overall viscosity is increased (the elastomeric phase with high elasticity is stretched and breaks into smaller particles due to high shear rates, intense elongational flow and high elasticity generated by cross-linkings (point 3), resulting in high mechanical stresses. At point 4, still under the effect of high shear rates, rubber particles break into smaller particles, and at point 5 there is a better distribution in the thermoplastic matrix. The end of the second shear zone (point 4) refers approximately to the optimum cure time of the elastomeric phase which, in the case of GTR5.5, is 44 s. The residence time of rubber from its introduction in the extruder to the end point of the

reaction must be equivalent to t_{90}, and this point should be in a high shear zone of the extruder for breakage of rubber particles in micrometric dimensions.

It is important to address here that, for both screw profiles used, the first mixing zone served to melt the HDPE, the second one to dynamically revulcanize the GTR phase and the last one to improve the distribution of the rubber particles in the HDPE. In the case of the blends produced through feeding mode 1 (Figure 65a), the high shear rate in the first mixing zone could bring about premature revulcanization of the rubber phase, since the components were added together. As the length of this zone and the corresponding residence time were short, the time for the reaction to go to completion was longer than the residence time on the zone, which probably happened in the second transport zone. Thus, the rubber domains were not sufficiently well dispersed and distributed in the HDPE matrix. However, in the case of the blends produced through feeding mode 2 (Figure 65b), the residence time of the rubber phase inside the extruder from its introduction to the end of the second mixing zone was closer to the optimum cure time of the GTR5.5 at 180°C (43.8 s). Therefore, the mixing zone was long enough for the revulcanization reaction to go to completion and the dispersed rubber domains to have its size reduced in the HDPE matrix.

The blend 250-2 presented higher finer morphology and consequently better mechanical properties, despite the fact that the compatibility and adhesion between the phases were poor. The finer morphology is due to good match between processing conditions and rheological properties of the GTR5.5. The residence times of the GTR5.5 inside the extruder from its introduction to the respective points shown in the Figure 70 were approximately 50 and 30 s, respectively, which were very close to the values of t_{90} and ts_1 (44 and 27 s, respectively).

The results presented in this Stage clearly demonstrate the importance of the choice of the optimal parameters for processing dynamically revulcanized blends, being that the kinetics of revulcanization of the elastomeric phase must be compulsorily complied. Such parameters will affect directly the morphology and, consequently, their mechanical properties.

Summarizing, the parameters chosen for the production of the other blends of the next Stage of the project were the screw profile 2 (Feeding mode 2) and speed of 250 rpm, according to Figure 65b.

8 - PARTIAL CONCLUSION

In the Stage 2, dynamically revulcanized blends 60GTR5.5+ad/40HDPE were produced, by using two different feeding modes, and in each of them the blends were produced with five different extrusion speeds. As in the literature it was not found similar system and among the works available the range of extrusion speed used is too large, it was necessary to check which processing parameters would better fit on the analysed system. As a way of analyzing the best parameters, mechanical and rheological properties were analyzed, as well as the SEM images of each blend.

The results found in this Stage clearly show the importance of the processing parameters (feeding mode and screw speed) involved in the production of blends of dynamically revulcanized rubber phase in a twin screw extruder, as well as the necessity of good match between the residence time of the rubber during processing and its revulcanization kinetics. Optimum processing conditions are responsible for fine morphology and good mechanical properties of the blend. For a highly cross-linked rubber, its residence time in the screw extruder is the most important factor.

The finest morphology and consequently the best mechanical properties were obtained when feeding mode 2 was used and the screw speed was high. Those processing conditions allowed matching the residence time with the revulcanization kinetics in such a way that the revulcanization of the rubber could happen at the same time as the high stress and strain rates were applied to the blend. Therefore, coalescence was avoided and the break-up of the particles was promoted. However, mechanical properties were still poor due to the insufficient compatibility and low adhesion between the phases.

The results found on this stage resulted in an article recently published on Journal of applied polymer science:

F.D.B. de Sousa. C.H. Scuracchio. G.H. Hu. S. Hoppe. Effects of processing parameters on the properties of microwave-devulcanized ground tire rubber/polyethylene dynamically revulcanized blends. Journal of applied polymer science 133(23), 2016.

STAGE 3: Characterization of the final properties of the blends

9 - MATERIALS AND METHODS

9.1 - Materials

9.1.1 - Phases of the blends

For the production of blends of Stage 3, was used as the thermoplastic phase the processed HDPE and HDPE/clays (as described in section 2.2.8), and as elastomeric phase the GTR5.5+ad, GTR5.5, GTR0+ad, and GTR0, as a way of comparing the results. The GTR5.5 was devulcanized for 5.5 minutes in the system described in section 2.2.2; GTR0 refers to the non devulcanized GTR, as received. The homogenization and the additivation of the elastomeric phase was described in section 6.2.1.

9.2 - Methods

The analyses carried out during Stage 3 of the project followed the flowchart shown in Figure 71.

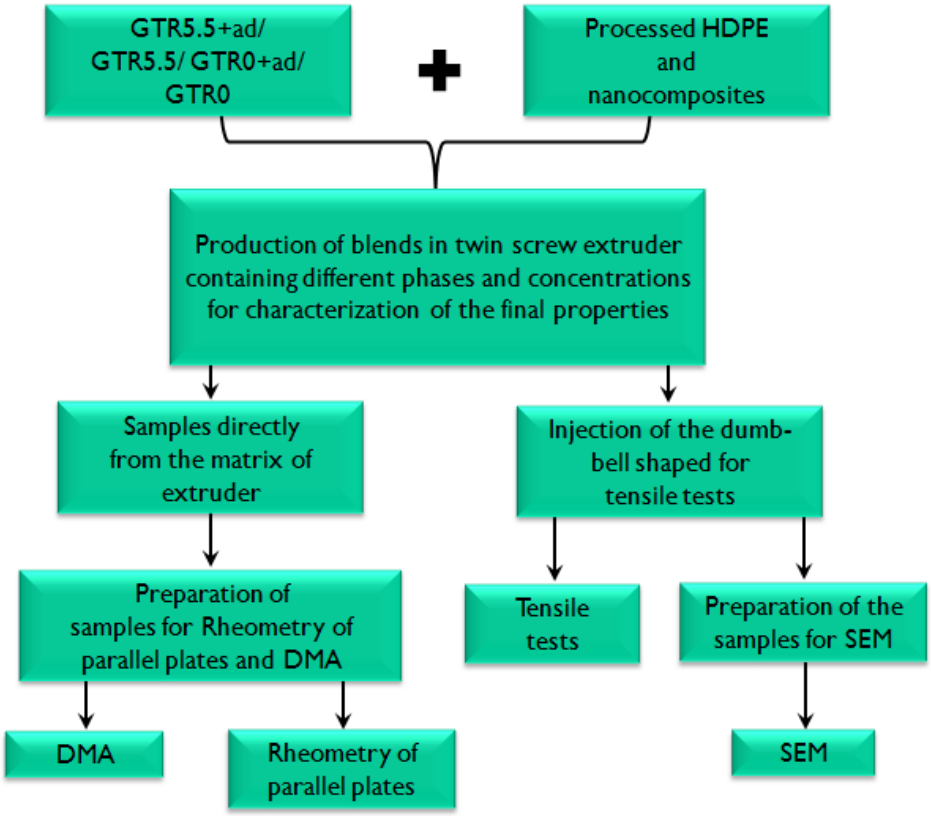

Figure 71: Flowchart of activities performed during Stage 3.

9.2.1 - Processing of blends in twin screw extruder

After checking the best conditions of processing performed in Stage 2, the blends were processed in twin screw extruder Process 11 Thermo Scientific to 250 rpm, with two feeders (the first one for the introduction of the thermoplastic or HDPE/clay nanocomposite and the second for the introduction of GTR) and screw profile present in Figure 65b (Feeding mode 2). The blends produced during this stage are present in Table 9.

The samples used in the analysis of DMA and rheology of parallel plates were made with materials from the extruder matrix (extruded material). Whereas the samples used for the SEM analysis were obtained from the specimens injected for tensile tests.

9.2.2 - Injection of specimens for tensile tests

The specimens for tensile tests have been injected in accordance with section 6.2.3.

Table 9: Blends analyzed during Stage 3 of the project.

Polymer blend	Concentration of GTR (%)	Concentration of HDPE (%)	Type of clay used
Blends containing GTR5.5			
20GTR5.5/80HDPE	20	80	—
20GTR5.5/80HDPE+20A	20	80	Cloisite 20A
20GTR5.5/80HDPE+Hal	20	80	Halloysite
40GTR5.5/60HDPE	40	60	—
40GTR5.5/60HDPE+20A	40	60	Cloisite 20A
40GTR5.5/60HDPE+Hal	40	60	Halloysite
60GTR5.5/40HDPE	60	40	—
60GTR5.5/40HDPE+20A	60	40	Cloisite 20A
60GTR5.5/40HDPE+Hal	60	40	Halloysite
80GTR5.5/20HDPE	80	20	—
80GTR5.5/20HDPE+20A	80	20	Cloisite 20A
80GTR5.5/20HDPE+Hal	80	20	Halloysite
Dynamically revulcanized blends containig GTR5.5			
20GTR5.5+ad/80HDPE	20	80	—
20GTR5.5+ad/80HDPE+20A	20	80	Cloisite 20A
20GTR5.5+ad/80HDPE+Hal	20	80	Halloysite
40GTR5.5+ad/60HDPE	40	60	—
40GTR5.5+ad/60HDPE+20A	40	60	Cloisite 20A
40GTR5.5+ad/60HDPE+Hal	40	60	Halloysite
60GTR5.5+ad/40HDPE	60	40	—
60GTR5.5+ad/40HDPE+20A	60	40	Cloisite 20A
60GTR5.5+ad/40HDPE+Hal	60	40	Halloysite
80GTR5.5+ad/20HDPE	80	20	—
80GTR5.5+ad/20HDPE+20A	80	20	Cloisite 20A
80GTR5.5+ad/20HDPE+Hal	80	20	Halloysite
Blends containing GTR0			
20GTR0/80HDPE	20	80	—
20GTR0/80HDPE+20A	20	80	Cloisite 20A
20GTR0/80HDPE+Hal	20	80	Halloysite
40GTR0/60HDPE	40	60	—
40GTR0/60HDPE+20A	40	60	Cloisite 20A
40GTR0/60HDPE+Hal	40	60	Halloysite
60GTR0/40HDPE	60	40	—
60GTR0/40HDPE+20A	60	40	Cloisite 20A
60GTR0/40HDPE+Hal	60	40	Halloysite
80GTR0/20HDPE	80	20	—
80GTR0/20HDPE+20A	80	20	Cloisite 20A
80GTR0/20HDPE+Hal	80	20	Halloysite
Dynamically revulcanized blends containig GTR0			
20GTR0+ad/80HDPE	20	80	—
20GTR0+ad/80HDPE+20A	20	80	Cloisite 20A
20GTR0+ad/80HDPE+Hal	20	80	Halloysite
40GTR0+ad/60HDPE	40	60	—
40GTR0+ad/60HDPE+20A	40	60	Cloisite 20A
40GTR0+ad/60HDPE+Hal	40	60	Halloysite
60GTR0+ad/40HDPE	60	40	—
60GTR0+ad/40HDPE+20A	60	40	Cloisite 20A
60GTR0+ad/40HDPE+Hal	60	40	Halloysite
80GTR0+ad/20HDPE	80	20	—
80GTR0+ad/20HDPE+20A	80	20	Cloisite 20A
80GTR0+ad/20HDPE+Hal	80	20	Halloysite

9.2.3 - SEM

The samples from the specimens for tensile tests injected were cut, cryogenically fractured and the sample preparation was carried out as described in section 6.2.5. Samples got stuck in a sort of clothesline and just the fractured surface was in contact with the solvent cyclohexane during the selective extraction of rubber phase of blends.
The morphology of blends was performed in a Scanning Electron Microscope JMS-6701F - Jeol, and the working distance used in each sample is present in the micrograph.

9.2.4 - Tensile tests

The mechanical properties of the blends were analyzed in a Universal Testing Machine Instron 5569 with 50 kN load cell. The test speed was 50 mm/min.

9.2.5 - DMA

The dynamic-mechanical properties of polymer blends were analyzed by using a dynamic-mechanical analyzer DMA Q800 of TA Instruments. The analyses were carried out in Single Cantilever mode, 1 Hz of frequency, in heating ramp from -100 to 140°C and heating rate of 3°C/min. Glass transition temperatures of the rubbers were extracted from the maximum value of the tan delta peak.
The samples were previously pressed in hydraulic press in rectangular mould with the dimensions of 17,5x12,5x2 mm to 180°C for 5 minutes.

9.2.6 - Rheometry of parallel plates

Rheological properties of the blends were analyzed by oscillatory rheometry in a parallel plate rheometer Anton Paar CTD450 (diameter 25 mm, gap 1.3 mm, 1 % of strain at 180°C). Frequency sweep experiments were carried out in the linear viscoelastic range to characterize the viscoelastic properties of the blends. The frequency ranged from 0.1 to 100 rad/s and pre-strain sweep tests were performed to determine the linear viscoelastic range of the blends.
The samples were previously pressed in hydraulic press in circular mould of 25 mm diameter and 1 mm in height to180°C for 5 minutes.

10 - RESULTS AND DISCUSSION

As quoted in the Organization of work, in this stage, the consequences of the different effects on dynamic-mechanical properties, rheological, mechanical and morphology of blends will be analyzed, namely: effect of devulcanization of elastomeric phase, revulcanization of elastomeric phase, addition of clays and concentration of the phases.

10.1 - SEM

First, it is important to understand what each part of the SEM images represents. In general, it appears that the particles, even having sizes of particles of sub micrometric order, they did not result in materials with good mechanical properties, in particular low elongation at break (section 10.4). When analyzed the images of SEM of blends with low magnifications, it turns out that, in general, the GTR particles are well dispersed, but badly distributed on thermoplastic matrix. As the analysis was carried out from the specimen of tensile test, and the same was injected, the morphology was probably a result of the injection process. The images can show three distinct regions:
(A) the region in which the GTR particles dispersed in sub-micrometer scale;
(B) the region in which the particles of GTR are in small concentration (or not present). These regions are formed preferentially by matrix phase, thanks to the concentration of stresses of large particles that are around these regions; and
(C) region with larger particles of GTR, in micrometric scale .
The regions described above are shown in Figure 72.

Generally, the region (A) is rougher and with the presence of small fibrils, while (B) is smoother. While the region (C) is generally well outlined and with a valley (empty) around. It's not always easy to distinguish between the regions, but their features were observed from the SEM images of neat phases of the blends.

In the next section, the effect of devulcanization of elastomeric phase on the morphology of blends will be analyzed.

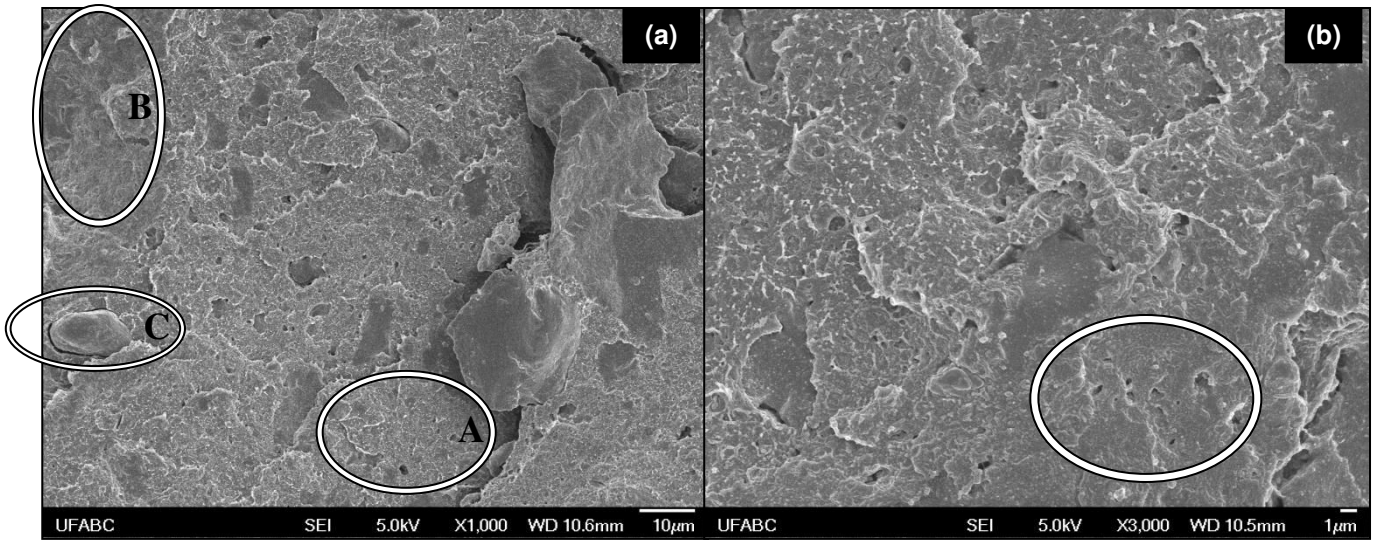

Figure 72: SEM images of the blend 60GTR5.5+ad/40HDPE with different magnifications, showing: (a) the different regions on the morphology (A - GTR sub micrometer particles well dispersed; B - the presence of a few particles; C - GTR micrometric particles); and (b) detail of the area B, in which some particles of GTR were selectively extracted by solvent.

10.1.1 - Effect of devulcanization of elastomeric phase

10.1.1.1 - Non revulcanized blends

The SEM images of non revulcanized blends without clay showing the effect of devulcanization of GTR phase on morphology of blends are present in Figure 73.

It is observed that GTR0 particles are much larger and more irregular-shaped in comparison to particles of GTR5.5. This fact is due to the fluidity of GTR5.5 as a result of the breakup of the cross-linkings during microwave devulcanization process. According to the DMA results (section 10.2.1.1), it was observed that the blend containing GTR0 presented the peak of tan δ concerning the elastomeric phase transition with less intensity than the peak of the blend containing GTR5.5 due to the constraint created by cross-linkings (greater rigidity) and that increased its E' value. This fact should possibly have hampered the breaking of the GTR0 particles during processing.

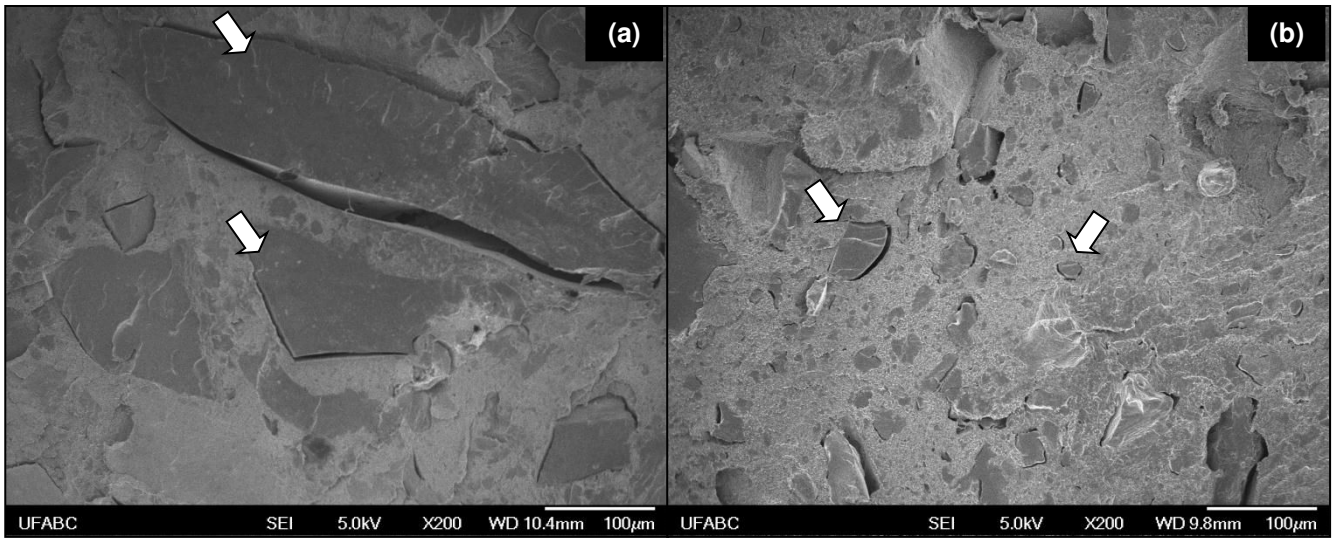

Figure 73: SEM images of the blends: (a) 80GTR0/20HDPE and (b) 80GTR5.5/20HDPE. The arrows show some particles of GTR.

As a result of devulcanization, apparently, there was no increase in the adhesion among particles of GTR and the matrix. The adhesion among phases will be discussed with more details in section 10.4 (mechanical properties of the blends).

10.1.1.2 - Revulcanized Blends

The SEM images of revulcanized blends without clay showing the effect of devulcanization of GTR phase in the final morphology of blends are presented in Figure 74.

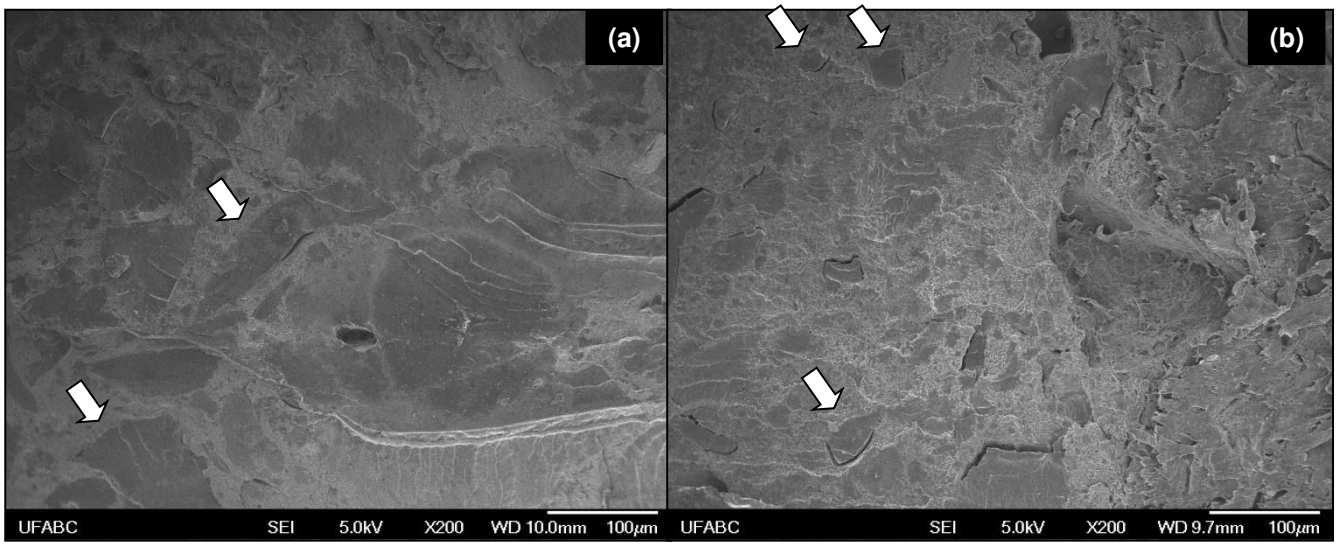

Figure 74: SEM images of the blends: (a) 80GTR0+ad/20HDPE and (b) 80GTR5.5ad+ad/20HDPE. The arrows show some particles of GTR.

According to the Figure 74, the devulcanization visibly reduced the size of the particles of the GTR phase due to greater fluidity. It can be also observed the lack of gaps between the particles shown with arrows and the matrix in Figure 74a and the presence of valleys between the particles and the matrix shown with arrows in Figure 74b. As will be discussed in section 10.4.1.2 (mechanical properties), in the case of revulcanized blends containing GTR0, there was no good mix between rubber and vulcanization additives added, since the GTR0 was in powder. For this same reason, it is believed that the vulcanization additives have been located on the interface, and so increased the adhesion among the phases.

In the following section will be analyzed the effect of revulcanization of the elastomeric phase on morphology of blends.

10.1.2 - Effect of revulcanization of elastomeric phase

10.1.2.1 - Blends without clay

The SEM images of blends without clay showing the effect of revulcanization of GTR phase on the final morphology of blends are presented in Figure 75. Figure 76 shows the images of the same blends with higher magnifications.

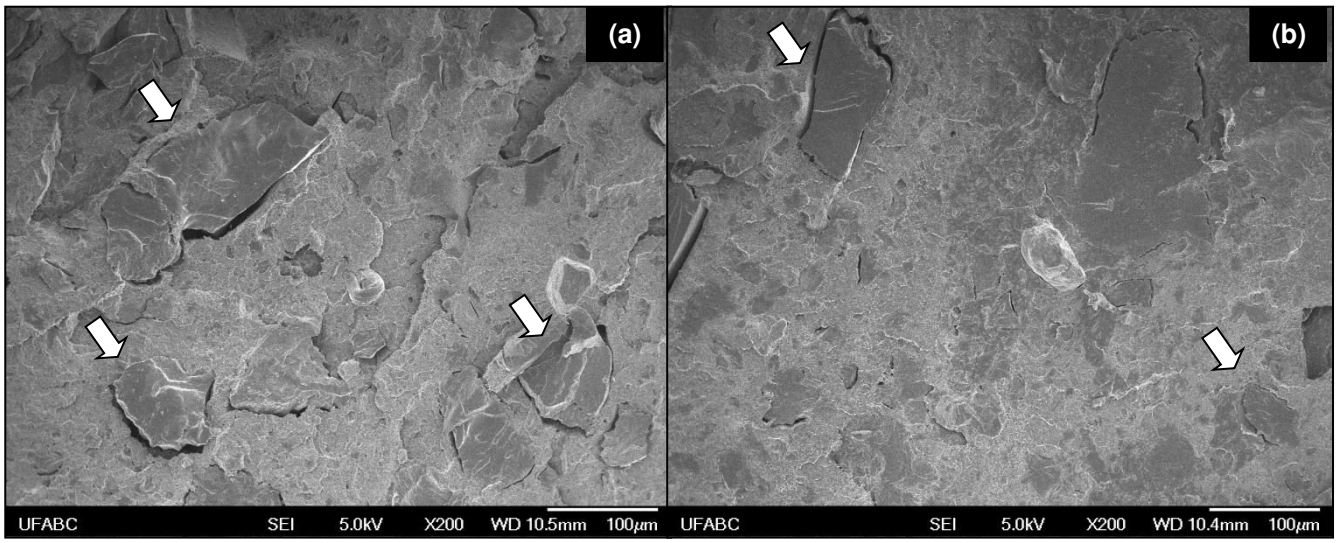

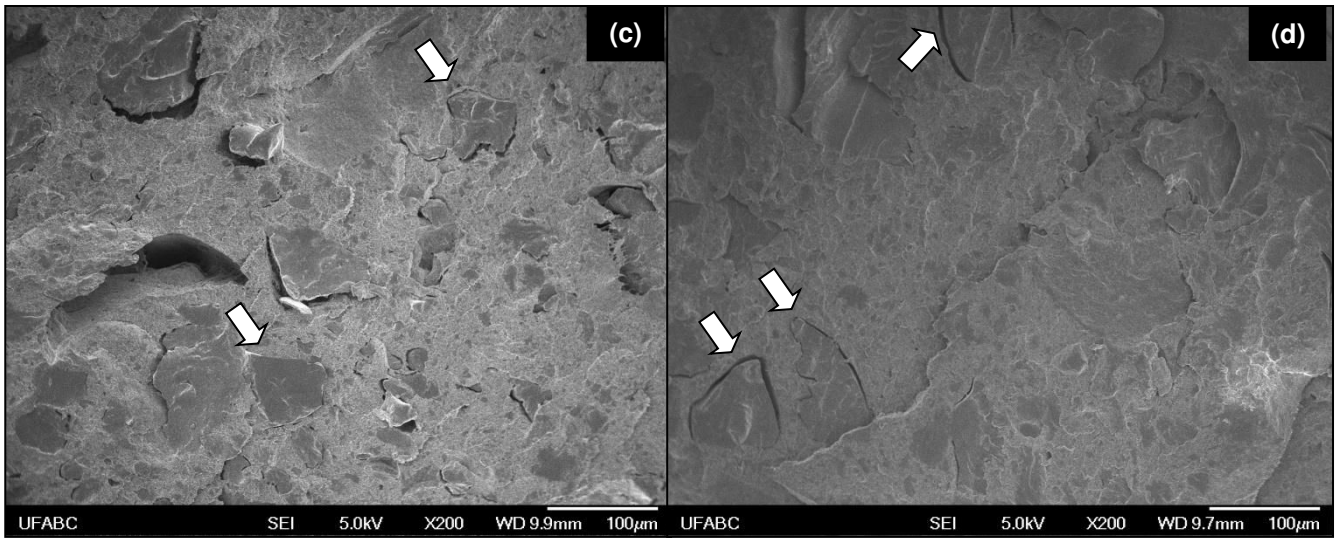

Figure 75: SEM images of the blends at low magnifications: (a) 60GTR5.5/40HDPE, (b) 60GTR5.5+ad/40HDPE, (c) 80GTR5.5/20HDPE and (d) 80GTR5.5+ad/20HDPE. The arrows show some particles of GTR.

In general, it is observed that the revulcanization apparently reduced the number of micrometric particles of GTR and also increased the adhesion among these particles and the HDPE matrix. The dynamic revulcanization is a stabilization process of the morphology, since it avoids the coalescence of rubber particles [223], which probably contributed to the reduction in the number of micrometric particles.

Figures 76b and 76d show that the revulcanization induced toughening processes by formation of microfibrils in the regions where the particles of GTR are well dispersed (sub micrometer GTR), some regions are in black circles in which can be observed the presence of thin ligaments or fibrils on thermoplastic matrix. According to Rabello [361], the particle size ideal for formation of microfibrils process lies in the range of 0.1 - 1 μm, which corresponds to the particle sizes of GTR present in these regions of the images. Still according to the same author [361], the essential condition for this process is the presence of dispersed particles and good adhesion among the phases. Babu et al. [250] also observed the formation of thin ligaments or microfibrils in the matrix of blend EOC/PP. According to the authors, it is the result of ductile fracture. Oommen and Thomas [362] report that the presence of microfibrils on fractured surface of blends indicates increase in interfacial adhesion.

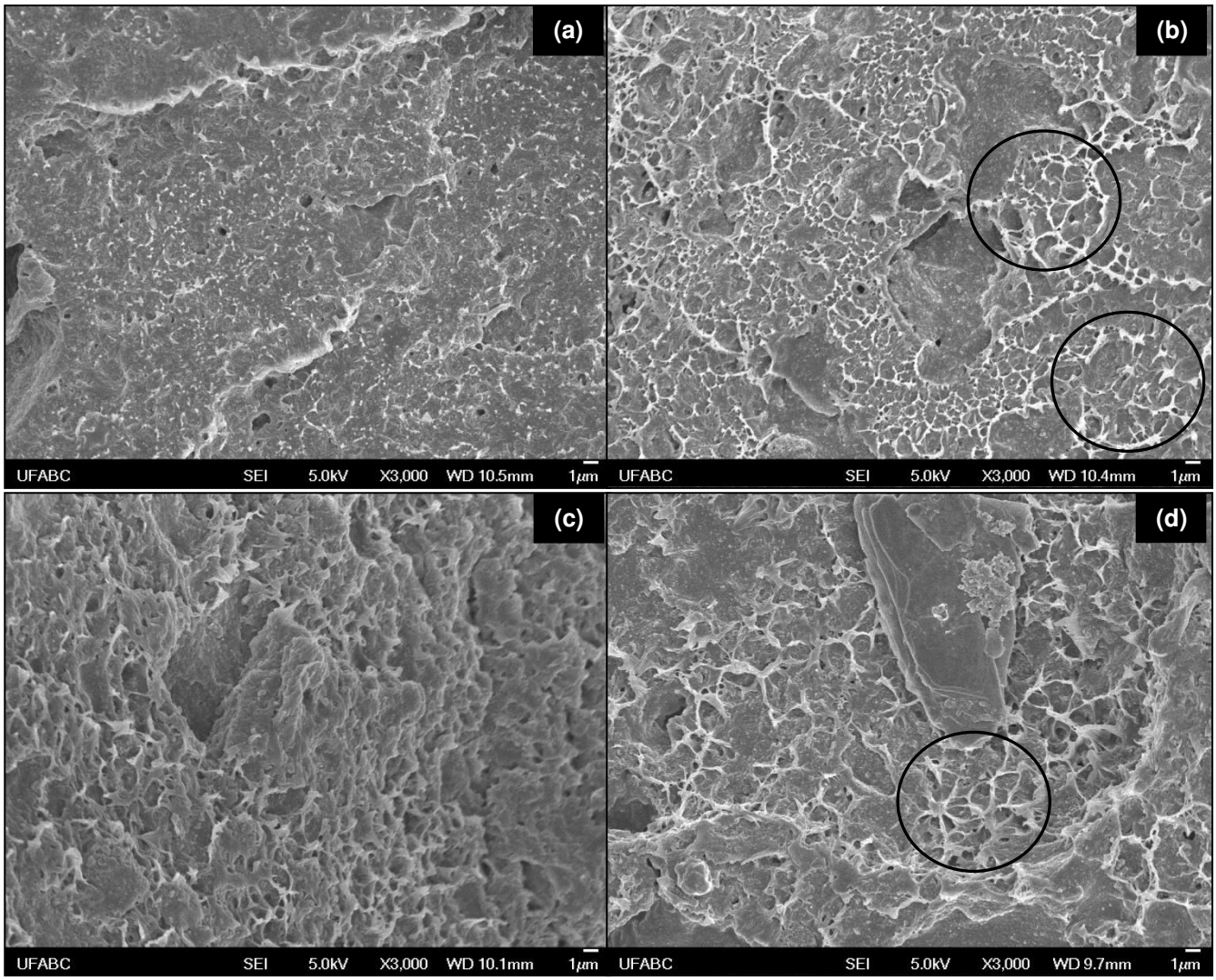

Figure 76: SEM images of the blends at high magnifications: (a) 60GTR5.5/40HDPE, (b) 60GTR5.5+ad/40HDPE, (c) 80GTR5.5/20HDPE and (d) 80GTR5.5+ ad/20HDPE. The circles exemplify some regions toughened by formation of microfibrils.

10.1.2.2 - Blends containing Cloisite 20A clay

The SEM images of blends containing Cloisite 20A clay showing the effect of revulcanization of GTR phase on morphology of blends are shown in Figure 77. Figure 78 shows images of the same blends with higher magnifications.

Comments on the effect of addition of clays will be made in the next section.

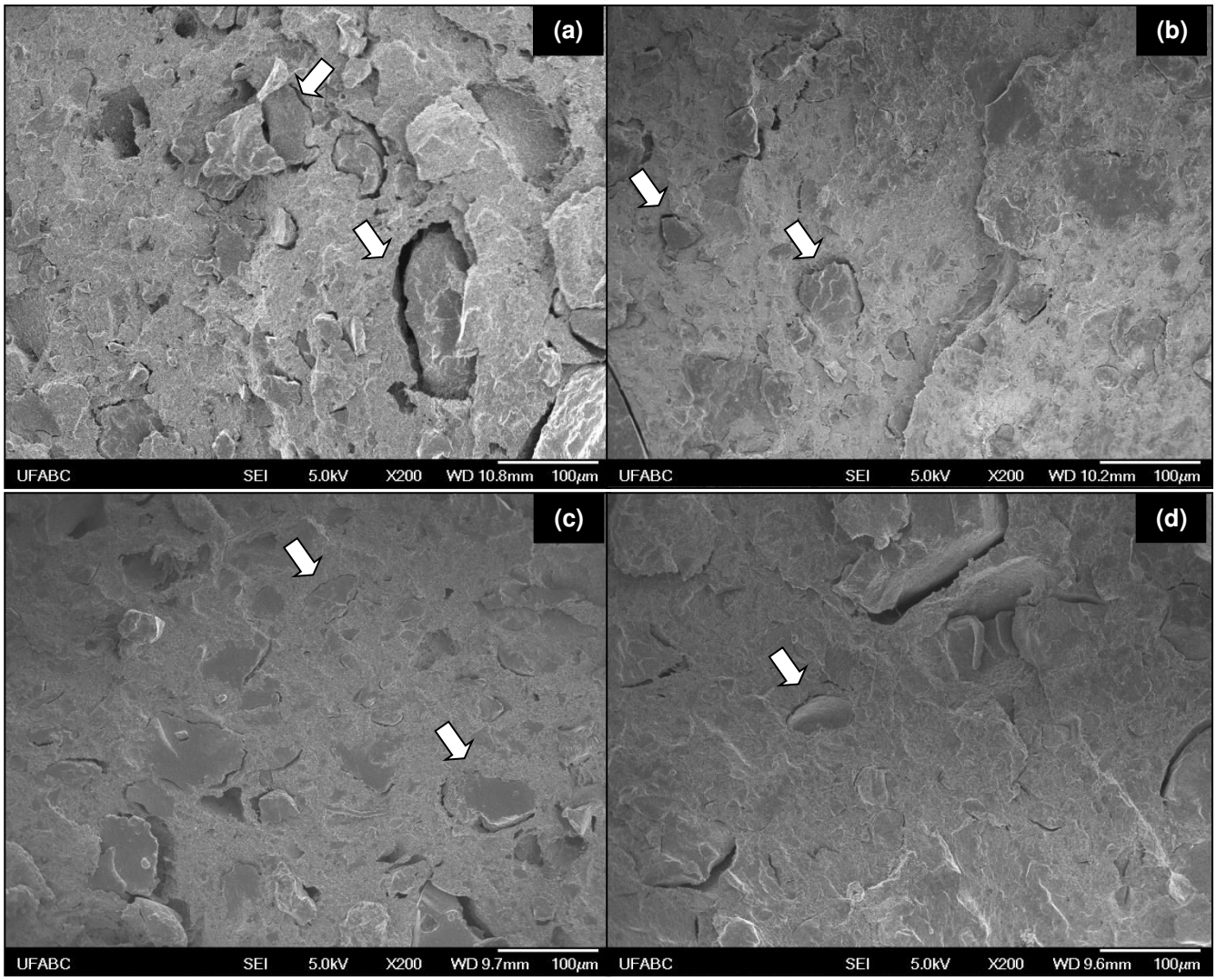

Figure 77: SEM images of the blends: (a) 60GTR5.5/40HDPE+20A, (b) 60GTR5.5+ad/40HDPE+20A, (c) 80GTR5.5/20HDPE+20A and (d) 80GTR5.5+ad/20HDPE+ 20A. The arrows show some particles of GTR.

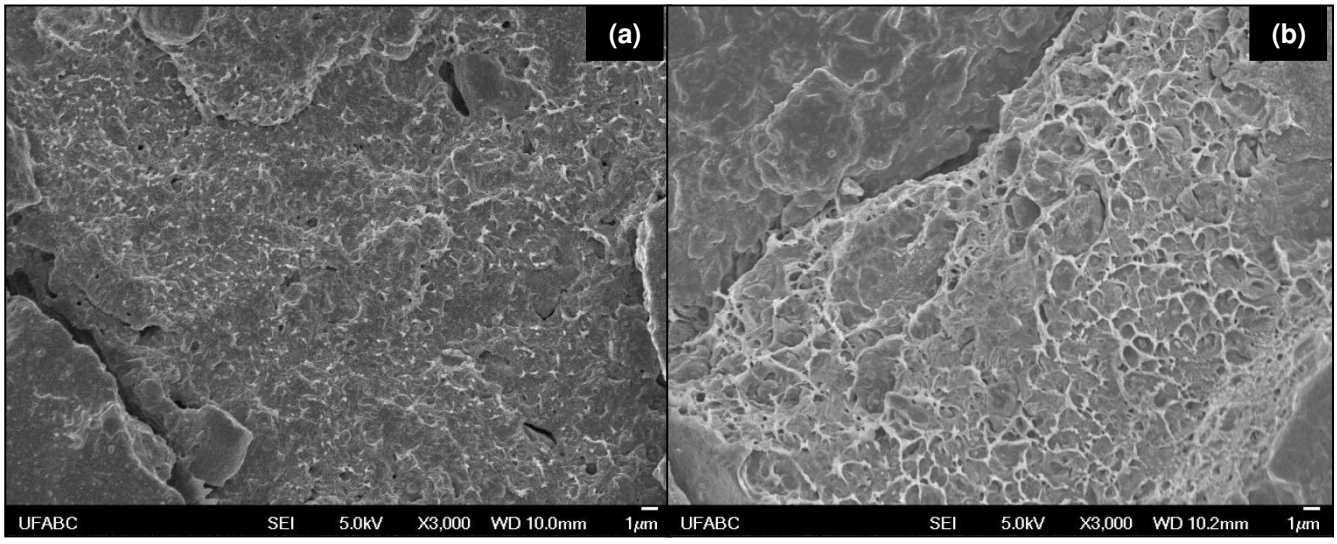

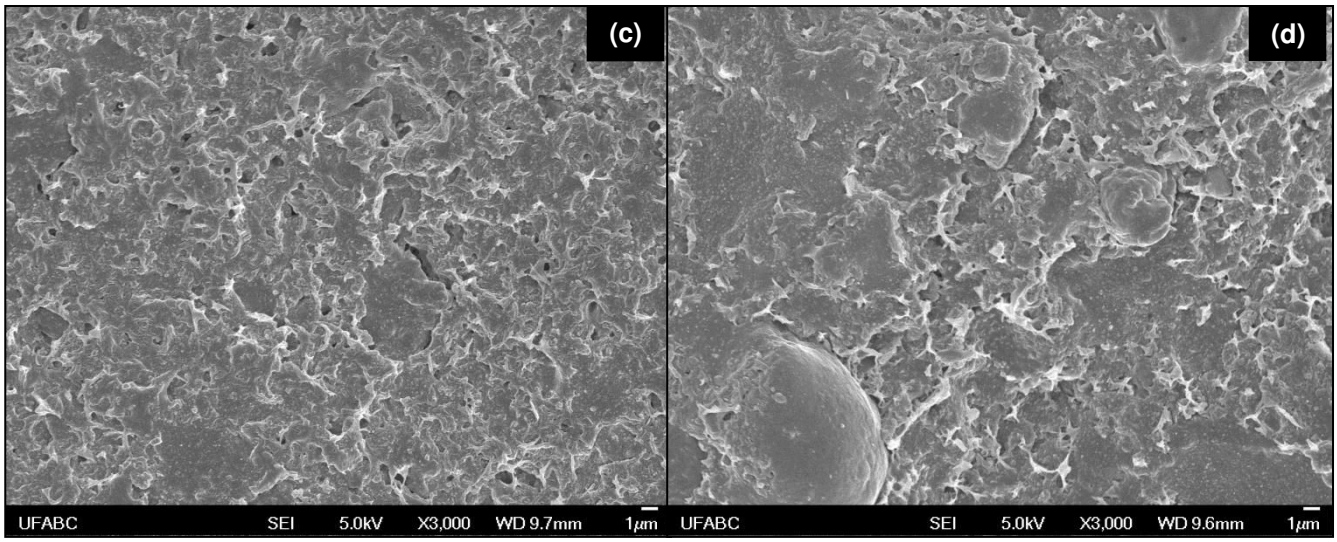

Figure 78: SEM images of the blends at high magnifications: (a) 60GTR5.5/40HDPE+20A, (b) 60GTR5.5+ad/40HDPE+20A, (c) 80GTR5.5/20HDPE+20A and (d) 80GTR5.5+ad/20HDPE+20A.

10.1.2.3 - Blends containing Halloysite clay

The SEM images of blends containing Halloysite clay showing the effect of revulcanization of GTR phase on the final morphology of blends are presented in Figure 79. Figure 80 shows the images of the same blends with higher magnifications.

Overall, the revulcanization of blends containing clay apparently reduced the size of the particles of micrometric GTR, especially in blends containing Halloysite, and improved the distribution of sub-micrometer particles in the matrix. This clay seems to have acted as a compatibilizing agent among the phases of the blend, and has apparently increased the adhesion among the particles of micrometric GTR and the matrix.

The revulcanization seems, also, have induced toughening processes by formation of microfibrils in the regions where the particles of GTR are well dispersed (sub-micrometers GTR), mostly in blends containing Cloisite 20A clay.

The effect of the presence of clays in the final morphology of blends will be examined in the next section.

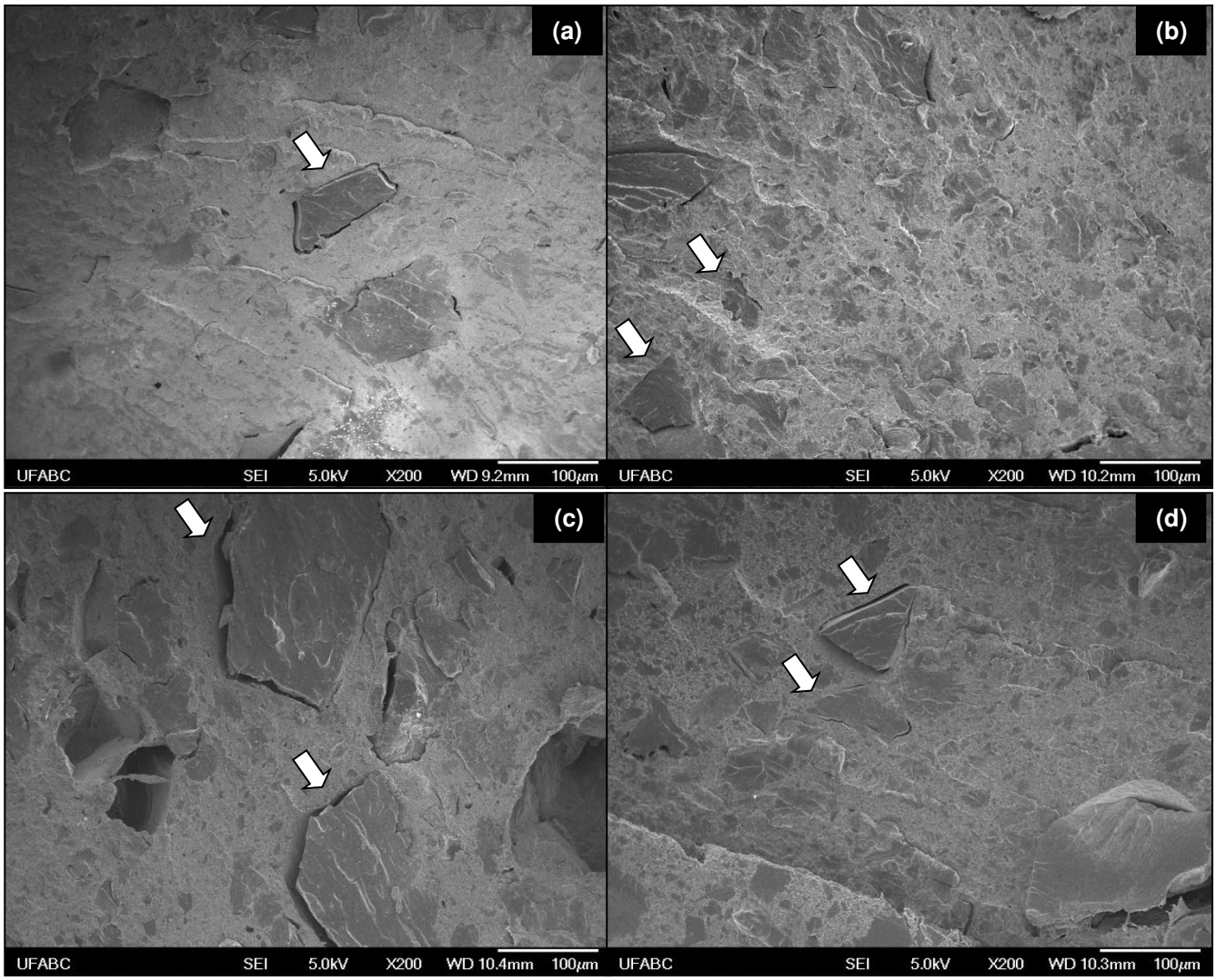

Figure 79: SEM images of the blends: (a) 60GTR5.5/40HDPE+Hal, (b) 60GTR5.5+ad/40HDPE+Hal, (c) 80GTR5.5/20HDPE+Hal and (d) 80GTR5.5+ad/20HDPE+Hal. The arrows show some particles of GTR.

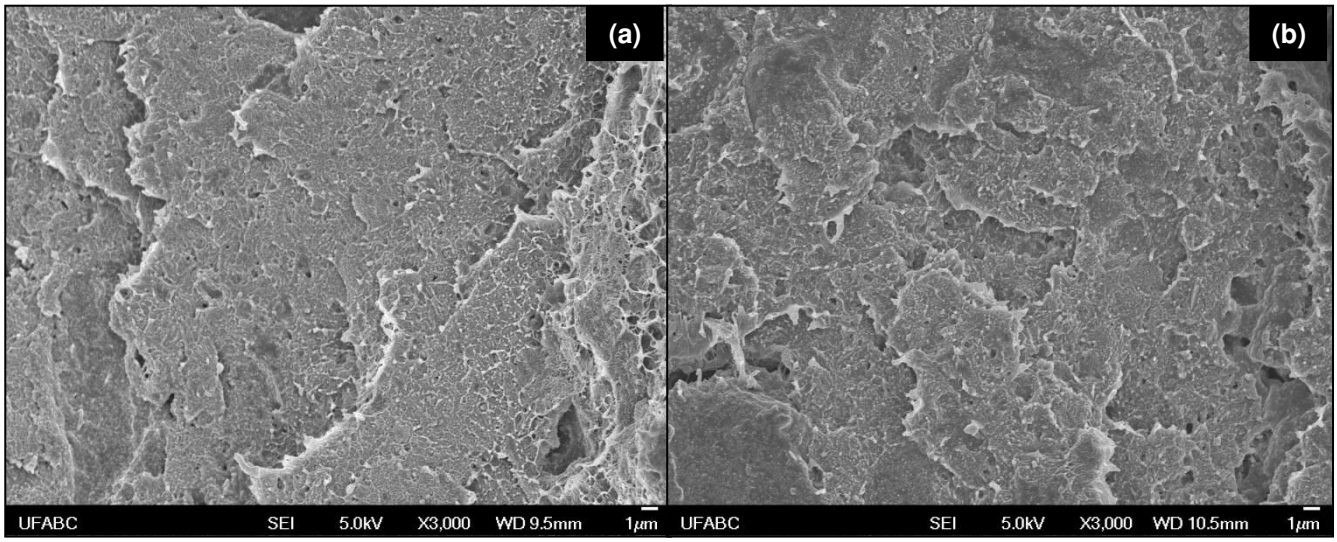

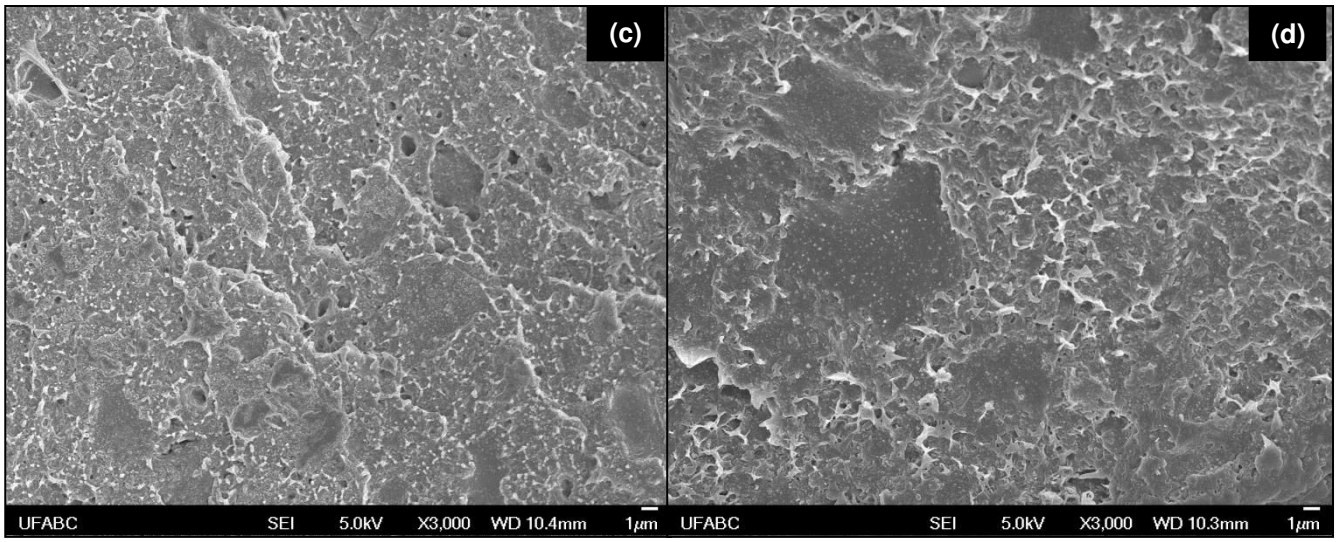

Figure 80: SEM images of the blends at high magnification: (a) 60GTR5.5/40HDPE+Hal, (b) 60GTR5.5+ad/40HDPE+Hal, (c) 80GTR5.5/20HDPE+Hal and (d) 80GTR5.5+ad/20HDPE+Hal.

10.1.3 - Effect of addition of clays

10.1.3.1 - Non revulcanized blends

The SEM images of blends showing the effect of addition of clays in the final morphology of blends are presented in Figure 81.

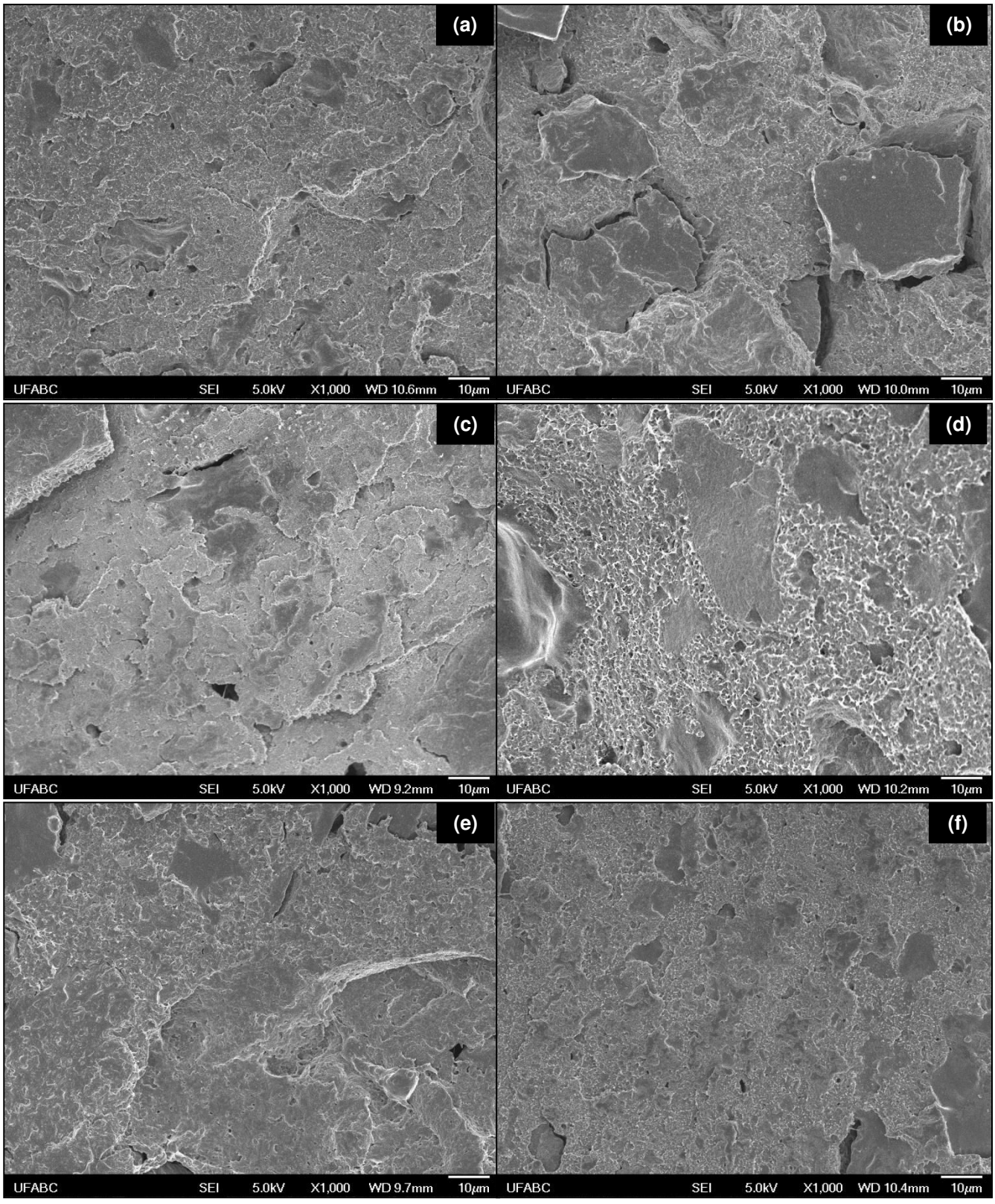

Figure 81: SEM images of the blends: (a) 60GTR5.5/40HDPE, (b) 60GTR5.5/40HDPE+20A, (c) 60GTR5.5/40HDPE+Hal, (d) 80GTR5.5/20HDPE, (e) 80GTR5.5/20HDPE+20A and (f) 80GTR5.5/20HDPE+Hal.

The addition of clays in non revulcanized blends apparently improved the distribution of sub-micrometer particles of GTR, especially the Halloysite clay. But, the presence of Cloisite 20A clay apparently reduced the interaction and the adhesion among phases, increasing the number of micrometric rubber particles and its detachment of the matrix phase. Wu et al. [252] also found that the increase in the concentration of clay in blend type TPV EPDM/PP led to the increase of size of the rubber particles and its detachment from the matrix due to the increase in the modulus of EPDM and reduction of interfacial interaction among the phases of the blend.

10.1.3.2 - Revulcanized blends

The SEM images of revulcanized blends showing the effect of addition of clays in the final morphology of blends are presented in Figure 82.

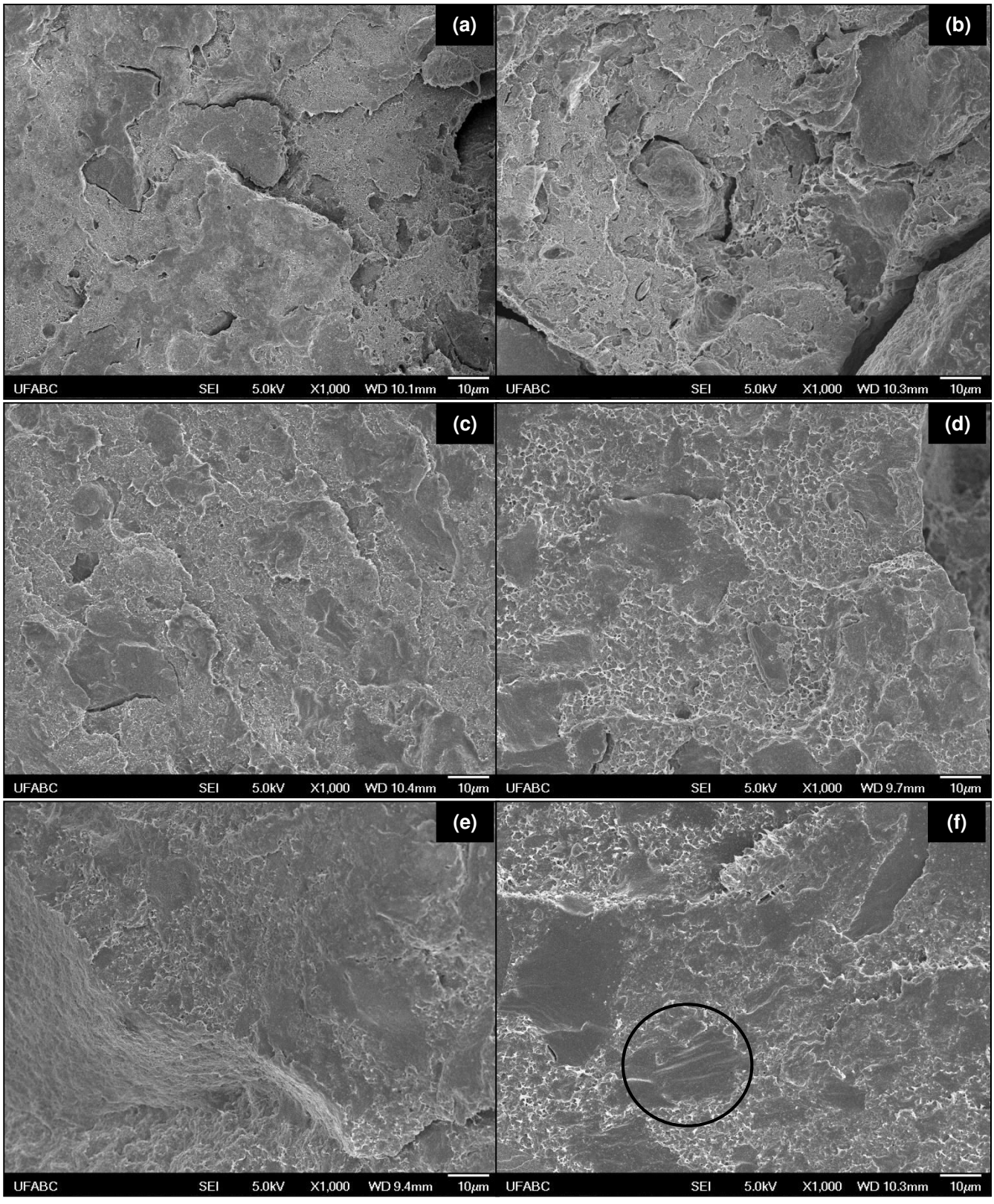

Figure 82: SEM images of the blends: (a) 60GTR5.5+ad/40HDPE, (b) 60GTR5.5+ad/40HDPE+20A (c) 60GTR5.5+ad/40HDPE+Hal, (d) 80GTR5.5+ad/20HDPE, (e) 80GTR5.5+ad/20HDPE+20A and (f) 80GTR5.5+ad/20HDPE+Hal.

The presence of clays in the revulcanized blends seems to have improved the distribution of sub-micrometer GTR particles in the matrix, in particular the Halloysite clay, which seems to have acted as a compatibilizing agent among the phases. The improvement in the distribution of the particles was more evident in blends containing 80% of GTR. In this blend, it also appears to have increased the roughness of the matrix phase.

The presence of Halloysite clay seems to have increased the thoughness and the roughness of the HDPE phase containing particles of sub-micrometer revulcanized GTR. Li et al. [313] added scrap rubber powder (it is not specified the exact composition of the dust, only that it is composed of a polar rubber and another apolar) to copolymer ethylene-octato (POE)/HDPE blend (being that it served as filler) and it was also observed increasing in thoughness of HDPE phase. According to the authors, there are two possible explanations for this increase: POE particles had dimensions ranging from submicron to micron and were finely dispersed in the matrix; POE encapsulated particles of fillers on the surface, which has increased the ability of elongation of the matrix around the fillers and increased its thoughness. In the case of this work, the first option took place and the second might have occurred in the case of blends containing Halloysite clay.

In general, it appears that even particles with sizes of the sub-micrometer order, did not resulted in materials with good mechanical properties (section 10.4), in particular low elongation at break. When analyzed the SEM images of blends with low magnifications, it turns out that, generally, the GTR particles are well dispersed, but badly distributed on thermoplastic matrix. As the analysis was carried out from the cryogenic break of tensile tests specimens, and the same was injected, the morphology was probably a result of the injection process adopted, as quoted previously.

In blends containing Cloisite 20A clay, which showed large depreciation on the results of mechanical properties (section 10.4.3), it is noted the presence of voids among the GTR particles and the matrix (Figure 83), indicating lack of adhesion among phases. Babu et al. [363] also observed such behavior in TPV blends EOC/PP and, according to the authors, the detachment of particles results in poor physical properties. In the regions with lower concentration of rubber particles, it is observed the existence of white lines on the fractured surfaces as a result of the stretch-induced crystallization [319], suggesting that the clay has served as nucleating agent in HDPE phase. The DMA results indicated that the presence of clays altered the crystallinity of HDPE

phase, and these white lines can be observed in some images of blends containing clay, as in the case of blend 80GTR5.5+ad/20HDPE+Hal (region inside the circle in Figure 82f).

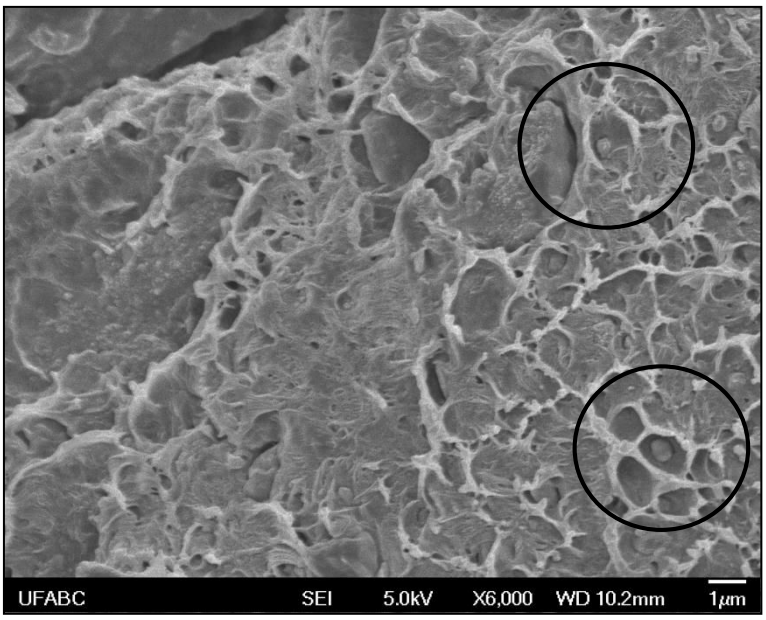

Figure 83: SEM image of the blend 60GTR5.5+ad/40HDPE+20A. The circles show the presence of GTR particles which were not extracted by solvent, being that the valley between the particles and the matrix indicates the lack of adhesion among the phases.

In the next section, the effect of the concentration of the phases on the morphology of blends will be analyzed.

10.1.4 - Effect of concentration of phases

10.1.4.1 - Non revulcanized blends

The SEM images of non revulcanized blends showing the effect of the concentration of the phases in the final morphology of blends are presented in Figure 84.

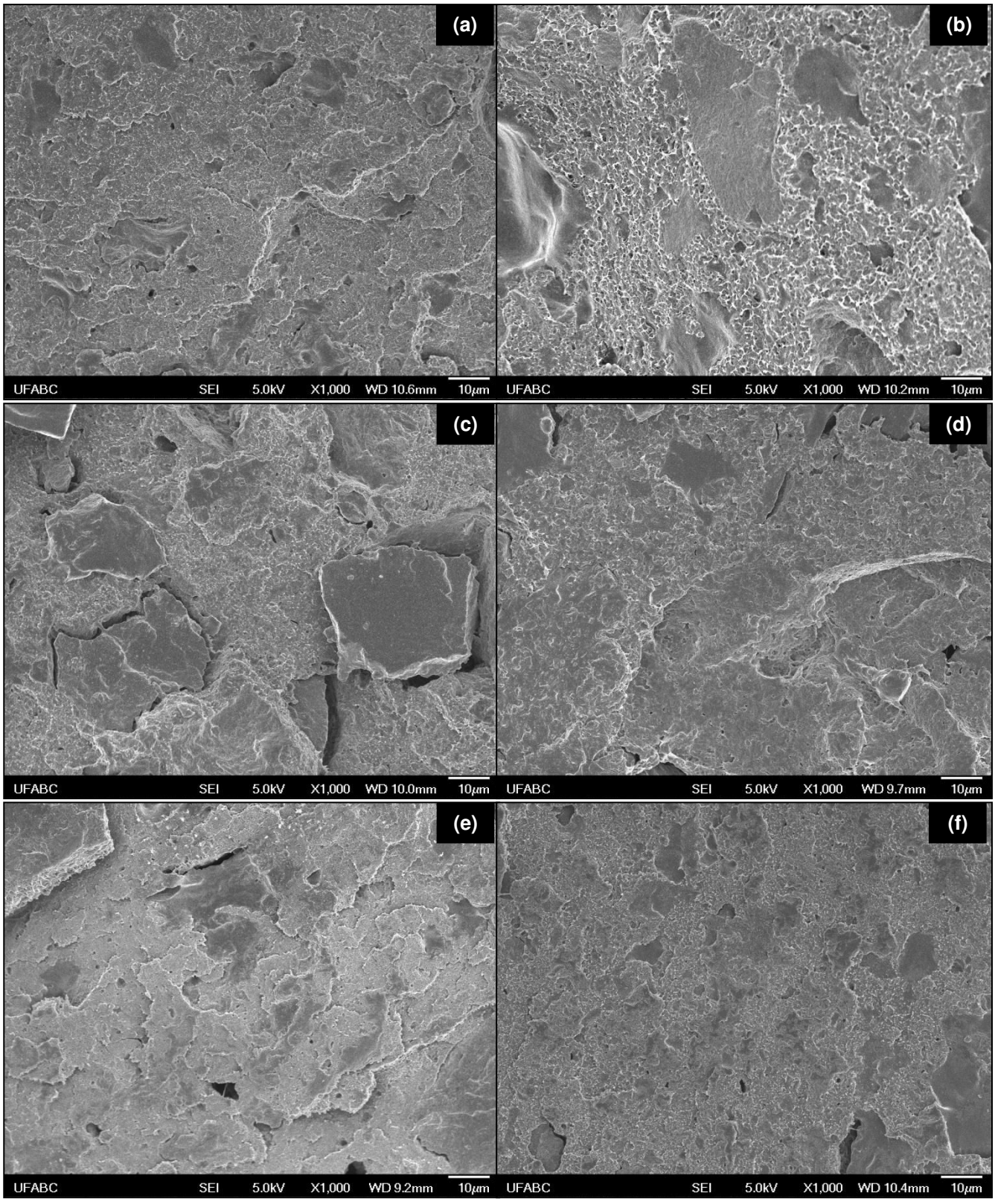

Figure 84: SEM images of the blends: (a) 60GTR5.5/40HDPE, (b) 80GTR5.5/20HDPE (c) 60GTR5.5/40HDPE+20A, (d) 80GTR5.5/20HDPE+20A, (e) 60GTR5.5/40HDPE+Hal and (f) 80GTR5.5/20HDPE+Hal.

The comments on these micrographs will be made in the next section.

10.1.4.2 - Revulcanized blends

The SEM images of revulcanized blends showing the effect of the concentration of the phases in the final morphology of blends are presented in Figure 85.

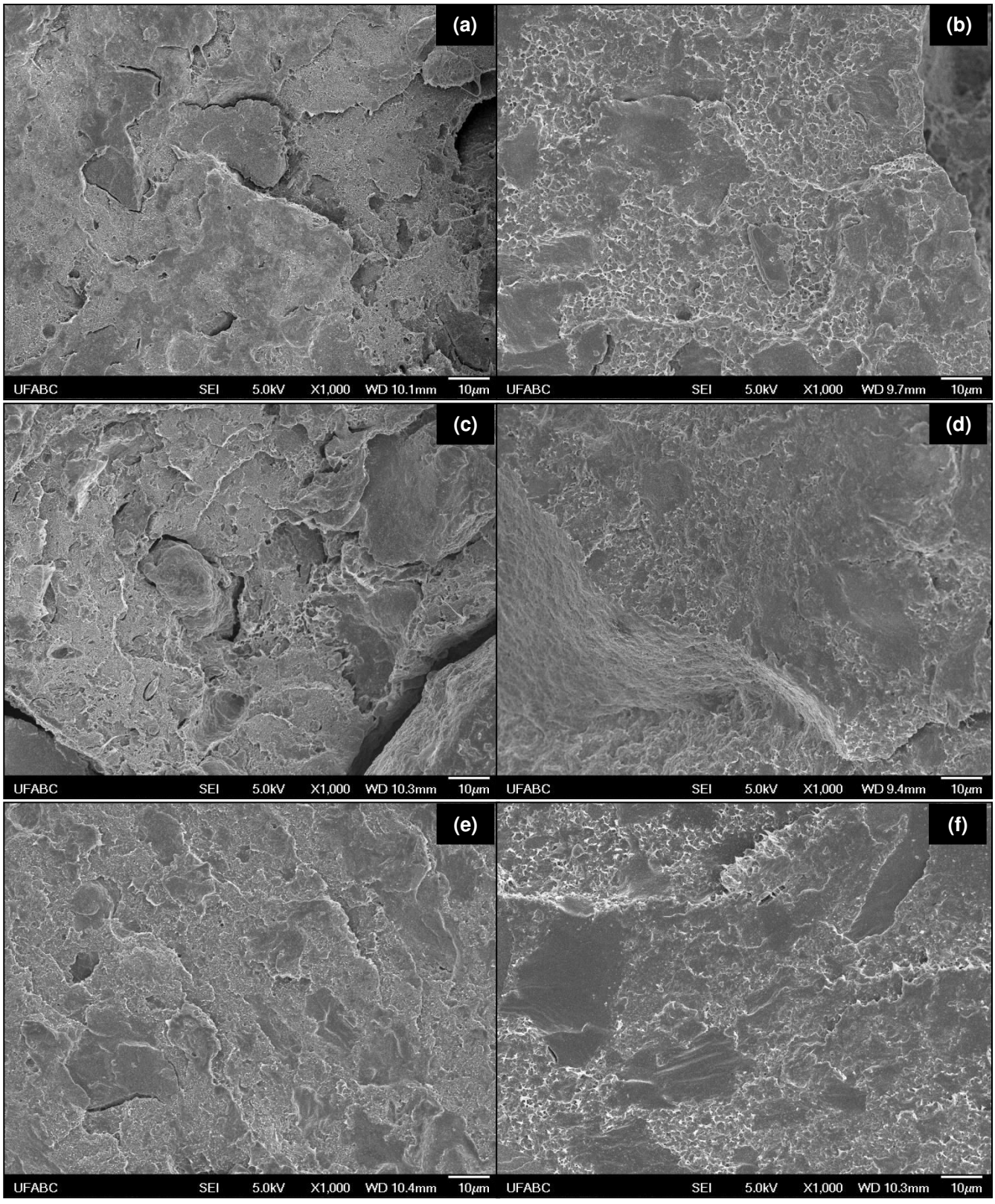

Figure 85: SEM images of the blends: (a) 60GTR5.5+ad/40HDPE, (b) 80GTR5.5+ad/20HDPE (c) 60GTR5.5+ad/40HDPE+20A, (d) 80GTR5.5+ad/20HDPE+20A, (e) 60GTR5.5+ad/40HDPE+Hal and (f) 80GTR5.5+ad/20HDPE+Hal.

The increase in the concentration of GTR, in both revulcanized and non revulcanized blends, seems to have increased the distribution of sub-micrometer particles of GTR in the matrix. The number of micrometric particles also seems to be reduced with the increase in the concentration of GTR in the blends.
However, in relation to the increase in distribution of sub-micrometer particles, a possible explanation may be the increased viscosity of the blend, which may have hampered the movement of particles of GTR on molten matrix during the injection process, avoiding possible agglomerations of particles.

In the next section, the consequences of the effects of devulcanization on elastomeric phase, revulcanization of elastomeric phase, and addition of clays and concentration of the phases in the dynamic-mechanical properties will be reviewed.

10.2 - DMA

The consequences of the different effects on dynamic-mechanical properties of the blends will be reviewed. In the next section, the effect of the devulcanization of elastomeric phase will be parsed.

10.2.1 - Effect of devulcanization of elastomeric phase

10.2.1.1 - Non revulcanized blends

Tan δ curves as function on the temperature of the blends containing GTR0 and GTR5.5 for verification of effect of GTR devulcanization on dynamic-mechanical properties of the non revulcanized blends are presented in Figure 86.

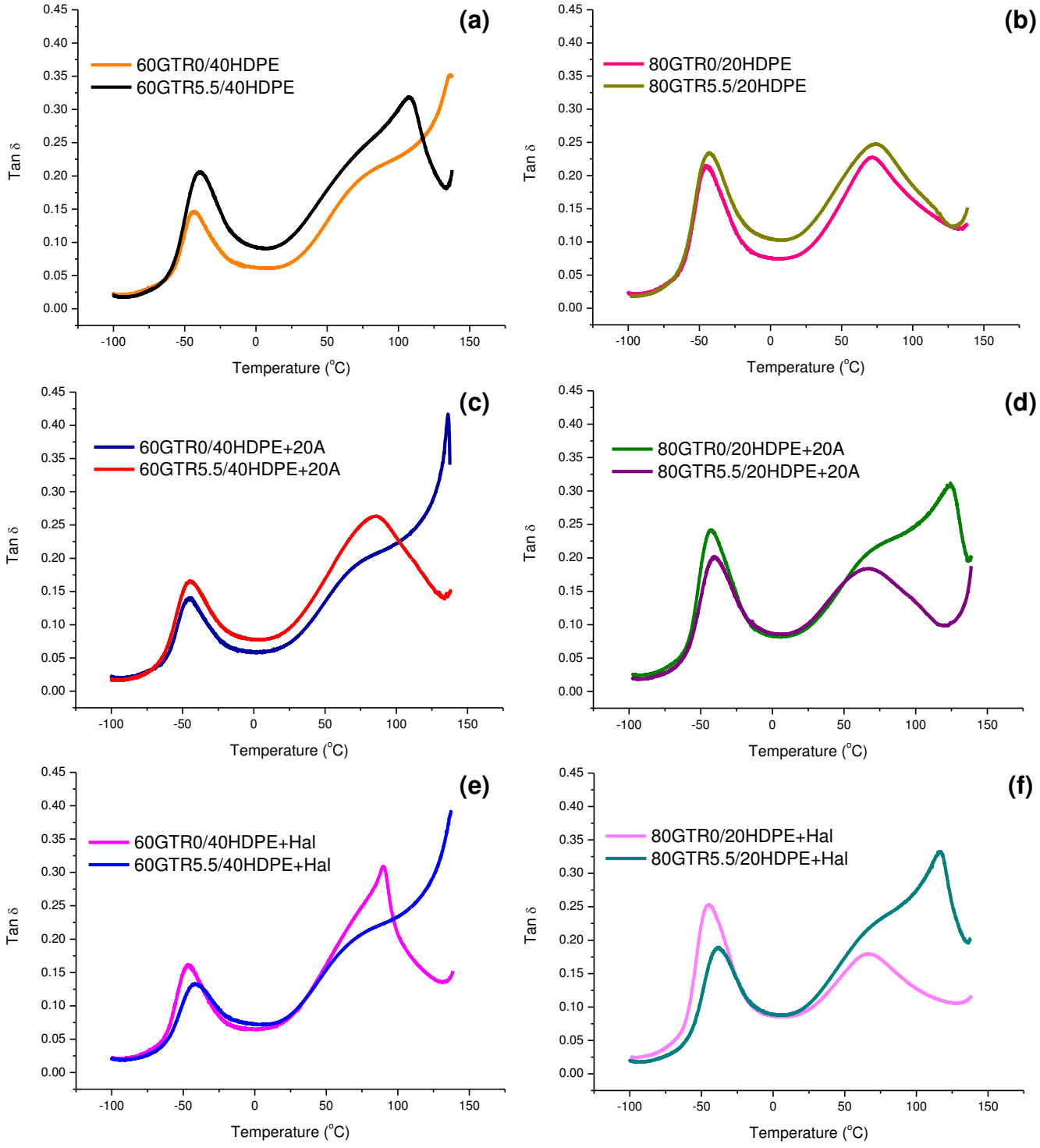

Figure 86: Tan δ curves as function on the temperature of the blends: (a) 60GTR/40HDPE, (b) 80GTR/20HDPE, (c) 60GTR/40HDPE+20A, (d) 80GTR/20HDPE+20A, (e) 60GTR/40HDPE+Hal and (f) 80GTR/20HDPE+Hal, containing GTR0 and GTR5.5 for verification of the effect of devulcanization in dynamic-mechanical properties of the non revulcanized blends.

According to Figure 86 , there are two transitions on the phases of the blends: around -

40° C refers to the T_g of the GTR and the other refers to the α transition of HDPE (T_α), which occurs around 100° C, and the same transitions were observed in all other blends to be analyzed over this section. The existence of two distinct transitions proves the character of immiscible blend. The temperature at which the transition α occurs is related to the crystallinity degree and the average thickness of the crystallites. It is also related to the occurrence of rotations of small molecular sequences in the crystallites [364], which can be subdivided into smaller subdivisions known as pre-melting temperature [365]. The transition refers to the relaxation of the limits of the grains, a subdivision of α transition known as α ' [366].

According to Molefi et al. [367], the increase of the crystallinity of the thermoplastic phase causes the increase in the intensity of this peak, which is often checked in the case of HDPE. The increase in intensity of the peaks relating to the transition of the thermoplastic phase was verified in some blends containing GTR5.5 because, as verified in the SEM images (section 10.1.1), the devulcanization of the elastomeric phase resulted in particle size smaller and well distributed in the matrix, which may, possibly, have changed the crystallinity of matrix phase. Similarly, variations in the region of curves were also verified related to the thermoplastic phase of blends containing clay, which possibly acted as nucleation points to HDPE [319].

According to Cao et al. [358], decrease of peak widths of tan δ in the region on the elastomeric phase transition is a result of the reduction of mobility of polymer chains. In the case of blends comprising of devulcanized GTR, extending the width of the peak in temperatures around -50° C as a result of the greater mobility of the GTR due to breaking of three-dimensional structure by devulcanization by microwaves. Also, in relation to the T_g values, were not observed large variations among the blends containing GTR0 and GTR5.5, to be checked next.

10.2.1.2 - Revulcanized blends

Tan δ curves as function on the temperature of the blends containing GTR0 and GTR5.5 for verification of effect of GTR devulcanization in dynamic-mechanical properties of the revulcanized blends are presented in Figure 87.

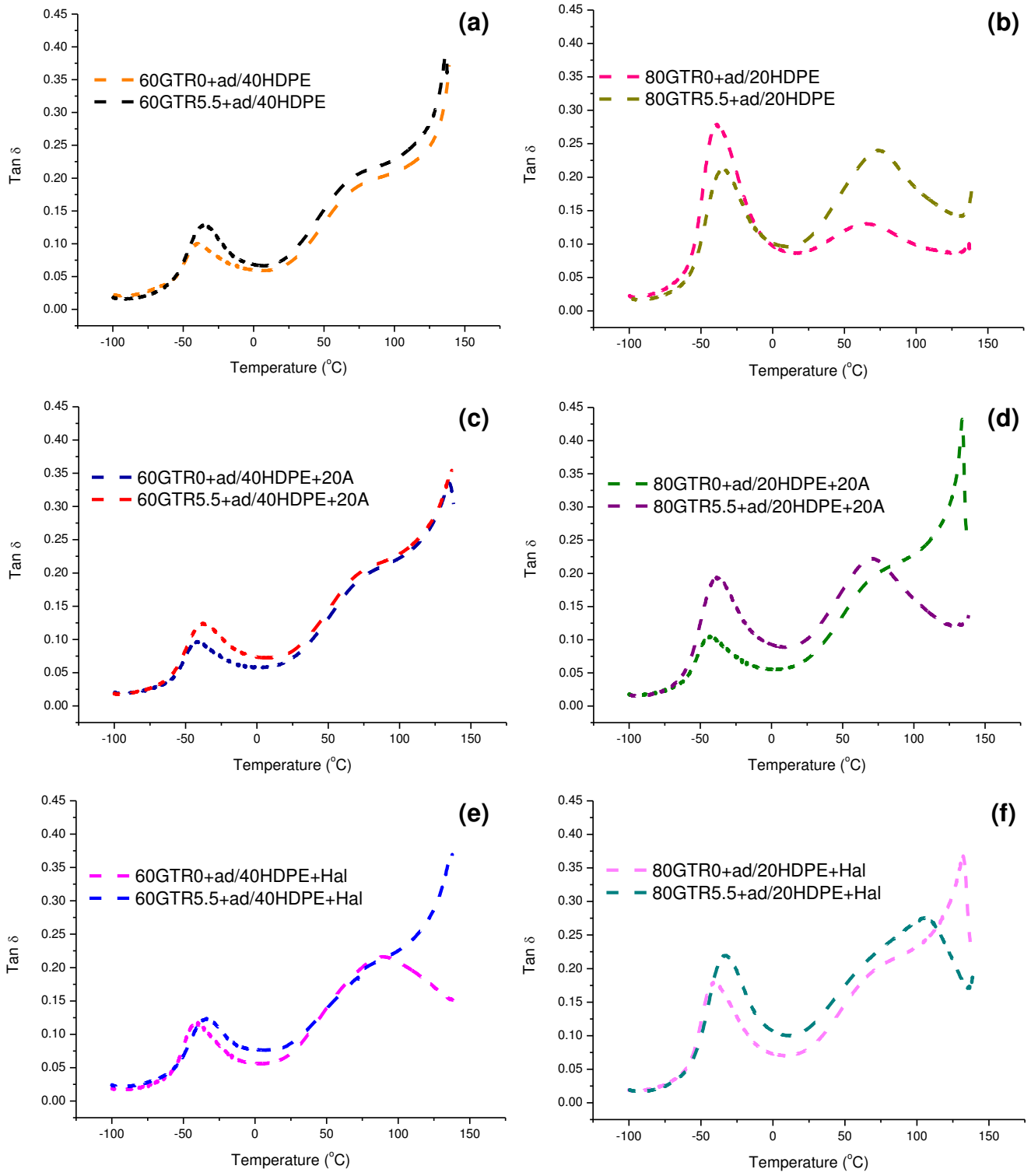

Figure 87: Tan δ curves as function on the temperature of the blends: (a) 60GTR+ad/40HDPE, (b) 80GTR+ad/20HDPE, (c) 60GTR+ad/40HDPE+20A, (d) 80GTR+ad/20HDPE+20A, (e) 60GTR+ad/40HDPE+Hal and (f) 80GTR+ad/20HDPE+Hal, containing GTR0 and GTR5.5 for verification of effect of devulcanization in dynamic-mechanical properties of revulcanized blends.

According to the Figure 87, it was observed reduction in the area under the T_g peak of GTR phase of blends containing GTR0 due to the restriction on the mobility of the chains by the increase of cross-linking density [368]. Such behavior is due to the probable coexistence of two three-dimensional networks, the first from the vulcanization of the GTR and the second of dynamic revulcanization, what does not mean that it has higher cross-linkings density. This is also due to the increase in the E' values of GTR0 phase, which probably hindered the breaking of the GTR0 particles during processing; resulting in larger rubber particles, as verified in the SEM images (section 10.1.1).

T_g values of GTR phase of the analyzed blends so far were determined from the maximum points from the first peak of tan δ curves as function of temperature, and they are presented in Figure 88.

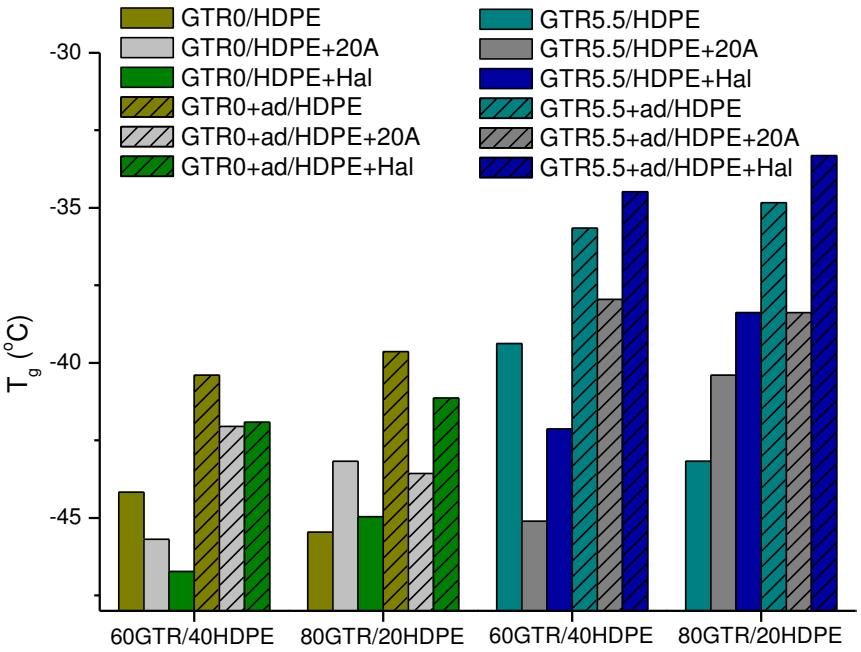

Figure 88: T_g values of elastomeric phase of revulcanized and non revulcanized blends GTR0/HDPE and GTR5.5/HDPE, with HDPE phase whether or not containing clay.

In general, in the blends containing revulcanized GTR0, T_g values are smaller in comparison to revulcanized blends containing the same concentration of GTR5.5. Due to the devulcanization, the polymeric chains displayed greater freedom during the

reactive processing, which probably has increased the number of effective shocks and resulted in increased cross-linkings density of elastomeric phase of blends containing GTR5.5. Also according to the FTIR results presented in Stage 1 of this work (section 3.4.1), the cross-linkings density in blends containing GTR5.5 was superior due probably to the formation of new bands C=C generated during the devulcanization process.

Whereas in relation to non revulcanized blends, they showed a slight difference among the T_g values of the blends containing or not clay, which is considered to be in the range of the experimental error of the analysis.

In the following section, the effect of revulcanization of elastomeric phase will be analyzed in the dynamic-mechanical properties blends.

10.2.2 - Effect of revulcanization of elastomeric phase

10.2.2.1 - Blends without clay

Tan δ curves as function of temperature of blends containing GTR5.5 in different concentrations for verification of the effect of revulcanization on dynamic-mechanical properties of the blends are presented in Figure 89.

According to the Figure 89, it was found the shift of T_g peak of the GTR to all blends containing revulcanized dispersed phase to higher temperatures, especially in the blends containing 40 and 80% of GTR. As the T_g value is extracted from the maximum point of this peak, its displacement in the direction to higher temperatures shows the increase in T_g values with the revulcanization of GTR phase due to the increase in cross-linking density. It was also observed a slight approaching among the peaks of revulcanized blends.

In general, there was reduction in the area under tan δ peak related to T_g of the elastomeric phase in revulcanized blends, especially in blends containing 60 and 80% of GTR, as a result of the restriction on the mobility of the rubber chains due to dynamic revulcanization [368].

In relation to the thermoplastic phase, a difference was observed in the crystallinity with revulcanization of blends containing 40 and 60% of GTR. Such variation of crystallinity

is probably due to changes in morphologies, as verified in the SEM images. However, for better analysis of changes in crystallinity of the thermoplastic phase it is necessary the performance of DSC analyses, which were not carried out in this work.

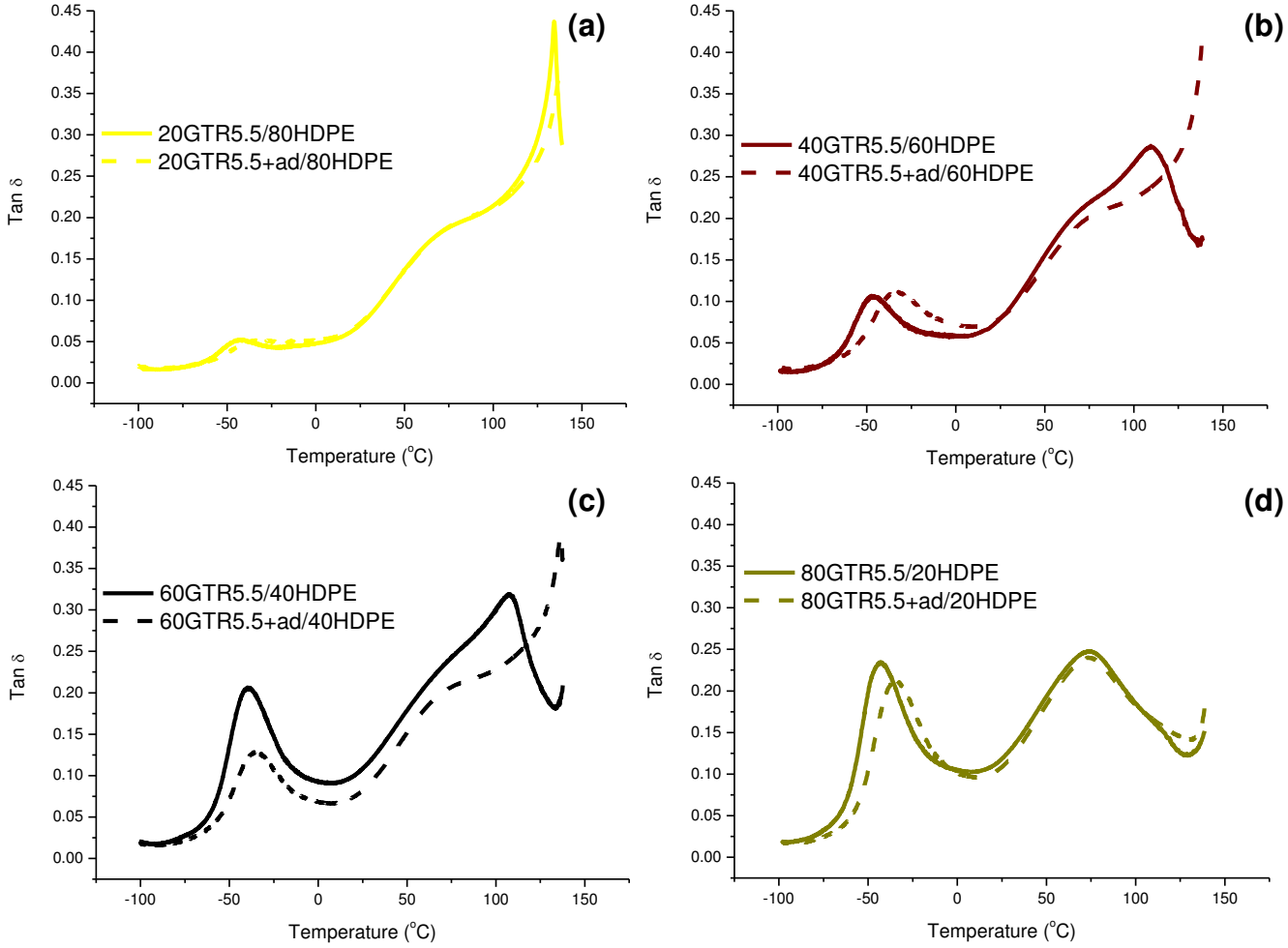

Figure 89: Tan δ curves as function of the temperature of revulcanized and non revulcanized blends:(a) 20GTR5.5/80HDPE, (b) 40GTR5.5/60HDPE, (c) 60GTR5.5/40HDPE and (d) 80GTR5.5/20HDPE for verification of the effect of revulcanization on dynamic-mechanical properties of the blends without the addition of clay.

10.2.2.2 - Blends containing Cloisite 20A clay

Tan δ curves as function of temperature of blends containing GTR5.5 in different concentrations containing Cloisite 20A clay for verification of the effect of revulcanization on dynamic-mechanical properties of the blends are presented in Figure 90.

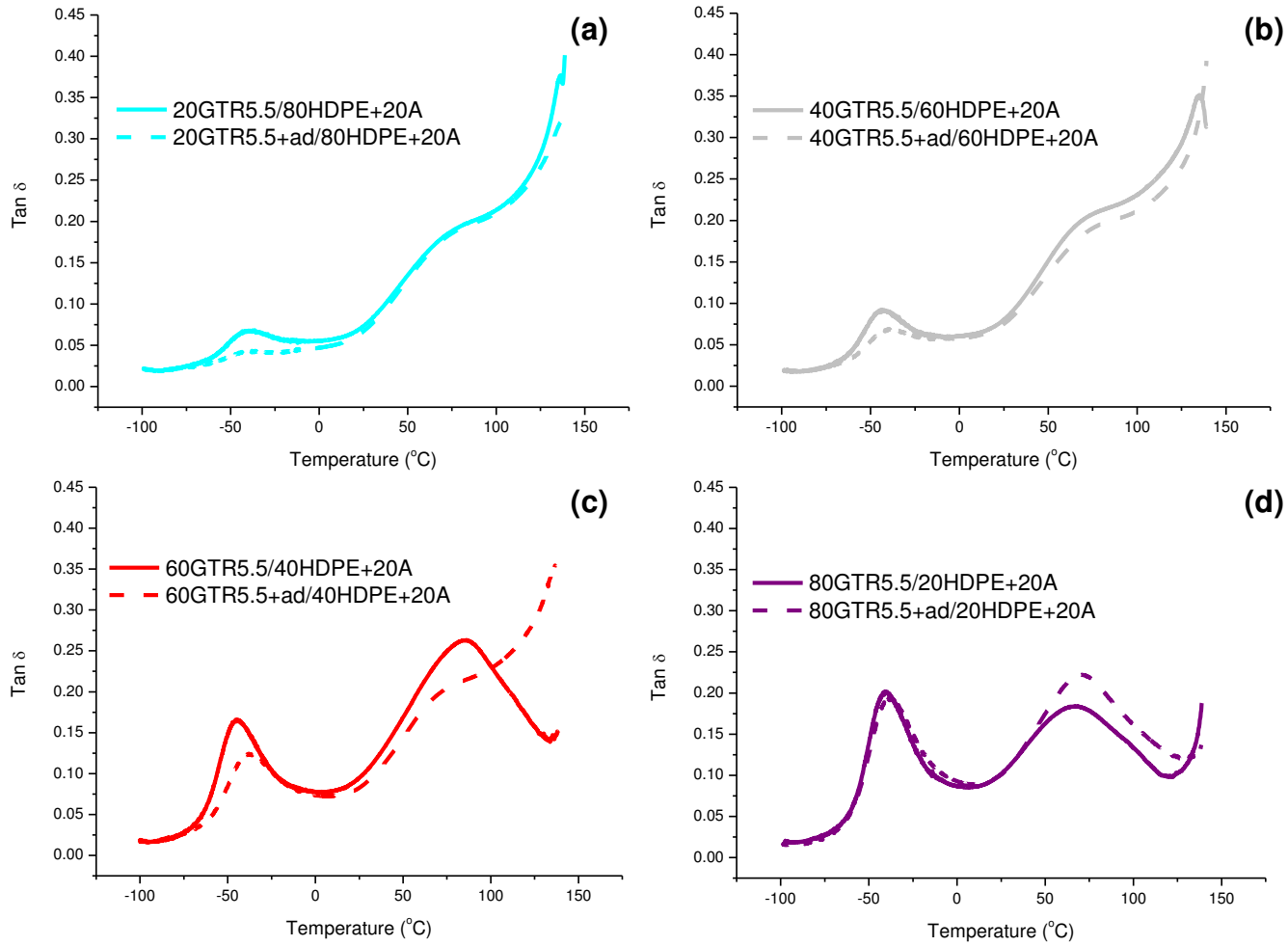

Figure 90: Tan δ curves as function of the temperature of revulcanized and non revulcanized blends: (a) 20GTR5.5/80HDPE+20A, (b) 40GTR5.5/60HDPE+20A, (c) 60GTR5.5/40HDPE+20A and (d) 80GTR5.5/20HDPE+20A for verification of the effect of revulcanization on dynamic-mechanical properties of blends containing Cloisite 20A clay.

As in blends without clay, it was verified the reduction in the area under the tan δ peak concerning the T_g of elastomeric phase in the revulcanized blends as a result of the restriction on the mobility of the rubber chains due to cross-linkings [368]. There was a slight shift of the T_g peak of elastomeric phase towards higher temperatures of revulcanized blends.

In relation to thermoplastic phase, the revulcanization of GTR phase of blends containing Cloisite 20A clay caused some change in crystallinity of the thermoplastic phase, especially in the blend containing 60% of GTR. Such variation is probably, as cited previously, to changes in morphology caused by dynamic revulcanization. However, as mentioned previously, for better analysis of changes in crystallinity of the

thermoplastic phase, it is necessary perform DSC analyses, which have not been carried out in this work.

10.2.2.3 - Blends containing Halloysite clay

The curves of tan δ as function of temperature of blends containing Halloysite clay and different concentrations of GTR5.5 for verification of the effect of revulcanization on dynamic-mechanical properties of the blends are presented in Figure 91.

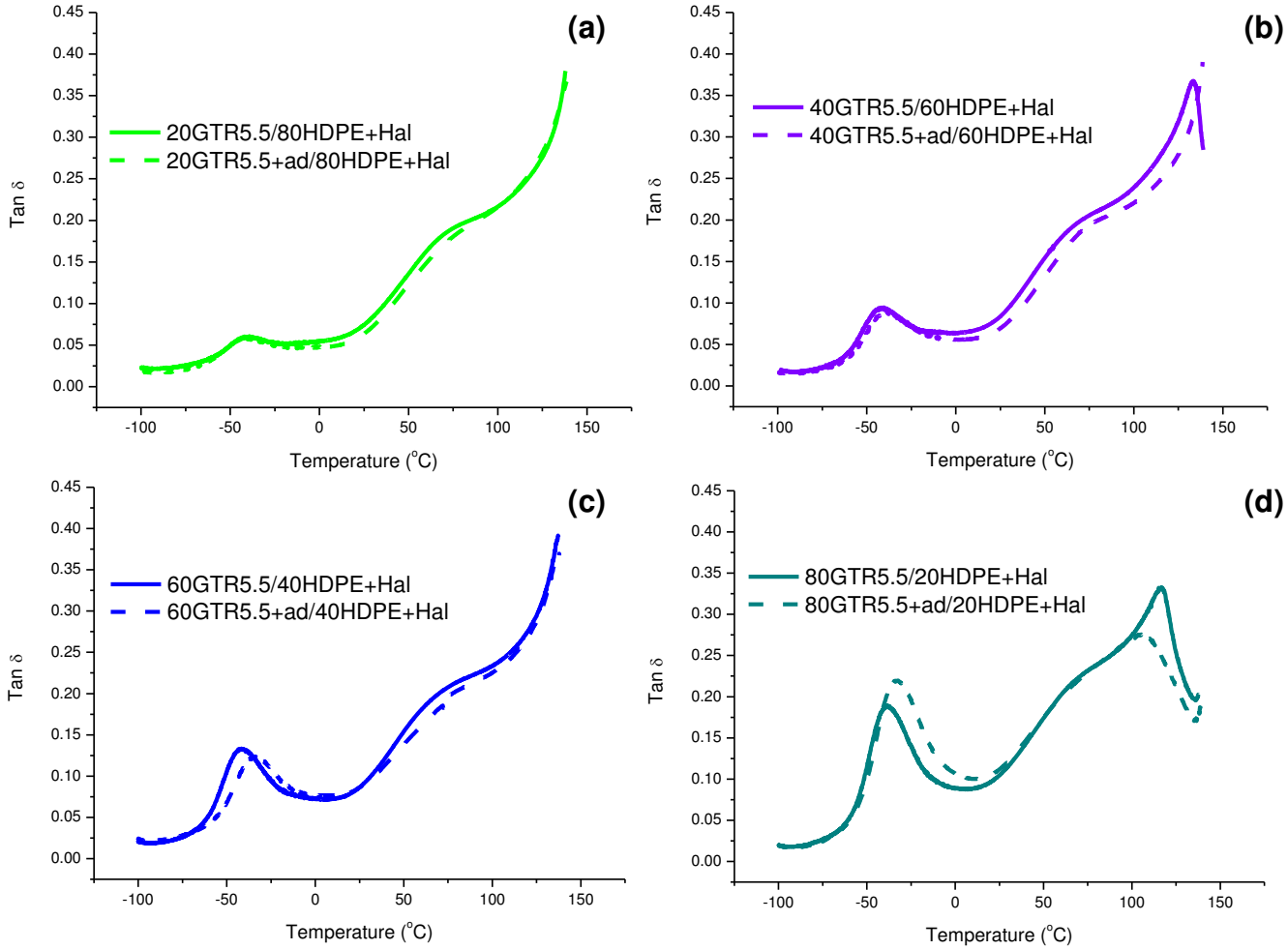

Figure 91: Tan δ curves as function of the temperature of revulcanized and non revulcanized blends: (a) 20GTR5.5/80HDPE+Hal, (b) 40GTR5.5/60HDPE+Hal, (c) 60GTR5.5/40HDPE+Hal and (d) 80GTR5.5/20HDPE+Hal for verification of the effect of revulcanization on dynamic-mechanical properties of blends containing Halloysite clay.

According to the Figure 91, there was a discrete peak shift of the T_g of elastomeric phase of revulcanized blends of all blends containing Halloysite clay, especially in

blends containing 60 and 80% of GTR. The displacement of these peaks towards higher temperatures shows the increase in T_g values with revulcanization of the GTR phase due to the increase in cross-linking density.

In relation to thermoplastic phase, the GTR revulcanization of blends containing Halloysite clay appears not to have changed significantly the crystallinity of the thermoplastic phase.

T_g values relative to the elastomeric phase of blends containing GTR5.5 are presented in Figure 92. The values were taken from the maximum point of the T_g peak of tan δ curves *versus* temperature.

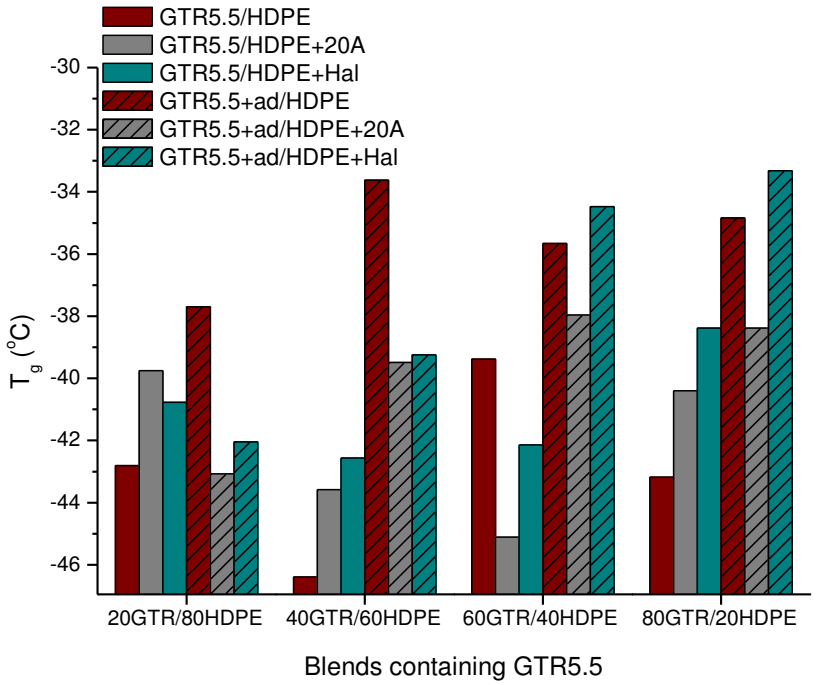

Figure 92: T_g values of elastomeric phase of revulcanized and non revulcanized blends containing GTR5.5.

In general (with the exception of a few blends containing 20% of GTR), the increase in the T_g value of the revulcanized blends in relation to the non revulcanized, what was expected, since in these blends the rubber revulcanized during processing and its cross-linking density became superior in comparison to the non revulcanized blend, causing the increase in T_g value. GTR phase of revulcanized blends with high concentrations of GTR5.5 (60 and 80%) containing Halloysite clay presented T_g values higher than those

blends without clay. Clay's presence increased the viscosity of the thermoplastic phase due to degradative processes observed (as verified on the results of Stage 1 of capillary rheometry, section 3.7), which generated a higher viscous heating and probably facilitated the revulcanization reaction.
The elastomeric phase of revulcanized blends containing Cloisite 20A clay presented lower T_g values than other blends. Even the clay being preferably present in HDPE phase of blends, it somehow acted negatively in the reaction of dynamic revulcanization of these blends, reducing the cross-linking density of GTR phase.
The T_g values variation observed in the non revulcanized blends due to the presence of clays was smaller and can be regarded as within the experimental error of the analysis.

In the next section will be analyzed the effect of addition of clays in the dynamic-mechanical properties of the blends.

10.2.3 - Effect of addition of clay

10.2.3.1 - Non revulcanized blends

The curves of tan δ as function of temperature of blends containing GTR5.5 for verification of the effect of addition of clays in the dynamic-mechanical properties of non revulcanized blends are presented in Figure 93.

The presence of clay has reduced the area under the peak of tan δ related to T_g of elastomeric phase, especially in blends containing 60 and 80% of GTR as a result of the restriction on the mobility of the rubber chains [368]. It has not been verified major displacements of T_g peak of elastomeric phase due to the presence of clays.
In blends containing 60 and 80% of GTR and Cloisite 20A clay, it is verified the peak shift for the α transition toward the T_g of elastomeric phase, indicating possible chemical interactions among the phases due to the presence of clays.

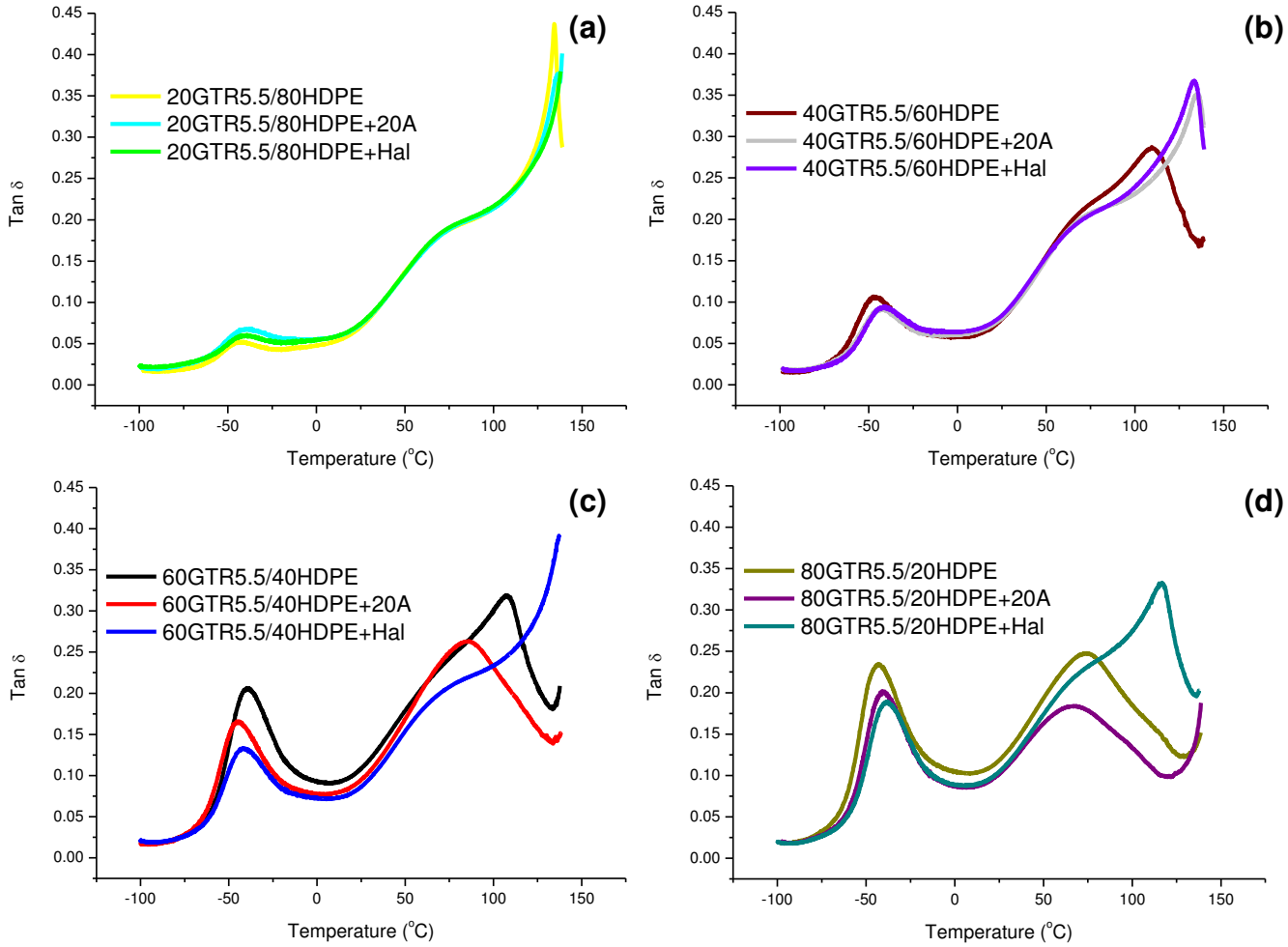

Figure 93: Tan δ curves in function on the temperature of the blends: (a) 20GTR5.5/80HDPE, (b) 40GTR5.5/60HDPE, (c) 60GTR5.5/40HDPE and (d) 80GTR5.5/20HDPE, whether or not containing Cloisite 20A and Halloysite clays to check influence of their addition on dynamic-mechanical properties of non revulcanized blends.

10.2.3.2 - Revulcanized blends

Tan δ curves as function of temperature of blends containing GTR5.5 for verification of the effect of addition of clays in the dynamic-mechanical properties of revulcanized blends are presented in Figure 94.

According to Figure 94, with the exception of blends containing 60% of GTR, slight changes were verified in relation to the T_g peaks of the GTR phase of revulcanized blends with the addition of clays. The T_g values and the influence of the presence of clays in these values are present in the section 10.2.2.3.

According to Jose et al. [273], the increase in peak intensity on the HDPE transition

implies the increased mobility of the phase, as well as to improve the toughness of the matrix. Such behavior was observed in 80GTR5.5+ad/20HDPE+Hal blend, and the toughness of the matrix was proven through SEM images.

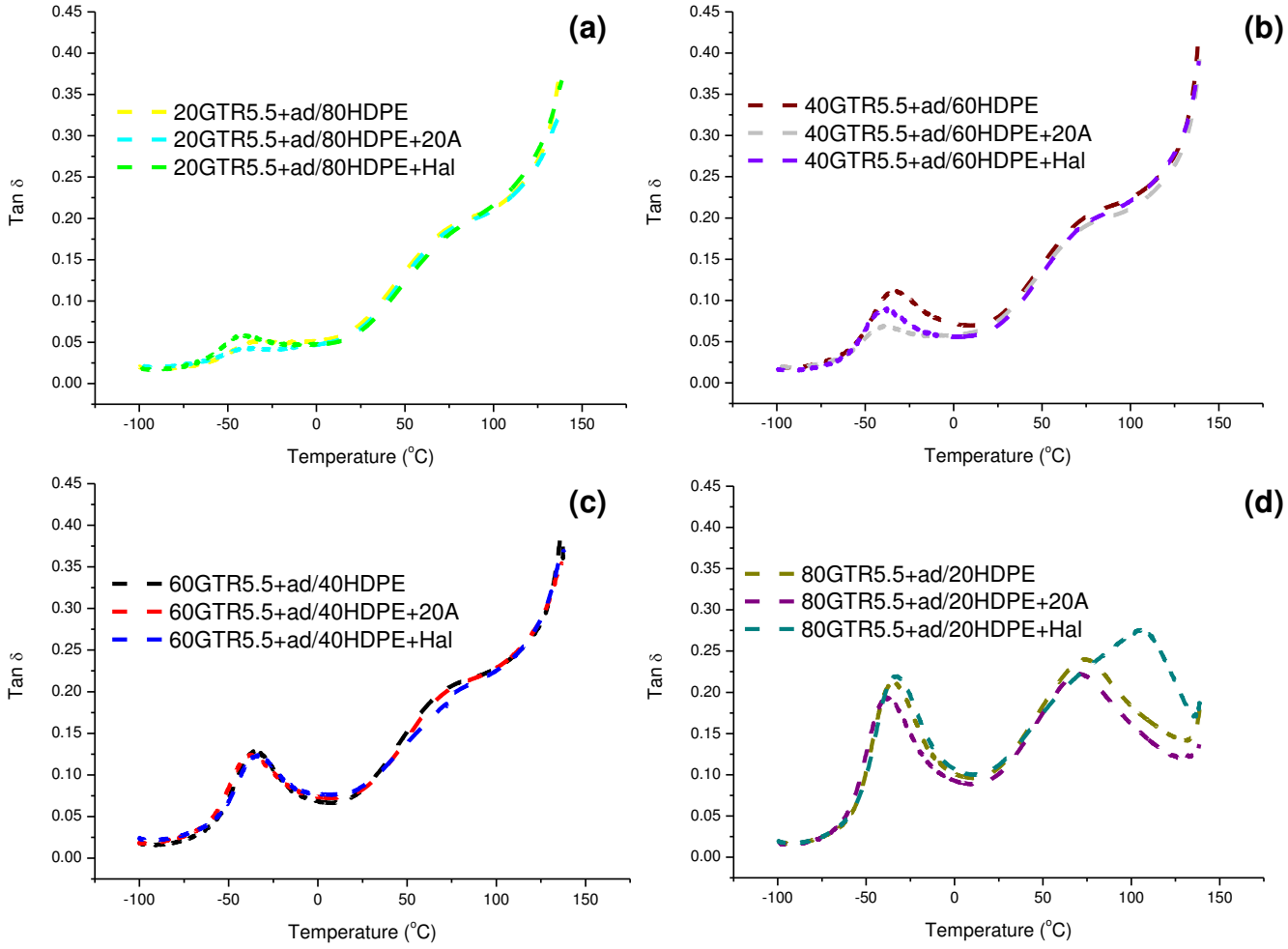

Figure 94: Tan δ curves as function on the temperature of the blends: (a) 20GTR5.5+ad/80HDPE, (b) 40GTR5.5+ad/60HDPE, (c) 60GTR5.5+ad/40HDPE and (d) 80GTR5.5+ad/20HDPE, whether or not containing Cloisite 20A and Halloysite clays to check the influence of their addition on the dynamic-mechanical properties of revulcanized blends.

In the next section will be analyzed the effect of the variation of concentration of the phases in the dynamic-mechanical properties of the blends.

10.2.4 - Effect of concentration of the phases

10.2.4.1 - Non revulcanized blends

E' and tan δ curves as function of temperature of blends containing GTR5.5 for verification of the effect of the concentration of the phases in the dynamic-mechanical properties of non revulcanized blends are presented in Figure 95.

As reported by Babu et al. [368], DMA analysis is a powerful tool for the study of phase morphology of blends. According to the same authors, the sudden reduction in the storage modulus with increase in temperature is due to the increased mobility of the segments. In general, at temperatures around -50°C there is a intense decline in the storage modulus of the blends due to the increase in mobility of GTR segments, which shows that the blend has the morphology of dispersed phase and the HDPE is the matrix phase. On the other hand, in the blends 20GTR5.5/80HDPE, 20GTR5.5/80HDPE+20A, and 20GTR5.5/80HDPE+Hal such decline is not observed, showing that the GTR phase restricts the movement of the HDPE segments due to the co-continuous morphology phase of these blends. The analysis of the obtained results is also in accordance with the work of other authors [305, 355, 369].

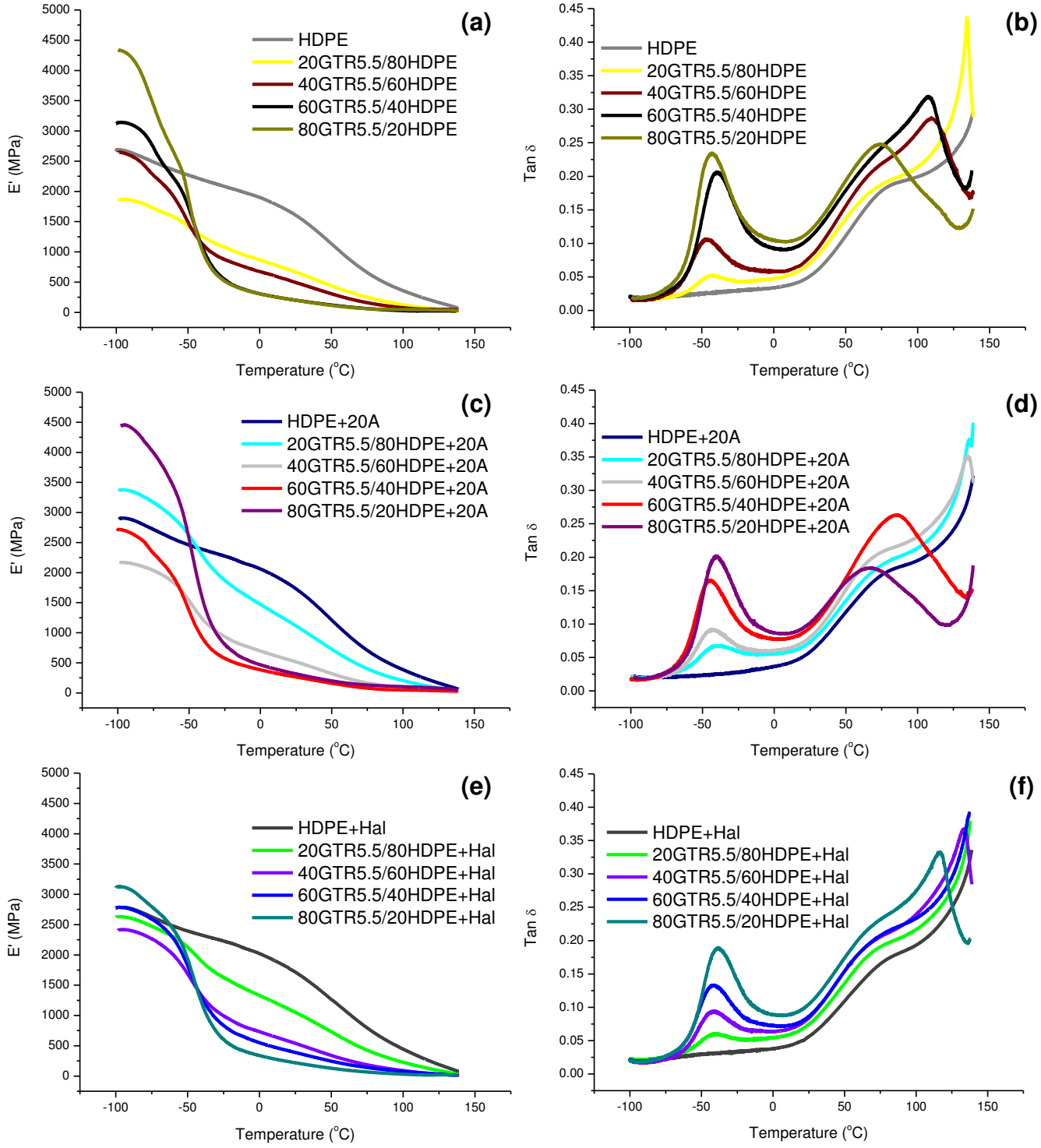

Figure 95: E' curves as function on the temperature of the blends: (a) GTR5.5/HDPE, (c) GTR5.5/HDPE+20A and (e) GTR5.5/HDPE+Hal, and tan δ curves as function on the temperature of the blends: (b) GTR5.5/HDPE, (d) GTR5.5/HDPE+20A and (f) GTR5.5/HDPE+Hal containing different concentrations of the phases for verification of this effect in the dynamic-mechanical properties of the non revulcanized blends.

10.2.4.2 - Revulcanized blends

E' and tan δ curves as function of temperature of blends containing GTR5.5 for verification of the effect of the concentration of the phases in the dynamic-mechanical properties of revulcanized blends are presented in Figure 96.

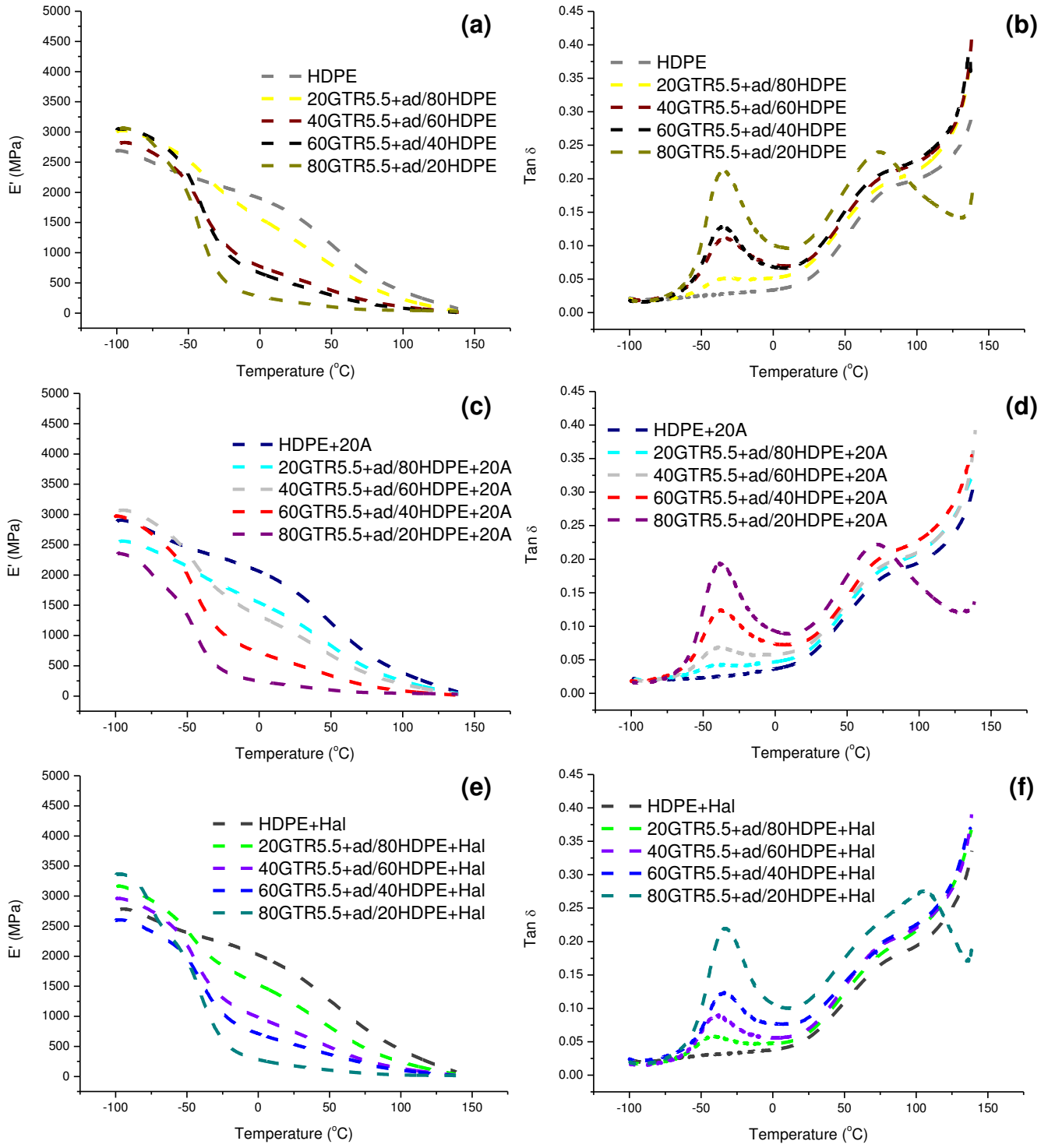

Figure 96: E' curves as function on the temperature of the blends: (a) GTR5.5+ad/HDPE, (c) GTR5.5+ad/HDPE+20A and (e) GTR5.5+ ad/HDPE +Hal, and tan δ curves as function on the

temperature of the blends: (b) GTR5.5+ad/HDPE, (d) GTR5.5+ad/HDPE+20A and (f) GTR5.5+ad/HDPE+Hal, containing different concentrations of the phases for verification of this effect in the dynamic-mechanical properties of revulcanized blends.

As previously mentioned, the decline of the storage modulus of the blends at temperatures around -50°C refers to the increased mobility of the GTR chains. In 20GTR5.5+ad/80HDPE, 20GTR5.5+ad/80HDPE+20A, 40GTR5.5+ad/60HDPE+20A and 20GTR5.5+ad/80HDPE+Hal blends, such decline is not observed, showing that one of the phases of the segments restricts another due to the morphology of these blends be of co-continuous phases. A difference of this group to the non revulcanized blends is that the non revulcanized blend containing 40% GTR and Cloisite 20A clay has dispersed morphology, while the revulcanized blend of same concentration has co-continuous morphology.

Another important observation was that the crystallinity of matrix phase has changed in all the blends containing 80% of GTR. As Jose et al. work cited earlier [273], the increase in peak intensity on the HDPE transition implies the increased mobility, as well as improvements in toughness of the matrix. The SEM images of these samples showed that GTR sub-micrometer particles induced toughness processes. SEM images have also shown that these blends presented smaller particle sizes possibly due to the high concentration of GTR present in blends, which may also have influenced the crystallinity of HDPE. However, as cited previously, for better analysis of changes in crystallinity of the thermoplastic phase it is necessary to perform DSC analyses, which were not carried out in this work.

The values of E' at 30°C of the analyzed blends are presented graphically in Figure 97.

The increase in the E' value is a sign of strengthening. The literature offers several forms of reinforcement in TPV type blends, either by adding a filler [284] or by an increase in the cross-linkings density of the elastomeric phase [370].

In general, it appears that there is a no direct link of the increased E' with the increase of T_g of the blend, which demonstrates that the reinforcement was not only result from the increase in cross-linkings density of the GTR phase.

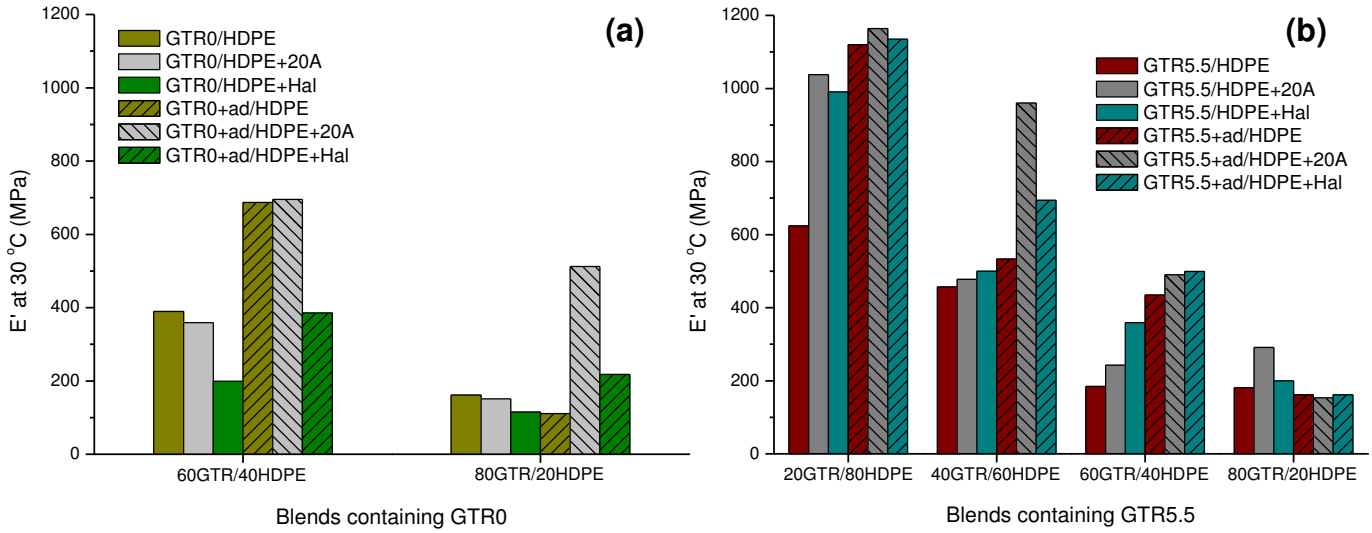

Figure 97: E' values at 30°C of the blends: (a) containing GTR0 and (b) containing GTR5.5.

ATR-FTIR results from Stage 1 showed that the presence of Halloysite clay caused the degradation of HDPE for branching and posterior cross-linking, and the results of rheology of parallel plates showed that the presence of clays acts both as strengthening agent, and as a "degrading" agent by changing the G' values of the blends (section 10.3.3). E' results presented in Figure 97 agree with the results of parallel plates rheology and, depending on the specific situation, E' value is influenced by reinforcing action of clay, degradation of the matrix, blend morphology or by cross-linking density of GTR phase.

An interesting example are the blends containing Cloisite 20A clay. On the results of rheology of parallel plates it was observed that, in revulcanized blend containing 60% of GTR, it acted as a strengthening agent, while in blend containing 80% of GTR it acted as a "degrading" agent. The results shown demonstrate the same behavior, and show that in the case of these blends, the cross-linking density of GTR phase does not influence effectively on the E' values, since the T_g values of these blends were lower compared to other blends with equal concentration of GTR.

In the next section, the consequences of the effects of devulcanization of the elastomeric phase, elastomeric revulcanization phase, addition of clays and concentration of the phases in the rheological properties will be reviewed.

10.3 - Rheometry of parallel plates in oscillatory regime

In the following section, the consequences of the effect of devulcanization on the elastomeric phase on rheological properties of the blends will be reviewed.

10.3.1 - Effect of devulcanization of elastomeric phase

10.3.1.1 - Non revulcanized blends

The curves of variation of the storage modulus and complex viscosity as a function of frequency at 180°C of blends containing GTR0 and GTR5.5 for verification of effect of devulcanization in rheological properties of non revulcanized blends are presented in Figure 98.

According to Figure 98, all blends showed reduced complex viscosity with increasing frequency, which suggests pseudoplastic behavior or characteristics of shear-thinning [247, 255]. In general, the blends containing GTR5.5 presented lower values of complex viscosity in comparison to blends containing GTR0 due to the higher flow capacity as a result of the breaking of the cross-linkings of the GTR due to devulcanization by microwaves.

According to Avgeropoulos et al. [336], the storage modulus of rubber/thermoplastic blends depends primarily on the composition and then on their morphology (dispersion of rubber in the thermoplastic phase and modulus of rubber phase, that depends on its cross-linking density), so the rheology is a technique of such importance.

Overall, it appears that the blends containing GTR0 present higher G' values of complex viscosity regarding to blends containing GTR5.5, what is probably due to the highest cross-linking density of the elastomeric phase of the blend containing non devulcanized rubber (GTR0), as shown on the results presented in Stage 1 of this work. The greater rigidity of the GTR0 phase (Figure 98d, e and f) in relation to GTR5.5 hinders the break of the GTR during processing, as well as reduces the interfacial interaction [252], as verified in the SEM images (section 10.1.1.1).

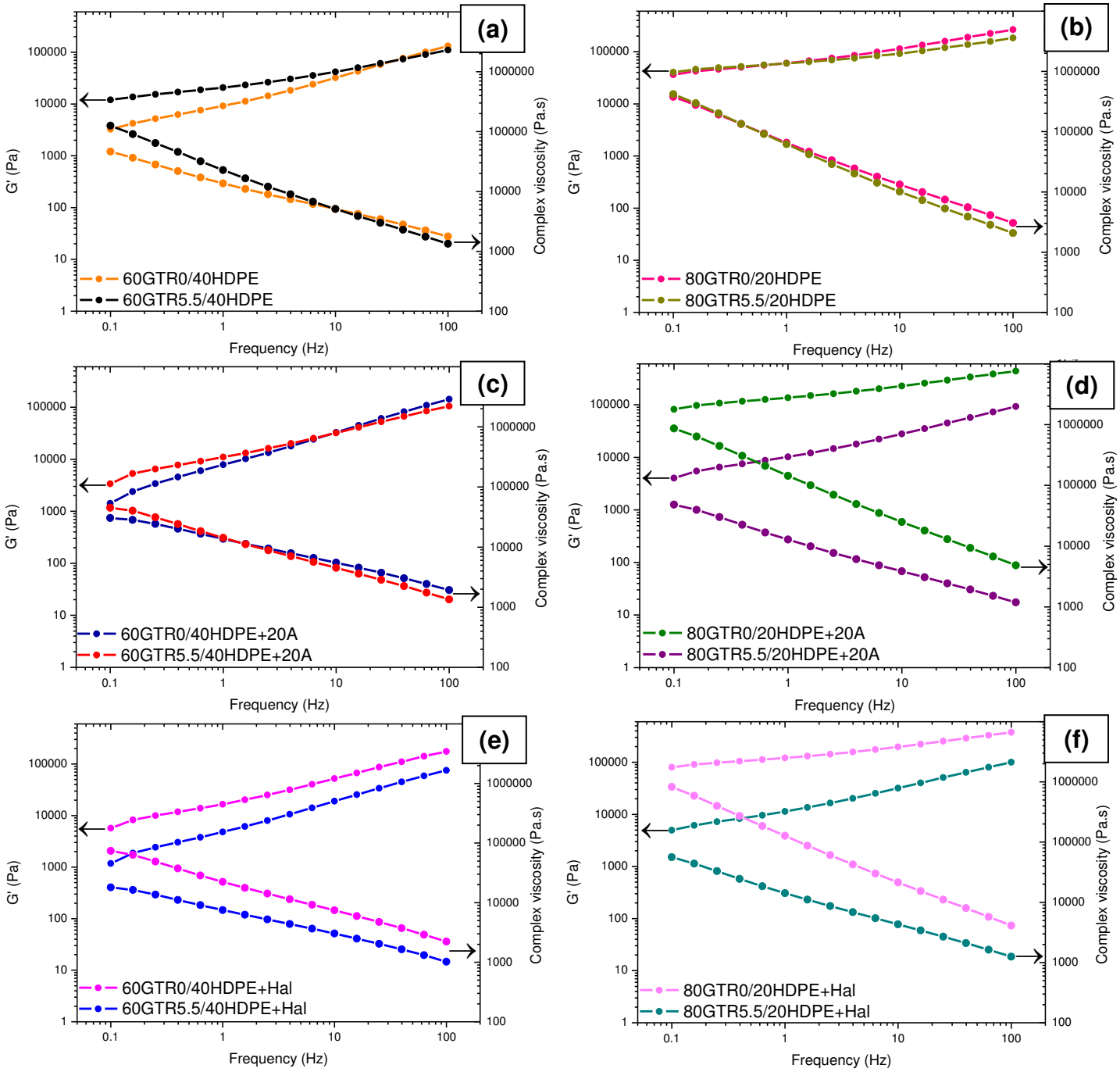

Figure 98: Evolution of the storage modulus and the complex viscosity with the frequency of the blends: (a) 60GTR/40HDPE, (b) 80GTR/20HDPE , (c) 60GTR/40HDPE+20A, (d) 80GTR/20HDPE+20A, (e) 60GTR/40HDPE+Hal and (f) 80GTR/20HDPE+Hal, containing GTR0 and GTR5.5 for verification of effect of devulcanization in rheological properties of non revulcanized blends.

Cao et al. [358] showed in their work that the TPV type blends with sharper reductions in the complex viscosity values with increasing frequency were those which presented dynamically vulcanized rubber agglomerates connected with the matrix around the

particles, forming a kind of interphase. With that, the blends containing devulcanized rubber without clays, there seems to be a greater interaction among the phases, the opposite of the same blends containing clay.

Figure 99 presents the G' variation in relation to the concentration of GTR to 0.1 and 100 Hz frequency of non revulcanized blends containing GTR0 and GTR5.5.

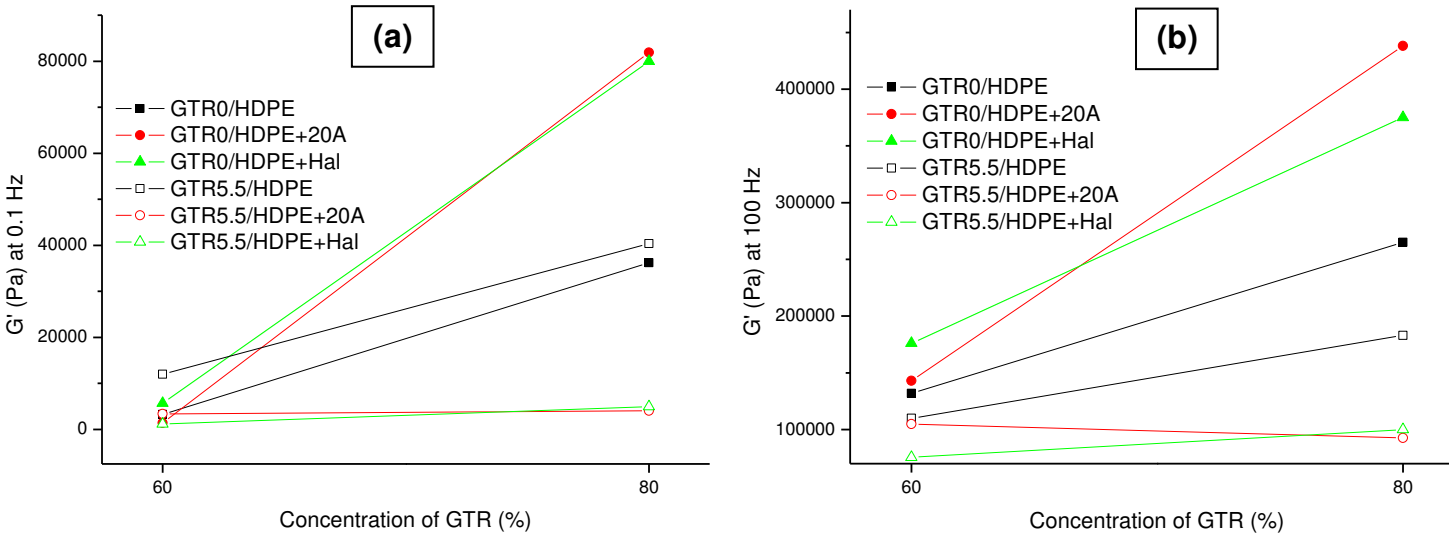

Figure 99: G' variation of non revulcanized blends containing GTR0 and GTR5.5 to (a) 0.1 and (b) 100 Hz of frequency.

The analysis of graphics allows the verification of some interesting behaviors. First, the results can be divided into two distinct groups: one group with the blends containing GTR0 (Group 1) and another group with the blends containing GTR5.5 (Group 2), regardless of whether they contain or not clays. In Group 1 it is observed the increase in the G' values with the increase in concentration of GTR in the blends, with a larger increase in blends containing clays. On the other hand, the Group 2 presents increase in G' values with the increase in concentration of GTR in blends, but smaller in relation to the former group or reduction of G' in relation to the increase in concentration, in the case of the blend containing Cloisite 20A clay. The increase in the G' values with the increase in concentration of GTR smaller in the Group 2 blends is due to the reduction in cross-linking density of devulcanized GTR phase. With regard to blends containing Cloisite 20A, it is noted that the values of G' remained practically constant with the increase in concentration of GTR5.5. A possible explanation for this fact is the formation of the network rheologically percolated, which will be addressed with more

detail in the following section.

10.3.1.2 - Revulcanized blends

The variation curves of the storage modulus and complex viscosity as a function of frequency at 180°C of blends containing GTR0 and GTR5.5 for verification of effect of devulcanization in rheological properties of revulcanized blends are presented in Figure 100.

In the case of revulcanized blends, the opposite occurs when observed on the results of non revulcanized blends: in general, the increase in the values of G' and in the complex viscosity blends containing GTR5.5 in relation to blends containing GTR0 due to the higher cross-linking density of elastomeric phase [250]. As verified through the results of FTIR of the GTRs in Stage 1 of this work (section 3.4.1), on GTR5.5 it was observed the formation of a new peak related to the formation of groups C=C in the chain of NR, which probably have been connected to other reactive sites during reactive processing [105, 309], and may be responsible for the increase in cross-linking density of the elastomeric phase of blends containing GTR5.5 and increased the G' values and the complex viscosity. As the GTR0 was in powder condition during mixing with the vulcanization additives, there was no effective mixing and may even contain a lower concentration of additives in relation to GTR5.5 due to losses during its addition to the extruder by mechanical feeder.

In blends containing clays and 80% of GTR5.5, the increase in G' value is possibly due to the greater interaction among the GTR particles. As verified in the SEM images, the presence of clays tended to reduce the particle size of GTR and to improve the level of distribution in the matrix, which reduces the distance among the particles, approaching them to each other, and forming a kind of interconnection among them. With this, the matrix around the particles becomes more rigid (also by the presence of clays), transferring better the tensions among phases and increasing the G' values. According to Babu et al. [272], the formation of three-dimensional structure (interconnected network) of small GTR particles hinders the process of relaxation of the polymer chains close these particles. In other words, the devulcanization apparently has aided in the formation of a rheologically percolated network.

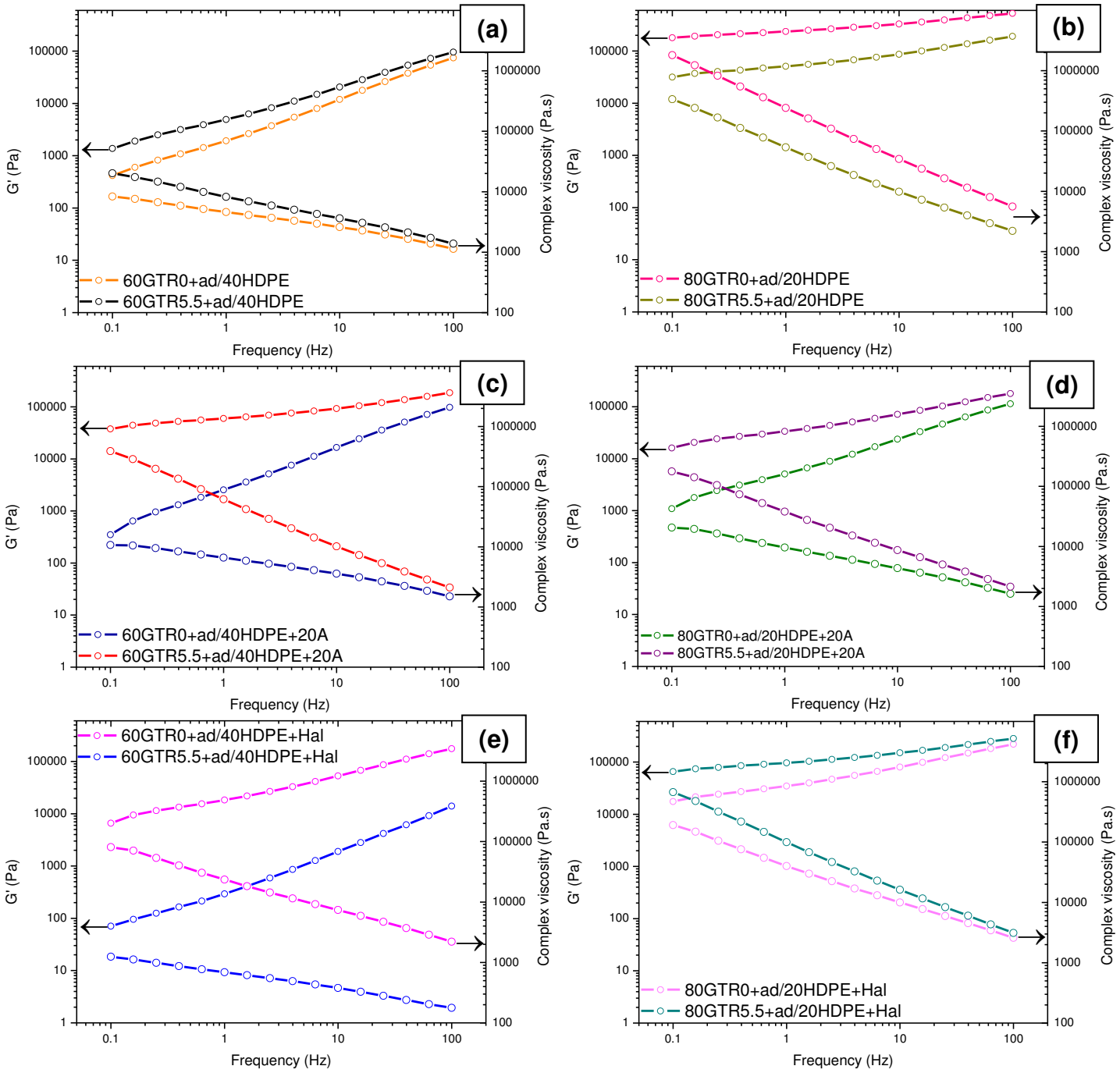

Figure 100: Evolution of the storage modulus and the complex viscosity with the frequency of the blends: (a) 60GTR+ad/40HDPE, (b) 80GTR+ad/20HDPE, (c) 60GTR+ad/40HDPE+20A, (d) 80GTR+ad/20HDPE+20A, (e) 60GTR+ad/40HDPE+Hal and (f) 80GTR+ad/20HDPE+Hal, containing GTR0 and GTR5.5 for verification of effect of devulcanization in rheological properties of revulcanized blends.

In the case of blend 60GTR5.5+ad/40HDPE+Hal, the reduction in G' values relative to blend containing GTR0 is probably due to the degradation of HDPE. According to the

results of FTIR presented in Stage 1 (section 3.4.2), the presence of Halloysite clay caused the degradation of HDPE for branching processes followed by cross-linking formation.

Figure 101 presents the graphs of G ' in relation to the concentration of GTR to 0.1 and 100 Hz frequency of revulcanized blends containing GTR0 and GTR5.5.

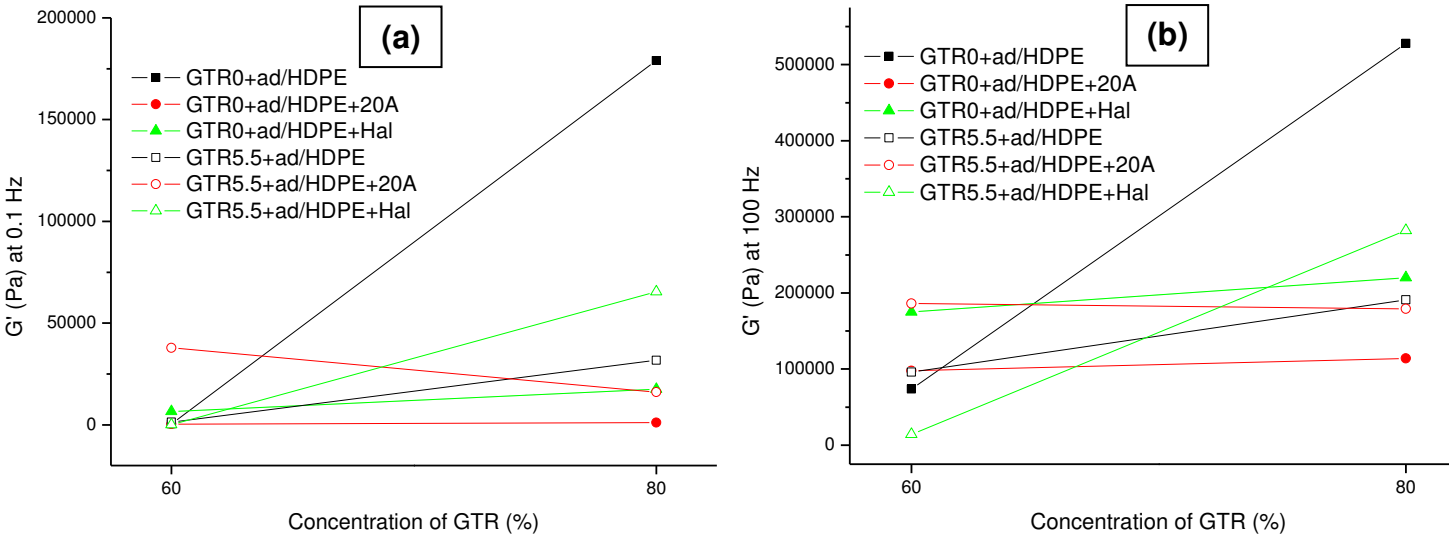

Figure 101: Variation of G' of revulcanized blends containing GTR0 and GTR5.5 to (a) 0.1 and (b) 100 Hz of frequency.

In the case of revulcanized blends, with the exception of the blend containing Cloisite 20A clay, it is verified the increase in G' values in relation to the increase in concentration of GTR on blend due possibly to the increase in viscosity caused by the increase in the cross-linking density.

In blends containing clay, two competing mechanisms appear to be occurring: strengthening and degradation. In some blends, the presence of clay seems to reinforce the blend and thus assists in increasing G' value, while in others it appears to contribute more effectively in the breakdown of HDPE, aiding in reducing the G' value.

The smallest G' value noted in the Figure 101b refers to blend 60GTR5.5+ad/40HDPE+Hal and is possibly the biggest HDPE degradation by the presence of Halloysite clay. It is worth remembering that the compound HDPE+Hal contains maleic anhydride compatibilizing agent, which also may have aided in the degrading process. The effect was more easily verified in the blend that contains higher concentration of matrix phase.

In the next section, the consequences of the revulcanization of elastomeric phase in the rheological properties of the blends will be reviewed.

10.3.2 - Effect of revulcanization of elastomeric phase

10.3.2.1 - Blends without clay

The curves of the storage modulus and complex viscosity as a function of frequency at 180°C of blends containing GTR5.5 in different concentrations for verification of the effect of revulcanization on the rheological properties of the blends are presented in Figure 102.

According to Lim and Park [371], the presence of a kind of plateau in G' curve symbolizes great interaction among phases. In the revulcanized and non revulcanized blends containing 20% of GTR5.5, this plateau can be observed, and this is due, possibly, to the morphology of co-continuous phases, identical conclusion to that found in the DMA results (section 10.2.4). Elastomeric co-continuous phase restricts the process of relaxation and movement of polymeric chains of molten thermoplastic phase, resulting in a plateau.

In the case of revulcanized blend containing 40% of GTR, the increase in the G' values and complex viscosity compared to non revulzanized blend is due to the higher cross-linking density of elastomeric phase [250], since the blend presented the greatest T_g value of elastomeric phase among the other blends (Figure 92).

In the case of non revulcanized blend containing 60% of GTR, the highest G' values and complex viscosity are possibly the largest sizes of rubber particles with lower cross-linking density, as Figure 92.

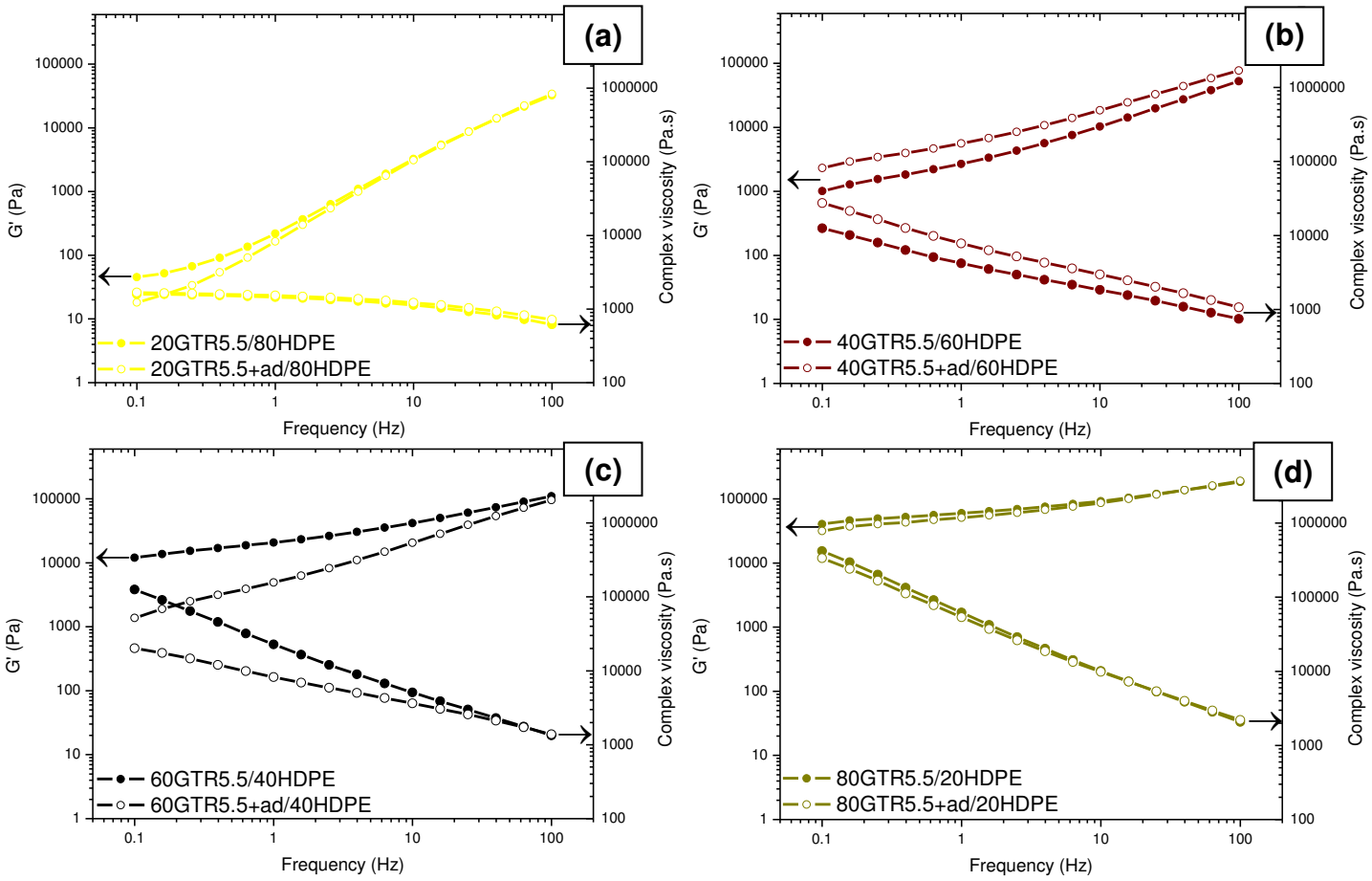

Figure 102: Evolution of the storage modulus and the complex viscosity with the frequency of the blends: (a) 20GTR5.5/80HDPE, (b) 40GTR5.5/60HDPE, (c) 60GTR5.5/40HDPE and (d) 80GTR5.5/20HDPE for verification of the effect of revulcanization on the rheological properties of the blends without the addition of clay.

However, in blends containing 80% of GTR, there is a sort of "competition" between the cross-linking density in elastomeric phase and its particle size. The cross-linking density of GTR phase of non vulcanized blend was smaller in relation to the revulcanized blend (Figure 92), while the average size of GTR particles was higher in non revulcanized blend, according to images of SEM from Stage 3. It was also observed in these blends the pseudosolid behavior by the formation of a possible network percolated, generated as a result of the reduction in particle sizes of GTR, as noted on the results of SEM presented.

Figure 103 shows the variation of G' in relation to the concentration of GTR5.5 to 0.1 and 100 Hz frequency of revulcanized and non revulcanized blends containing GTR5.5.

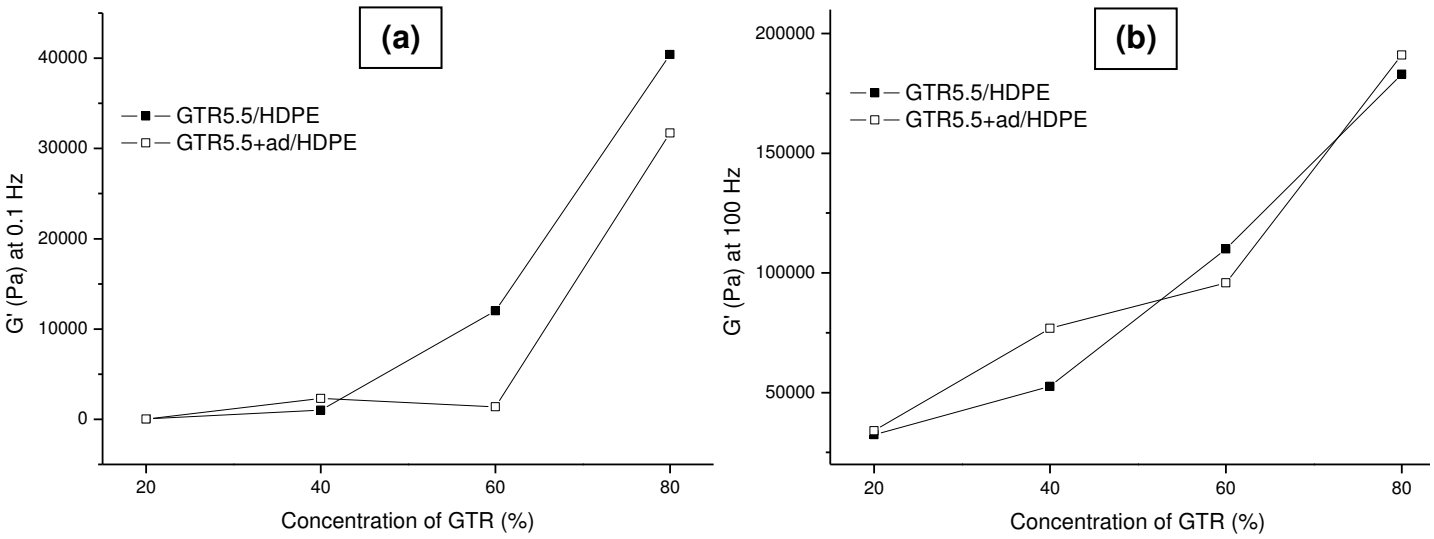

Figure 103: Variation of G' of revulcanized and non revulcanized blends containing GTR5.5 to (a) 0.1 and (b) 100 Hz of frequency.

The curves show the tendency to growth on the G' values of the blends with the increase in concentration of GTR on blend. In this case, a "competition" between the particle size of GTR and cross-linking density, as described earlier, can be noted. The presence of vulcanization additives apparently assisted in the "degradation" of the G' values in blends containing high concentrations of GTR. The lack of adhesion among phases also has, probably, influenced the results.

10.3.2.2 - Blends containing Cloisite 20A clay

The curves of storage modulus and complex viscosity as a function of frequency at 180°C of blends containing GTR5.5 in different concentrations and Cloisite 20A clay for verification of the effect of revulcanization on the rheological properties of the blends are presented in Figure 104.

In the same way as in 20GTR5.5/80HDPE blends, in the curves of blends containing 20% of GTR are checked a kind of plateau, and the same is due, possibly, to the morphology of co-continuous phases which was also observed in the DMA results (section 10.2.4). The blend 40GTR5.5+ad/60HDPE+20A which also features a plateau in G' curve, has morphology of co-continuous phase , according to the DMA results presented in the same section.

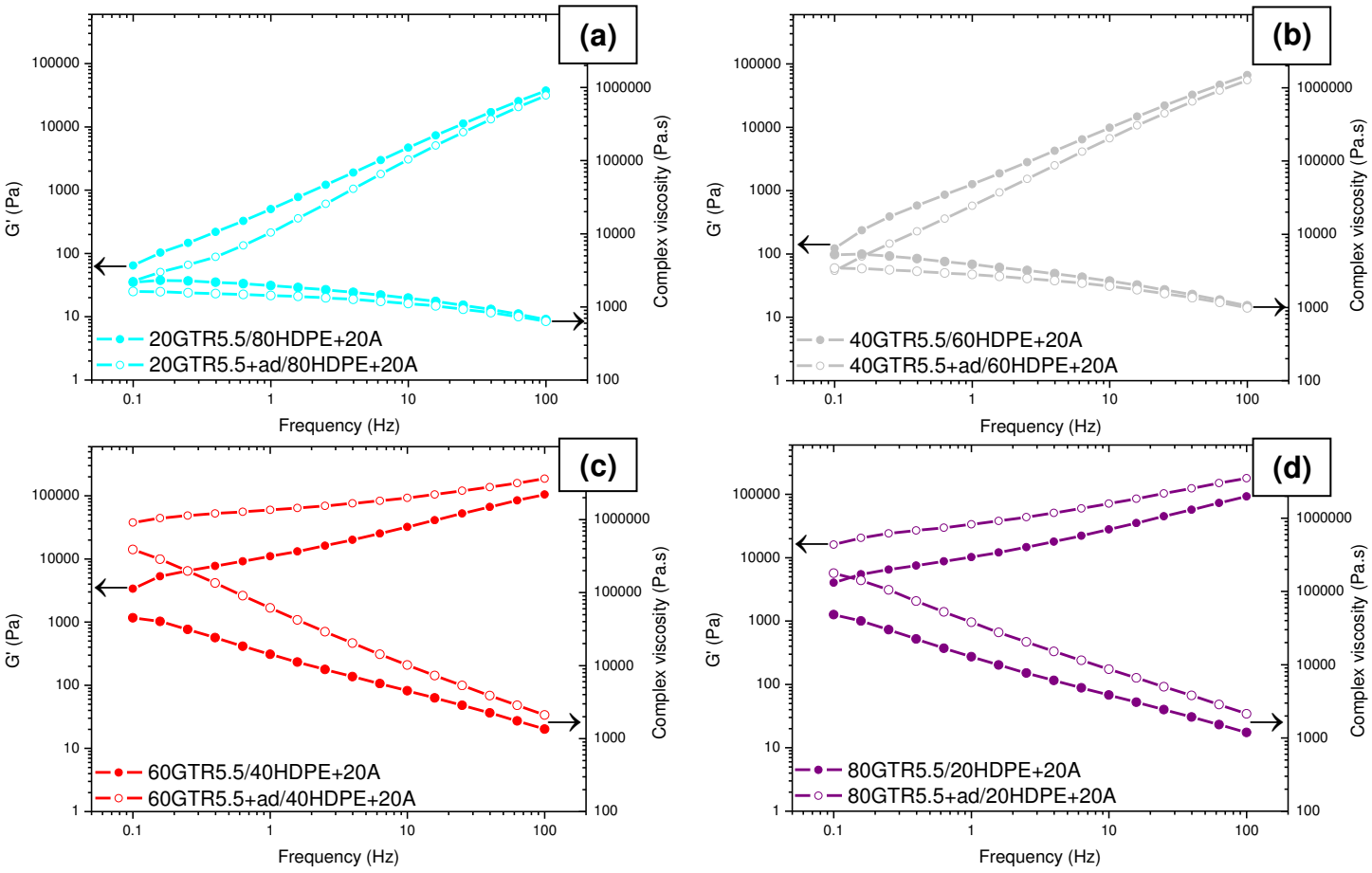

Figure 104: Evolution of the storage modulus and the complex viscosity with the frequency of revulcanized and non revulcanized blends: (a) 20GTR5.5/80HDPE+20A, (b) 40GTR5.5/60HDPE+20A, (c) 60GTR5.5/40HDPE+20A and (d) 80GTR/20HDPE+20A for verification of the effect of revulcanization on the rheological properties of blends containing Cloisite 20A clay.

The revulcanized blends containing 60 and 80% of GTR present higher G' values and complex viscosity compared to their non revulcanized blends due to the higher cross-linking density on elastomeric phase [250] (Figure 92). These blends also presented the GTR particles smaller in relation to non revulcanized blends (according to the SEM images) which, as described before, may have formed a kind of interconnection (interconnected network) due to greater closeness among them, making the matrix around the particles more rigid and aiding in the highest transference of tension of the matrix to the dispersed phase, which consequently increased the values of G'. The result can be described, in other words, in terms of rheological percolation.

Figure 105 presents the variation of G' in relation to the concentration of GTR5.5 to 0.1

and 100 Hz frequency of revulcanized and non revulcanized blends containing GTR5.5 and Cloisite 20A clay.

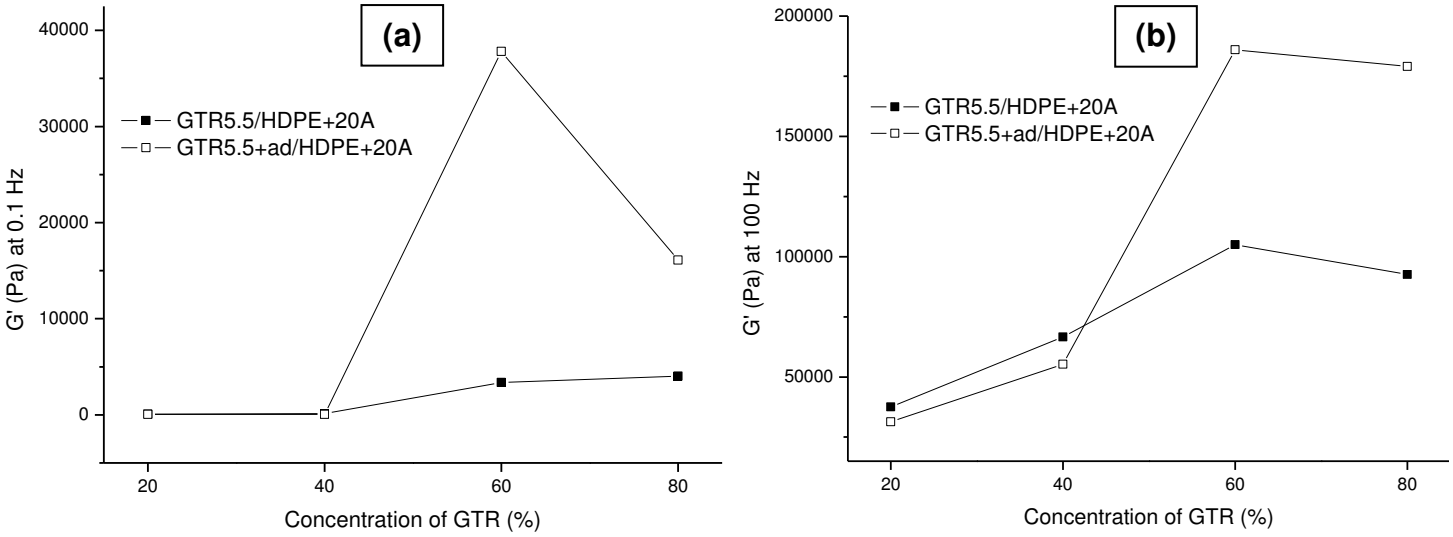

Figure 105: Variation of G' of revulcanized and non revulcanized blends containing GTR5.5 and Cloisite 20A clay to (a) 0.1 and (b) 100 Hz of frequency.

The results of the storage modulus at 30°C (Figure 97) showed that, just as in Figure 105, there was an increase in the modulus of blends containing 60% of GTR and a reduction in blends containing 80% of GTR. As mentioned in section 10.2.4.2, E' can be influenced by reinforcing action of clay, degradation of the matrix, blend morphology or by cross-linking density of GTR phase. As the T_g value of the GTR phase of the blend containing 60% of GTR was lower compared to the blend containing 80% of GTR, the clay has probably served as a reinforce agent to HDPE in blend containing 60% of GTR. The value of Young's modulus of the blend 60GTR5.5+ad/40HDPE+20A was also higher than among the other analyzed blends (section 10.4.2), which proves the other results obtained. The reduction of G' on 80% rubber composition may be due to lack of adhesion among phases or even to the agglomeration of rubber in this concentration, forming larger particles and, therefore, less stress transfer in the interface between filler and matrix. However, this behavior needs to be better studied by other techniques (such as TEM) for a better understanding of the phenomenon.

10.3.2.3 - Blends containing Halloysite clay

The variation of the storage modulus and complex viscosity as a function of frequency

at 180°C of blends containing GTR5.5 in different concentrations and Halloysite clay for verification of the effect of revulcanization on the rheological properties of the blends are presented on Figure 106.

According to the results of DMA (section 10.2.4), blends containing 20% of GTR have morphology of co-continuous phases. However, in the case of blends containing Halloysite clay, it has not been possible to verify a plateau in the G' curve as in other blends containing 20% of GTR.

The revulcanized blend containing 60% of GTR, which presents smaller particle sizes and higher cross-linking density on GTR phase [250] in comparison to non revulcanized blend and should, therefore, present higher values of G' and complex viscosity compared to non revulcanized blend, however the opposite is observed. Such behavior is due, possibly, to the degradation of HDPE by the presence of Halloysite clay, which has generated degradative processes by branch followed by cross-linking formation of polymer chains of HDPE (section 3.4.2).

In the case of blends containing 80% of GTR, the revulcanized blend presents greater values of G' and complex viscosity that non revulcanized blends due to the higher cross-linking density on elastomeric phase [250] (Figure 92). The elastomeric phase must, probably, be responsible for the largest observed properties due to the low concentration of degraded HDPE. The clay probably served as compatibilizing agent among the phases of revulcanized blend according to other results, which also helps in the increase of the G' values and complex viscosity [359]. Another possibility is that there has been the formation of the interconnected network among small particles of GTR next to each other and the filler on the thermoplastic phase, as described earlier.

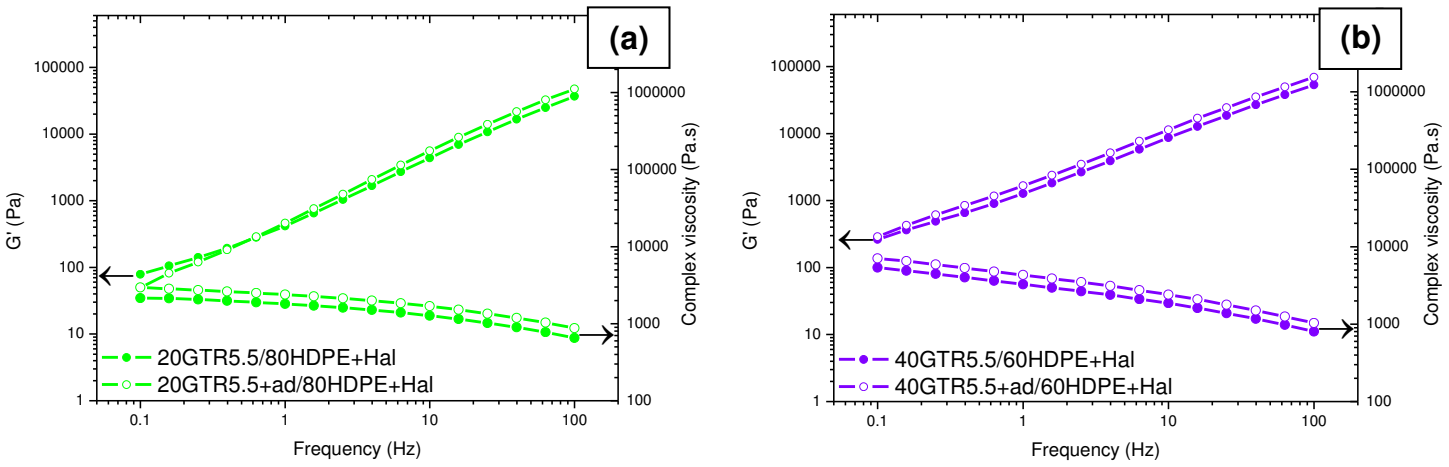

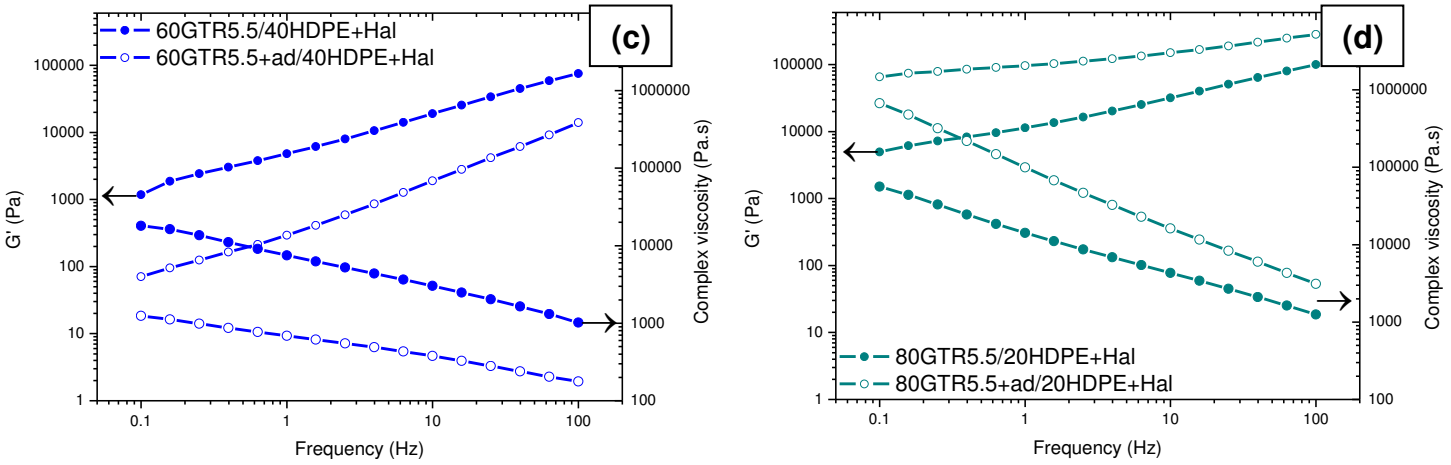

Figure 106: Evolution of the storage modulus and the complex viscosity with the frequency of revulcanized and non revulcanized blends: (a) 20GTR5.5/80HDPE+Hal, (b) 40GTR5.5/60HDPE+Hal, (c) 60GTR5.5/40HDPE+Hal and (d) 80GTR5.5/20HDPE+Hal for verification of the effect of revulcanization on the rheological properties of blends containing Halloysite clay.

Figure 107 presents the variation of G' in relation to the concentration of GTR5.5 to 0.1 and 100 Hz frequency of revulcanized and non revulcanized blends containing GTR5.5 and Halloysite clay.

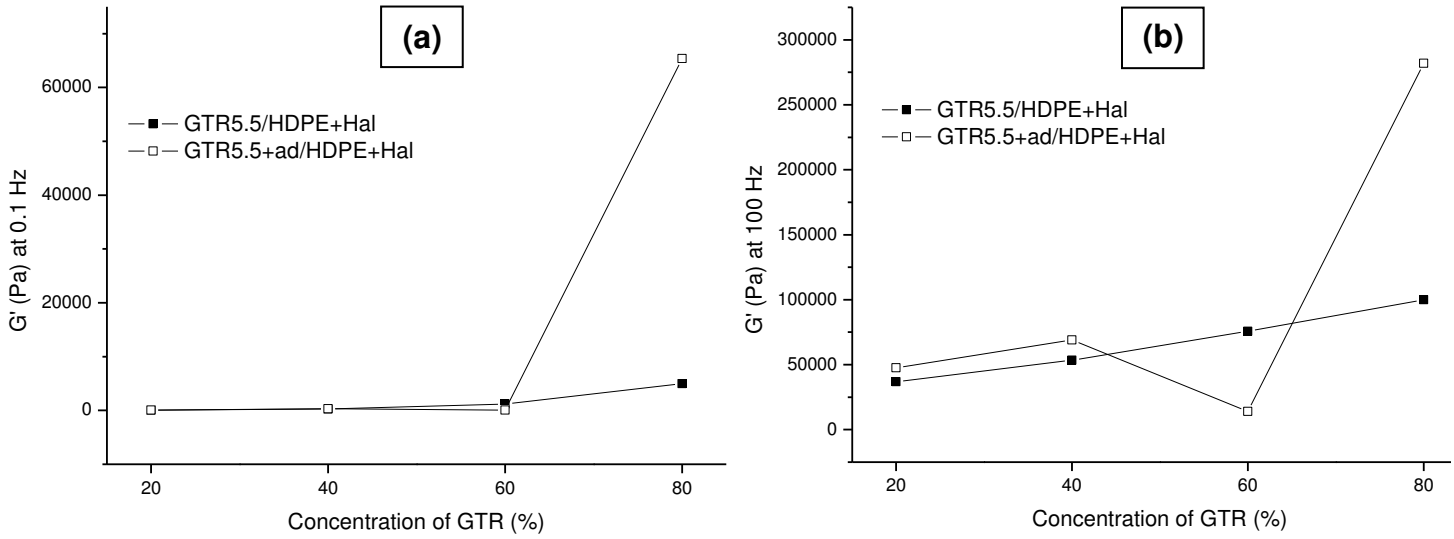

Figure 107: Variation of G' of revulcanized and non revulcanized blends containing GTR5.5 and Halloysite clay at a frequency of (a) 0.1 and (b) 100 Hz.

In the case of non revulcanized blends, it is perceived just a discrete increase in values of G' with the increase in concentration of GTR in blends, probably due to the degradation of HDPE by the presence of clay (section 3.4.2).

In the case of revulcanized blend containing 60% of GTR, HDPE degradation generated by the presence of clay seems to have influenced the G' values, while in revulcanized blends containing 80% of GTR, the high concentration of rubber on small particles generated interconnected networks and increased the G' values (rheologically percolated network).

In the next section, the effect of the addition of clays in the rheological properties of the blends will be analyzed.

10.3.3 - Effect of addition of clays

10.3.3.1 - Non revulcanized blends

The variation of the storage modulus and complex viscosity as a function of frequency at 180°C of blends containing GTR5.5 for verification of the effect of addition of clays in the rheological properties of non revulcanized blends are presented in Figure 108.

In non revulcanized blends containing low concentrations of GTR (20 and 40%), the presence of clay did not significantly alter the G' values and complex viscosity.
In the case of blends containing 60% of GTR, the presence of clays has reduced the G' value of the blends, possibly due to the low adhesion among phases. The blend containing Halloysite clay presented the lowest G' value, possibly due to degradation of HDPE by the presence of clay (section 3.4.2).

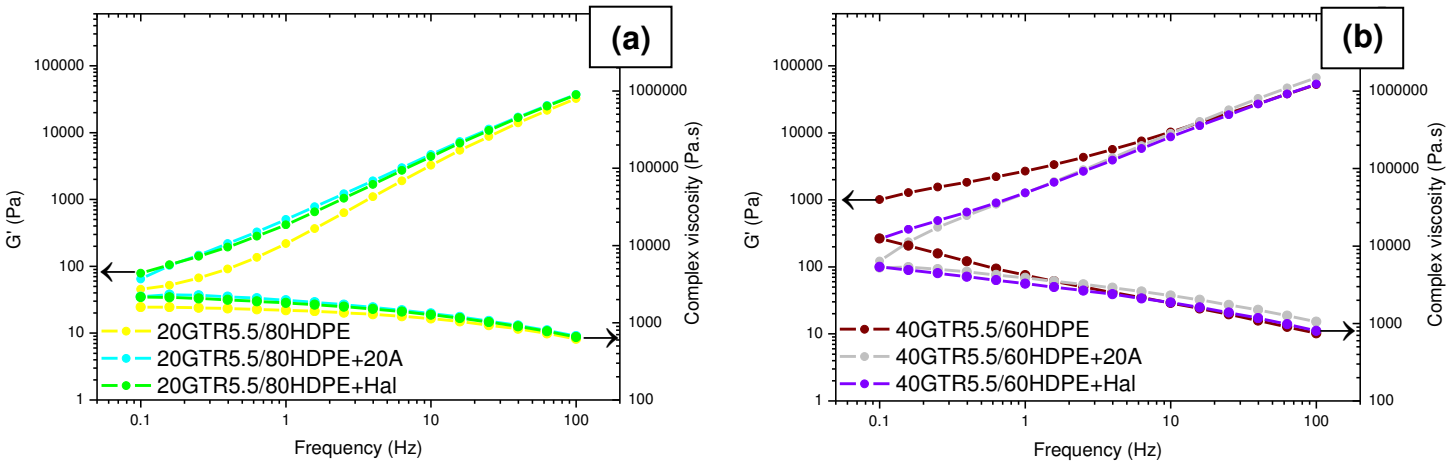

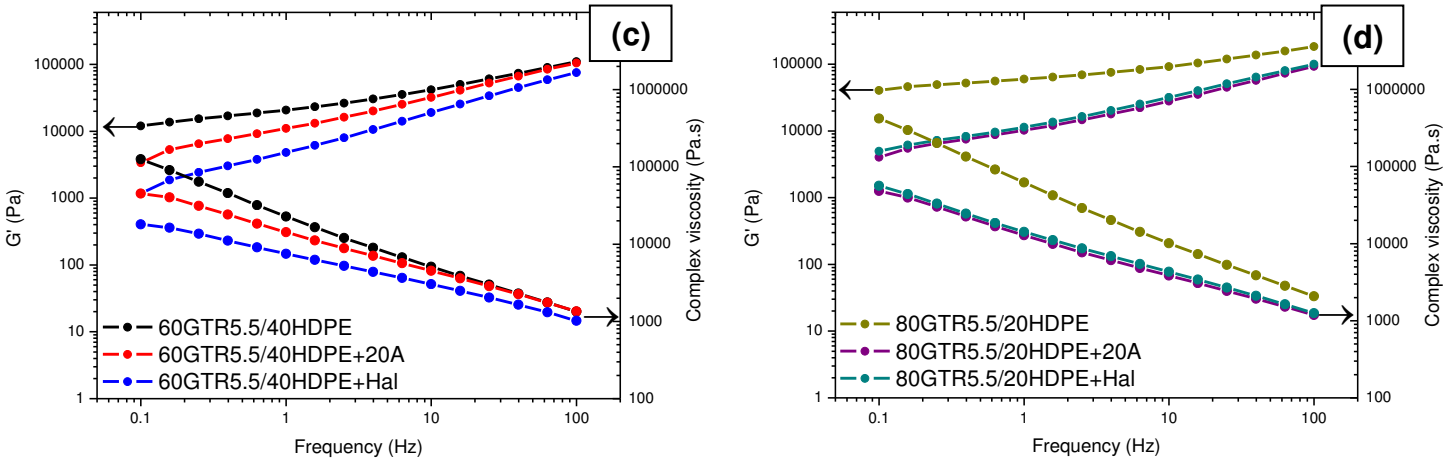

Figure 108: Evolution of the storage modulus and the complex viscosity with the frequency of the blends: (a) 20GTR5.5/80HDPE, (b) 40GTR5.5/60HDPE, (c) 60GTR5.5/40HDPE and (d) 80GTR5.5/20HDPE containing Cloisite 20A and Halloysite clays to check their influence on the rheological properties of non revulcanized blends.

In the case of blends containing 80% of GTR, on Halloysite clay-containing blend, possibly, the formation of a rheologically percolated network among the rubber particles in high concentration and the clay occurred, so it showed the highest G' value among the other blends containing 80% of GTR5.5.

Figure 109 presents the variation of G ' in relation to the concentration of GTR5.5 to 0.1 and 100 Hz frequency of non revulcanized blends containing GTR5.5.

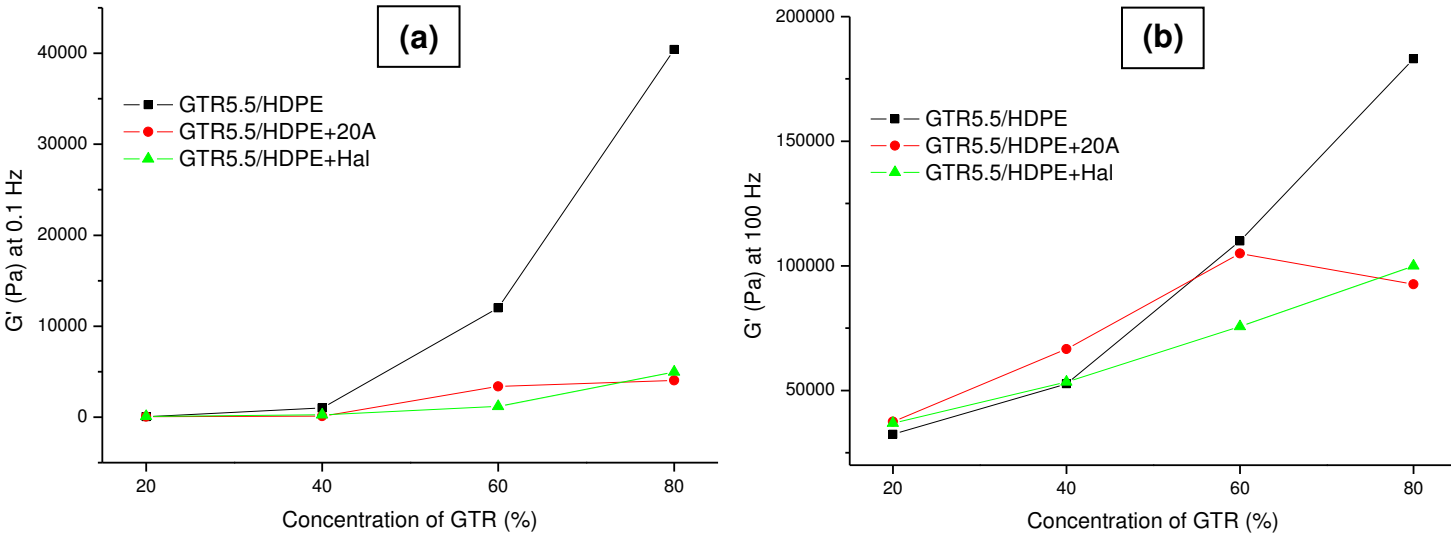

Figure 109: Variation of G' of non revulcanized blends containing GTR5.5 at a frequency of (a) 0.1 and (b) 100 Hz.

According to the results of morphological analysis of the blends (section 10.1.3), the presence of clays in the non revulcanized blends apparently increased the particle distribution of GTR in the matrix and the presence of Halloysite clay increased roughness of the matrix, which indicates greater adhesion among phases. However, it is known that the same clay degraded HDPE by branching and cross-linking process, which may have influenced in the low values of G' obtained on blends containing high concentrations of GTR.

Even knowing that the presence of clays has increased the distribution of GTR particles in the matrix, it can be observed the low adhesion among phases of blends containing Cloisite 20A clay (section 10.1.3.1). The low adhesion among phases may also have influenced the fall of the G' values observed in non revulcanized blends containing high concentrations of GTR and Cloisite 20A.

10.3.3.2 - Revulcanized blends

The curves of the storage modulus and complex viscosity as a function of frequency to 180°C of blends containing GTR5.5 for verification of the effect of addition of clays in the rheological properties of revulcanized blends are presented in Figure 110.

As in non revulcanized blends, in revulcanized blends containing low concentrations of GTR (20 and 40%), the presence of clay did not alter significantly the G' values and complex viscosity of blends.

In the case of blends containing 60% of GTR, it was found in the analysis of the SEM images that the presence of clays has improved the distribution of sub-micrometer rubber particles in the matrix. Small rubber particles close to each other probably have formed a kind of interconnected network, which caused the increase in G' values. However, in the blend containing Halloysite clay, degradation of HDPE was prevalent, resulting in reduction in G ' values and complex viscosity.

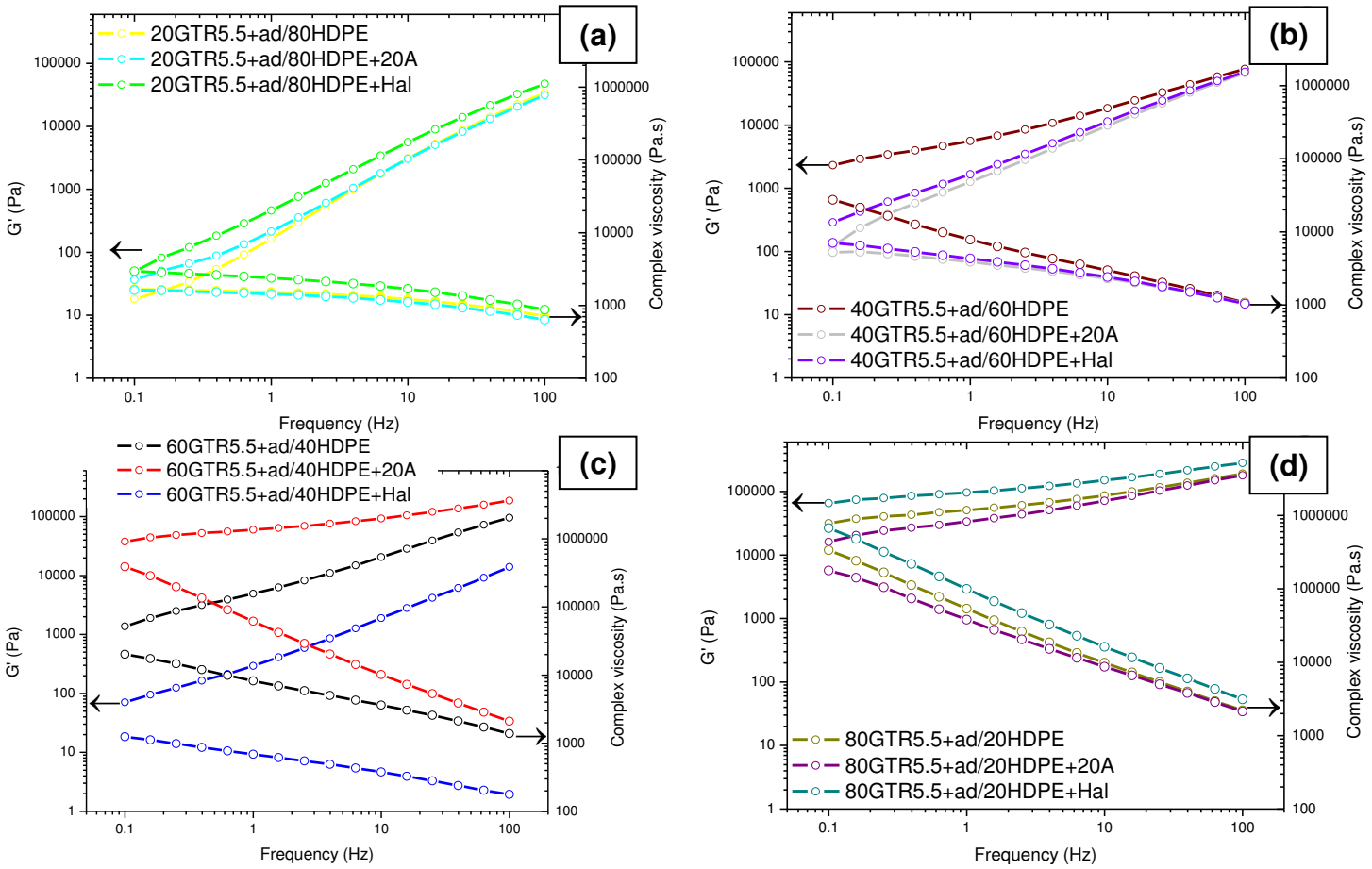

Figure 110: Evolution of the storage modulus and the complex viscosity with the frequency of the blends: (a) 20GTR5.5+ad/80HDPE, (b) 40GTR5.5+ad/60HDPE, (c) 60GTR5.5+ad/40HDPE and (d) 80GTR5.5+ad/20HDPE containing Cloisite 20A and Halloysite clays to check their influence on the rheological properties of revulcanized blends.

It is observed that the blend 80GTR5.5+ad/20HDPE+Hal has the highest viscosity compared to the others with the same concentration of GTR. According to George et al. [263], in the non compatibilized blends can occur easily the sliding among the layers of the material, which causes reduction in viscosity. In the blends containing compatibilizing agent, it reduces interfacial tension and makes the mixture among the phases (interphase), which causes an increase in viscosity of compatibilized blends. Then, in revulcanized blends containing clay, these possibly acted as compatibilizing agents among the phases, which resulted in the increase of the complex viscosity observed. Therefore, as previously mentioned, Halloysite clay seems to have acted as a compatibilizing agent on revulcanized blends containing 80% of GTR. According to the results of FTIR presented in Stage 1 (section 3.4.2), it was found that the addition of this

clay resulted in degradation of HDPE by branching and subsequent cross-linking process, which may have helped in increasing the complex viscosity of the blend.

Figure 111 features the variation of G' in relation to the concentration of GTR5.5 to 0.1 and 100 Hz frequency of revulcanized blends containing GTR5.5.

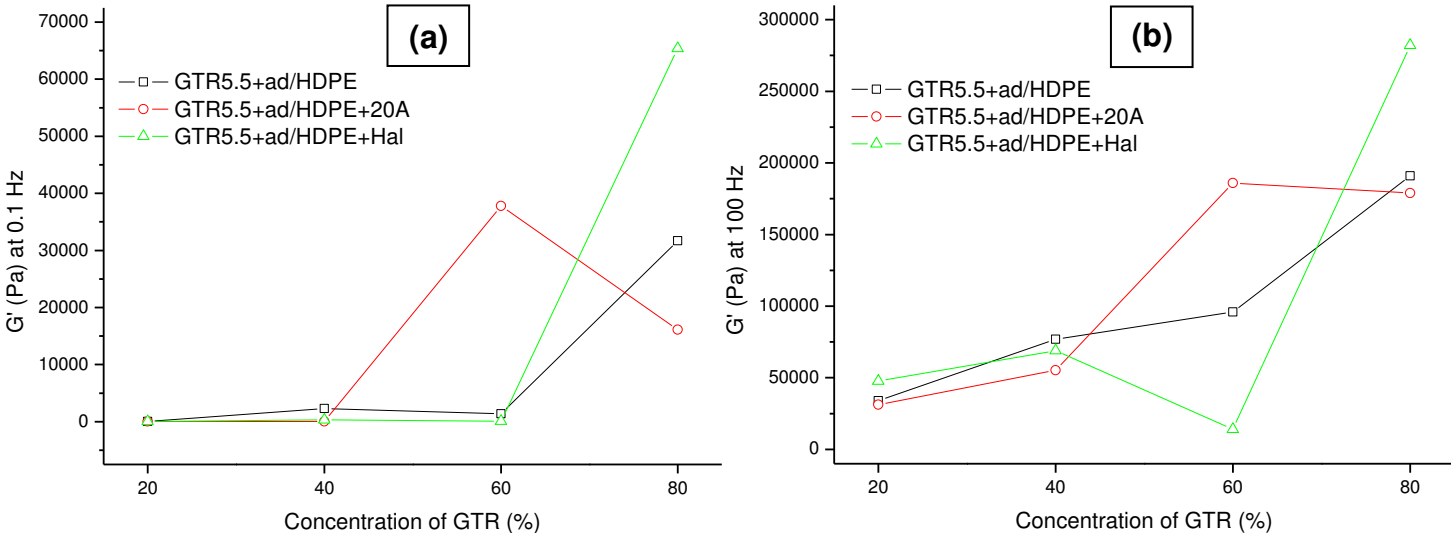

Figure 111: Variation of G' of revulcanized blends containing GTR5.5 at a frequency of (a) 0.1 and (b) 100 Hz..

The curves demonstrate clearly the issue of competing mechanisms. In the case of blend 60GTR5.5+ad/40HDPE+20A, Cloisite 20A clay acted as a reinforce agent, resulting in the increase of the G'; in the case of blend 80GTR5.5+ad/20HDPE+20A, the same clay acted as 'degrading' agent. The opposite can be verified in blends containing Halloysite clay: on 60GTR5.5+ad/40HDPE+Hal blend, clay served as a 'degrading' agent, resulting in the reduction of G', while in 80GTR5.5+ad/20HDPE+Hal blend it has acted as a reinforce.

An important observation to be made is about the limit of rheological percolation. Based on the results presented on the Figures 110 and 111, it appears that the limit for the blends without clay and for those containing Halloysite clay is between 60 and 80% of GTR, and blends containing Cloisite 20A clay the limit is between 40 and 60% of GTR. In other words, the presence of Cloisite 20A clay reduced the percolation rheological limit of revulcanized blends. So, for the threshold in these blends to be the same compared to other blends, the concentration of clay should be smaller, which indicates that possibly there is concentration higher than the optimum concentration

needed, what might be helping in the reduction of G' values observed.

In the following section, the effect of the concentration of the phases on the rheological properties of the blends will be analyzed.

10.3.4 - Effect of concentration of phases

10.3.4.1 - Non revulcanized blends

The curves of the storage modulus and complex viscosity as a function of frequency at 180°C of blends containing GTR5.5 for verification of the effect of the concentration of the phases on the rheological properties of non revulcanized blends are presented in Figure 112.

In general, it is observed that there is an increase in complex viscosity of blends with the increase in concentration of GTR, since rubber is more viscous than HDPE. The same behavior can also be observed with the G' values, what happens due to different contributions, namely: the morphology (distribution and dispersion of the dispersed phase in the matrix), cross-linking density of elastomeric phase, presence or absence of clays that can act in different ways, and degradation of HDPE. However, the values of the properties of the blends containing clay are, generally, smaller than those of the blends without the addition of clay, and the possible causes for this phenomenon were cited in the previous section.

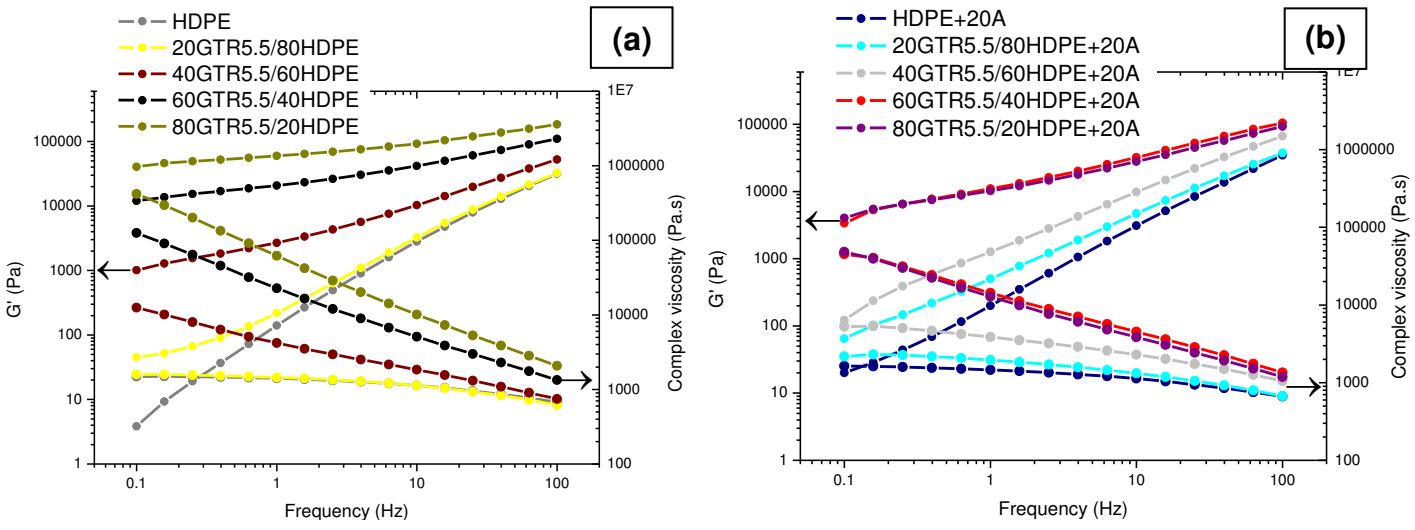

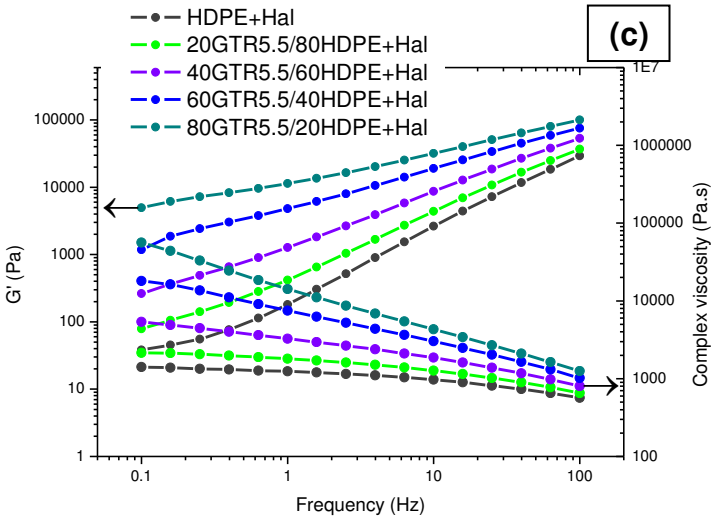

Figure 112: Evolution of the storage modulus and the complex viscosity with the frequency of the blends: (a) GTR5.5/HDPE, (b) GTR5.5/HDPE+20A and (c) GTR5.5/HDPE+Hal containing different concentrations of the phases for verification of this effect on rheological properties of non revulcanized blends.

10.3.4.2 - Revulcanized blends

The curves of the storage modulus and complex viscosity as a function of frequency at 180°C of blends containing GTR5.5 for verification of the effect of the concentration of the phases on the rheological properties of the revulcanized blends are presented in Figure 113.

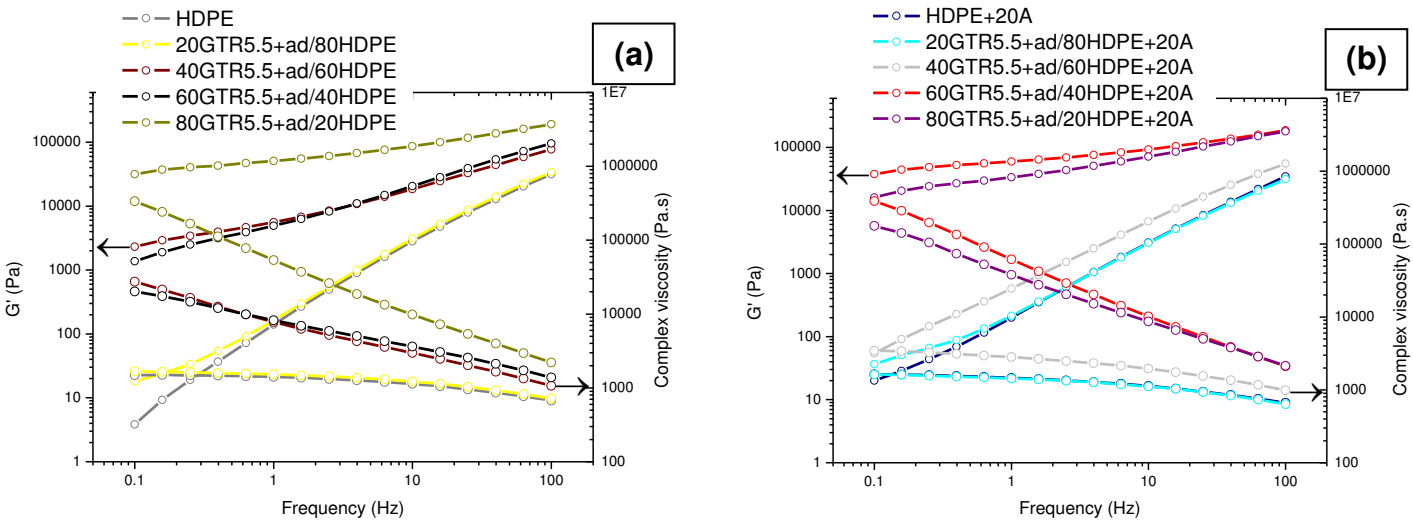

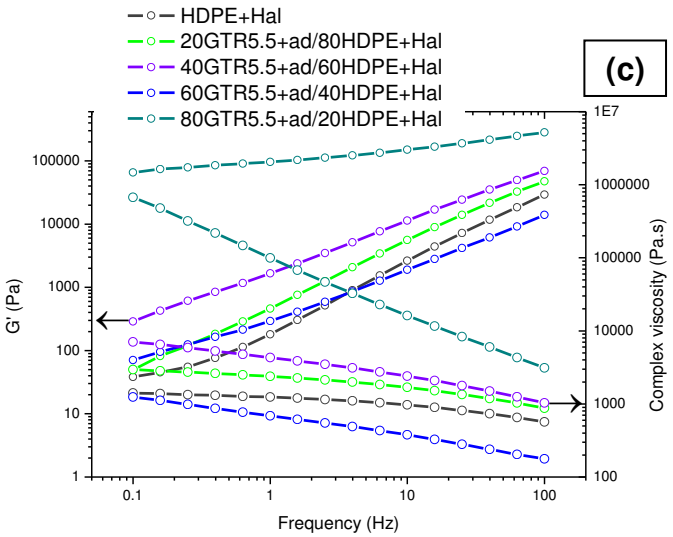

Figure 113: Evolution of the storage modulus and the complex viscosity with the frequency of the blends: (a) GTR5.5+ad/HDPE, (b) GTR5.5+ad/HDPE+20A and (c) GTR5.5+ad/HDPE+Hal containing different concentrations of the phases for verification of this effect on rheological properties of revulcanized blends.

In general, it is observed that the blends that showed higher values of complex viscosity and G' of each analyzed group were those with higher concentrations of GTR, however there is a tendency of reduction of values with the reduction in the concentration of GTR, as verified in the case of non revulcanized blends.

The blends containing clays and high concentrations of GTR presented the highest values of G' and complex viscosity. In these blends, the complex viscosity decreased more pronounced at higher frequencies, which means the rubber particles form interconnected networks, with improvement in the interphases [247, 251, 255, 272, 358]. The greatest distribution of sub-micrometer particles in the matrix of these blends was also verified through the pictures of SEM. According to Babu et al. [272], with the reduction in the size of the particles of the dispersed phase, the greater number of chains in the matrix can be adsorbed by rubber particles and the particle-particle distance may decrease. This causes an energy barrier against relaxation, increasing the values of complex viscosity and frequency scanning tests, which may have occurred on the results in question.

Apparently, with the increase in concentration of GTR in the blend, the formation of a network structure formed by the increase in the area of the GTR particles and increase in concentration of particles. Particle-particle interactions of GTR begin to dominate the

system [372], restricting the relaxations of the polymeric chains around and causing the value of G' does not vary with increase in frequency. So, the blends containing high concentrations of GTR tended to present rheological percolation.

According to the additivity rule for blends, the viscosity of the blend is equal to the sum of the viscosities of the phases multiplied by its respective concentration (Equation 16)

$$\log\eta = \phi_1 \log\eta_1 + \phi_2 \log\eta_2 \qquad \text{Equation 16 [255]}$$

where η is the viscosity of the blend, η_1 and η_2 are the viscosities of the phases, and, Φ_1 and Φ_2 are the mass fractions of the respective phases.
When the analyzed systems present a negative deviation to the rule, that is, when the experimental values are smaller than the ones calculated, it means that the phases of the blend are incompatible [255]. The calculation can be done using the values of viscosities from capillary rheometry tests or oscillatory rheometry. In the case of the present work, it has not been possible to perform the test of GTR5.5+ad for both techniques due to the high viscosity, which made it impossible for the calculations. However, based on the analysis of the results presented in this Stage, the blends are incompatible and probably would present negative deviation to the additivity rule.

In the next section, the consequences of the effects of devulcanization of the elastomeric phase, revulcanization of elastomeric phase, addition of clays and concentration of the phases on the mechanical properties will be reviewed.

10.4 - Tensile tests

First, it is important to note that, according to the results of SEM presented, it was found that the particles of sub-micrometer GTR were well dispersed and badly distributed on thermoplastic matrix due to the injection process adopted for the production of specimens for tensile tests. Thus, the results presented here are not a good indicative for analysis of the process adopted in the production of blends, but only a consequence of their morphology in specimens. Still, the factors analyzed showed consequences on morphology (as verified through the analysis of the images of SEM, section 10.1), as well as on the results presented below.

In sections 10.4.1, 10.4.2 and 10.4.3, as the goal of the figures presented was not to compare the properties according to the variation in the concentration of the phases, the graphics are with different scales from one another on the y-axis.

In the next section, the effect of devulcanization of the elastomeric phase on mechanical properties of the blends will be analyzed.

10.4.1 - Effect of devulcanization of the elastomeric phase

10.4.1.1 - Non revulcanized blends

The effect of devulcanization of elastomeric phase on mechanical properties of non revulcanized blends is verified through the Figure 114.

According to the SEM images of non revulcanized blends (section 10.1.1.1), it was found that those containing GTR0 showed much larger particle sizes compared to the particles of GTR5.5. However, in the case of blends containing GTR5.5 it turns out that, even having particle sizes in sub micrometric range, during the injection process occurred agglomeration, resulting in particles badly distributed in the matrix. In blends containing GTR0, there is a better distribution of large particles of GTR on matrix, which probably resulted in the improvement of some properties in comparison to blends containing GTR5.5.

It can be perceived that the stress at break of blends containing GTR0 without clay were superior to the same blends containing GTR5.5. According to Ismail and Suryadiansyah [242], the increase in values of stress at break and Young's modulus of blends containing recycled rubber is due to previous vulcanization of the rubber. This behavior has also been observed in some revulcanized blends (results will be presented in the next section) what, in this particular case, the increase is due to the presence of two co-existing three-dimensional networks, one from the first vulcanization of GTR and the second from the revulcanization.

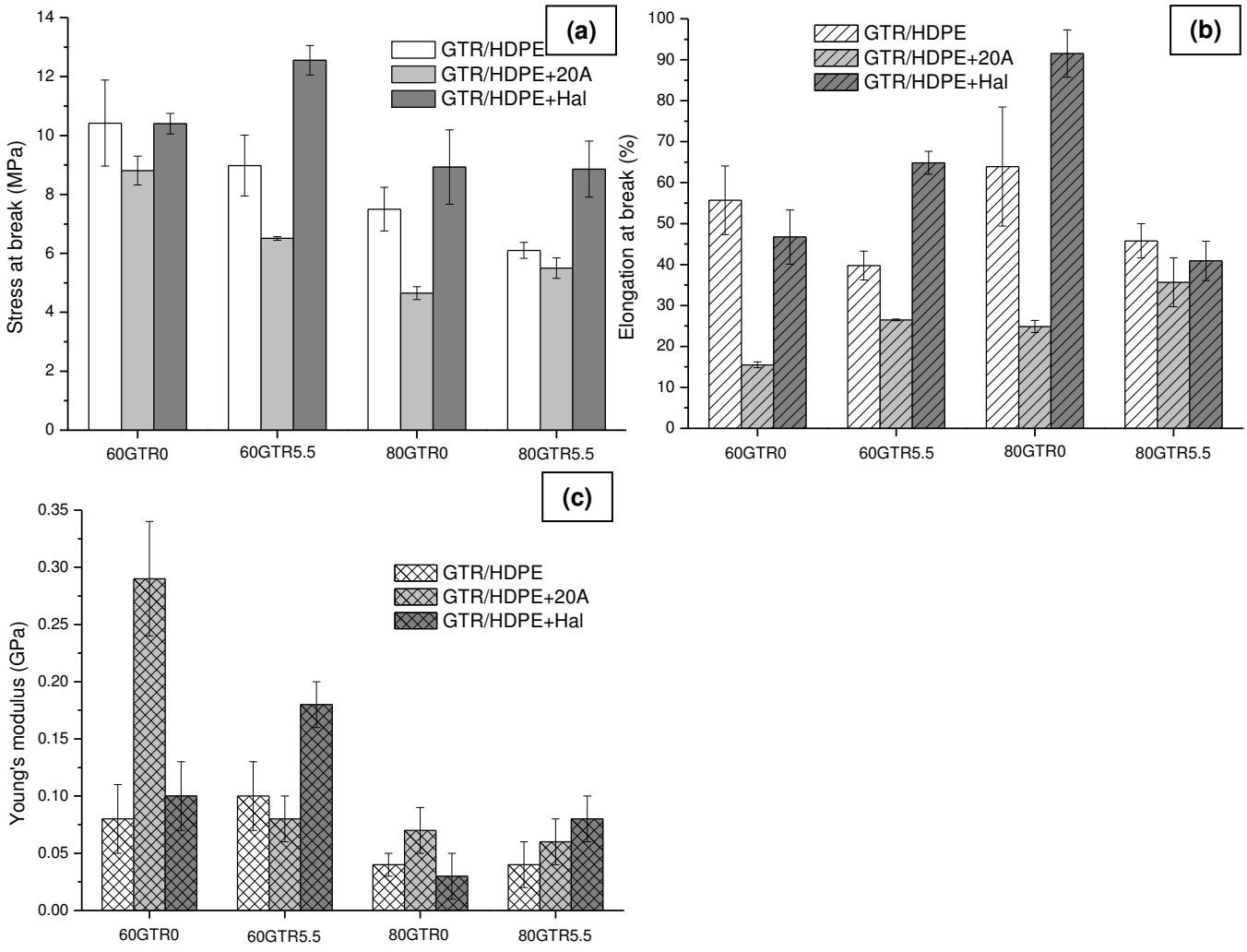

Figure 114: Mechanical properties of non revulcanized blends containing GTR0 and GTR5.5 with different concentrations of GTR: (a) stress at break, (b) elongation at break and (c) Young's modulus. The x-axis of the figures represents the elastomeric phase composition of the blends.

10.4.1.2 - Revulcanized blends

The effect of devulcanization of elastomeric phase on mechanical properties of the revulcanized blends is verified through the Figure 115.

According to the SEM images of non revulcanized blends (section 10.1.1.1), it was found that those containing GTR0 showed much larger particle sizes compared to the particles of GTR5.5. However, in the case of blends containing GTR5.5 it turns out that, even having particle sizes in sub micrometric range, during the injection process occurred agglomeration, resulting in particles badly distributed in the matrix. In blends containing GTR0, there is a better distribution of large particles of GTR on matrix,

which probably resulted in the improvement of some properties in comparison to blends containing GTR5.5.

It can be perceived that the stress at break of blends containing GTR0 without clay were superior to the same blends containing GTR5.5. According to Ismail and Suryadiansyah [242], the increase in values of stress at break and Young's modulus of blends containing recycled rubber is due to previous vulcanization of the rubber. This behavior has also been observed in some revulcanized blends (results will be presented in the next section) what, in this particular case, the increase is due to the presence of two co-existing three-dimensional networks, one from the first vulcanization of GTR and the second from the revulcanization.

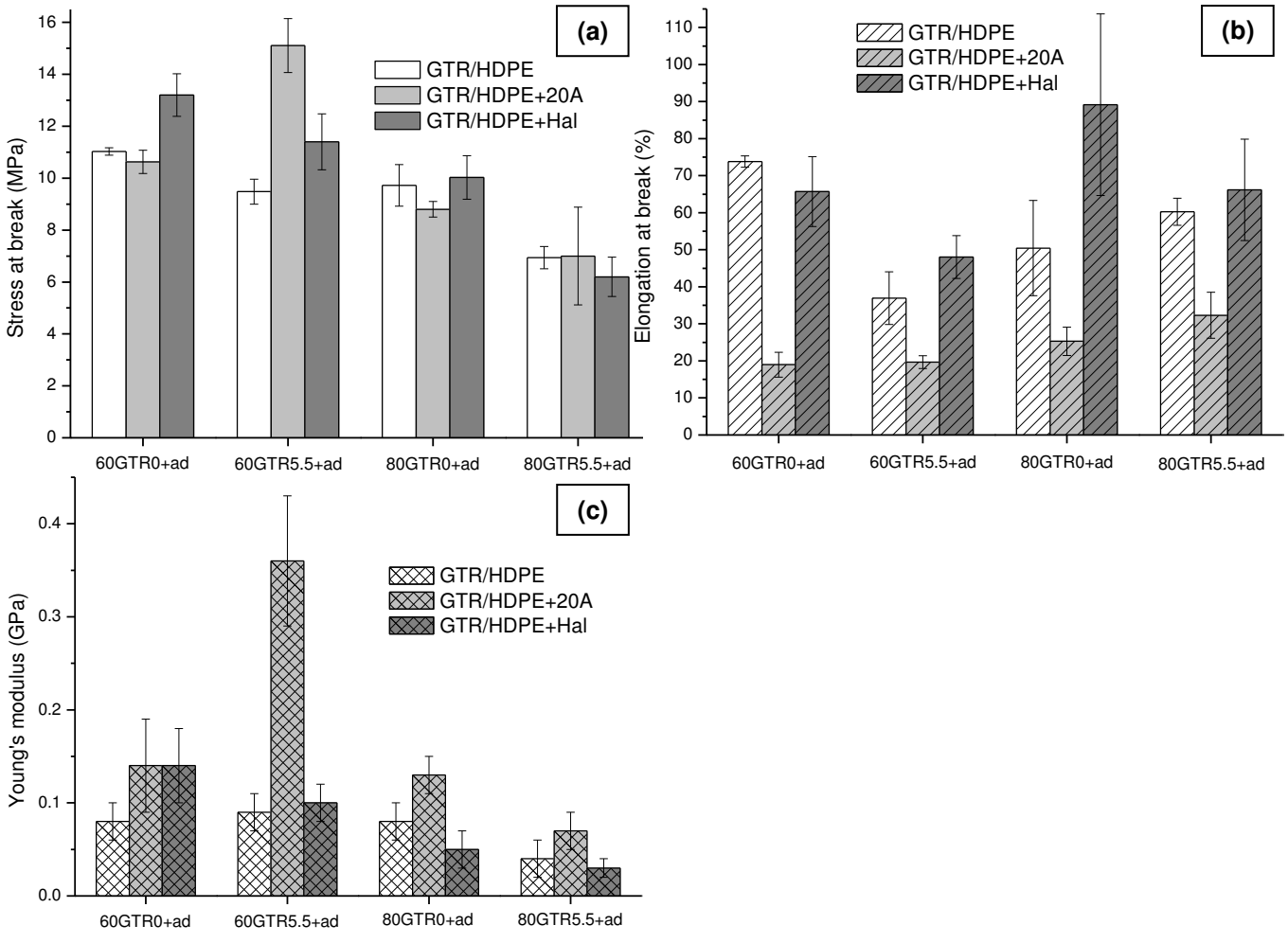

Figure 115: Mechanical properties of revulcanized blends containing GTR0 and GTR5.5 with different concentrations of GTR: (a) stress at break, (b) elongation at break and (c) Young's modulus. The x-axis of the figures represents the elastomeric phase composition of the blends.

According to the results, it appears that the revulcanized blends containing GTR0 presented their mechanical properties slightly superior to blends containing GTR5.5, especially in the blends containing HDPE and HDPE+Hal. According to the SEM images (section 10.1.1.2) it was possible to observe that the devulcanization improved the fluidity of the GTR during processing, since particles of GTR5.5 were lower compared to GTR0 ones. However, the vulcanization additives were not well mixed to GTR0, since both were in powder. With this it is believed that, during processing, the additives have stayed on the interface and not acted effectively on increasing the cross-linking density of GTR0. Also according to SEM images, better adhesion between phases of the blend containing GTR0 was observed, probably because of the location of the vulcanization additives, which may have increased the values of elongation at break of these blends.

Another possibility for the increase in mechanical properties of blends containing GTR0 is the coexistence of two networks of cross-linkings on the elastomeric phase: one from the first vulcanization and the other from revulcanization, even knowing the additives have not been well mixed to GTR0.

In the next section, the effect of the revulcanization of elastomeric phase on the mechanical properties of the blends will be analyzed.

10.4.2 - Effect of revulcanization of elastomeric phase

The effect of revulcanization of elastomeric phase in the mechanical properties of the blends is verified through the Figures 116 to 118.

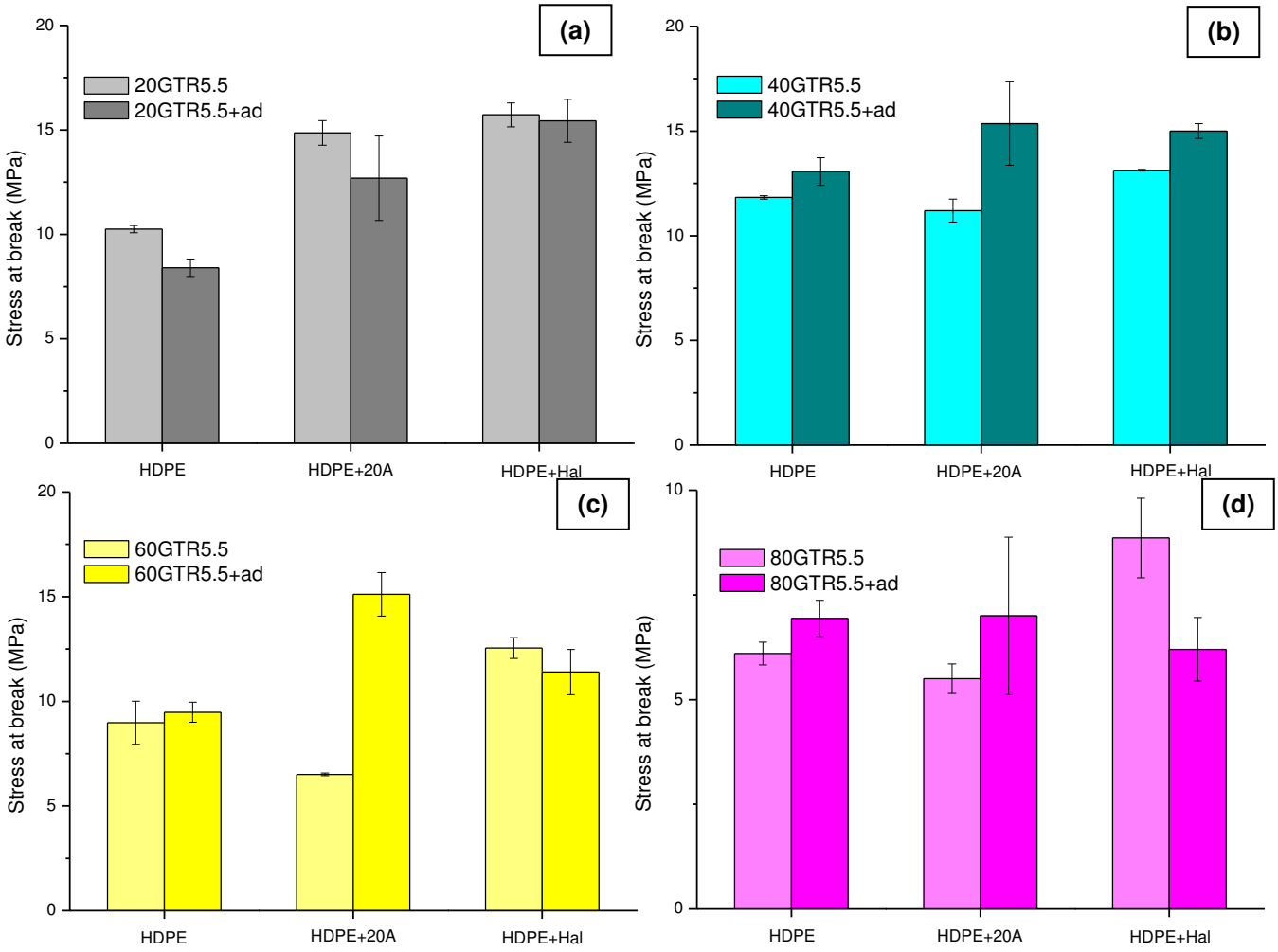

Figure 116: Stress at break of revulcanized and non revulcanized blends whether or not containing clay in different concentrations: (a) 20GTR5.5/80HDPE, (b) 40GTR5.5/60HDPE, (c) 60GTR5.5/40HDPE and (d) 80GTR5.5/20HDPE. The x-axis of the figures represents the thermoplastic phase composition.

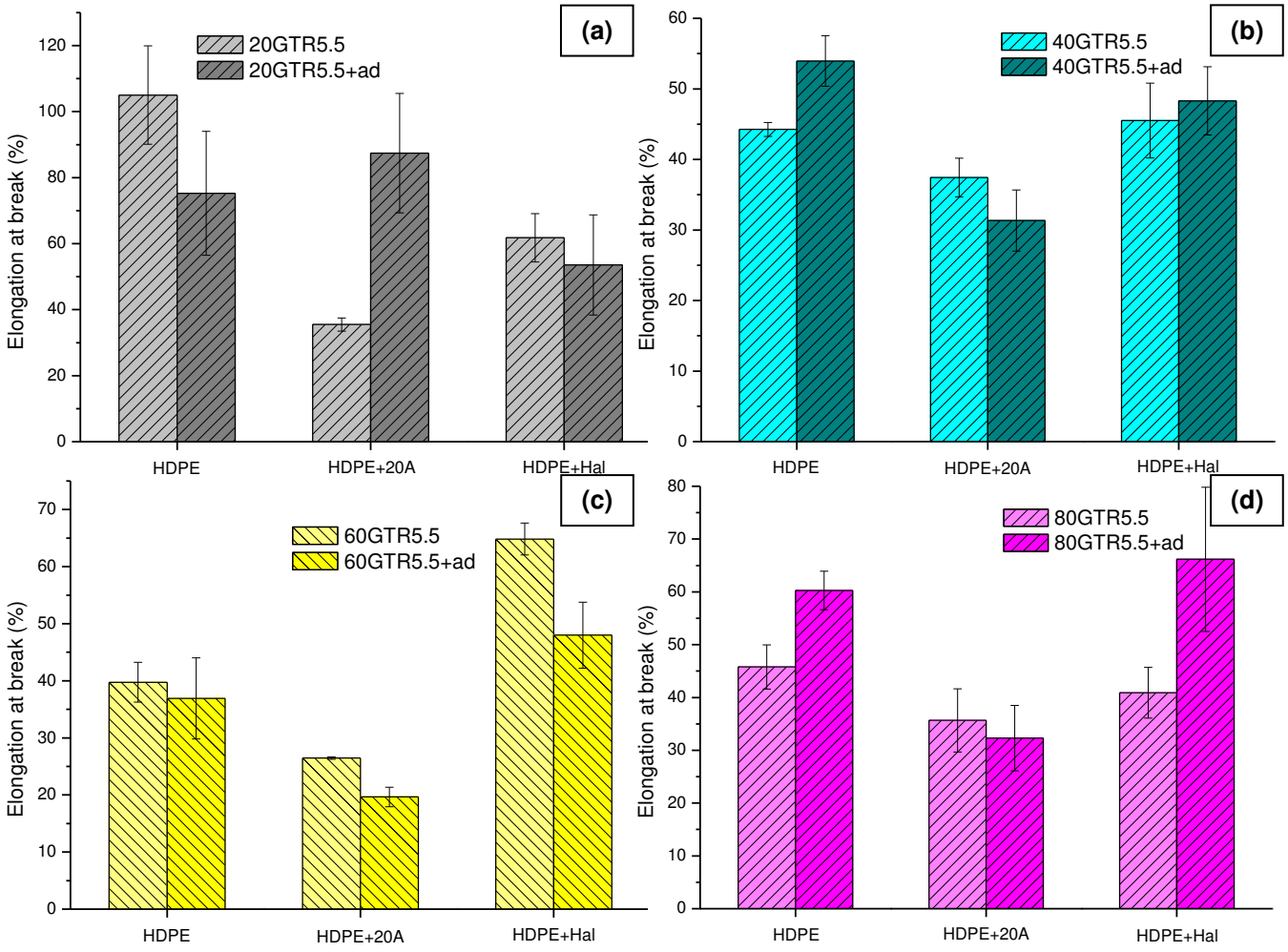

Figure 117: Elongation at break of revulcanized and non revulcanized blends whether or not containing clay in different concentrations: (a) 20GTR5.5/80HDPE, (b) 40GTR5.5/60HDPE, (c) 60GTR5.5/40HDPE and (d) 80GTR5.5/20HDPE. The x-axis of the figures represents the thermoplastic phase composition.

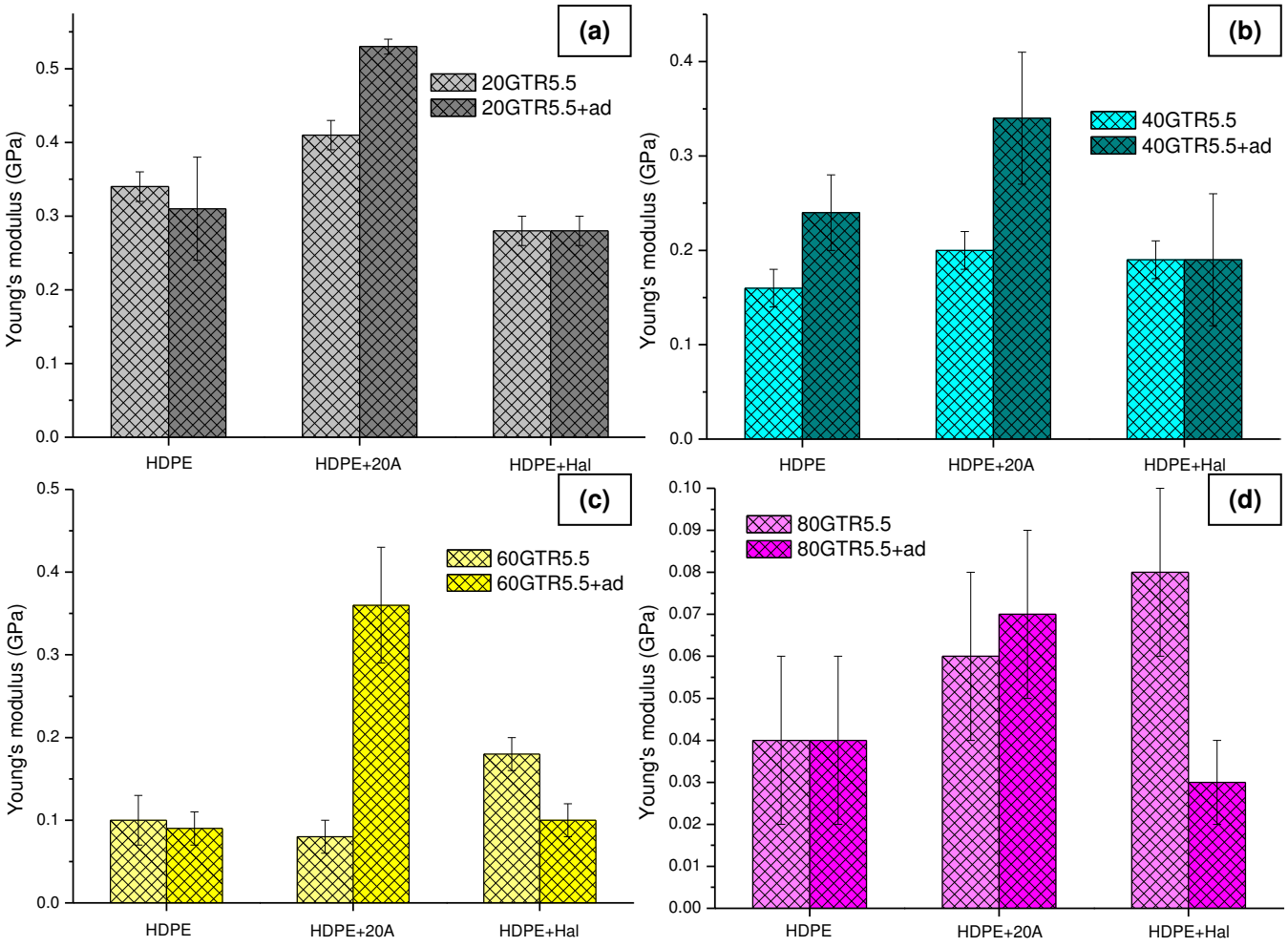

Figure 118: Young's modulus of revulcanized and non revulcanized blends whether or not containing clay in different concentrations: (a) 20GTR5.5/80HDPE, (b) 40GTR5.5/60HDPE, (c) 60GTR5.5/40HDPE and (d) 80GTR5.5/20HDPE. The x-axis of the figures represents the thermoplastic phase composition.

The literature reports improvements in mechanical properties of dynamically vulcanized blends [251, 260-262, 264-266, 271, 273, 358]. However, only in some blends were observed improvements with the occurrence of dynamic revulcanization. The literature also reports that blends containing high concentrations of GTR showed a depreciation in their results of mechanical properties [120, 134, 253, 268, 306, 308, 373, 374], primarily the elongation at break, due to lack of adhesion among phases. SEM images of the Stage 3 (section 10.1.2) showed that, in general, the occurrence of dynamic revulcanization induced toughening processes by formation of microfibrils due to the increase in the adhesion among phases, since in the revulcanized blends the images showed reduced number of GTR particles extracted, due precisely to the greater

adhesion among phases by the occurrence of dynamic revulcanization. As previously mentioned, the results presented here are due to the blend morphology generated by injection process adopted, which complicates the analysis of the real contribution of revulcanization on the results of mechanical properties.

The effect of addition of clays in the mechanical properties of the blends will be examined in the following section.

10.4.3 - Effect of addition of clays

The effect of addition of clays in the mechanical properties of the revulcanized and non revulcanized blends is verified through the Figures 119 to 121.

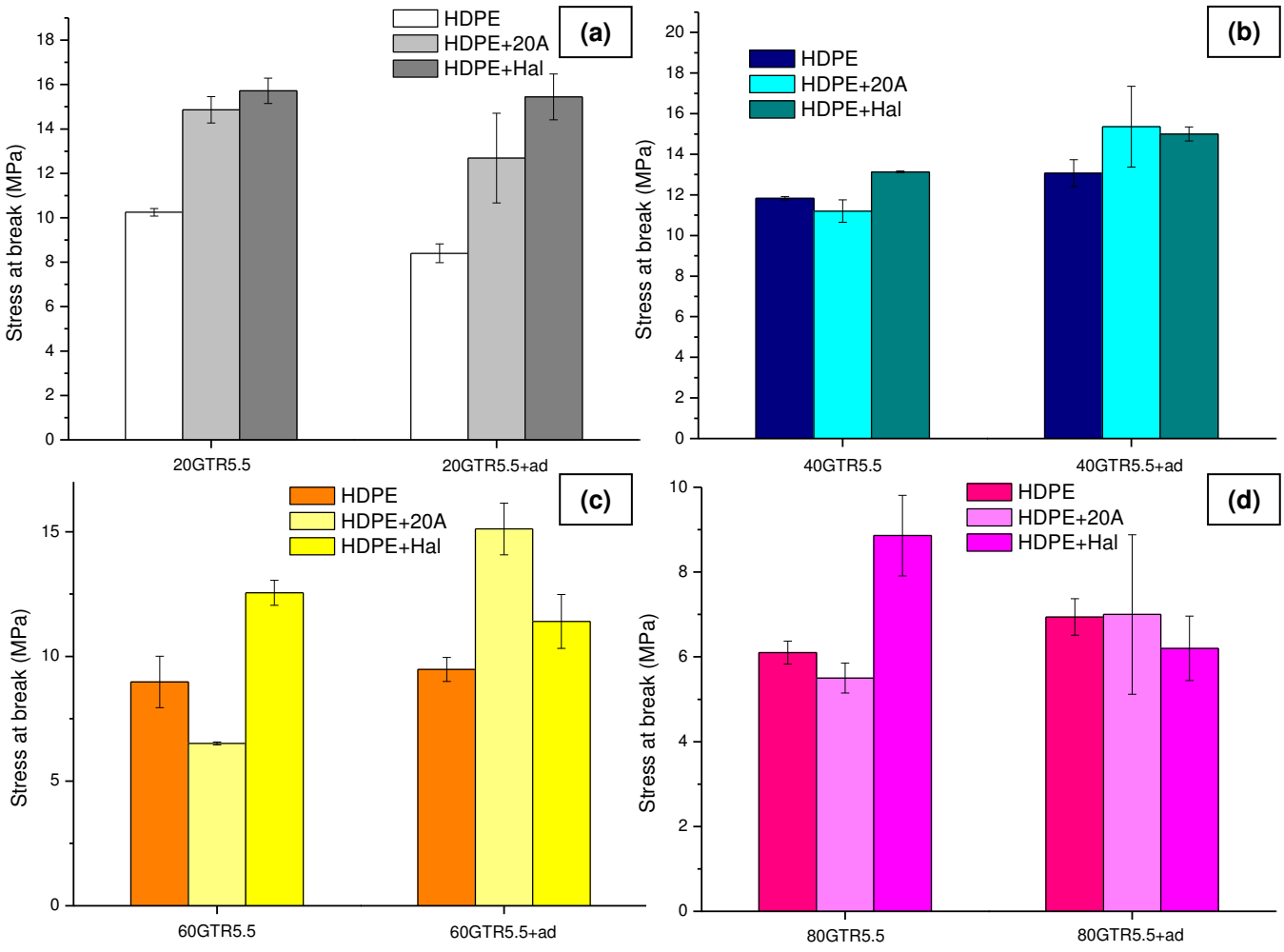

Figure 119: Stress at break of revulcanized and non revulcanized blends whether or not containing clay in different concentrations: (a) 20GTR5.5/80HDPE, (b) 40GTR5.5/60HDPE, (c) 60GTR5.5/40HDPE and (d) 80GTR5.5/20HDPE. The x-axis of the figures represents the composition of the elastomeric phase.

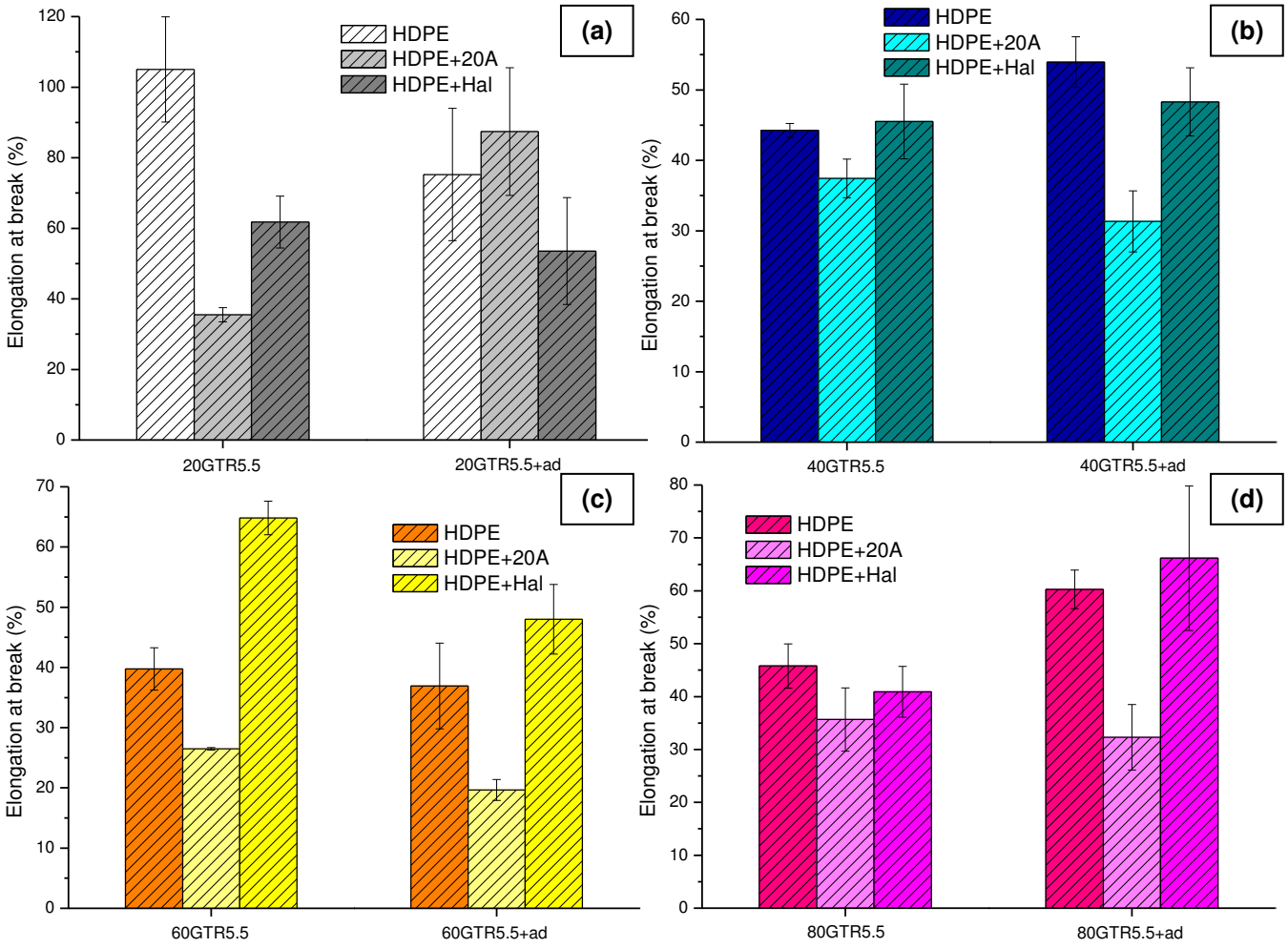

Figure 120: Elongation at break of revulcanized and non revulcanized blends whether or not containing clay in different concentrations: (a) 20GTR5.5/80HDPE, (b) 40GTR5.5/60HDPE, (c) 60GTR5.5/40HDPE and (d) 80GTR5.5/20HDPE. The x-axis of the figures represents the composition of the elastomeric phase.

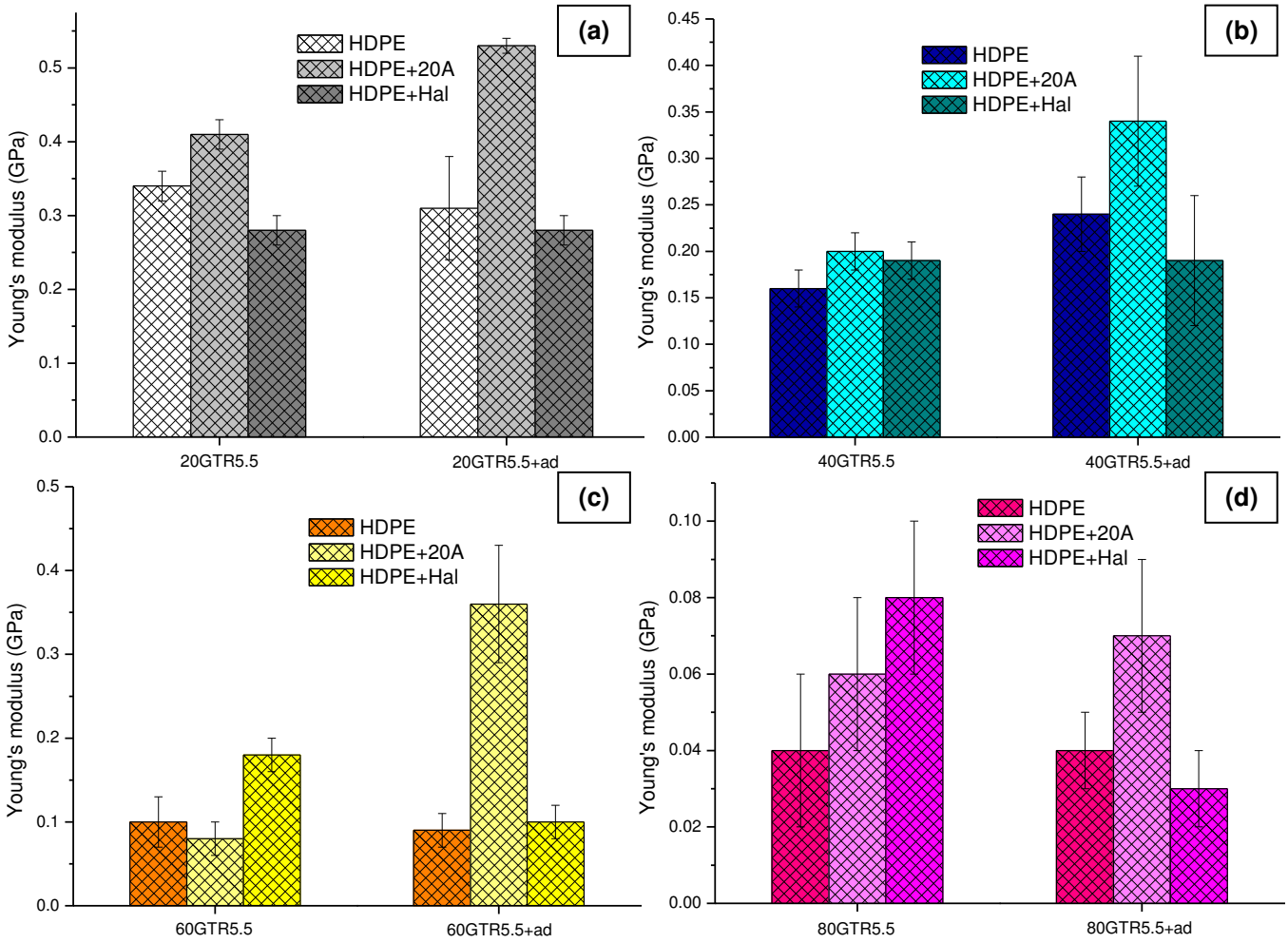

Figure 121: Young's modulus of revulcanized and non revulcanized blends whether or not containing clay in different concentrations: (a) 20GTR5.5/80HDPE, (b) 40GTR5.5/60HDPE, (c) 60GTR5.5/40HDPE and (d) 80GTR5.5/20HDPE. The x-axis of the figures represents the composition of the elastomeric phase.

The presence of clays did not significantly alter the values of stress at break, except few exceptions, one of which is the blend 60GTR5.5+ad/40HDPE+20A that presented higher value among the blends containing 60% of GTR due, probably, that the presence of clay have been acting as nucleating agent and have increased the crystallinity of matrix phase.

In the case of elongation at break, the presence of Cloisite 20A clay served in the reduction of this property because, as verified in the SEM images, it reduced the adhesion among phases, as well as having served as reinforcement to the matrix. Similarly, Tsai et al. [319] observed that the presence of OMMT in EPDM/PP blends also acted as nucleating agent in the thermoplastic phase, increasing the tensile strength and elongation at break. The presence of Halloysite clay seems to have acted as a

compatibilizing agent among the phases, since the elongation in the blends containing this clay was slightly higher compared to the others. The SEM images (section 10.1.3) showed that it improved the distribution of sub-micrometer GTR particles in the matrix and also improved its adhesion, due to the occurrence of toughness on matrix phase.
In modulus of blends containing Halloysite clay was, in general, minor in comparison to the other blends due to the occurrence of degradation. As seen in rheometry results of parallel plates of blends and ATR-FTIR in Stage 1, the presence of this clay increased degradation of HDPE for branching and later cross-linking and, possibly, this degradation of the matrix have influenced the reduction in moduli of blends containing clay.
In short, Halloysite clay seems to have acted as a compatibilizing agent among the phases of the blends, Cloisite 20A clay seems to have increased the crystallinity of matrix phase and acted as reinforcement in the revulcanized blends.

In the following section, the effect of the concentration of the phases on the mechanical properties of the blends will be analyzed.

10.4.4 - Effect of concentration of phases

The effect of the concentration of the phases on the mechanical properties of the revulcanized and non revulcanized blends is verified through the Figure 122.

In general, the properties decreased with the increase in concentration of GTR in blends, both in revulcanized and in the non revulcanized. The increase in concentration of rubber decreased the stress at break of the blends, what was expected, especially in the revulcanized ones, since the presence of sub-micrometer particles of rubber induced toughening processes in the matrix, as verified on the SEM results (section 10.1.2). George et al. [375] also observed depreciation on the results of NBR/PP blends which, according to the authors, is due to poor interfacial adhesion, which causes low stress transfer between the matrix and the dispersed phase. The modulus has decreased with the increase in concentration of rubber on the blend as response to the effect of the incorporation of a more flexible material [265]. According to Awang et al. [187], the reduction in tensile properties with the increase in concentration of rubber is due to the increase in particle-particle interaction, due to an increase on its concentration. The

same behavior was observed in other works available on literature [241, 242].

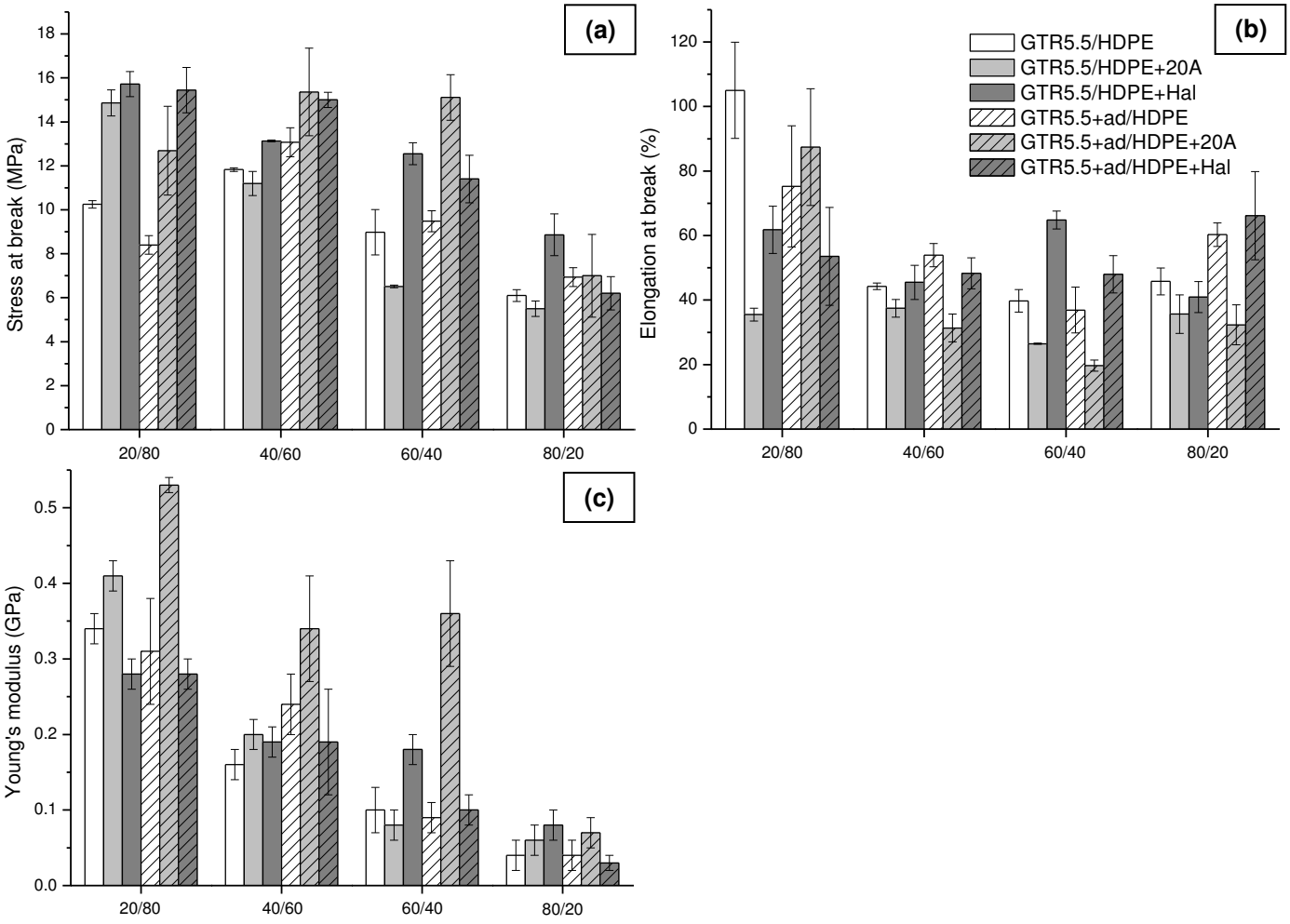

Figure 122: Mechanical properties of revulcanized and non revulcanized blends whether or not containing clay with different concentrations of GTR: (a) stress at break, (b) elongation at break and (c) Young's modulus. The x-axis of the figures represents the composition of the blends (GTR/thermoplastic).

According to Rabello [361], the presence of microfibrils generated by toughness implies in lower tensile strength and lower elastic modulus. According to the SEM images, it was observed that the dynamic revulcanization induced toughening processes in the regions of blends where sub-micrometer particles are well dispersed. According to Rabello [361], one of the conditions for the toughening process is that there is good adhesion among the phases. In general, it was observed that the presence of clays in the revulcanized blends apparently increased the toughness, especially the Halloysite clay, which was supported by the low value of modulus of 80GTR5.5+ad/20HDPE+Hal blend. The same clay also improved the distribution of sub-micrometer particles of GTR in the matrix and its adhesion, as verified in the SEM images, which was also

corroborated by the result of elongation at break of 60GTR5.5+ad/40HDPE+Hal and 80GTR5.5+ad/20HDPE+Hal blends, which were the largest values in the revulcanized blends.

Cloisite 20A clay decreased the adhesion among phases, even sub-micrometer particles, as verified through the SEM images, which was also borne out by the low values of elongation at break obtained on blends containing this clay, both in revulcanized and non revulocanized. According to Lee et al. [297], the low values of elongation at break reflect the delamination occurring during elongation due to poor interfacial adhesion. Similarly, for Zhang et al. [100], the elongation at break of blends depends on the compatibility among the phases, as this property is the best evidence of multiphase polymeric blends compatibility.

In general has also been observed that the values of stress at break of revulcanized blends containing Cloisite 20A were high, since the presence of this clay altered the crystallinity of phase matrix, as verified through the DMA results (section 10.2.3). The presence of the same clay also increased the Young's modulus of revulcanized blends due to its reinforcing character.

For a blend to be considered a thermoplastic vulcanized, the elongation at break is at least 100% [100, 260, 294, 305, 308], which was not verified on the results of tensile tests. Even obtaining particle sizes in sub micrometric scale, which shows that the processing adopted in the production of blends has been effective, the injection process of the specimens for tensile tests resulted in uneven distribution of these particles in the matrix, causing depreciation of the values of mechanical properties of these blends. Anyway, through the results, is observed the weak interaction among phases of the blend, since it is main feature for composites presenting good mechanical properties [100, 294]. It was expected that the results of the mechanical properties of revulcanized blends were higher in relation to non revulcanized blends, which was not checked in many blends, especially in blends containing Halloysite clay. This behavior is probably due to the HDPE degradation because of the presence of this clay, as verified in ATR-FTIR results from Stage 1 (section 3.4.2).

For mechanical properties results consistent with the actual properties of the blends, are required later studies adopting other methods to produce specimens for tensile tests. However, other results presented in this work should be taken into consideration as a means of analyzing the process adopted and quality of obtained materials, since the injection process used showed up not to be effective.

11 - PARTIAL CONCLUSION

In Stage 3 of this work, the consequences of the different effects on dynamic-mechanical, rheological and mechanical properties, as well as morphology of blends were analyzed, being they: effect of devulcanization and revulcanization of elastomeric phase, the addition of clays and the concentration of the phases.

In general, the analysis of the morphology of blends showed that the devulcanization of GTR was effective in the increase of its flow ability during processing, since the blends containing GTR0 showed much larger particle sizes in relation to particles of GTR5.5. The GTR5.5, more fluid and less viscous, facilitated the process of particle breakage during processing in twin screw extruder.

Concerning the revulcanization of the elastomeric phase, it was observed that, in general, this, apparently reduced the number of micrometric particles of GTR. It has been observed that the revulcanization induced thoughening processes by formation of microfibrils in the regions where the sub-micrometer particles were well distributed, which shows that the revulcanization increased the adhesion among phases.

As for the addition of clays, it was observed that they apparently have improved the distribution of particles of GTR in the matrix. However, in non revulcanized blends, the presence of Cloisite 20A clay seems to have reduced the interaction and adhesion among phases, possibly due to increased E' observed through the DMA results.

In relation to the increase in concentration of GTR phase, apparently there was an increase in the distribution of sub-micrometer particles of GTR in the matrix. The number of micrometric particles also seems to have been reduced with the increase of GTR concentration in the blends.

According to the DMA results, two transitions were verified for the phases of the blends: the first, around -40°C refers to the T_g of the GTR and the second refers to the α transition of HDPE (T_α), which occurs around 100°C, being that the same transitions were observed in all the analyzed blends. The existence of these different transitions proves the character immiscible of the blends.

Even knowing that for better analysis of changes in crystallinity of the thermoplastic phase it is necessary to carry out DSC analysis, and that they have not been performed in this work, some changes in crystallinity of HDPE phase could be observed on the basis of the DMA results.

The devulcanization of GTR phase changed the crystallinity of HDPE phase of some blends, possibly because of changes in sizes of particles of GTR5.5 and its distribution in the matrix.

In general, in revulcanized blends containing GTR0, T_g values are smaller in comparison to blends containing the same concentration of GTR5.5. Due to devulcanization, the polymeric chains have greater freedom during the reactive processing, which probably has increased the number of effective shocks and resulted in increased cross-linking density of elastomeric phase of blends containing GTR5.5.

In relation to revulcanization, the elastomeric phase, generally, it was observed the shift of the T_g peak of the GTR to higher temperatures, and reduction in the area under the peak of tan δ for the T_g of the same phase, as a result of the restriction on the mobility of the GTR by dynamic revulcanization. Similarly, has also been observed change in crystallinity of HDPE phase of some blends. As was expected, the dynamic revulcanization increased the T_g of the elastomeric phase in most blends (except in blends containing 20% of GTR).

Even being preferably on HDPE phase, the presence of clays altered the T_g of elastomeric phase of revulcanized blends. The T_g of the GTR phase of blends containing Halloysite clay was the largest of all the analyzed blends, due possibly to the greatest number of effective shocks during processing, since the presence of clay increased the viscosity of the HDPE due to degrading processes. On the other hand, the T_g of the GTR phase of blends containing Cloisite 20A clay was the smallest among the other blends. The presence of clays also altered the crystallinity of HDPE phase of some blends, especially those which are non revulcanized.

As to the concentration of the phases, the DMA results showed that the 20GTR5.5/80HDPE, 20GTR5.5/80HDPE+20A, 20GTR5.5/80HDPE+Hal, 20GTR5.5+ad/80HDPE, 20GTR5.5+ad/80HDPE+20A, 40GTR5.5+ad/60HDPE+20A and 20GTR5.5+ad/80HDPE+Hal blends have morphologies of co-continuous phases. In revulcanized blends, the crystallinity of matrix phase has changed in all the blends containing 80% of GTR, possibly as a result of their morphologies (as the analysis of the SEM results).

The results of rheometry of parallel plates showed that all blends presented reduced complex viscosity with increasing frequency, which suggests pseudoplastic behavior or characteristics of shear-thinning.

About the devulcanization of GTR phase, in general, the blends containing GTR5.5 presented smaller values of complex viscosity in comparison to blends containing GTR0 due to the higher flow capacity, as a result of the breaking of the cross-linkings of the GTR during devulcanization by microwaves. The non revulcanized blends containing GTR0 presented, in general, higher G' values as compared to blends containing GTR5.5 due to the higher cross-linking density of the elastomeric phase of the blend containing GTR0 (non devulcanized). In the case of revulcanized blends, an opposite behavior has occurred. The devulcanization of GTR apparently assisted in the formation of a network rheologically percolated.

As for the revulcanization of GTR phase, a clear trend has not been verified. The G' values have been influenced by several factors: reinforcement action of clay, degradation of matrix, blend morphology, and cross-linking density of the elastomeric phase. In each blend, depending on the concentration of the phases and the presence or not of clay, one of the factors was prevalent, and sometimes there was a "competition" among some of them. The lack of adhesion among phases also influenced the obtained results.

As for the addition of clays, depending on the concentration of the phases and adding of a specific clay type, it seems to have acted as a "reinforcement" or "degrading" agent in rheological properties. The presence of clay influenced on formation of rheologically percolated networks in blends, however different percolation thresholds were observed for each clay. Cloisite 20A clay reduced the rheological percolation threshold (between 40 and 60% of GTR on blend), and for the other blends the percolation threshold was met between 60 and 80% of GTR.

In relation to the concentration of the phases, to the non revulcanized blends, the G' and η^* values increased according to the increase of GTR concentration present in the blend. In the case of revulcanized blends, this trend was not observed. With the increase of GTR concentration of these blends, greater tendency to the formation of a rheologically percolated network, possibly due to the largest proximity among the particles of revulcanized GTR with smaller diameters.

The results of mechanical properties were consequence of morphology of the injected specimens that, as cited previously, showed well dispersed and bad distributed particles.

As for the GTR devulcanization , the blends containing GTR0 revulcanized showed slightly higher mechanical properties in relation to blends containing GTR5.5, possibly

due to higher adhesion among phases (as SEM images). As the GTR0 and vulcanization additives were powder and for this reason the last ones probably were not well mixed to the GTR, it is believed that, during processing, the additives have stayed in the interface, which somehow seems to have increased the adhesion. Another possibility for the increase in mechanical properties of blends containing GTR0 is the coexistence of two networks of cross-linking in the elastomeric phase, one from the vulcanization and the other from revulcanization, even knowing that the additives have not been well mixed to GTR0.

In relation to the revulcanization of elastomeric phase, only in some blends were observed improvements in mechanical properties. The SEM results showed that the dynamic revulcanization increased the adhesion among phases, however were not observed relevant improvements in the mechanical properties of the blends possibly due to the morphology of the injected specimens.

The presence of clays did not significantly alter the stress at break, except for a few exceptions. Cloisite 20A clay reduced the elongation at break, possibly for having reduced adhesion among phases and have apparently changed the crystallinity of HDPE. Halloysite clay has increased the property for having acted possibly as compatibilizing agent. The Young's modulus of blends containing Halloysite was smaller in relation to the value of the other blends due, possibly, to the toughness of the matrix and degradation of HDPE.

As to the concentration of the phases, in general and with some exceptions, the properties decreased with the increase in GTR concentration in the blends, both in revulcanized and non revulcanized ones.

However, it is noteworthy that the 60GTR5.5/40HDPE+20A blend presented high stress at break in relation to other blends analyzed in the work, which was a very positive outcome, given the high concentration of recycled material present in the blend concerned.

The results of mechanical properties of the obtained blends did not characterize them as TPVs.

Figure 52 (section 5.2) outlines and helps to understand the real contributions of devulcanization and revulcanization of elastomeric phase in the final morphology of blends. The devulcanization makes the rubber more fluid and this helps the breakage during processing, helping in the reduction of the particle size. With this, it helps in the

refinement of morphology, which consequently increases the contact area among the phases and increases the transmission of tensions. The revulcanization increases the adhesion among phases, as well as stabilizes the morphology by reducing the coalescence among the particles of revulcanized rubber.

12 - GENERAL CONCLUSIONS

In Stage 1, it was analyzed the efficiency of process of devulcanization of GTR by microwaves. The results showed that the process was efficient, because the breakdown of cross-linkings occurred and, consequently, the gel fraction was reduced, chemical changes occurred in the structure of the GTR by devulcanization and the rubber was able to flow. In this stage were also analyzed the best time of devulcanization (in this case was of 5.5 minutes) and the properties of the phases of the blends that were produced in the following stages. Based on the results, the method of microwave devulcanization proved to be an option for recycling vulcanized rubbers, helping in the reduction of the great environmental and public health problem that is the disposal of solid waste.

In Stage 2 were analyzed the best parameters involved in the production of blends, by processing of blends 60GTR5.5+ad/40HDPE in twin screw extruder, using different feeding modes and extrusion speeds. The stage was held due to difficulty in finding studies of systems in the literature which are at least similar. The results underscored the importance in the choice of the optimal processing parameters for each system in particular, since each system is unique, respecting the revulcanization kinetics of elastomeric phase previously known. These parameters affect directly the morphology and, consequently, the mechanical properties of the blends.

In Stage 3 were analyzed the consequences of effects: devulcanization and revulcanization of elastomeric phase, addition of clays and concentration of the phases in the dynamic-mechanical, rheological, mechanical properties, and on the morphology of blends. Based on the results presented in this stage of the work, it was found that the devulcanization and the revulcanization of elastomeric phase altered the rheological properties, dynamic-mechanical and morphology of blends. The addition of clays also altered the properties due to change in the rheological percolation threshold, change in crystallinity of HDPE phase of some blends and the possible performance as compatibilizing agent among the phases. However, it did not significantly alter the immiscible character of blends. The concentration of the stages completely changed all the properties analyzed.

However, due to the injection process used in the work to produce specimens for tensile tests, the mechanical properties were influenced by the morphology of the specimens, which hindered the analysis of the effects mentioned in those properties.

Though, even with all the complexity of the work in question, it fulfilled all of its main goals. The publication of results will fill in some gaps found in the current literature on the various aspects involved in the production of dynamically revulcanized blends containing residues of truck tires devulcanized by microwaves, as well as the proposed method for the production of the blends may be an option for the recycling of vulcanized rubber helping, thus, in the solution of the huge global problem that is the provision of solid waste, which causes serious environmental and public health problems.

13 - REFERENCES

[1] <http://www.resol.com.br/textos/Reciclagem%20de%20pneus.pdf>, acsess in 6/12/12.
[2] <http://www.inmetro.gov.br/painelsetorial/palestras/Zilda-Maria-Faria-Veloso-Ciclo-Vida-Pneus.pdf>, access in 18/7/14..
[3] J.M. Vergnaud, I.D. Rosca, Methods of Recycling Waste Tire Rubber, Rubber curing and properties, Taylor & Francis Group, Boca Raton, 2008, pp. 177-195.
[4] C.A.F. Lagarinhos, J.A.S. Tenorio, Reverse Logistics for Post-Consumer Tires in Brazil, Polimeros-Ciencia E Tecnologia 23(1) (2013) 49-58.
[5] S.K. De, A.I. Isayev, K. Khait, Rubber recycling, CRC Press, United States, 2005.
[6] C.R. Kumar, I. Fuhrmann, J. Karger-Kocsis, LDPE-based thermoplastic elastomers containing ground tire rubber with and without dynamic curing, Polymer Degradation and Stability 76(1) (2002) 137-144.
[7] C.H. Scuracchio, D.A. Waki, R.E.S. Bretas, Caracterização Térmica e Reológica de Borracha de Pneu Desvulcanizada por Microondas, Polímeros: Ciência e Tecnologia 16(1) (2006) 46-52.
[8] F.D.B. de Sousa, J.R. Gouveia, P.M.F. de Camargo Filho, S.E. Vidotti, C.H. Scuracchio, L. Amurin, T.S. Valera, Blends Ground Tire Rubber devulcanized by microwaves/HDPE - Part B: Influence of clay addition, Polimeros-Ciencia E Tecnologia 25(4) (2015) 382-391.
[9] A. Taguet, P. Cassagnau, J.M. Lopez-Cuesta, Structuration, selective dispersion and compatibilizing effect of (nano)fillers in polymer blends, Progress in Polymer Science 39(8) (2014) 1526-1563.
[10] J.H. Koo, Polymer Nanocomposites: Processing, characterization, and applications, McGraw-Hill, Mexico, 2006.
[11] F.D.B. de Sousa, Nanocompósitos de Borracha Nitrílica com Argilas Montmoriloníticas e Bentonitas, Universidade Federal do ABC, Santo André, 2010.
[12] C.E. Carraher Jr., Polymer Chemistry, Marcel Dekker, New York, 2003.
[13] T. Peprnicek, J. Duchet, L. Kovarova, J. Malac, J.F. Gerard, J. Simonik, Poly(vinyl chloride)/clay nanocomposites: X-ray diffraction, thermal and rheological behaviour, Polymer Degradation and Stability 91(8) (2006) 1855-1860.
[14] C.Y. Wan, X.Y. Qiao, Y. Zhang, Y.X. Zhang, Effect of different clay treatment on morphology and mechanical properties of PVC-clay nanocomposites, Polymer Testing 22(4) (2003) 453-461.
[15] H. Ismail, R. Ramli, Organoclay Filled Natural Rubber Nanocomposites: The Effects of Filler Loading and Mixing Method, Journal of Reinforced Plastics and Composites 27(16-17) (2008) 1909-1924.
[16] H. Fischer, Polymer nanocomposites: from fundamental research to specific applications, Materials Science & Engineering C-Biomimetic and Supramolecular Systems 23(6-8) (2003) 763-772.
[17] P.M. Ajayan, S.L. S., B.P. V., Nanocomposite Science and Technology, Wiley-VCH Verlag, Weinheim, 2003.
[18] S. Joly, G. Garnaud, R. Ollitrault, L. Bokobza, J.E. Mark, Organically modified layered silicates as reinforcing fillers for natural rubber, Chemistry of Materials 14(10) (2002) 4202-4208.
[19] E.P. Giannelis, R. Krishnamoorti, E. Manias, Polymer-silicate nanocomposites: Model systems for confined polymers and polymer brushes, Polymers in Confined Environments 138 (1999) 107-147.
[20] K. Okamoto, S.S. Ray, M. Okamoto, New poly(butylene succinate)/layered silicate nanocomposites. II. Effect of organically modified layered silicates on structure, properties, melt rheology, and biodegradability, Journal of Polymer Science Part B-Polymer Physics 41(24) (2003) 3160-3172.
[21] B.K.G. Theng, Interactions between montmorillonite and fulvic acid, Geoderma 15 (1974) 243-251.
[22] A. Bandyopadhyay, M. Maiti, A.K. Bhowmick, Synthesis, characterisation and properties of clay and silica based rubber nanocomposites, Materials Science and Technology 22(7) (2006) 818-828.
[23] M. Mondragon, E.M. Hernandez, J.L. Rivera-Armenta, F.J. Rodriguez-Gonzalez, Injection molded thermoplastic starch/natural rubber/clay nanocomposites: Morphology and mechanical properties, Carbohydrate Polymers 77(1) (2009) 80-86.
[24] A. Das, F.R. Costa, U. Wagenknecht, G. Heinrich, Nanocomposites based on chloroprene rubber: Effect of chemical nature and organic modification of nanoclay on the vulcanizate properties, European Polymer Journal 44(11) (2008) 3456-3465.
[25] S.S. Ray, M. Okamoto, Polymer/layered silicate nanocomposites: a review from preparation to processing, Progress in Polymer Science 28(11) (2003) 1539-1641.
[26] B.C. Guo, F. Chen, Y.D. Lei, X.L. Liu, J.J. Wan, D.M. Jia, Styrene-butadiene rubber/halloysite nanotubes nanocomposites modified by sorbic acid, Applied Surface Science 255(16) (2009) 7329-7336.
[27] M.X. Liu, B.C. Guo, M.L. Du, F. Chen, D.M. Jia, Halloysite nanotubes as a novel beta-nucleating agent for isotactic polypropylene, Polymer 50(13) (2009) 3022-3030.
[28] L.N. Carli, J.S. Crespo, R.S. Mauler, PHBV nanocomposites based on organomodified montmorillonite and halloysite: The effect of clay type on the morphology and thermal and mechanical

properties, Composites Part a-Applied Science and Manufacturing 42(11) (2011) 1601-1608.
[29] M.X. Liu, Y. Zhang, C.R. Zhou, Nanocomposites of halloysite and polylactide, Applied Clay Science 75-76 (2013) 52-59.
[30] M.L. Du, B.C. Guo, Y.D. Lei, M.X. Liu, D.M. Jia, Carboxylated butadiene-styrene rubber/halloysite nanotube nanocomposites: Interfacial interaction and performance, Polymer 49(22) (2008) 4871-4876.
[31] R. Barbosa, T.S. Alves, E.M. Araujo, T.J.A. Melo, G. Camino, A. Fina, E.N. Ito, Flammability and morphology of HDPE/clay nanocomposites, Journal of Thermal Analysis and Calorimetry 115(1) (2014) 627-634.
[32] T.D. Fornes, P.J. Yoon, H. Keskkula, D.R. Paul, Nylon 6 nanocomposites: the effect of matrix molecular weight, Polymer 42(25) (2001) 9929-9940.
[33] H.R. Dennis, D.L. Hunter, D. Chang, S. Kim, J.L. White, J.W. Cho, D.R. Paul, Effect of melt processing conditions on the extent of exfoliation in organoclay-based nanocomposites, Polymer 42(23) (2001) 9513-9522.
[34] M. Alexandre, P. Dubois, Polymer-layered silicate nanocomposites: preparation, properties and uses of a new class of materials, Materials Science & Engineering R-Reports 28(1-2) (2000) 1-63.
[35] P. Cassagnau, Melt rheology of organoclay and fumed silica nanocomposites, Polymer 49(9) (2008) 2183.
[36] J. Jancar, J.F. Douglas, F.W. Starr, S.K. Kumar, P. Cassagnau, A.J. Lesser, S.S. Sternstein, M.J. Buehler, Current issues in research on structure-property relationships in polymer nanocomposites, Polymer 51(15) (2010) 3321-3343.
[37] L.A. Goettler, K.Y. Lee, H. Thakkar, Layered silicate reinforced polymer nanocomposites: Development and applications, Polymer Reviews 47(2) (2007) 291-317.
[38] I. Dabrowska, L. Fambri, A. Pegoretti, G. Ferrara, Organically modified hydrotalcite for compounding and spinning of polyethylene nanocomposites, Express Polymer Letters 7(11) (2013) 936-949.
[39] L. Minkova, Y. Peneva, M. Valcheva, S. Filippi, M. Pracella, I. Anguillesi, P. Magagnini, Morphology, Microhardness, and Flammability of Compatibilized Polyethylene/Clay Nanocomposites, Polymer Engineering and Science 50(7) (2010) 1306-1314.
[40] K.M. Lee, C.D. Han, Effect of hydrogen bonding on the rheology of polycarbonate/organoclay nanocomposites, Polymer 44(16) (2003) 4573-4588.
[41] J.M. Barbas, A.V. Machado, J.A. Covas, Evolution of dispersion along the extruder during the manufacture of polymer-organoclay nanocomposites, Chemical Engineering Science 98 (2013) 77-87.
[42] S. Al-Malaika, H. Sheena, D. Fischer, E. Masarati, Influence of processing and clay type on nanostructure and stability of polypropylene-clay nanocomposites, Polymer Degradation and Stability 98(12) (2013) 2400-2410.
[43] H. Sadeghipour, H. Ebadi-Dehaghani, D. Ashouri, S. Mousavian, M. Hashemi-Fesharaki, M.S. Gahrouei, Effects of modified and non-modified clay on the rheological behavior of high density polyethylene, Composites Part B-Engineering 52 (2013) 164-171.
[44] M.L. Du, B.C. Guo, M.X. Liu, X.J. Cai, D.M. Jia, Reinforcing thermoplastics with hydrogen bonding bridged inorganics, Physica B-Condensed Matter 405(2) (2010) 655-662.
[45] R.A. da Paz, A.M.D. Leite, E.M. Araujo, T.J.A. de Melo, L.A. Pessan, F.R. Passador, Mechanical and Rheological Properties of Nanocomposites of Polyamide 6 with National Organoclay, Polimeros-Ciencia E Tecnologia 23(5) (2013) 682-689.
[46] D. Komatsu, H. Otaguro, A.C. Ruvolo, Comparative Evaluation between Montmorillonite Clay/LLDPE and Potassium Hexaniobate/LLDPE Nanocomposites: Characterization of Mechanical and Transport Properties, Polimeros-Ciencia E Tecnologia 24(1) (2014) 37-44.
[47] M.F.L. de Oliveira, M.G. de Oliveira, M. Leite, Nanocomposites of Polyamide 6 and Organoclay: Crystallinity and Study of Mechanical Properties, Polimeros-Ciencia E Tecnologia 21(1) (2011) 78-82.
[48] A. Arrillaga, A.M. Zaldua, R.M. Atxurra, A.S. Farid, Techniques used for determining cure kinetics of rubber compound, European Polymer Journal 43(11) (2007) 4783-4799.
[49] H.M. da Costa, L.L.Y. Visconte, R.C.R. Nunes, C.R.G. Furtado, Aspéctos Históricos da Vulcanização, Polímeros: Ciência e Tecnologia 13(2) (2003) 125-129.
[50] F.R. Passador, L.A. Pessan, A. Rodolfo, PVC/NBR blends by reactive processing I: In situ dynamic vulcanization process, Polimeros-Ciencia E Tecnologia 17(2) (2007) 80-84.
[51] M. Morton, Rubber Technology, Robert & Krieger Publishing Company, Florida, 1981.
[52] V.Y. Levin, S.H. Kim, A.I. Isayev, J. Massey, E. vonMeerwall, Ultrasound devulcanization of sulfur vulcanized SBR: Crosslink density and molecular mobility, Rubber Chemistry and Technology 69(1) (1996) 104-114.
[53] B. Wu, M.H. Zhou, Recycling of waste tyre rubber into oil absorbent, Waste Management 29(1) (2009) 355-359.

[54] N. Roche, M.N. Ichchou, M. Salvia, A. Chettah, Dynamic Damping Properties of Thermoplastic Elastomers Based on EVA and Recycled Ground Tire Rubber, Journal of Elastomers and Plastics 43(4) (2011) 317-340.
[55] K. Masaki, S.I. Ohkawara, T. Hirano, M. Seno, T. Sato, Devulcanization of nitrile butadiene rubber in nitrobenzene, Journal of Applied Polymer Science 91(5) (2004) 3342-3353.
[56] J. Scheirs, Rubber tyre recycling, in: J. Scheirs (Ed.), Polymer recycling: science, technology and applications, Wiley, London, 1998, pp. 125–137.
[57] M.M. Hassan, N.A. Badway, M.Y. Elnaggar, E.A. Hegazy, Effects of Peroxide and Gamma Radiation on Properties of Devulcanized Rubber/Polypropylene/Ethylene Propylene Diene Monomer Formulation, Journal of Applied Polymer Science 131(16) (2014).
[58] C.H. Scuracchio, D.A. Waki, M. da Silva, Thermal analysis of ground tire rubber devulcanized by microwaves, Journal of Thermal Analysis and Calorimetry 87(3) (2007) 893-897.
[59] Y. Saeki, Methodology, technology and economy of polymer recycling, International rubber conference, 1995, pp. 594–601.
[60] J.R. White, S.K. De, Rubber technologist's handbook, Rapra Technology, Reino Unido, 2001.
[61] V.K. Sharma, F. Fortuna, M. Mincarini, M. Berillo, G. Cornacchia, Disposal of waste tyres for energy recovery and safe environment, Applied Energy 65(1-4) (2000) 381-394.
[62] E.C. Orr, J.A. Burghard, W. Tuntawiroon, L.L. Anderson, E.M. Eyring, Coprocessing waste rubber tire material and coal, Fuel Processing Technology 47(3) (1996) 245-259.
[63] H.M. Wang, M. Davidson, Y. Zuo, Z.Y. Ren, Recycled tire crumb rubber anodes for sustainable power production in microbial fuel cells, Journal of Power Sources 196(14) (2011) 5863-5866.
[64] J. Fiksel, B.R. Bakshi, A. Baral, E. Guerra, B. DeQuervain, Comparative life cycle assessment of beneficial applications for scrap tires, Clean Technologies and Environmental Policy 13(1) (2011) 19-35.
[65] M. Stelmachowski, K. Slowinski, Conversion of waste rubber as an alternative rout to renewable fuel production, Energy and Sustainability Ii 121 (2009) 501-510.
[66] C. Lin, C.L. Huang, C.C. Shern, Recycling waste tire powder for the recovery of oil spills, Resources Conservation and Recycling 52(10) (2008) 1162-1166.
[67] I.H. Hwang, S. Yokono, T. Matsuto, Pretreatment of automobile shredder residue (ASR) for fuel utilization, Chemosphere 71(5) (2008) 879-885.
[68] M. Myhre, D.A. MacKillop, Rubber recycling, Rubber Chemistry and Technology 75(3) (2002) 429-474.
[69] Y.H. Li, S.H. Zhao, Y.Q. Wang, Microbial Desulfurization of Ground Tire Rubber by sp.: A Novel Technology for Crumb Rubber Composites, Journal of Polymers and the Environment 20(2) (2012) 372-380.
[70] M. Sienkiewicz, J. Kucinska-Lipka, H. Janik, A. Balas, Progress in used tyres management in the European Union: A review, Waste Management 32(10) (2012) 1742-1751.
[71] J.S. Oh, A.I. Isayev, Continuous ultrasonic devulcanization of unfilled butadiene rubber, Journal of Applied Polymer Science 93(3) (2004) 1166-1174.
[72] T. Kleps, M. Piaskiewicz, W. Parasiewicz, The use of thermogravimetry in the study of rubber devulcanization, Journal of Thermal Analysis and Calorimetry 60(1) (2000) 271-277.
[73] W.C. Warner, Methods of devulcanization, Rubber Chemistry and Technology 67(3) (1994) 559-566.
[74] <http://www.etrma.org/uploads/Modules/Documentsmanager/chemrisk--09-12-16-end-of-life-tyre.pdf>, access in 5/9/12.
[75] X.M. Sun, A.I. Isayev, Continuous ultrasonic devulcanization comparison of carbon black filled synthetic isoprene and natural rubbers, Rubber Chemistry and Technology 81(1) (2008) 19-46.
[76] K. Fukumori, M. Matsushita, H. Okamoto, N. Sato, Y. Suzuki, K. Takeuchi, Recycling technology of tire rubber, Jsae Review 23(2) (2002) 259-264.
[77] X.X. Zhang, C.H. Lu, M. Liang, Properties of natural rubber vulcanizates containing mechanochemically devulcanized ground tire rubber, Journal of Polymer Research 16(4) (2009) 411-419.
[78] S.H. Lee, Z.X. Zhang, D. Xu, D. Chung, G.J. Oh, J.K. Kim, Dynamic Reaction Involving Surface Modified Waste Ground Rubber Tire Powder/Polypropylene, Polymer Engineering and Science 49(1) (2009) 168-176.
[79] S.Y. Li, J. Lamminmaki, K. Hanhi, Effect of ground rubber powder and devulcanizates on the properties of natural rubber compounds, Journal of Applied Polymer Science 97(1) (2005) 208-217.
[80] R. Rios, M. Gontijo, V.P. Ferraz, R.M. Lago, M.H. Araujo, Devulcanization of styrenebutadiene (SBR) waste tire by controlled oxidation, Journal of the Brazilian Chemical Society 17(3) (2006) 603-608.
[81] B. Maridass, B.R. Gupta, Performance optimization of a counter rotating twin screw extruder for recycling natural rubber vulcanizates using response surface methodology, Polymer Testing 23(4) (2004)

377-385.
[82] B. Maridass, B.R. Gupta, Process Optimization of Devulcanization of Waste Rubber Powder From Syringe Stoppers by Twin Screw Extruder Using Response Surface Methodology, Polymer Composites 29(12) (2008) 1350-1357.
[83] H. Yazdani, M. Karrabi, I. Ghasmi, H. Azizi, G.R. Bakhshandeh, Devulcanization of Waste Tires Using a Twin-Screw Extruder: The Effects of Processing Conditions, Journal of Vinyl & Additive Technology 17(1) (2011) 64-69.
[84] X.X. Zhang, C.H. Lu, M. Liang, Preparation of Thermoplastic Vulcanizates Based on Waste Crosslinked Polyethylene and Ground Tire Rubber Through Dynamic Vulcanization, Journal of Applied Polymer Science 122(3) (2011) 2110-2120.
[85] P. Sutanto, F.L. Laksmana, E. Picchioni, L. Janssen, Modeling on the kinetics of an EPDM devulcanization in an internal batch mixer using an amine as the devulcanizing agent, Chemical Engineering Science 61(19) (2006) 6442-6453.
[86] P. Sutanto, F. Picchioni, L. Janssen, Modelling a continuous devulcanization in an extruder, Chemical Engineering Science 61(21) (2006) 7077-7086.
[87] P. Sutanto, F. Picchioni, L. Janssen, The use of experimental design to study the responses of continuous devulcanization processes, Journal of Applied Polymer Science 102(5) (2006) 5028-5038.
[88] P. Sutanto, F. Picchioni, L. Janssen, K.A.J. Dijkhuis, W.K. Dierkes, J.W.M. Noordermeer, EPDM rubber reclaim from devulcanized EPDM, Journal of Applied Polymer Science 102(6) (2006) 5948-5957.
[89] S. Rooj, G.C. Basak, P.K. Maji, A.K. Bhowmick, New Route for Devulcanization of Natural Rubber and the Properties of Devulcanized Rubber, Journal of Polymers and the Environment 19(2) (2011) 382-390.
[90] E. Bilgili, A. Dybek, H. Arastoopour, B. Bernstein, A new recycling technology: Compression molding of pulverized rubber waste in the absence of virgin rubber, Journal of Elastomers and Plastics 35(3) (2003) 235-256.
[91] B. Maridass, B.R. Gupta, Effect of carbon black on devulcanized ground rubber tire-natural rubber vulcanizates: Cure characteristics and mechanical properties, Journal of Elastomers and Plastics 38(3) (2006) 211-229.
[92] K.A.J. Dijkhuis, I. Babu, J.S. Lopulissa, J.W.M. Noordermeer, W.K. Dierkes, A mechanistic approach to EPDM devulcanization, Rubber Chemistry and Technology 81(2) (2008) 190-208.
[93] A.A. Yehia, M.N. Ismail, Y.A. Hefny, E.M. Abdel-Bary, M.A. Mull, Mechano-chemical reclamation of waste rubber powder and its effect on the performance of NR and SBR vulcanizates, Journal of Elastomers and Plastics 36(2) (2004) 109-123.
[94] X.X. Zhang, Z.X. Lu, D. Tian, H. Li, C.H. Lu, Mechanochemical devulcanization of ground tire rubber and its application in acoustic absorbent polyurethane foamed composites, Journal of Applied Polymer Science 127(5) (2013) 4006-4014.
[95] H. Yazdani, I. Ghasemi, M. Karrabi, H. Azizi, G.R. Bakhshandeh, Continuous devulcanization of waste tires by using a Co-rotating twin screw extruder: Effects of screw configuration, temperature profile, and devulcanization agent concentration, Journal of Vinyl & Additive Technology 19(1) (2013) 65-72.
[96] S.K. Mandal, N. Alam, S.C. Debnath, Reclaiming of Ground Rubber Tire by safe multifunctional rubber additives: I. Tetra Benzylthiuram Disulfide, Rubber Chemistry and Technology 85(4) (2012) 629–644.
[97] A.R. Tripathy, J.E. Morin, D.E. Williams, S.J. Eyles, R.J. Farris, A novel approach to improving the mechanical properties in recycled vulcanized natural rubber and its mechanism, Macromolecules 35(12) (2002) 4616-4627.
[98] M.A.L. Verbruggen, L. van der Does, J.W.M. Noordermeer, M. van Duin, H.J. Manuel, Mechanisms involved in the recycling of NR and EPDM, Rubber Chemistry and Technology 72(4) (1999) 731-740.
[99] F. Sadaka, I. Campistron, A. Laguerre, J.F. Pilard, Controlled chemical degradation of natural rubber using periodic acid: Application for recycling waste tyre rubber, Polymer Degradation and Stability 97(5) (2012) 816-828.
[100] S.L. Zhang, Z.X. Zhang, J.K. Kim, Study on Thermoplastic Elastomers (TPEs) of Waste Polypropylene/Waste Ground Rubber Tire Powder, Journal of Macromolecular Science Part B-Physics 50(4) (2011) 762-768.
[101] A. Bani, G. Polacco, G. Gallone, Microwave-Induced Devulcanization for Poly(ethylene-propylene-diene) Recycling, Journal of Applied Polymer Science 120(5) (2011) 2904-2911.
[102] V. Pistor, A.J. Zattera, Degradation kinetics of ethylene propylene diene terpolymer residues devulcanized by microwaves, Journal of Elastomers and Plastics 44 (2012) 1-15.
[103] V. Pistor, C.H. Scuracchio, P.J. Oliveira, R. Fiorio, A.J. Zatteral, Devulcanization of Ethylene-Propylene-Diene Polymer Residues by Microwave-Influence of the Presence of Paraffinic Oil, Polymer

Engineering and Science 51(4) (2011) 697-703.
[104] V. Pistor, F.G. Ornaghi, R. Fiorio, A.J. Zattera, P.J. Oliveira, C.H. Scuracchio, Devulcanization of Ethylene-Propylene-Diene Polymer Residues (EPDM-r) by Microwaves, Polimeros-Ciencia E Tecnologia 20(3) (2010) 165-169.
[105] D. Hirayama, C. Saron, Chemical Modifications in Styrene-Butadiene Rubber after Microwave Devulcanization, Industrial & Engineering Chemistry Research 51(10) (2012) 3975-3980.
[106] L. Landini, S.G. de Araujo, A.B. Lugao, H. Wiebeck, Preliminary analysis to BIIR recovery using the microwave process, European Polymer Journal 43(6) (2007) 2725-2731.
[107] A. Zanchet, L.N. Carli, M. Giovanela, J.S. Crespo, C.H. Scuracchio, R.C.R. Nunes, Characterization of Microwave-Devulcanized Composites of Ground SBR Scraps, Journal of Elastomers and Plastics 41(6) (2009) 497-507.
[108] A. Zanchet, L.N. Carli, M. Giovanela, R.N. Brandalise, J.S. Crespo, Use of styrene butadiene rubber industrial waste devulcanized by microwave in rubber composites for automotive application, Materials & Design 39 (2012) 437-443.
[109] G.D. Paulo, D. Hirayama, C. Saron, Microwave devulcanization of waste rubber with inorganic salts and nitric acid, 2012, pp. 1072-1075.
[110] N. Sombatsompop, C. Kumnuantip, Comparison of physical and mechanical properties of NR/carbon black/reclaimed rubber blends vulcanized by conventional thermal and microwave irradiation methods, Journal of Applied Polymer Science 100(6) (2006) 5039-5048.
[111] C.H. Scuracchio, R.E.S. Bretas, A.I. Isayev, Blends of PS with SBR devulcanized by ultrasound: Rheology and morphology, Journal of Elastomers and Plastics 36(1) (2004) 45-75.
[112] S. Ghose, A.I. Isayev, Ultrasonic devulcanization of carbon black filled polyurethane rubber, Journal of Elastomers and Plastics 36(3) (2004) 213-239.
[113] V.V. Yashin, A.I. Isayev, The effect of polydispersity on structure of ultrasonically treated rubbers, Polymer 45(17) (2004) 6083-6094.
[114] W.L. Feng, A.I. Isayev, Blends of ultrasonically devulcanized tire-curing bladder and butyl rubber, Journal of Materials Science 40(11) (2005) 2883-2889.
[115] W.L. Feng, A.I. Isayev, High-power ultrasonic treatment of butyl rubber gum: Structure and properties, Journal of Polymer Science Part B-Polymer Physics 43(3) (2005) 334-344.
[116] A.I. Isayev, B. Sujan, Nonisothermal vulcanization of devulcanized GRT with reversion type behavior, Journal of Elastomers and Plastics 38(4) (2006) 291-318.
[117] J.K. Kim, S.H. Lee, S.H. Hwang, Study on the thermoplastic vulcanizate using ultrasonically treated rubber powder, Journal of Applied Polymer Science 90(9) (2003) 2503-2507.
[118] X. Sun, A.I. Isayev, Ultrasound devulcanization: comparison of synthetic isoprene and natural rubbers, Journal of Materials Science 42(17) (2007) 7520-7529.
[119] C.K. Hong, A.I. Isayev, Continuous ultrasonic devulcanization of carbon black-filled NR vulcanizates, Journal of Applied Polymer Science 79(13) (2001) 2340-2348.
[120] C.K. Hong, A.I. Isayev, Plastic/rubber blends of ultrasonically devulcanized GRT with HDPE, Journal of Elastomers and Plastics 33(1) (2010) 47-71.
[121] J. Yun, A.I. Isayev, S.H. Kim, M. Tapale, Comparative analysis of ultrasonically devulcanized unfilled SBR, NR, and EPDM rubbers, Journal of Applied Polymer Science 88(2) (2003) 434-441.
[122] S.H. Zhu, A. Penlidis, C. Tzoganakis, E. Ginzel, Ultrasonic properties and morphology of devulcanized rubber blends, Journal of Applied Polymer Science 124(3) (2012) 2062-2070.
[123] A.I. Isayev, S.P. Yushanov, J. Chen, Ultrasonic devulcanization of rubber vulcanizates .1. Process model, Journal of Applied Polymer Science 59(5) (1996) 803-813.
[124] A.I. Isayev, S.P. Yushanov, J. Chen, Ultrasonic devulcanization of rubber vulcanizates .2. Simulation and experiment, Journal of Applied Polymer Science 59(5) (1996) 815-824.
[125] A.I. Isayev, S.P. Yushanov, S.H. Kim, V.Y. Levin, Ultrasonic devulcanization of waste rubbers: Experimentation and modeling, Rheologica Acta 35(6) (1996) 616-630.
[126] J.L. Massey, J.C. Parr, T.A. Wagler, E. von Meerwall, C.K. Hong, A.I. Isayev, Ultrasound devulcanization of unfilled natural rubber networks, studied via component molecular mobility, Polymer International 56(7) (2007) 860-869.
[127] J.S. Oh, S. Ghose, A.I. Isayev, Effects of ultrasonic treatment on unfilled butadiene rubber, Journal of Polymer Science Part B-Polymer Physics 41(22) (2003) 2959-2968.
[128] J.S. Oh, A.I. Isayev, T. Wagler, P.L. Rinaldi, E. Von Meerwall, Molecular mobility and structure of ultrasonically treated unfilled butadiene rubber, Journal of Polymer Science Part B-Polymer Physics 42(10) (2004) 1875-1887.
[129] S.E. Shim, A.I. Isayev, Effects of the presecne of water on ultrasonic devulcanization of polydimethylsiloxane, Journal of Applied Polymer Science 88(11) (2003) 2630-2638.
[130] S.E. Shim, S. Ghose, A.I. Isayev, Formation of bubbles during ultrasonic treatment of cured

poly(dimethyl siloxane), Polymer 43(20) (2002) 5535-5543.
[131] S.E. Shim, J.C. Parr, E. von Meerwall, A.I. Isayev, NMR relaxation and pulsed gradient NMR diffusion measurements of ultrasonically devulcanized poly (dimethylsiloxane), Journal of Physical Chemistry B 106(46) (2002) 12072-12078.
[132] S.H. Lee, S.H. Hwang, M. Kontopoulou, V. Sridhar, Z.X. Zhang, D. Xu, J.K. Kim, The Effect of Physical Treatments of Waste Rubber Powder on the Mechanical Properties of the Revulcanizate, Journal of Applied Polymer Science 112(5) (2009) 3048-3056.
[133] J.S. Oh, A.I. Isayev, Ultrasonically treated polypropylene/ground tire rubber blends, Rubber Chemistry and Technology 75(4) (2002) 617-625.
[134] T. Luo, A.I. Isayev, Rubber/plastic blends based on devulcanized ground tire rubber, Journal of Elastomers and Plastics 30(2) (1998) 133-160.
[135] B. Diao, A.I. Isayev, V.Y. Levin, Basic study of continuous ultrasonic devulcanization of unfilled silicone, Rubber Chemistry and Technology 72(1) (1999) 152-164.
[136] A.I. Isayev, J. Chen, A. Tukachinsky, Novel ultrasonic technology for devulcanization of waste rubbers, Rubber Chemistry and Technology 68(2) (1995) 267-280.
[137] A.I. Isayev, J. Chen, S.P. Yushanov, Ultrasonic devulcanization of waste rubbers - Experimentation and modeling, Simulation of Materials Processing: Theory, Methods and Applications - Numiform 95 (1995) 77-85.
[138] J. Yun, J.S. Oh, A.I. Isayev, Ultrasonic devulcanization reactors for recycling of GRT: Comparative study, Rubber Chemistry and Technology 74(2) (2001) 317-330.
[139] S.P. Yushanov, A.I. Isayev, S.H. Kim, Ultrasonic devulcanization of SBR rubber: Experimentation and modeling based on cavitation and percolation theories, Rubber Chemistry and Technology 71(2) (1998) 168-190.
[140] V.V. Yashin, A.I. Isayev, A model for rubber degradation under ultrasonic treatment: Part I. Acoustic cavitation in viscoelastic solid, Rubber Chemistry and Technology 72(4) (1999) 741-757.
[141] V.V. Yashin, A.I. Isayev, A model for rubber degradation under ultrasonic treatment: Part II. Rupture of rubber network and comparison with experiments, Rubber Chemistry and Technology 73(2) (2000) 325-339.
[142] J.S. Yun, A.I. Isayev, The effect of high power ultrasound on EPDM gum in extrusion process, Journal of Applied Polymer Science 105(6) (2007) 3698-3707.
[143] S. Ghose, A.I. Isayev, E. von Meerwall, Effect of ultrasound on thermoset polyurethane: NMR relaxation and diffusion measurements, Polymer 45(11) (2004) 3709-3720.
[144] W.L. Feng, A.I. Isayev, E. von Meerwall, Molecular mobility in ultrasonically treated butyl gum and devulcanized butyl rubber, Polymer 45(25) (2004) 8459-8467.
[145] X. Sun, A.I. Isayev, T.R. Joshi, E. von Meerwall, Molecular mobility of unfilled and carbon-black-filled isoprene rubber: Proton NMR transverse relaxation and diffusion, Rubber Chemistry and Technology 80(5) (2007) 854-872.
[146] A. Tukachinsky, D. Schworm, A.I. Isayev, Devulcanization of waste tire rubber by powerful ultrasound, Rubber Chemistry and Technology 69(1) (1996) 92-103.
[147] M. Alexandre-Franco, C. Fernandez-Gonzalez, M. Alfaro-Dominguez, J.M.P. Latasa, V. Gomez-Serrano, Devulcanization and Demineralization of Used Tire Rubber by Thermal Chemical Methods: A Study by X-ray Diffraction, Energy & Fuels 24 (2010) 3401-3409.
[148] A.M. Shanmugharaj, J.K. Kim, S.H. Ryu, UV surface modification of waste tire powder: Characterization and its influence on the properties of polypropylene/waste powder composites, Polymer Testing 24(6) (2005) 739-745.
[149] D. De, A. Das, B. Dey, S.C. Debnath, B.C. Roy, Reclaiming of ground rubber tire (GRT) by a novel reclaiming agent, European Polymer Journal 42(4) (2006) 917-927.
[150] R. Sonnier, E. Leroy, L. Clerc, A. Bergeret, J.M. Lopez-Cuesta, Polyethylene/ground tyre rubber blends: Influence of particle morphology and oxidation on mechanical properties, Polymer Testing 26(2) (2007) 274-281.
[151] U.S. Ishiaku, C.S. Chong, H. Ismail, Determination of optimum De-Link R concentration in a recycled rubber compound, Polymer Testing 18(8) (1999) 621-633.
[152] G.K. Jana, R.N. Mahaling, C.K. Das, A novel devulcanization technology for vulcanized natural rubber, Journal of Applied Polymer Science 99(5) (2006) 2831-2840.
[153] M. Kojima, M. Tosaka, Y. Ikeda, Chemical recycling of sulfur-cured natural rubber using supercritical carbon dioxide, Green Chemistry 6(2) (2004) 84-89.
[154] A.R. Tripathy, D.E. Williams, R.J. Farris, Rubber plasticizers from degraded/devulcanized scrap rubber: A method of recycling waste rubber, Polymer Engineering and Science 44(7) (2004) 1338-1350.
[155] B. Vega, L. Montero, S. Lincoln, N. Agullo, S. Borros, Control of vulcanizing/devulcanizing behavior of diphenyl disulfide with microwaves as the heating source, Journal of Applied Polymer

Science 108(3) (2008) 1969-1975.
[156] K.A. Dubkov, S.V. Semikolenov, D.P. Ivanov, D.E. Babushkin, G.I. Panov, V.N. Parmon, Reclamation of waste tyre rubber with nitrous oxide, Polymer Degradation and Stability 97(7) (2012) 1123-1130.
[157] S.K. Lai, A. Batra, C. Cohen, Characterization of polydimethylsiloxane elastomer degradation via cross-linker hydrolysis, Polymer 46(12) (2005) 4204-4211.
[158] D. De, S. Maiti, B. Adhikari, Reclaiming of rubber by a renewable resource material (RRM). II. Comparative evaluation of reclaiming process of NR vulcanizate by RRM and diallyl disulfide, Journal of Applied Polymer Science 73(14) (1999) 2951-2958.
[159] Y.H. Li, S.H. Zhao, L.Q. Zhang, Y.Q. Wang, W.Y. Yu, The effect of different Fe2+ concentrations in culture media on the recycling of ground tyre rubber by Acidithiobacillus ferrooxidans YT-1, Annals of Microbiology 63(1) (2013) 315-321.
[160] Y.H. Li, S.H. Zhao, Y.Q. Wang, Microbial desulfurization of ground tire rubber by Thiobacillus ferrooxidans, Polymer Degradation and Stability 96(9) (2011) 1662-1668.
[161] K. Bredberg, B.E. Andersson, E. Landfors, O. Holst, Microbial detoxification of waste rubber material by wood-rotting fungi, Bioresource Technology 83(3) (2002) 221-224.
[162] M. Christiansson, B. Stenberg, L.R. Wallenberg, O. Holst, Reduction of surface sulphur upon microbial devulcanization of rubber materials, Biotechnology Letters 20(7) (1998) 637-642.
[163] O. Holst, B. Stenberg, M. Christiansson, Biotechnological possibilities for waste tyre-rubber treatment, Biodegradation 9(3-4) (1998) 301-310.
[164] G.M. Jiang, S.H. Zhao, J.Y. Luo, Y.Q. Wang, W.Y. Yu, C.R. Zhang, Microbial Desulfurization for NR Ground Rubber by Thiobacillus ferrooxidans, Journal of Applied Polymer Science 116(5) (2010) 2768-2774.
[165] G.M. Jiang, S.H. Zhao, W.J. Li, J.Y. Luo, Y.Q. Wang, Q.S. Zhou, C.R. Zhang, Microbial desulfurization of SBR ground rubber by Sphingomonas sp. and its utilization as filler in NR compounds, Polymers for Advanced Technologies 22(12) (2011) 2344-2351.
[166] S. Sato, Y. Honda, M. Kuwahara, H. Kishimoto, N. Yagi, K. Muraoka, T. Watanabe, Microbial scission of sulfide linkages in vulcanized natural rubber by a white rot basidiornycete, Ceriporiopsis subvermispora, Biomacromolecules 5(2) (2004) 511-515.
[167] A. Tsuchii, Y. Tokiwa, Microbial degradation of tyre rubber particles, Biotechnology Letters 23(12) (2001) 963-969.
[168] C. Yao, S.H. Zhao, M.H. Hu, B.W. Wang, L.Q. Zhang, Half-Submerged Cultivation Method for the Microbial Desulfurization of Waste Latex Rubber, Journal of Applied Polymer Science 131(21) (2014).
[169] K. Khait, J.M. Torkelson, Solid-state shear pulverization of plastics: A green recycling process, Polymer-Plastics Technology and Engineering 38(3) (1999) 445-457.
[170] E. Bilgili, H. Arastoopour, B. Bernstein, Pulverization of rubber granulates using the solid state shear extrusion process Part II. Powder characterization, Powder Technology 115(3) (2001) 277-289.
[171] E. Bilgili, H. Arastoopour, B. Bernstein, Pulverization of rubber granulates using the solid-state shear extrusion (SSSE) process: Part I. Process concepts and characteristics, Powder Technology 115(3) (2001) 265-276.
[172] T. Chaubey, H. Arastoopour, Studying the Pulverization Mechanism of Rubber with a Modified Design of the Solid-State Shear Extrusion Process, Journal of Applied Polymer Science 119(2) (2011) 1075-1083.
[173] N. Shahidi, H. Arastoopour, G. Ivanov, Pulverization of rubber using modified solid state shear extrusion process (SSSE), Journal of Applied Polymer Science 102(1) (2006) 119-127.
[174] D.D. Stanojevic, M.B. Rajkovic, D.V. Toskovic, Management of used tyres, accomplishments in the world, and situation in Serbia, Hemijska Industrija 65(6) (2011) 727-738.
[175] M. Llompart, L. Sanchez-Prado, J.P. Lamas, C. Garcia-Jares, E. Roca, T. Dagnac, Hazardous organic chemicals in rubber recycled tire playgrounds and pavers, Chemosphere 90(2) (2013) 423-431.
[176] S. Kocevski, S. Yagneswaran, F.P. Xiao, V.S. Punith, D.W. Smith, S. Amirkhanian, Surface modified ground rubber tire by grafting acrylic acid for paving applications, Construction and Building Materials 34 (2012) 83-90.
[177] D.S. Novotny, R.I. Marsh, F.C. Masters, D.N. Tally, Microwave devulcanization of rubber, 1978.
[178] B. Adhikari, D. De, S. Maiti, Reclamation and recycling of waste rubber, Progress in Polymer Science 25(7) (2000) 909-948.
[179] D.M. Pozar, Microwave Engineering, John Wiley & Sons, Toronto, 1998.
[180] C. Leonelli, T.J. Mason, Microwave and ultrasonic processing: Now a realistic option for industry, Chemical Engineering and Processing 49(9) (2010) 885-900.
[181] T. Amari, N.J. Themelis, I.K. Wernick, Resource recovery from used rubber tires, Resources Policy 25(3) (1999) 179-188.

[182] V.V. Rajan, W.K. Dierkes, R. Joseph, J.W.M. Noordermeer, Science and technology of rubber reclamation with special attention to NR-based waste latex products, Progress in Polymer Science 31(9) (2006) 811-834.
[183] E.T. Thostenson, T.W. Chou, Microwave processing: fundamentals and applications, Composites Part a-Applied Science and Manufacturing 30(9) (1999) 1055-1071.
[184] A.C. Metaxas, Foundations of Electroheat: A Unified Approach, John Wiley & Sons1996.
[185] K.S. Loganathan, Rubber engineering, McGraw-Hill, New York, 2000.
[186] D. De, G.M. Singharoy, Reclaiming of ground rubber tire by a novel reclaiming agent. I. Virgin natural rubber/reclaimed GRT vulcanizates, Polymer Engineering and Science 47(7) (2007) 1091-1100.
[187] M. Awang, H. Ismail, M.A. Hazizan, Polypropylene-based blends containing waste tire dust: Effects of trans-polyoctylene rubber (TOR) and dynamic vulcanization, Polymer Testing 26(6) (2007) 779-787.
[188] C.F. Antunes, A.V. Machado, M. van Duin, Morphology development and phase inversion during dynamic vulcanisation of EPDM/PP blends, European Polymer Journal 47(7) (2011) 1447-1459.
[189] F.P. J., J. Rehner Jr, Statistical mechanics of cross-linked polymer networks. II. Swelling, Journal of Chemical Physics 11 (1943) 521-526.
[190] M. Banda, A.K. Naskar, K.P.U. Perera, C. Moreland, T. Hodge, K. Wallace, H.W. Beckham, D.W. Smith, Functionalization of used tire rubber by hydrosilylation, Rubber Chemistry and Technology 85(1) (2012) 68-79.
[191] S.E. Shim, I. Isayev, E.V. Meerwall, Molecular mobility of ultrasonically devulcanized silica-filled poly(dimethyl siloxane), Journal of Polymer Science Part B-Polymer Physics 41(5) (2003) 454-465.
[192] S.T. Johnston, J. Massey, E. vonMeerwall, S.H. Kim, V.Y. Levin, A.I. Isayev, Ultrasound devulcanization of SBR: Molecular mobility of gel and sol, Rubber Chemistry and Technology 70(2) (1997) 183-193.
[193] A. Zanchet, N. Dal'Acqua, T. Weber, J.S. Crespo, R.N. Brandalise, R.C.R. Nunes, Cure characteristics, mechanical properties and morphology of composites developed with addition of elastomeric vulcanized ground scraps, Polimeros-Ciencia E Tecnologia 17(1) (2007) 23-27.
[194] T. Weber, A. Zanchet, J.S. Crespo, M.G. Oliveira, J.C.M. Suarez, R.C.R. Nunes, Caracterização de Artefatos Elastoméricos obtidos por Revulcanização de Resíduo Industrial de SBR(Copolímero de Butadieno e Estireno), Polímeros: Ciência e Tecnologia 21(5) (2011) 429-435.
[195] R. Ding, A.I. Leonov, A kinetic model for sulfur accelerated vulcanization of a natural rubber compound, Journal of Applied Polymer Science 61(3) (1996) 455-463.
[196] S.H. Chough, D.H. Chang, Kinetics of sulfur vulcanization of NR, BR, SBR, and their blends using a rheometer and DSC, Journal of Applied Polymer Science 61(3) (1996) 449-454.
[197] G.C. Santos, D.M. Carmo, C.G.F. Rezende, A.J. Zattera, M.G. Oliveira, P.J. Oliveira, Use of EPDMSDD as Compatibilizer Agent for EPDM/EPDMR Blends: Rheologic, Mechanical, and Morphologic Properties, Journal of Applied Polymer Science 122(2) (2011) 948-955.
[198] R.M. Mariano, P.H.D. Picciani, R.C.R. Nunes, L.L.Y. Visconte, Preparation, Structure, and Properties of Montmorillonite/Cellulose II/Natural Rubber Nanocomposites, Journal of Applied Polymer Science 120(1) (2011) 458-465.
[199] B. Karaagac, M. Inal, V. Deniz, Artificial neural network approach for predicting optimum cure time of rubber compounds, Materials & Design 30(5) (2009) 1685-1690.
[200] J.S. Dick, H. Pawlowski, Applications for the curemeter maximum cure rate in rubber compound development process control and cure kinetic studies, Polymer Testing 15(3) (1996) 207-243.
[201] F. Ignatz-Hoover, B.H. To, Rubber Compounding: Chemistry and Applications, Marcel Dekker, New York, 2004.
[202] M.R. Krejsa, J.L. Koenig, A review of sulfur cross-linking fundamentals for accelerated and unaccelerated vulcanization, Rubber Chemistry and Technology 66(3) (1993) 376-410.
[203] < http://www.braskem.com.br/site.aspx/Consultar-Produtos?codProduto=228&grd=true&Familia=13&nmFam=PE&Aplicacao=&Processo=2&CurrentPage=0>, access in 24/6/13.
[204] < http://www.chemtura.com/deployedfiles/staticfiles/businessunits/polymer_additives-en-us/TechnicalDataSheets/files/Polybond%203029%20and%203039%20TDS.pdf/Polybond%203029%20and%203039%20TDS.pdf>, access in 13/8/14.
[205] D.A. Baeta, J.A. Zattera, M.G. Oliveira, P.J. Oliveira, The use of styrene-butadiene rubber waste as a potential filler in nitrile rubber: Order of addition and size of waste particles, Brazilian Journal of Chemical Engineering 26(1) (2009) 23-31.
[206] A.J. Marzocca, Evaluation of the polymer–solvent interaction parameter v for the system cured styrene butadiene rubber and toluene 43 (2007) 2682–2689.
[207] J.A. Menendez, A. Arenillas, B. Fidalgo, Y. Fernandez, L. Zubizarreta, E.G. Calvo, J.M. Bermudez,

Microwave heating processes involving carbon materials, Fuel Processing Technology 91(1) (2010) 1-8.
[208] F.D. de Sousa, C.H. Scuracchio, The Role of Carbon Black on Devulcanization of Natural Rubber by Microwaves, Materials Research-Ibero-American Journal of Materials 18(4) (2015) 791-797.
[209] P.S. Garcia, F.D.B. de Sousa, J.A. de Lima, S.A. Cruz, C.H. Scuracchio, Devulcanization of ground tire rubber: Physical and chemical changes after different microwave exposure times, Express Polymer Letters 9(11) (2015) 1015-1026.
[210] K.A. Dubkov, S.V. Semikolenov, D.P. Ivanov, D.E. Babushkin, V.D. Voronchikhin, Scrap tyre rubber depolymerization by nitrous oxide: products and mechanism of reaction, Iranian Polymer Journal 23(11) (2014) 881-890.
[211] M.M. Hassan, R.O. Aly, S.E.A. Aal, A.M. El-Masry, E.S. Fathy, Mechanochemical devulcanization and gamma irradiation of devulcanized waste rubber/high density polyethylene thermoplastic elastomer, Journal of Industrial and Engineering Chemistry 19(5) (2013) 1722-1729.
[212] A. Kebritchi, H. Firoozifar, K. Shams, A. Jalali-Arani, Effect of pre-devulcanization and temperature on physical and chemical properties of waste tire pyrolytic oil residue, Fuel 112 (2013) 319-325.
[213] S. Yagneswaran, W.J. Storer, N. Tomar, M.N. Chaur, L. Echegoyen, D.W. Smith, Surface-grafting of ground rubber tire by poly acrylic acid via self-initiated free radical polymerization and composites with epoxy thereof, Polymer Composites 34(5) (2013) 769-777.
[214] A.P. Izhik, N.B. Uriev, Surface properties and specific features of structurization of disperse carbon black with different degrees of oxidation, Colloid Journal 64(5) (2002) 562-566.
[215] G. Socrates, Infrared characteristic group frequencies, John Wiley & Sons, New York, 1980.
[216] M. Khavarnia, S.O. Movahed, Butyl rubber reclamation by combined microwave radiation and chemical reagents Journal of applied polymer science 133(17) (2016).
[217] H. Hinsken, S. Moss, J.R. Pauquet, H. Zweifel, Degradation of polyolefins during melt processing, Polymer Degradation and Stability 34(1-3) (1991) 279-293.
[218] L.A. Pinheiro, M.A. Chinelatto, S.V. Canevarolo, The role of chain scission and chain branching in high density polyethylene during thermo-mechanical degradation, Polymer Degradation and Stability 86(3) (2004) 445-453.
[219] J.D. Silvano, S.A. Rodrigues, J. Marini, R.E.S. Bretas, S.V. Canevarolo, B.D. Carvalho, L.A. Pinheiro, Effect of reprocessing and clay concentration on the degradation of polypropylene/montmorillonite nanocomposites during twin screw extrusion, Polymer Degradation and Stability 98(3) (2013) 801-808.
[220] H. Cui, J.L. Yang, Z.Y. Liu, Thermogravimetric analysis of two Chinese used tires, Thermochimica Acta 333(2) (1999) 173-175.
[221] M.J. Fernandez-Berridi, N. Gonzalez, A. Mugica, C. Bernicot, Pyrolysis-FTIR and TGA techniques as tools in the characterization of blends of natural rubber and SBR, Thermochimica Acta 444(1) (2006) 65-70.
[222] Y.J. Hong, K.M. Jeong, P. Saha, J. Suh, J.K. Kim, Processing and Characterization of Microwave and Ultrasonically Treated Waste-EPDM/LDPE Polymer Composites, Polymer Engineering and Science 55(3) (2015) 533-540.
[223] F.D.B. de Sousa, J.R. Gouveia, P.M.F. de Camargo, S.E. Vidotti, C.H. Scuracchio, L.G. Amurin, T.S. Valera, Blends of ground tire rubber devulcanized by microwaves/HDPE - Part A: influence of devulcanization process, Polimeros-Ciencia E Tecnologia 25(3) (2015) 256-264.
[224] F.D.B. de Sousa, C.H. Scuracchio, G.H. Hu, S. Hoppe, Effects of processing parameters on the properties of microwave-devulcanized ground tire rubber/polyethylene dynamically revulcanized blends Journal of applied polymer science 133(23) (2016).
[225] R.E.S. Bretas, M.A. D'Ávila, Reologia de polímeros fundidos, 2 ed., EduFSCar, São Carlos-SP, 2010.
[226] S. Wu, Formation of dispersed phase in incompatible polymer blends: Interfacial and rheological effects, Polymer engineering and science 27(5) (1987) 335-343.
[227] Y. Soeda, X.M. Zhang, Y. Matsuda, S. Tasaka, Lamellar Structure of a Reactive Blend of 1,2-Polybutadiene and Nylon 11, Journal of Thermoplastic Composite Materials 22(4) (2009) 353-364.
[228] C. Harrats, S. Thomas, G. Groeninckx, Micro and Nanostructured Multiphase Polymer Blend Systems: Phase Morphology and Interfaces Taylor & Francis, United States, 2006.
[229] J. Oderkerk, G. Groeninckx, Morphology development by reactive compatibilisation and dynamic vulcanisation of nylon6/EPDM blends with a high rubber fraction, Polymer 43(8) (2002) 2219-2228.
[230] H. Schmitt, K. Prashantha, J. Soulestin, M.F. Lacrampe, P. Krawczak, Preparation and properties of novel melt-blended halloysite nanotubes/wheat starch nanocomposites, Carbohydrate Polymers 89(3) (2012) 920-927.
[231] S.S. Ray, S. Pouliot, M. Bousmina, L.A. Utracki, Role of organically modified layered silicate as an

active interfacial modifier in immiscible polystyrene/polypropylene blends, Polymer 45(25) (2004) 8403-8413.
[232] F.D.B. de Sousa, G.L. Mantovani, C.H. Scuracchio, Mechanical properties and morphology of NBR with different clays, Polymer Testing 30(8) (2011) 819-825.
[233] G. Naderi, P.G. Lafleur, C. Dubois, Microstructure-properties correlations in dynamically vulcanized nanocomposite thermoplastic elastomers based on PP/EPDM, Polymer Engineering and Science 47(3) (2007) 207-217.
[234] C. Harrats, Multiphase polymer-based materials, CRC Press, United States, 2009.
[235] C.F. Antunes, M. van Duin, A.V. Machado, Morphology and phase inversion of EPDM/PP blends - Effect of viscosity and elasticity, Polymer Testing 30(8) (2011) 907-915.
[236] L. Ackcelrud, Fundamentos da ciência dos polímeros, Manole, Barueri, SP, 2007.
[237] H.M. da Costa, V.D. Ramos, W.S. da Silva, A.S. Sirqueira, Analysis and optimization of polypropylene (PP)ethylene-propylene-diene monomer (EPDM)/scrap rubber tire (SRT) mixtures using RSM methodology, Polymer Testing 29(5) (2010) 572-578.
[238] P.A. Bhadane, J. Cheng, M.D. Ellul, B.D. Favis, Decoupling of reactions in reactive polymer blending for nanoscale morphology control, Journal of Polymer Science Part B-Polymer Physics 50(23) (2012) 1619-1629.
[239] L.A. Utracki, Polymer blends handbook, Kluwer Academic Publishers, Netherlands, 2002.
[240] P. Nevatia, T.S. Banerjee, B. Dutta, A. Jha, A.K. Naskar, A.K. Bhowmick, Thermoplastic elastomers from reclaimed rubber and waste plastics, Journal of Applied Polymer Science 83(9) (2002) 2035-2042.
[241] H. Ismail, Suryadiansyah, Thermoplastic elastomers based on polypropylene/natural rubber and polypropylene/recycle rubber blends, Polymer Testing 21(4) (2002) 389-395.
[242] H. Ismail, Suryadiansyah, A comparative study of the effect of degradation on the properties of PP/NR and PP/RR blends, Polymer-Plastics Technology and Engineering 43(2) (2004) 319-340.
[243] T. Chatterjee, S. Wiessner, K. Naskar, G. Heinrich, Novel thermoplastic vulcanizates (TPVs) based on silicone rubber and polyamide exploring peroxide cross-linking, Express Polymer Letters 8(4) (2014) 220-231.
[244] A. Fainleib, O. Grigoryeva, O. Starostenko, I. Danilenko, L. Bardash, Reactive compatibilization of recycled low density polyethylene/butadiene rubber blends during dynamic vulcanization, Macromolecular Symposia 202 (2003) 117-126.
[245] J.G. Drobny, Handbook of thermoplastic elastomer, Plastic Design Library, United States, 2007.
[246] M. van Duin, A.V. Machado, EPDM-based thermoplastic vulcanisates: Crosslinking chemistry and dynamic vulcanisation along the extruder axis, Polymer Degradation and Stability 90(2) (2005) 340-345.
[247] R.R. Babu, N.K. Singha, K. Naskar, Melt Viscoelastic Properties of Peroxide Cured Polypropylene-Ethylene Octene Copolymer Thermoplastic Vulcanizates, Polymer Engineering and Science 50(3) (2010) 455-467.
[248] A.Y. Coran, Vulcanization: Convetional and dynamic, Rubber chemistry and technology 68 (1995) 351-375.
[249] J.T. Yeh, S.C. Lin, Optimized Processing Conditions for the Preparation of Dynamically Vulcanized EPDM/PP Thermoplastic Elastomers Containing PP Resins of Various Melt Indexes, Journal of Applied Polymer Science 114(5) (2009) 2806-2815.
[250] R.R. Babu, N.K. Singha, K. Naskar, Dynamically Vulcanized Blends of Polypropylene and Ethylene-Octene Copolymer: Comparison of Different Peroxides on Mechanical, Thermal, and Morphological Characteristics, Journal of Applied Polymer Science 113(3) (2009) 1836-1852.
[251] Y.C. Tang, K. Lu, X.J. Cao, Y.J. Li, Nanostructured Thermoplastic Vulcanizates by Selectively Cross-Linking a Thermoplastic Blend with Similar Chemical Structures, Industrial & Engineering Chemistry Research 52(35) (2013) 12613-12621.
[252] H.G. Wu, N.Y. Ning, L.Q. Zhang, H.C. Tian, Y.P. Wu, M. Tian, Effect of additives on the morphology evolution of EPDM/PP TPVs during dynamic vulcanization in a twin-screw extruder, Journal of Polymer Research 20(10) (2013).
[253] X. Lu, W.W. Wang, L. Yu, Waste Ground Rubber Tire Powder/Thermoplastic Vulcanizate Blends: Preparation, Characterization, and Compatibility, Journal of Applied Polymer Science 131(3) (2014).
[254] J.E. Mark, B. Erman, F.R. Eirich, Science and technology of rubber Elsevier, United States, 2005.
[255] R.R. Babu, N.K. Singha, K. Naskar, Phase morphology and melt rheological behavior of uncrosslinked and dynamically crosslinked polyolefin blends: role of macromolecular structure, Polymer Bulletin 66(1) (2011) 95-118.
[256] C. Nakason, P. Wannavilai, A. Kaesaman, Effect of vulcanization system on properties of thermoplastic vulcanizates based on epoxidized natural rubber/polypropylene blends, Polymer Testing 25(1) (2006) 34-41.

[257] C. Jacob, P.P. De, A.K. Bhowmick, S.K. De, Recycling of EPDM waste. II. Replacement of virgin rubber by ground EPDM vulcanizate in EPDM/PP thermoplastic elastomeric composition, Journal of Applied Polymer Science 82(13) (2001) 3304-3312.
[258] S. Joseph, Z. Oommen, S. Thomas, Melt elasticity and extrudate characteristics of polystyrene/polybutadiene blends, Materials Letters 53(4-5) (2002) 268-276.
[259] F.R. Passador, L.A. Pessan, A. Rodolfo, PVC/NBR blends by reactive processing II: Physical-mechanical and morphological characterization, Polimeros-Ciencia E Tecnologia 18(2) (2008) 87-91.
[260] S. Anandhan, A.K. Bhowmick, Thermoplastic vulcanizates from post consumer computer plastics/nitrile rubber blends by dynamic vulcanization, Journal of Material Cycles and Waste Management 15(3) (2013) 300-309.
[261] B.E. Corley, H.J. Radusch, Intensification of interfacial interaction in dynamic vulcanization, Journal of Macromolecular Science-Physics B37(2) (1998) 265-273.
[262] R.R. Babu, N.K. Singha, K. Naskar, Studies on the influence of structurally different peroxides in polypropylene/ethylene alpha olefin thermoplastic vulcanizates (TPVs), Express Polymer Letters 2(3) (2008) 226-236.
[263] J. George, K.T. Varughese, S. Thomas, Dynamically vulcanised thermoplastic elastomer blends of polyethylene and nitrile rubber, Polymer 41(4) (2000) 1507-1517.
[264] Supri, H. Ismail, Effects of dynamic vulcanization and glycidyl methacrylate on properties of recycled poly(vinyl chloride)/acrylonitrile butadiene rubber blends, Polymer Testing 25(3) (2006) 318-326.
[265] M.K.A. Wahab, H. Ismail, N. Othman, Effects of dynamic vulcanization on the physical, mechanical, and morphological properties of high-density polyethylene/(natural rubber)/(thermoplastic tapioca starch) blends, Journal of Vinyl & Additive Technology 18(3) (2012) 192-197.
[266] S.M. Gheno, F.R. Passador, L.A. Pessan, Investigation of the Phase Morphology of Dynamically Vulcanized PVC/NBR Blends Using Atomic Force Microscopy, Journal of Applied Polymer Science 117(6) (2010) 3211-3219.
[267] S. George, K.T. Varughese, S. Thomas, Thermal and crystallisation behaviour of isotactic polypropylene/nitrile rubber blends, Polymer 41(14) (2000) 5485-5503.
[268] J. Chen, J.W. Chen, H.M. Chen, J.H. Yang, C. Chen, Y. Wang, Effect of compatibilizer and clay on morphology and fracture resistance of immiscible high density polyethylene/polyamide 6 blend, Composites Part B-Engineering 54 (2013) 422-430.
[269] S. Li, F.Z. Lang, Z.B. Wang, Zinc Dimethacrylate-Reinforced Thermoplastic Vulcanizates Based on Ethylene-Vinyl Acetate Copolymer/Chlorinated Polyethylene Rubber/Nitrile Butadiene Rubber Blends, Polymer-Plastics Technology and Engineering 52(7) (2013) 683-689.
[270] S. Li, T. Liu, L.J. Wang, Z.B. Wang, Dynamically Vulcanized Nitrile Butadiene Rubber/Ethylene-vinyl Acetate Copolymer Blends Compatibilized by Chlorinated Polyethylene, Journal of Macromolecular Science Part B-Physics 52(1) (2013) 13-21.
[271] R.R. Babu, N.K. Singha, K. Naskar, Interrelationships of morphology, thermal and mechanical properties in uncrosslinked and dynamically crosslinked PP/EOC and PP/EPDM blends, Express Polymer Letters 4(4) (2010) 197-209.
[272] R.R. Babu, N.K. Singha, K. Naskar, Dynamically Vulcanized Blends of Polypropylene and Ethylene Octene Copolymer: Influence of Various Coagents on Mechanical and Morphological Characteristics, Journal of Applied Polymer Science 113(5) (2009) 3207-3221.
[273] J. Jose, A. Nag, G.B. Nando, Processing and Characterization of Recycled Polypropylene and Acrylonitrile Butadiene Rubber Blends, Journal of Polymers and the Environment 18(3) (2010) 155-166.
[274] M. van Duin, Recent developments for EPDM-based thermoplastic vulcanisates, Macromolecular Symposia 233 (2006) 11-16.
[275] T.A. Huy, T. Luepke, H.J. Radusch, Characterization of the elongation behavior of dynamic vulcanizates by FTIR spectroscopy, Journal of Applied Polymer Science 80(2) (2001) 148-158.
[276] J. Oderkerk, G. de Schaetzen, B. Goderis, L. Hellemans, G. Groeninckx, Micromechanical elongation and recovery processes of nylon-6 rubber thermoplastic vulcanizates as studied by atomic force microscopy and transmission electron microscopy, Macromolecules 35(17) (2002) 6623-6629.
[277] J.K. Mishra, J.H. Ryou, G.H. Kim, K.J. Hwang, I. Kim, C.S. Ha, Preparation and properties of a new thermoplastic vulcanizate (TPV)/organoclay nanocomposite using maleic anhydride functionalized polypropylene as a compatibilizer, Materials Letters 58(27-28) (2004) 3481-3485.
[278] Z. Fang, C. Harrats, N. Moussaif, G. Groeninckx, Location of a nanoclay at the interface in an immiscible poly(epsilon-caprolactone)/poly(ethylene oxide) blend and its effect on the compatibility of the components, Journal of Applied Polymer Science 106(5) (2007) 3125-3135.
[279] Z.P. Fang, Y.Z. Xu, L.F. Tong, Effect of clay on the morphology of binary blends of polyamide 6 with high density polyethylene and HDPE-graft-acrylic acid, Polymer Engineering and Science 47(5)

(2007) 551-559.
[280] F. Fenouillot, P. Cassagnau, J.C. Majeste, Uneven distribution of nanoparticles in immiscible fluids: Morphology development in polymer blends, Polymer 50(6) (2009) 1333-1350.
[281] F. Razmjooei, G. Naderi, G. Bakhshandeh, Preparation of dynamically vulcanized thermoplastic elastomer nanocomposites based on LLDPE/reclaimed rubber, Journal of Applied Polymer Science 124(6) (2012) 4864-4873.
[282] Q. Zhang, H. Yang, Q. Fu, Kinetics-controlled compatibilization of immiscible polypropylene/polystyrene blends using nano-SiO2 particles, Polymer 45(6) (2004) 1913-1922.
[283] L. Elias, F. Fenouillot, J.C. Majeste, P. Cassagnau, Morphology and rheology of immiscible polymer blends filled with silica nanoparticles, Polymer 48(20) (2007) 6029-6040.
[284] B. Baghaei, S.H. Jafari, H.A. Khonakdar, I. Rezaeian, L. As'habi, S. Ahmadian, Interfacially compatibilized LDPE/POE blends reinforced with nanoclay: investigation of morphology, rheology and dynamic-mechanical properties, Polymer Bulletin 62(2) (2009) 255-270.
[285] S. Mani, P. Cassagnau, M. Bousmina, P. Chaumont, Morphology Development in Novel Composition of Thermoplastic Vulcanizates Based on PA12/PDMS Reactive Blends, Macromolecular Materials and Engineering 296(10) (2011) 909-920.
[286] A. Goldel, G. Kasaliwal, P. Potschke, Selective Localization and Migration of Multiwalled Carbon Nanotubes in Blends of Polycarbonate and Poly(styrene-acrylonitrile), Macromolecular Rapid Communications 30(6) (2009) 423-429.
[287] A. Goldel, A. Marmur, G.R. Kasaliwal, P. Potschke, G. Heinrich, Shape-Dependent Localization of Carbon Nanotubes and Carbon Black in an Immiscible Polymer Blend during Melt Mixing, Macromolecules 44(15) (2011) 6094-6102.
[288] A. Goldel, G.R. Kasaliwal, P. Potschke, G. Heinrich, The kinetics of CNT transfer between immiscible blend phases during melt mixing, Polymer 53(2) (2012) 411-421.
[289] K.Y. Lee, L.A. Goettler, Structure-property relationships in polymer blend nanocomposites, Polymer Engineering and Science 44(6) (2004) 1103-1111.
[290] L.Y. Zhang, C.Y. Wan, Y. Zhang, Investigation on Morphology and Mechanical Properties of Polyamide 6/Maleated Ethylene-propylene-diene Rubber/Organoclay Composites, Polymer Engineering and Science 49(2) (2009) 209-216.
[291] J.Y. Feng, C.M. Chan, J.X. Li, A method to control the dispersion of carbon black in an immiscible polymer blend, Polymer Engineering and Science 43(5) (2003) 1058-1063.
[292] <http://www.mma.gov.br/port/conama/res/res99/res25899.html>, access in 14/10/14.
[293] O. Bianchi, R. Fiorio, J.N. Martins, A.J. Zattera, C.H. Scuracchio, L.B. Canto, Crosslinking Kinetics of Blends of Ethylene Vinyl Acetate and Ground Tire Rubber, Journal of Elastomers and Plastics 41(2) (2009) 175-189.
[294] J. Canavate, P. Casas, X. Colom, F. Nogues, Formulations for thermoplastic vulcanizates based on high density polyethylene, ethylene-propylene-diene monomer, and ground tyre rubber, Journal of Composite Materials 45(11) (2011) 1189-1200.
[295] S. Anandhan, P.P. De, A.K. Bhowmick, S.K. De, S. Bandyopadhyay, Thermoplastic elastomeric blend of nitrile rubber and poly(styrene-co-acrylonitrile). II. Replacement of nitrile rubber by its vulcanizate powder, Journal of Applied Polymer Science 90(9) (2003) 2348-2357.
[296] M. Magioli, A.S. Sirqueira, B.G. Soares, The effect of dynamic vulcanization on the mechanical, dynamic-mechanical and fatigue properties of TPV based on polypropylene and ground tire rubber, Polymer Testing 29(7) (2010) 840-848.
[297] S.H. Lee, M. Balasubramanian, J.K. Kim, Dynamic reaction inside co-rotating twin screw extruder. I. Truck tire model material/polypropylene blends, Journal of Applied Polymer Science 106(5) (2007) 3193-3208.
[298] S.H. Lee, M. Balasubramanian, J.K. Kim, Dynamic reaction inside co-rotating twin screw extruder. II. Waste ground rubber tire powder/polypropylene blends, Journal of Applied Polymer Science 106(5) (2007) 3209-3219.
[299] R. Magaraphan, R. Skuarriya, S. Kohjiya, Morphological study of LLDPE-NR reactive blending with maleic anhydride, Journal of Applied Polymer Science 105(4) (2007) 1914-1921.
[300] P. Punnarak, S. Tantayanon, V. Tangpasuthadol, Dynamic vulcanization of reclaimed tire rubber and high density polyethylene blends, Polymer Degradation and Stability 91(12) (2006) 3456-3462.
[301] S.H. Zhu, C. Tzoganakis, Effect of Interfacial Strengthening in Blends of Reclaimed Rubber and Polypropylene, Journal of Applied Polymer Science 118(2) (2010) 1051-1059.
[302] S. Satapathy, A. Nag, G.B. Nando, Thermoplastic elastomers from waste polyethylene and reclaim rubber blends and their composites with fly ash, Process Safety and Environmental Protection 88(2) (2010) 131-141.
[303] A.K. Naskar, S.K. De, A.K. Bhowmick, Thermoplastic elastomeric composition based on maleic

anhydride-grafted ground rubber tire, Journal of Applied Polymer Science 84(2) (2002) 370-378.
[304] R. Scaffaro, N.T. Dintcheva, M.A. Nocilla, F.P. La Mantia, Formulation, characterization and optimization of the processing condition of blends of recycled polyethylene and ground tyre rubber: Mechanical and rheological analysis, Polymer Degradation and Stability 90(2) (2005) 281-287.
[305] A.K. Naskar, A.K. Bhowmick, S.K. De, Thermoplastic elastomeric composition based on ground rubber tire, Polymer Engineering and Science 41(6) (2001) 1087-1098.
[306] Z. Hrdlicka, A. Kuta, J. Hajek, Thermoplastic elastomer blends based on waste rubber and low-density polyethylene, Polimery 55(11-12) (2010) 832-838.
[307] O. Grigoryeva, A. Fainleib, A. Tolstov, P. Pissis, A. Spanoudaki, A. Vatalis, C. Delides, Thermal analysis of thermoplastic elastomers based on recycled polyethylenes and ground tyre rubber, Journal of Thermal Analysis and Calorimetry 86(1) (2006) 229-233.
[308] O.P. Grigoryeva, A.M. Fainleib, A.L. Tolstov, O.M. Starostenko, E. Lievana, J. Karger-Kocsis, Thermoplastic Elastomers based on recycled high-density polyethylene, ethylene-propylene-diene monomer rubber, and ground tire rubber, Journal of Applied Polymer Science 95(3) (2005) 659-671.
[309] M.R. Abadchi, A.J. Arani, H. Nazockdast, Partial Replacement of NR by GTR in Thermoplastic Elastomer Based on LLDPE/NR Through Using Reactive Blending: Its Effects on Morphology, Rheological, and Mechanical Properties, Journal of Applied Polymer Science 115(4) (2010) 2416-2422.
[310] R.I.N. Cespedes, J.F.H. Gamez, M.G.N. Velazquez, F.A. Belmontes, R.E.D. de Leon, O.S.R. Fernandez, C.A.A. Orta, E.H. Hernandez, Thermoplastic Elastomers Based on High-Density Polyethylene, Ethylene-Propylene-Diene Terpolymer, and Ground Tire Rubber Dynamically Vulcanized with Dicumyl Peroxide, Journal of Applied Polymer Science 131(4) (2014).
[311] H. Ismail, S. Ishak, Z.A.A. Hamid, Effect of blend ratio on cure characteristics, tensile properties, thermal and swelling properties of mica-filled (ethylene-propylene-diene monomer)/(recycled ethylene-propylene-diene monomer) (EPDM/r-EPDM) blends, Journal of vinyl & additive technology (2014).
[312] Y. Li, Y. Zhang, Y.X. Zhang, Structure and mechanical properties of SRP/HDPE/POE (EPR or EPDM) composites, Polymer Testing 22(8) (2003) 859-865.
[313] Y. Li, Y. Zhang, Y.X. Zhang, Morphology and mechanical properties of HDPE/SRP/elastomer composites: effect of elastomer polarity, Polymer Testing 23(1) (2004) 83-90.
[314] H. Nabil, H. Ismail, Blending of Natural Rubber/Recycled Ethylene-Propylene-diene Rubber: Promoting the Interfacial Adhesion Between Phases by Natural Rubber Latex, International Journal of Polymer Analysis and Characterization 19(2) (2014) 159-174.
[315] M.C.G. Rocha, M.E. Leyva, M.G. de Oliveira, Thermoplastic Elastomers Blends Based on Linear Low Density Polyethylene, Ethylene-1-Octene Copolymers and Ground Rubber Tire, Polimeros-Ciencia E Tecnologia 24(1) (2014) 23-29.
[316] O. Grigoryeva, A. Fainleib, J. Grenet, J.M. Saiter, Reactive compatibilization of recycled polyethylenes and scrap rubber in thermoplastic elastomers: chemical and radiation-chemical approach, Rubber Chemistry and Technology 81(5) (2008) 737-752.
[317] A. Tolstov, O. Grigoryeva, A. Fainleib, I. Danilenko, A. Spanoudaki, P. Pissis, J. Grenet, Reactive compatibilization of polyethylene/ground tire rubber inhomogeneous blends via interactions of pre-functionalized polymers in interface, Macromolecular Symposia 254 (2007) 226-232.
[318] L. Elias, F. Fenouillot, J.C. Majeste, P. Alcouffe, P. Cassagnau, Immiscible polymer blends stabilized with nano-silica particles: Rheology and effective interfacial tension, Polymer 49(20) (2008) 4378-4385.
[319] Y. Tsai, J.H. Wu, Y.T. Wu, C.H. Li, M.T. Leu, Reinforcement of dynamically vulcanized EPDM/PP elastomers using organoclay fillers, Science and Technology of Advanced Materials 9(4) (2008).
[320] K.A. Moly, Z. Oommen, S.S. Bhagawan, G. Groeninckx, S. Thomas, Melt rheology and morphology of LLDPE/EVA blends: Effect of blend ratio, compatibilization, and dynamic crosslinking, Journal of Applied Polymer Science 86(13) (2002) 3210-3225.
[321] O. Grigoryeva, A. Fainleib, O. Starostenko, A. Tolstov, W. Brostow, Thermoplastic elastomers from rubber and recycled polyethylene: chemical reactions at interphases for property enhancement, Polymer International 53(11) (2004) 1693-1703.
[322] A. Thitithammawong, C. Nakason, K. Sabakaro, J.W.M. Noordermeer, Thermoplastic vulcanizates based on epoxidized natural rubber/polypropylene blends: Selection of optimal peroxide type and concentration in relation to mixing conditions, European Polymer Journal 43(9) (2007) 4008-4018.
[323] D.R. Paul, C.B. Bucknall, Polymer Blends: Formulation, Wiley-Interscience, United States, 2000.
[324] L.A. Ultracki, Polymer Alloys and Blends, Hanser Publishers, New York, 1989.
[325] S. Manrich, Processamento de termoplásticos, Artliber, São Paulo, 2005.
[326] H.A. Khonakdar, U. Wagenknecht, S.H. Jafari, R. Hassler, H. Eslami, Dynamic-mechanical properties and morphology of polyethylene/ethylene vinyl acetate copolymer blends, Advances in

Polymer Technology 23(4) (2004) 307-315.
[327] K. Naskar, J.W.M. Noordermeer, Influence of various peroxides in PP/EPDM thermoplastic vulcanizates at varied blend ratios, Journal of Elastomers and Plastics 38(2) (2006) 163-180.
[328] M. He, Y. Li, B. Qiao, X. Ma, J. Song, M. Wang, Effect of dicumyl peroxide and phenolic resin as a mixed curing system on the mechanical properties and morphology of TPVs based on HDPE/ground tire rubber, Polymer composites (2014).
[329] P. Sengupta, J.W.M. Noordermeer, Effects of composition and processing conditions on morphology and properties of thermoplastic elastomer blends of SEBS-PP-oil and dynamically vulcanized EPDM-PP-oil, Journal of Elastomers and Plastics 36(4) (2004) 307-331.
[330] S. Shahbikian, P.J. Carreau, M.C. Heuzey, M.D. Ellul, J. Cheng, P. Shirodkar, H.P. Nadella, Morphology development of EPDM/PP uncross-linked/dynamically cross-linked blends, Polymer Engineering and Science 52(2) (2012) 309-322.
[331] H.W. Xiao, S.Q. Huang, T. Jiang, S.Y. Cheng, Miscibility of blends of ethylene-propylene-diene terpolymer and polypropylene, Journal of Applied Polymer Science 83(2) (2002) 315-322.
[332] F.D.B. de Sousa, S.E. Vidotti, C.H. Scuracchio, G.H. Hu, S. Hoppe, Thermoplastic Vulcanized HDPE/GTR devulcanized by microwaves, 12 Congresso Brasileiro de Polímeros, Florianópolis, 2013.
[333] G. Taylor, The formation of emulsions in definable fields of flow, Proceedings of the Royal Society of London Series A 146 (1934) 501-523.
[334] J.K. Lee, C.D. Han, Evolution of polymer blend morphology during compounding in a twin-screw extruder, Polymer 41(5) (2000) 1799-1815.
[335] H.P. Grace, Dispersion phenomena in high viscosity immiscible fluid systems and application of static mixers as dispersion devices in such systems, Chemical Engineering Communications 14 (1982) 225-277.
[336] G.N. Avgeropoulos, F.C. Wessert, P.H. Biddinson, G.G.A. Boehm, Heterogeneous blends of polymers: Rheology and morphology, Rubber chemistry and technology 49 (1976) 93-104.
[337] G.M. Jordhamo, J.A. Manson, L.H. Sperling, Phase continuity and inversion in polymer blends and simultaneous interpenetrating networks, Polymer engeneering and science 26 (1986) 517-524.
[338] A.K. Barick, J.Y. Jung, M.C. Choi, Y.W. Chang, Thermoplastic vulcanizate nanocomposites based on thermoplastic polyurethane and millable polyurethane blends reinforced with organoclay prepared by melt intercalation technique: Optimization of processing parameters via statistical methods, Journal of Applied Polymer Science 129(3) (2013) 1405-1416.
[339] V. Yquel, A.V. Machado, J.A. Covas, J.J. Flat, Contribution of the Melting Stage to the Evolution of the Morphology and Chemical Conversion of Immiscible Polyamide/Polyethylene Blends in Twin-Screw Extruders, Journal of Applied Polymer Science 114(3) (2009) 1768-1776.
[340] J.A. Covas, O.S. Carneiro, J.M. Maia, S.A. Filipe, A.V. Machado, Evolution of chemistry, morphology and rheology of various polymer systems along a twin-screw extruder, Canadian Journal of Chemical Engineering 80(6) (2002) 1065-1074.
[341] A. Mousa, U.S. Ishiaku, Z.A.M. Ishak, Rheological properties of dynamically vulcanized poly(vinyl chloride)/epoxidized natural rubber thermoplastic elastomers: effect of processing variables, Polymer Testing 19(2) (2000) 193-204.
[342] B. John, K.T. Varughese, Z. Oommen, S. Thomas, Melt Rheology of HDPE/EVA Blends: The Effects of Blend Ratio, Compatibilization, and Dynamic Vulcanization, Polymer Engineering and Science 50(4) (2010) 665-676.
[343] F. Goharpey, R. Foudazi, H. Nazockdast, A.A. Katbab, Determination of twin-screw extruder operational conditions for the preparation of thermoplastic vulcanizates on the basis of batch-mixer results, Journal of Applied Polymer Science 107(6) (2008) 3840-3847.
[344] A.V. Machado, J.A. Covas, M. van Duin, Evolution of morphology and of chemical conversion along the screw in a corotating twin-screw extruder, Journal of Applied Polymer Science 71(1) (1999) 135-141.
[345] S. Joseph, S. Thomas, Morphology, morphology development and mechanical properties of polystyrene/polybutadiene blends, European Polymer Journal 39(1) (2003) 115-125.
[346] E. Kalkornsurapranee, C. Nakason, C. Kummerlowe, N. Vennemann, Development and preparation of high-performance thermoplastic vulcanizates based on blends of natural rubber and thermoplastic polyurethanes, Journal of Applied Polymer Science 128(4) (2013) 2358-2367.
[347] I. Pesneau, M.F. Champagne, M.A. Huneault, PP/EMA TPV: Dynamic cross-linking through an alcoholysis reaction, Polymer Engineering and Science 42(10) (2002) 2016-2031.
[348] A. Verbois, P. Cassagnau, A. Michel, J. Guillet, C. Raveyre, New thermoplastic vulcanizate, composed of polypropylene and ethylene-vinyl acetate copolymer crosslinked by tetrapropoxysilane: evolution of the blend morphology with respect to the crosslinking reaction conversion, Polymer International 53(5) (2004) 523-535.

[349] U. Sundararaj, C.W. Macosko, R.J. Rolando, H.T. Chan, Morphology development in polymer blends, Polymer Engineering and Science 32(24) (1992) 1814-1823.
[350] A.V. Machado, J.A. Covas, M. Van Duin, Chemical and morphological evolution of PA-6/Epm/Epm-g-MA blends in a twin screw extruder, Journal of Polymer Science Part a-Polymer Chemistry 37(9) (1999) 1311-1320.
[351] M. van Duin, A.V. Machado, J. Covas, A look inside the extruder: Evolution of chemistry, morphology and rheology along the extruder axis during reactive processing and blending, Macromolecular Symposia 170 (2001) 29-39.
[352] A. Machado, M. van Duin, Dynamic vulcanisation of EPDM/PE-based thermoplastic vulcanisates studied along the extruder axis, Polymer 46(17) (2005) 6575-6586.
[353] Y.Z. Chen, Y.R. Cao, H.L. Li, Effect of ultrasound on extrusion of polypropylene/ethylene-propylene-diene terpolymer blend: Processing and mechanical properties, Journal of Applied Polymer Science 90(13) (2003) 3519-3525.
[354] M. Hernandez, J. Gonzalez, C. Albano, M. Ichazo, D. Lovera, Effects of composition and dynamic vulcanization on the rheological properties of PP/NBR blends, Polymer Bulletin 50(3) (2003) 205-212.
[355] J. Oderkerk, G. Groeninckx, M. Soliman, Investigation of the elongation and recovery behavior of nylon-6/rubber thermoplastic vulcanizates on the molecular level by infrared-strain recovery measurements, Macromolecules 35(10) (2002) 3946-3954.
[356] R. l'Abee, R. Sablong, H. Goossens, M. van Duin, A. Spoelstra, R. Duchateau, Thermoplastic Vulcanizates Based on Highly Compatible Blends of Isotactic Poly(propylene) and Copolymers of Atactic Poly(propylene) and 5-Ethylidene-2-norbornene, Macromolecular Chemistry and Physics 211(3) (2010) 334-344.
[357] P. Mahallati, D. Rodrigue, Effect of Feeding Strategy on the Properties of PP/Recycled EPDM Blends, International Polymer Processing 30(2) (2015) 276-283.
[358] L.M. Cao, X.D. Cao, X.J. Jiang, C.H. Xu, Y.K. Chen, In situ reactive compatibilization and reinforcement of peroxide dynamically vulcanized polypropylene/ethylene-propylene-diene monomer tpv by zinc dimethacrylate, Polymer Composites 34(8) (2013) 1357-1366.
[359] L.M. Cui, Z. Zhou, Y. Zhang, Y.X. Zhang, X.F. Zhang, W. Zhou, Rheological behavior of polypropylene/novolac blends, Journal of Applied Polymer Science 106(2) (2007) 811-816.
[360] R. Rajeshbabu, U. Gohs, K. Naskar, V. Thakur, U. Wagenknecht, G. Heinrich, Preparation of polypropylene (PP)/ethylene octene copolymer (EOC) thermoplastic vulcanizates (TPVs) by high energy electron reactive processing, Radiation Physics and Chemistry 80(12) (2011) 1398-1405.
[361] M.S. Rabello, Aditivação de polímeros, Artliber, São Paulo, 2007.
[362] Z. Oommen, S. Thomas, Mechanical properties and failure mode of thermoplastic elastomers from natural rubber poly(methyl methacrylate) natural rubber-g-poly(methyl methacrylate) blends, Journal of Applied Polymer Science 65(7) (1997) 1245-1255.
[363] R.R. Babu, N.K. Singha, K. Naskar, Effects of mixing sequence on peroxide cured polypropylene (PP)/ethylene octene copolymer (EOC) thermoplastic vulcanizates (TPVs). Part. I. Morphological, mechanical and thermal properties, Journal of Polymer Research 17(5) (2010) 657-671.
[364] A.J. Peacock, Handbook of polyethylene: Structures, properties and applications, Marcel Dekker, United States, 2000.
[365] <www.thermalsupport.com>, access in 19/9/13.
[366] <http://www.hitachi-hitec-science.com/en/documents/technology/thermal_analysis/application_DMS_005e.pdf>, access in 03/7/14.
[367] J.A. Molefi, A.S. Luyt, I. Krupa, Comparison of the influence of copper micro- and nano-particles on the mechanical properties of polyethylene/copper composites, Journal of Materials Science 45(1) (2010) 82-88.
[368] R.R. Babu, N.K. Singha, K. Naskar, Effects of mixing sequence on peroxide cured polypropylene (PP)/ethylene octene copolymer (EOC) thermoplastic vulcanizates (TPVs). Part. II. Viscoelastic characteristics, Journal of Polymer Research 18(1) (2011) 31-39.
[369] M. Mondal, U. Gohs, U. Wagenknecht, G. Heinrich, Polypropylene/natural rubber thermoplastic vulcanizates by eco-friendly and sustainable electron induced reactive processing, Radiation Physics and Chemistry 88 (2013) 74-81.
[370] F.D.B. de Sousa, J.R. Gouveia, P.M.F. de Camargo Filho, S.E. Vidotti, C.H. Scuracchio, G.H. Hu, S. Hoppe, Viscoelastic properties of blends type TPV HDPE/Ground Tire Rubber devulcanized by microwave, The 28th International Conference of Polymer Processing Society, Pattaya, 2012.
[371] Y.T. Lim, O.O. Park, Phase morphology and rheological behavior of polymer/layered silicate nanocomposites, Rheologica Acta 40(3) (2001) 220-229.
[372] Q.H. Zhang, S. Rastogi, D.J. Chen, D. Lippits, P.J. Lemstra, Low percolation threshold in single-walled carbon nanotube/high density polyethylene composites prepared by melt processing technique,

Carbon 44(4) (2006) 778-785.
[373] A.W.M. Kahar, H. Ismail, N. Othman, Properties of HVA-2 vulcanized high density polyethylene/natural rubber/thermoplastic tapioca starch blends, Journal of Applied Polymer Science 128(4) (2013) 2479-2488.
[374] S. Jose, S.V. Nair, S. Thomas, J. Karger-Kocsis, Effect of reactive compatibilisation on the phase morphology and tensile properties of PA12/PP blends, Journal of Applied Polymer Science 99(5) (2006) 2640-2660.
[375] S. George, R. Joseph, S. Thomas, K.T. Varughese, Blends of isotactic polypropylene and nitrile rubber - Morphology, mechanical-properties and compatibilization, Polymer 36(23) (1995) 4405-4416.

Étude des mélanges de polyéthylène renforcé avec des nanocharges et résidus de pneus régénérés par micro-ondes

RÉSUMÉ

Ces dernières années, la recherche de solutions au problème de l'élimination de déchets polymères, notamment les déchets issus de pneumatiques qui posent de graves problèmes environnementaux, connait un développement croissant. Dans ce contexte, ce projet de recherche a pour objectif de contribuer au développement et à la promotion de solutions innovantes qui font appel aux connaissances développées dans les domaines des nanotechnologies, de la science et l'ingénierie des matériaux nouveaux et du génie des procédés et des produits. Il s'agit plus particulièrement de d'étudier la possibilité de valoriser les déchets issus de pneumatiques en les utilisant comme matière première (en tant que agents de renfort ou agents de modification de la résistance aux chocs) pour l'élaboration de matériaux nanostructurés. Ce travail met l'accent sur l'étude des mélanges de polyéthylène haute densité (PEHD) contenant des particules d'argile (dispersées à l'échelle du nanomètre) et des déchets de caoutchouc issus de pneumatiques usagés (ou Ground Rubber Tire ou GRT). Il est attendu que ce matériau présente des propriétés typiques des mélanges de polymères appelés Vulcanisats Thermoplastiques (TPVs), résultant de la vulcanisation dynamique de la phase de caoutchouc pendant le traitement à l'état de fondu (extrusion). Dans le système étudié, la matrice est le PEHD et la phase dispersée de la poudrette de pneu, préalablement dévulcanisée par micro-ondes. L'argile dispersée dans la phase de la matrice, agit comme un agent compatibilisant entre les phases du mélange et comme agent de renforcement, apportant une amélioration des propriétés mécaniques des matériaux préparés. La caractérisation des mélanges met l'accent sur leur morphologie et leur structure ainsi que sur leurs propriétés rhéologiques, thermiques et mécaniques. Une étude approfondie de l'évolution de la morphologie du mélange au cours de l'extrusion a été effectuée car ce paramètre est la clé pour optimiser le procédé et obtenir les meilleures propriétés pour le matériau final. Ceci représente la contribution plus importante de ces travaux de recherche.

Mots Clés : Mélanges de polymères, résidus de pneus, revulcanisation dynamique, nanocomposites, dévulcanisation par micro-ondes, argiles.

Polyethylene blends reinforced with nanometric fillers and tire waste devulcanized by microwaves

ASTRACT

The main objective of this work was the production of dynamically revulcanized blends containing HDPE and GTR devulcanized by microwaves. It comes against a big global problem which is the waste disposal of vulcanized elastomers, especially tires, which bring with them serious environmental and public health problems, since these materials require long periods of time to degrade naturally due to their structure of cross-linkings, and the presence of stabilizers and other additives in its formulation.

A way of using the GTR that has been widely studied by researchers is as polymer blends in which one of the phases is a thermoplastic polymer. In this context, the role of elastomers devulcanization is to increase the interaction between raw and recycled material, reducing the degradation of properties of the finished product with its incorporation and making it possible the increase of the recycled rubber amount in the compound recycled rubber/thermoplastic. The devulcanization transformes devulcanized elastomer into a fluid material, allowing a better control of the particle size during the mixing process of the blend by breaking processes in the application of high shear rates. In addition, by becoming a fluid material, it is possible the incorporation of a higher amount of elastomer to the thermoplastic without great damage to its processability.

However, the literature does not have works in which the study of the processing parameters of dynamically revulcanized blends containing devulcanized elastomer, as well as the influence of addition of clays from different shapes (lamellar and tubular) on their final properties, especially on rheological properties, which sets out the present work.

Summarizing, this work aims to propose a possible solution to the problem of solid waste disposing by producing a dynamically revulcanized blend containing HDPE and GTR devulcanized by microwaves, in addition to decrease some gaps observed currently in the literature from the obtained results.

Key words : Polymer blends, Ground Tire Rubber (GTR), dynamic revulcanization, nanocomposites, devulcanization by microwaves, clays